12-2020

Design of hFGF1 Variant(s) with Increased Stability and Enhanced Bioactivity

Shilpi P. Agrawal
University of Arkansas, Fayetteville

Design of hFGF1 Variant(s) with Increased Stability and Enhanced Bioactivity

A dissertation submitted in partial fulfillment
of the requirements for the degree of
Doctor of Philosophy in Chemistry

by

Shilpi P. Agrawal
Gujarat University
Bachelor of Science in Biochemistry and Vocational Biotechnology, 2013
Vellore Institute of Technology
Master of Science in Biotechnology, 2015

December 2020
University of Arkansas

This dissertation is approved for recommendation to the Graduate Council.

Suresh Kumar Thallapuranam, Ph.D.
Dissertation Director

Josh Sakon, Ph.D.
Committee Member

Frank Millett, Ph.D.
Committee Member

Roger Koeppe, Ph.D.
Committee Member

Jingi Chen, Ph.D.
Committee Member

Paul Adams, Ph.D.
Committee Member

Abstract

Fibroblast growth factors (FGFs) are involved in various cellular processes such as cell growth, proliferation, differentiation, migration, angiogenesis, wound healing and embryonic development. Human acidic fibroblast growth factor (hFGF1) binds non-selectively to all the four FGF-receptors and is therefore considered as a powerful mitogen with broadest specificity. However, pharmacological applications of hFGF1 are restricted due to the low thermal stability of the growth factor. hFGF1 has low thermodynamic stability under physiological temperatures which leads to impairment of cellular signaling process thereby preventing its potential mitogenic properties. hFGF1 has a heparin binding pocket at the C-terminus which comprises of positively charges residues. The interaction between the positively charged amino acids lead to electrostatic repulsions, thereby rendering instability. To overcome this instability, hFGF1 binds to the glycosaminoglycan, heparin which decreases the repulsion (s) between the positively charged residues. However, binding of heparin poses a challenge for the use of hFGF1 in wound healing. Thrombin converts fibrinogen to fibrin and works as first line of defense by blocking the loss of blood. Intriguingly, thrombin also binds to heparin. Studies on wtFGF1 have demonstrated the presence of secondary thrombin cleavage site in hFGF1. Thus, thrombin is known to cleave hFGF1 at Arg 136 and render it biologically inactive. Usually, it is considered that dependency of hFGF1 to heparin increases the plausibility of thrombin-induced degradation of the growth factor. To tackle these downfalls, I have designed and constructed several point mutations in hFGF1 to improve the thermal stability and cell proliferation ability and to subside the heparin binding affinity of the growth factor.

In this dissertation, I studied single, double, triple, quadruple, and penta variants of Q54P, S61L, H107S, K126N, and R136E and examined the thermal stability, bioactivity, and heparin

dependency of the protein. These studies indicate that site - directed mutagenesis in hFGF1 can impact the inherent stability of the growth factor and role of heparin in hFGF1-FGFR receptor interaction and activation.

Acknowledgments

First and foremost, I would like to thank Lord Ganesha, who has granted countless blessings and opportunity throughout my life.

The success of this dissertation required a lot of guidance and assistance from many people. Most importantly, I would like to express my deepest gratitude to my advisor Dr. Suresh Kumar Thallapuranam, for providing me an opportunity to work on this research topic and for his endless support throughout my Ph.D. journey. Dr. Kumar is a humble and patient person who always encouraged new ideas and believed in me. This work would not have been possible without his support and constant guidance. I am extending my heartfelt thanks to his wife, Sujatha Suresh Kumar for her love and prayers. I would also like to thank Dr. Paul Adams, Dr. Frank Millett, Dr. Josh Sakon, Dr. Roger Koeppe, and Dr. Jingi Chen for taking time out of their busy schedule to serve on my dissertation committee and providing invaluable suggestions. I especially want to thank Dr. Mahmoud Moradi for sharing his knowledge to perform molecular dynamic simulations. I am also thankful to Vivek Govind Kumar, who performed the simulations to support the experimental results. I would like to extend my gratitude to the professors and the staff at the University of Arkansas, particularly the Chemistry and Biochemistry Department, who provided me an advanced education.

I am grateful to receive financial assistance provided by the Department of Energy (grant number DE-FG02-01ER15161), the National Institutes of Health/National Cancer Institute (NIH/NCI) (1 RO1 CA 172631) and the NIH through the COBRE program (P30 GM103450), and the Arkansas Biosciences Institute.

Thanks to my amazing parents, Prem Agrawal and Rashmi Agrawal, and my little brother, Utsav Agrawal. The countless times you helped me throughout my journey in United States; all

your efforts will gain something great in the near future. I am extremely grateful for their love, care, and sacrifices for educating and preparing me for my future. I won't be this stronger without you as my inspiration. Special thanks to Nehal Agarwal for being with me always. Nehal, I will never forget that when things went rough in my life, you stepped up and stood by my side.

I would not forget the support I received from my colleagues in the Kumar Laboratory: Dr. Srinivas Jayanthi, Dr. Ravi Gundampati, Dr. Sanhita Maity, Zeina Al-Raawi, Mercede Furr, Musaab Al-ameer, Patience Okoto, Ryan Layes, and Amanda Raley. We had endless brainstorming sessions when I got stuck with research, and they helped me see the issue with a different viewpoint. I also would like to thank the undergraduates in our lab who kept me motivated throughout my Ph.D. journey.

Finally, I would like to thank my friends especially, Sumana Venkat, Likitha Jonnagurakala, Adithya Polasa, Bhuvan Pathak, Anamika Gupta, and everybody in Summit Terrace for their love, opinion, support, and sense of humor. I would also like to thank my labmate and close friend, Shiva Kumar Sonnaila. Shiva, you have been a constant pillar of support and strength. Thank you for the effortless encouragement.

Table of contents

Chapter I	1
References	37
Chapter II	48
References	79
Chapter III	82
References	118
Chapter IV	122
References	156
Chapter V	161
References	186
Chapter VI	190
Appendix	195

Abbreviations

FGF - Fibroblast growth factor, human acidic fibroblast growth factor-1 (hFGF1); wildtype hFGF1 (wt-hFGF1); site directed mutagenesis (SDM); circular dichroism (CD); heteronuclear single quantum coherence (HSQC); American Type Culture Collection (ATCC); Visual Molecular Dynamics (VMD); isothermal titration calorimetry (ITC), GAG – Glycosaminoglycan, RAS - Retrovirus-associated DNA sequences, MAPK - Mitogen-activated protein kinase, HS - Heparin sulfate, ECM - Extra cellular matrix, HBS - Heparin binding site, FHF - FGF homologous factors, FGFR - Fibroblast growth factor receptor, FRS1 - phospholipase C (PLC) γ substrate 1, FRS2 - FGFR substrate 2, FRS2α - FGF receptor substrate 2α, PLCγ - phospholipase Cγ, PI3K - phosphoinositide 3-kinase, AKT - Protein kinase B, STAT - Signal Transducer and Activator of Transcription, CRKL - CRK Like Proto-Oncogene, GRB2 - Growth factor receptor-bound 2, SHP2- SH2 domain-containing protein tyrosine phosphatase-2, ETS - E26 transformation-specific, FOXO1 - Forkhead box class transcription factor, TSC2 - Tuberous sclerosis complex 2, IP3- Inositol triphosphate, DAG - Diacylglycerol, PKC - Protein kinase C, Ig – Immunoglobulin, SH2 - Src homology2, RTK - Receptor tyrosine kinase, KGF - Keratinocyte growth factor, rh-FGF1 - Recombinant human acidic fibroblast growth factor 1, rh-FGF2 - Recombinant human acidic fibroblast growth factor 2, MI - Myocardial infarction, MDD - Major depressive disorder, 1,25$(OH)_2$D - 1,25 dihydroxy vitamin D, CKD-MBD - Chronic kidney disease-mineral and bone disorder, HPT – Hyperparathyroidism, TIO - Tumor-induced osteomalacia, CYP27B1 - Cytochrome P450 Family 27 Subfamily B Member 1, CYP24A1 - Cytochrome P450 Family 24 Subfamily A Member 1, TG – Triglyceride, GLUT1 - Glucose transporter 1, UCP1 - Uncoupling protein 1

CHAPTER I

INTRODUCTION

Growth factors

Growth factors play a substantial role in intercommunication between cells *via* ligand/receptor cell signaling. Cell signaling can be mediated by several different types of ligands/effector molecules, including proteins. With protein ligands, cell signaling occurs in three clear modes in succession - reception of the signal, transduction through relay molecules, and cellular response by the target cell. Between cells, intercommunication begins with an extracellular ligand binding to a specific receptor in an extracellular compartment of the target cell. This reception is detected by a ligand that triggers the transduction signal, a chemical input that acts inside the cell. Once the chemical signal has reached its target intracellularly, cell undergoes the ligand-specific response. Growth factors, a family of proteins that are pertinent to cell signaling influence growth and replication of new cells, cell repair, cell differentiation, and cell survival in higher animals *via* the process of cell signaling.

In coordination with the process of cell signaling, four modes of signaling can occur (Table 1). One mode is autocrine secretion in which a cell signals itself by releasing a hormone that binds to autocrine receptors on the same cell. Another mode of secretion is the paracrine secretion wherein neighboring cells release factors onto each other's extracellular receptors. Third mode of secretion is intracrine secretion wherein the cell stimulates itself by a cellular product that acts inside the cell. Endocrine signaling is in contrast to other modes of signaling as the signal(s) is transported to cells via the bloodstream [1,2].

Classification of the fibroblast growth factor family

According to sequence homology and phylogeny, the mammalian fibroblast growth factor (FGF) family can be subdivided into 7 subfamilies (Table 1, Fig. 1) which are in contrast to gene location analysis; wherein the FGF family is classified into 6 subfamilies (Table 2) [1-3]. Except for the FGF11 subfamily which acts in an intracrine manner and FGF19 subfamily which are endocrine FGFs, most of the FGF subfamilies act in the paracrine manner (FGF1, FGF4, FGF7, FGF8, and FGF9 subfamilies). Only the members of paracrine subfamily bind to the heparan sulfate [2].

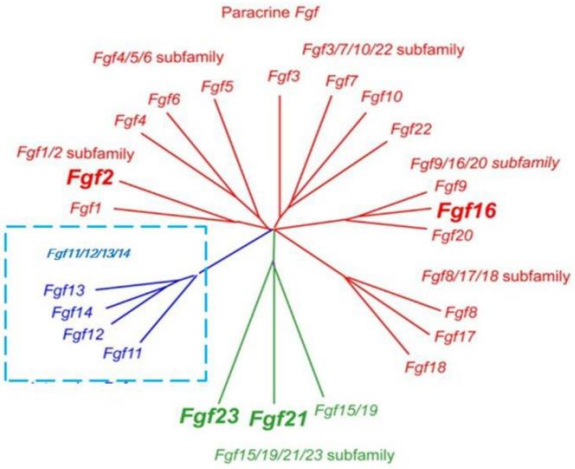

Fig. 1: Phylogenetic tree of the Human FGF family. Sequence homology and phylogenetic analysis reveals that FGFs can be arranged into 7 subfamilies. The branch length of each FGF member is directly proportional to the evolutionary distance between each gene. FGF19, FGF21, and FGF23 act as endocrine secretions [1].

Table 1: Phylogenetic analysis of the human FGF family. The human FGF gene family can be subdivided into 7 subfamilies.

FGF subfamily	Members of the subfamily	Mode of action
FGF1	FGF1, FGF2	Paracrine [1]
FGF4	FGF4, FGF5, FGF6	Paracrine [2]
FGF7	FGF3, FGF7, FGF10, FGF22	Paracrine [1]
FGF8	FGF8, FGF17, FGF18	Paracrine [2]
FGF9	FGF9, FGF16, FGF20	Paracrine [1]
FGF11	FGF11, FGF12, FGF13, FGF14	Intracrine [1]
FGF19	FGF19, FGF21, FGF23	Endocrine [1]

Table 2: Gene location analysis of the human FGF family.

FGF subfamily	Members of the subfamily	Gene location
FGF1	FGF1	5q31.3 [3]
	FGF2	4q27 [3]
	FGF5	4q21.21 [3]
FGF4	FGF3	11q13.3 [3]
	FGF4	11q13.3 [3]
	FGF6	12p13.32 [3]
	FGF19	11q13.3 [3]
	FGF21	19q13.32[3]
	FGF23	12p13.32[3]
FGF7	FGF7	15q21.2[3]
	FGF10	5p12 [3]
	FGF22	19p13.3 [3]
FGF8	FGF8	10q24.32 [3]
	FGF17	8p21.3[3]
	FGF18	5q35.1[3]
FGF9	FGF9	13q12.11 [3]
	FGF16	Xq21.1[3]
	FGF20	8p22[3]
FGF11	FGF11	17p13.1[3]
	FGF12	3q28[3]
	FGF13	Xq26.3[3]
	FGF14	13q33.1[3]

FGF is a prototype member of the family consisting of 23 related proteins with a molecular weight ranging from 17 to 34 kDa [5]. They are largely responsible for growth and development and strongly influence mitogenic events in endothelial and epithelial cells, angiogenesis, wound healing, and regulation of cell growth and differentiation [6]. FGF induces the metabolic processes by binding and activating specific tyrosine kinase fibroblast growth factor receptors (FGFRs). This FGF-FGFR complex, in turn, induces downstream signaling through common pathways such as the retrovirus-associated DNA sequences (RAS)/mitogen-activated protein kinase (MAPK), phosphoinositide-3-kinase (PI3K) / Protein kinase B (AKT), and phospholipase-Cγ (PLCγ) pathways [5]. However, the structural bases for the specificity of events triggered by individual members of the FGF family is still not known. Most FGFs are

homologous to each other in their amino acid composition [6]. The FGF family consists of structurally related polypeptide growth factors that share high affinity for heparin, interact with FGFRs, and carry out distinct functions.

FGFs predominantly have a β-trefoil structure consisting of 12 antiparallel β-strands [7]. This globular β-trefoil core domain is flanked by N- and C-terminal regions that are highly divergent in both length and sequence amongst different members of the FGF family. FGFs and their target cells are widely distributed and expressed in several types of tissues. Biosynthesis and activity of FGFs is complex and regulated at all levels of processing, including activation of transcription, post-transcriptional modifications (capping, splicing, polyadenylation, and mRNA stability), translation initiation, post-translational modifications (O-linked glycosylation, N-linked glycosylation, phosphorylation, acetylation, methylation, and ribosylation), intracellular trafficking, secretion, bioavailability, and ligand-receptor interactions [8].

Structure and function of the FGF family

FGF1 subfamily

The FGF1 subfamily is also known as the prototypical or archetypal family. FGF1, also known as an acidic fibroblast growth factor and FGF2, also known as a basic fibroblast growth factor, were the first FGFs to be isolated and identified. The prototypical Fgf genes comprise of 3 coding exons, out of which exon 1 contains the initiating codon- methionine. Even though this subfamily is considered as paracrine FGFs, it behaves in an intracrine manner. None of the FGFs from this group are secreted by the cell nor do they have the N-terminal hydrophobic sequence instead, they are directly translocated to the nucleus [9-12]. The mRNA structure of this subfamily is unique when compared to other FGFs because it does not include a signal peptide sequence that targets FGFs for secretion through the classic ER-Golgi complex secretory

pathway. FGFs employ a non-classical pathway to be secreted [11]. Also, the open reading frame in FGF1 is edged by the termination codons, whereas FGF2 contains 5' transcribed sequence that initiates from upstream CUG codons for translation [12].

FGF1 and FGF2 differ significantly in both size and sequence, but both contain a core region of homology encompassing 120–130 residues; which suggests that they are originated from a common ancestral gene. Both the structurally related proteins have 53% protein sequence homology. Both bind tightly to heparin and share many biochemical and biological properties [13]. Thus, in the FGF1 subfamily, both FGF1 and FGF2 have a similar preference for N-sulfate and 2-Osulfate, but FGF1 differs in that it also binds saccharide structures with 6-O-sulfated heparin. This subfamily possesses three Heparin Binding Sites (HBS), the primary HBS1 and the secondary binding sites HBS2 and HBS3 [14].

FGF1 is a single chain positively charged polypeptide with a molecular weight of about 15,967 Da and a pI of 7.73 [5]. FGF1 was originally purified from the brain using standard chromatographic techniques such as ion-exchange chromatography, gel filtration, isoelectric focusing, and reverse-phase HPLC. FGF-1 has a strong affinity for heparin and its purification is greatly facilitated by heparin sepharose chromatography. Initially, FGF1 was recognized as a polypeptide containing 140 amino acids. However, subsequent sequence analysis showed that FGF1 was a 154 amino acids polypeptide. The shorter form represents a truncated version, where 14 amino acids are chopped off the N-terminus. FGF1 is fairly well conserved among species, with 11 amino acids differing between human and bovine FGF1. FGF1 also has 19-25% sequence homologies with interleukin-l-alpha and interleukin-l-beta but there is no evidence of these homologies being biologically significant. However, it is of interest that these interleukins, like FGF1 and FGF2, are not secreted proteins. FGF1 contains characteristic β-trefoil structure

which is made up of 12 antiparallel β strands [5,6]. Human FGF1 contains three cysteine residues (Cys 30, Cys 97, C131), unlike FGF2 which has four. Two of these, Cys 30 and Cys 97 are conserved in all FGF family members. Key residues responsible for interaction between FGF1 and heparin or its receptor are characterized by the crystal structure [6]. FGF1 is unique among FGFs because of its ability to bind and activate all known FGFRs, FGF-1 is considered to be the universal FGFR ligand [15].

FGF2 has a molecular weight of 18 kDa and is well conserved among the other species. Human FGF2 contains four cysteine residues (Cys 33, Cys 77, Cys 95, and Cys 100). As mentioned in hFGF1, two of these cysteine residues (Cys 33 and cys 100) are conserved in all FGF family members. Several studies have shown that none of the cysteine residues form disulfide bonds. Site directed mutagenesis studies report that substitution of Cys 77, 95, and 100 to serine did not alter the cell proliferation activity of FGF2. On the other hand, substitution of Cys 33 to serine led to 60% reduction in the biological activity of hFGF2. Baird and colleagues showed that cell surface receptor-binding and heparin-binding domains of FGF2 are the same.

FGF1 and FGF2 are prototype members of the FGF family. They control a broad range of biological functions from developmental processes during embryogenesis to various physiological roles in the adult state, including the regulation of angiogenesis, wound healing, organ development (eye, skin, brain, lung, limb, muscle, bone, blood, and heart), and metabolism. FGF1 and FGF2 also possess broad mitogenic and cell survival activities, such as cell growth, cell differentiation, tissue repair, tumor growth, and invasion. FGF1 and FGF2 are known to play an important role in neurogenesis. FGF2 knock-out mice shows impaired brain development, wound repair, and deformed bone formation [16]. FGF1 and FGF2 has been used more widely for wound healing than FGF7 and FGF10. Also, recombinant human FGF1 (rh-

FGF1) and recombinant human FGF2 (rh-FGF2) showed effective healing effects for the treatment of ulcers and diabetic foot ulcers compared to FGF7 and FGF10. rh-FGF1 and rh-FGF2 has a positive influence in curing ulcers, diabetic foot abscess, and second-degree burns [17].

FGF4 subfamily

The FGF4 subfamily involves FGF4, FGF5 and FGF6. Human FGF4 is located in extracellular space and nucleus. It has been reported that FGF4 and FGF6 are more stable than FGF3 and FGF17 in absence of heparin [14]. Examination of crystal structure of FGF4 identified 2 heparin binding sites (HBS). The first heparin binding site spans the area between β6 and β7, β9 and β10, and β10 and β12 strands which involve Lys 142, 144, 147, 183, 186, 188, and 189, respectively. The second heparin binding site consists of three lysine residues (Lys 65, 81, and 158). Similarly, FGF6 also has two heparin binding sites. HBS1 spans the region between β10 and β12 strand and involves Lys 144, 185, and 194. HBS2 includes Lys 83 (found near the N-terminal of β1 strand) and Lys 158 on the β8 strand.

FGF5 is composed of a highly conserved core region which comprises of 12 β strands and a signal peptide at the N terminus [18]. Human FGF4 plays an important role in the regulation of embryonic development, cell proliferation, and cell differentiation. It is required for normal limb and cardiac valve development during embryogenesis [19]. Human FGF5 plays an important role in the regulation of cell proliferation and differentiation and is required for normal regulation of the hair growth cycle. FGF5 functions as an inhibitor of hair elongation by promoting progression from anagen, the growth phase of the hair follicle, into catagen the apoptosis-induced regression phase [20]. Human FGF6 plays an important role in the regulation of cell

proliferation, cell differentiation, angiogenesis and myogenesis, and is required for normal muscle regeneration and differentiation [21].

FGF7 subfamily

The FGF7 subfamily involves FGF3, FGF7, FGF10 and FGF22. The FGF7 subfamily is unique among FGFs because its members are expressed exclusively by mesenchymal cells and interact specifically with the b splice variant of FGFR2 (FGFR2b) resident in overlying epithelium [22]. Members of the FGF7 subfamily are essential for organogenesis and tissue patterning in the embryo, and mediate wound healing and tissue homeostasis in adult mammals [23]. The varied functional roles of this subfamily is responsible for causing numerous diseases such as congenital deafness (LAMM syndrome), lacrimo-auriculo-dento-digital (LADD) syndrome, inflammatory bowel disease, Apert syndrome (AS), and prostate cancer [24].

FGF7 is also known as Keratinocyte Growth Factor (KGF). It has 10 well-defined beta strands, which form five double stranded anti-parallel beta sheets. There is a single beta-sheet hydrogen bond (which is also called as the 6^{th} Beta sheet) between residues 137 and 141. This poorly defined sixth beta- sheet has a helix-like nature in high resolution FGF-2 NMR structure [25]. Apart from these little dissimilarities, the structures of KGF, FGF-1, and FGF-2 are very similar with a Root Mean Square Deviation (RMSD) of about 0.89 Å based on the C-alpha atoms [26]. Overlay of the heparin bound KGF structure on the heparin bound FGF-2 structure shows that only Gln-152 of KGF superimposes very well with Gln-135 of FGF1 and FGF2, whereas other residues in KGF differ from FGF1 and FGF2. Talking about the non-heparin binding region, the nonpolar residue Val-143 of KGF superimposes with the high-affinity residue Lys-126 of bFGF [25]. However, when the structures are superimposed, residue Thr-154 of KGF appears to be pointing toward the heparin-binding pocket, and thus may contribute to the

binding energy lost by the valine. FGF7 plays an important role in the regulation of embryonic development, cell proliferation and cell differentiation and is required for normal branching morphogenesis [27].

FGF10 controls the epithelial-mesenchymal interactions that are important for lung development [28]. FGF10 is 20 kDa heparin-binding protein essentially expressed by mesenchymal cells and it binds strongly to FGFR2-IIIb while binds weakly to FGFR1-IIIb [29]. FGF10 can prevent lung-specific inflammation induced by traumatic or infectious lung injury. The effect of FGF10 on lung-resident mesenchymal stem cells (LR-MSCs) was studied by delivering FGF10 into the lungs of rats and it was found that FGF10 led to an increase of LR-MSCs in treated lungs [30].

Terauchi *et al.*, have reported that the hippocampus region of the mouse brain uses FGF22 as a target-derived presynaptic organizer [31]. The Cornu Ammonis, subfield 3 pyramidal neuron is located within the hippocampus of the brain's temporal lobe. This pyramidal neuron releases FGF22 which stimulates the differentiation of the excitatory presynaptic terminals. FGF22-dependent presynaptic differentiation requires two FGF receptors (FGFRs), FGFR2b and FGFR1b, in dentate granule cells (DGCs), the major presynaptic neurons for CA3 pyramidal neurons, and the downstream signaling molecules FGFR substrate 2 (FRS2) and PI-3 kinase [31]. Signals mediated by FRS2 and PI-3 kinase are known to regulate gene expression.

There are significant differences in the heparin binding affinity of the FGF7 subfamily, with minimum or no binding observed in FGF3 and FGF22. This difference conferred distinct biological properties and functions to this subfamily [22]. According to the amino acid sequence alignment, FGF3 was similarly stabilized by unmodified heparin and any of the singly desulfated heparins [22]. In the case of FGF10, there was no obvious difference in the stabilizing effect of

heparin and the singly desulfated heparins. Thus, the binding preferences of FGF10 are similar but not equal to those of FGF3.

FGF8 subfamily

It includes FGF8, FGF17, and FGF18. Unlike other FGFs, an alternative splicing event occurs at the N termini of FGF8 and FGF17 resulting in four FGF8 isoforms (FGF8a, FGF8b, FGF8e, and FGF8f) and 2 FGF17 isoforms (FGF17a and FGF17b) [32]. FGF8a, the smallest FGF8 isoform, represents the common core region of FGF8b, FGF8e, and FGF8f and the remaining isoforms differ by the presence of additional N-terminal amino acid sequences of variable length and sequence [33]. FGF17a and FGF17b resemble FGF8a and FGF8b, respectively. On the other hand, FGF18 is not subjected to alternative splicing [34].

Members of FGF8 subfamily adopt a different conformation than the rest of the FGF family members. They exhibit a well conserved N-terminus and a one-residue insertion (S95) in the β4–β5 loop [35]. FGF8 plays a key role in the regulation of embryonic limb development, embryonic brain development, and development of the gonadotropin-releasing hormone (GnRH) neuronal system [36]. It is also required for cell proliferation, cell differentiation and cell migration. FGF17 is also essential for embryonic eye, ear, and limb development, and as signaling molecule in the induction and patterning of the embryonic brain [37]. FGF18 is reported to play a crucial role in osteogenesis, cartilage formation, cell proliferation, cell differentiation, and cell migration [38].

FGF9 subfamily

The FGF9 subfamily includes FGF9, FGF16, and FGF20. FGF9 is a potent mitogen which is primarily produced by neurons [39]. FGF9 is broadly expressed in high levels throughout the brain and kidney. FGF16 is highly expressed in olfactory bulb and heart, where it

is required for cardiac cell proliferation [40]. FGF20 is a neurotrophic factor expressed in the substantia nigra pars compacta and is associated with Parkinson's disease [41]. FGF20 is expressed at low levels in a limited set of tissues including adrenal tissues.

The FGF9 subfamily is the only subfamily which undergoes reversible homodimerization [42]. This family shares approximately 62–73% amino acid sequence similarity and exhibit high sequence homology between human and mouse. The FGF9 subfamily is important for epithelial-mesenchymal interactions. This subfamily also controls the morphogenesis of lungs, small intestine, inner ear, and cecum [43].

FGF11 subfamily

The FGF11 subfamily consists of FGF11, FGF12, FFG13, and FGF14. This subfamily is an exclusion from the other FGF sub-families but shares high structural and sequence homology. Members of the FGF11 subfamily are also known as FGF homologous factors (FHFs) and is functionally different from the other FGF families. They share between 58-71% sequence identity with each other and less than 30% sequence identity with other members of the FGF family. These members regulate channel gating and intracellular signal trafficking by interacting with the cytoplasmic C-terminal tails of voltage-gated sodium channels [13].

FGF19 subfamily

FGF19 subfamily consists of FGF19, FGF21, and FGF23. Unlike usual FGFs, FGF19 subfamily members lack a classic heparin-binding domain. This characteristic protects them from the capture by local cells; therefore, they are secreted into the bloodstream and function as hormones. Thus, this subfamily acts in an endocrine manner. However, the FGF19 subfamily has a low affinity for heparin sulfate, and another co-receptor named Klotho is required to allow the FGF19 subfamily to exert their biological functions. Relative to the five paracrine-acting FGF

subfamilies, the FGF 19 subfamily displays the least sequence identity amongst its members. The pairwise sequence identity between the core regions of members of FGF19 subfamily ranges between 33% for FGF21 and FGF23 and 38% for FGF19 and FGF21. When compared, the identity between the core regions of members of paracrine FGF subfamilies is significantly higher and ranges between 88% for FGF9 and FGF16 to 54% for FGF7 and FGF10. Most of the sequence divergence between FGF19 subfamily members shoots from the heparin binding regions, specifically the β1-β2 loop and the segment between the β10 and β12 strands of the paracrine ligands. Elimination of the heparin binding region from the sequence alignment data increases the identity between FGF19 subfamily members and other FGF subfamilies to more than 40%. Members of the FGF19 subfamily have varied functions such as regulating the enterohepatic circulation of bile acid, regulating glucose and lipid metabolism, and maintaining phosphate/vitamin D homeostasis [13].

FGF21 is a hormone secreted by the liver (hepatokine) but the bioactivity of FGF21 and the actual mode of action still remains elusive [44]. FGF21 is an important inducer of glucose uptake in adipocytes. When overexpressed in transgenic mice, it was found to reduce the diet-induced obesity, blood glucose, and the triglyceride (TG) levels [45]. FGF21 has appeared as an essential metabolic hormone contributing towards managing glucose, lipid, and energy homeostasis. Recombinant FGF21 have impressive effect in normalizing plasma glucose levels, increasing insulin sensitivity, and reducing plasma TG and cholesterol levels in different diabetic animal models including rhesus monkeys. Recombinant FGF21 serves as a potential unique treatment to cure metabolic disorders [46]. FGF21 improves insulin-independent glucose uptake into cultured 3T3-L1 mouse adipocytes and human adipocytes by the upregulation of glucose transporter 1 (GLUT1) expression. Studies indicate that FGF21 controls adipocyte lipolysis and

enhances adiponectin expression and secretion [47]. Reconstitution of adipose tissue by transplanting white adipose tissue (WAT) from wild-type mice to lipoatrophic mice restores FGF21 responsiveness. FGF21 controls the gene expression of uncoupling protein 1 (UCP1) in brown adipose tissue (BAT) and WAT and significantly increases the presence of "brown-like" adipocytes in subcutaneous WAT [48]. These outcomes may result in the thermogenic activities of FGF21 and controlled weight-loss under high fat conditions. In mice, FGF21 expression is upregulated in response to cold exposure and β-adrenergic stimulation [48]. In rats, exposure to cold climate activate a distinct release of FGF21 from BAT, suggesting an endocrine role of BAT as a source of FGF21 that can be related to thermogenic activation. In humans, changes in the serum FGF21 concentrations correlate positively with thermogenesis and circulating FGF21 levels correspond to BAT activity during severe cold exposure in male individuals which suggests that FGF21 maintains normothermia [49]. FGF21 agonist aids in the treatment of type 2 diabetes and obesity [50]. FGF21 plays an essential role in the regulation of glucose and lipid metabolism in obese rodents and primates. FGF21, a hepatokine growth factor, has a satisfactory role in glucose and lipid metabolism in mice. The first clinical trials of FGF21 analogs in type 2 diabetic patients exhibited lowered glucose efficacy [51]. Immunostaining of the pancreatic islets revealed that the number of islets and insulin amount were elevated in FGF21 injected db/db mice [52]. FGF21 is significantly expressed in pancreas and exerts its inflammatory role in experimental pancreatitis [53,54].

FGF23 is secreted mainly by osteocytes and it acts as a phosphaturic factor that inhibits 1,25 dihydroxy vitamin D ($1,25(OH)_2D$) and parathyroid hormone. FGF23 regulates the concentration of phosphate that is important in cellular signaling, regulating plasma pH, bone mineralization, and bone development. Increased serum FGF23 concentration has been

associated with the progression of chronic kidney disease. To study the effects of FGF23 on chronic kidney disease-mineral and bone disorder (CKD-MBD) and secondary hyperparathyroidism (HPT), scientists conducted a study where they used FGF23 antibodies to neutralize the effect of FGF23 using rat model. CKD-MBD rat models were fed on a high-phosphorus diet and were treated with either a high dose or a low dose of monoclonal FGF23 antibody. The results showed that treatment with the monoclonal FGF23 antibody inhibited the occurrence of HPT which decreased parathyroid hormone levels, increased vitamin D and calcium levels, and restored bone markers back to normal level [55]. Tumor-induced osteomalacia (TIO) is a type of a paraneoplastic condition recognized by hypophosphatemia resulting from renal phosphate wasting. Overexpression of FGF23 leads to TIO while mutations in the FGF23 gene cause autosomal dominant hypophoshatemic rickets [56]. FGF23 is a dynamic player of vitamin D and phosphate metabolism [57]. FGF23 stops the expression of Cytochrome P450 Family 27 Subfamily B Member 1 (CYP27B1) that encodes a protein which controls the production of $1,25(OH)_2D$. FGF23 also induces Cytochrome P450 Family 24 Subfamily A Member 1 (CYP24A1) expression that encodes an enzyme that acts to reduce $1,25(OH)_2D$ level [58]. A segment of FGF23 protein is divided into inactive N-terminal and C-terminal parts before or during the secretion process of FGF23.

hFGF1 structure

hFGF1 is the prototype member of fibroblast growth factor (FGF) family, a superfamily that promotes cell signaling. Human acidic fibroblast growth factor (hFGF1) is a 16 kDa, single-chain globular protein with characteristic β-trefoil fold consisting of six β-strand pairs, three of which form a six-stranded β-barrel structure [59]. Proteins that share the β-trefoil structure with

FGFs are the Kunitz soybean trypsin inhibitors, the ricin-like plant and bacterial toxins, interleukins, and various carbohydrate-binding proteins such as xylanase [60].

Sweet and coworkers were the first group to observe β -trefoil fold in the soybean trypsin inhibitor. β -trefoil structural architecture was then characterized by Chothia and group [61]. hFGF1 comprises of 12 β -strands that form 6 β -hairpins (Fig. 2). Overall β- trefoil structure of hFGF1 can be divided into a 6-stranded β-barrel, (top half, consisting of β-strands 1, 4, 5, 8, 9, and 12) and a β -hairpin triplet (bottom part, comprising of β-strands 2, 3, 6, 7, 10, and 11).

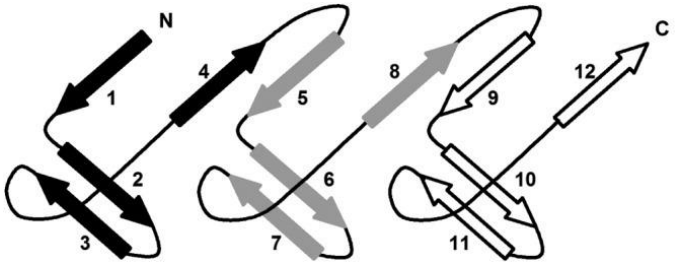

Fig. 2: Secondary structure of hFGF1. Twelve β-strands are folded into β-trefoil structure [59].

A central axis of 3-fold symmetry separates the barrel into three trefoil subdomains of approximately 40 amino acids each. hFGF1 structure is functionally divided into two parts - heparin binding and receptor binding [62]. The heparin binding region (β-strands 6-12) are more rigid and compact whereas the receptor binding part (β-strands 1-5).

Heparan Sulfate Glycosaminoglycan (HSGAG) binding and hFGF1-heparin interaction

FGFs are known for their potential biological functions such as cell proliferation and cell differentiation, but FGFs have a short half-life *in vivo* and are readily degradable. They bind to heparin present on the surface of cells. FGF signaling has been suggested to require heparin or heparin sulfate (HS) [5,6]. HS is a highly sulfated linear polymer of alternating glucuronate (GlcA) and N-acetylglucosamine (GlcNAc) monosaccharide units that undergo heterogenous

deacetylation (N-sulfation on GlcNAc and O-sulfation on both GlcA and GlcNAc). HS regulates FGF-FGFR signal transduction by stabilizing the FGF-FGFR binding, regulating FGF protein level in extracellular matrix (ECM), and also conferring protection to FGFs against thermal denaturation and proteolytic degradation [63]. In addition to facilitating the FGF-FGFR binding, HS also acts as a storage reservoir for ligand and determines the radius of ligand diffusion by controlling the gradients of paracrine FGFs in ECM. Amongst all the paracrine FGF subfamilies, FGF22 is the only FGF that does not bind to HS. All the other paracrine FGFs interact with HS with different affinities with FGF1, FGF2 and FGF7 having the highest binding affinity. The positively charged residues in the heparin binding pocket of hFGF1 interacts with the negatively charged heparin molecule. Heparin-binding site (HBS) in all FGFs is located within the core region and spans residues in the ß1- ß2 loop and ß9 to ß12 strands [13, 59]. SDM studies infer that charge reversal mutations of the lysine residues (K132, K127, K114, and K115) at the C-terminal of FGFs leads to loss of heparin binding affinity. Crystallographic and NMR studies confirm that residues 126-142 (present at the C-terminal) of hFGF1 is responsible for heparin binding. Interestingly the crystal structure contains no protein-protein interactions and each monomer binds the heparin sulfate groups on opposing sides of the polysaccharide [59].

Crystal structure data on the FGF-FGFR-HS ternary complex revealed that heparin promotes FGF signaling through the formation of a 2:2:2 and 2:2:1 (FGF: FGFR: HS) complex. Schlessinger *et al.*, reported a putative 2:2:2 complex formed between FGF2, FGFR1c, and deca-saccharide heparin (dp10) [64]. The positively charged residues in hFGF1 facilitating the heparin binding are K126, K127, N128, K132, R133, R136, and K142.

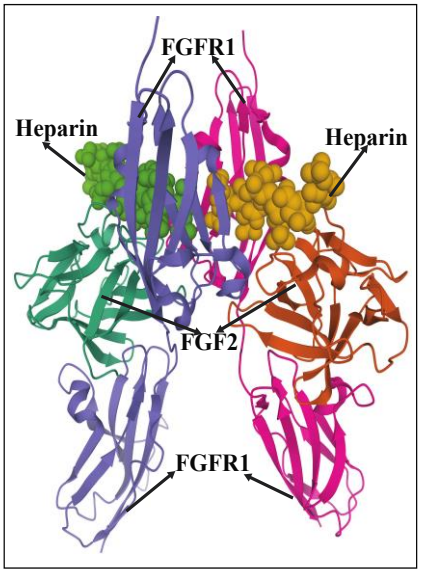

Fig. 3: The FGF2-FGFR1-heparin ternary complex. FGFR1 domains 2 (D2) and 3 (D3) are purple and magenta, respectively, and FGF1 is green and orange. The heparin molecule is in Corey-Pauling-Koltun (CPK) representation [12].

One half of this structure (1:1:1 complex) consists of a heparin chain bound to both FGF2 and FGFR1c, enhancing the ligand-receptor interaction (Fig. 3) [64]. The two 1:1:1 complex were then held together through direct receptor (FGFR1c) contacts, together with the secondary ligand-receptor (FGF2- FGFR1c) and heparin-receptor interactions. Contrary to this, Pellegrini *et al.*, pointed out a potential 2:2:1 FGF1-FGFR2c- deca-saccharide heparin (dp10) ternary complex structure in which a single heparin chain bridged the gap between two FGF1-FGFR2c complexes, making additional contacts with one of the receptor subunits [65].

Role of heparin in hFGF1-FGFR signaling

Heparin's role in hFGF1-FGFR interaction and subsequent activation is an ongoing topic of research. It is assumed that in addition to stabilizing hFGF1, heparin is also necessary for receptor binding and activation [66]. From the crystal structures obtained previously, it is evident that heparin plays a pivotal role in various biological processes, including hFGFR dimerization and FGFR activation [67, 68]. For hFGF1 dimerization and FGFR activation, binding of heparin

is crucial. In order to understand the biological activity of hFGF1, sucrose octasulfate (SOS), a mimic of heparin was used [69]. This study showed that the monomeric form maintained by hFGF1 retains its mitogenic activity to significant amounts, thereby inferring that oligomeric form of hFGF1 is not important for its biological functioning [69].

Angulo *et al.,* reported that length and sulfation patterns of glycosaminoglycans (such as heparin) has a considerable impact on the bioactivity of hFGF1 [70]. They also showed that dimerization of two hFGF1 monomers is not a mandatory step in hFGF1 activation. Their study uses two synthetic hexasaccharides with different sulfation patterns [71]. These hexasaccharaides bind to hFGF1 in its monomeric form. Numerous studies have reported that heparin is not an absolute requirement for the cell proliferation activity of hFGF1 [72]. Heparin is only known to stabilize the inherently unstable hFGF1 molecule. hFGF1 is known to have a short half-life *in vivo*. Culajay *et al.,* found that hFGF1 mutants, C30S, C97S, and C131S, increases the half-life of hFGF1, yet these mutants were found to decrease the thermal stability of the growth factor [73].

Apart from aiding in receptor activation, heparin also helps in stabilizing hFGF1 from thermal degradation. In order to validate this concept, site directed mutagenesis were performed on the growth factor. Out of all the variants generated on hFGF1, L58F exhibited considerable increase in the thermal stability of hFGF1 [62]. In a varied approach, three other individual substitutions (H35Y, H116Y, and F122Y) were tried and finally a quadruple mutant with L58F was generated. H35Y/H116Y/F122Y/L58F displayed 7.8°C increase in the thermal stability and also maintained the same mitogenic activity as wtFGF1 in spite of heparin independency [74]. Zakrzewska *et al.,* combined three other mutations to the quadruple mutant to form a septa mutant (H35Y/Q54P/S61I/L58F/H107G/H116Y/F122Y) to investigate if the inherent thermal

and proteolytic stability of hFGF1 can be further enhanced [75]. As a result of this study, it was found that the thermal stability of the septa mutant was 27°C higher than wtFGF1. Wong *et al.,* showed that substitution of lysine to glutamine at position 132 in the heparin binding site displays reduced heparin binding affinity, but still activates FGFR and induces early intermediate gene transcription [76]. Interestingly, in the absence of heparin a quadruple mutant with the K132E mutation plus the triple mutant Q54P/S61I/H107G was found to have mitogenic activity equivalent to heparin-bound wildtype hFGF1 [77]. These studies conclude that heparin is not mandatory for the biological activity of hFGF1.

One interesting study analyzing the intramolecular bonds of hFGF1 found that inclusion of disulfide bonds at the N and C terminal could yield better stabilization of the growth factor which led to the generation of K26C and P148C mutants [78]. These mutants were thought to form a disulfide bond and lead to increase in the inherent stability of the growth factor. Conversely, the mutants did exhibit increased thermal stability and mitogenic activity, in spite of no disulfide bond formation. In conclusion, numerous efforts have been taken to improve the thermal stability, proteolytic stability, and cell proliferation activity of the growth factor in a heparin independent manner, yet a substantial understanding still remains elusive.

Interestingly, several other mutations in hFGF1 such as K132E, cysteine mutations (C97S, C30S, C131S), H107G, and L58F have shown higher thermal stability, lack of heparin dependent FGF-FGFR activation. Except for K132E mutation, all the other hFGF1 variants exhibited higher mitogenic activity than wtFGF1 [79,80]. Studies have shown that hFGF1 can lead to endocrinization, which demonstrates that mitogenic activity of hFGF1 can be differentiated from the metabolic activity [81,82]. Xia *et al.,* and Huang *et al.,* have reported that phosphorylation of S116R and combination of K126D, K127Q, and K132E mutations lead to

decreased mitogenic activity but increased glucose-lowering activity. These variants of hFGF1 may be a potential therapeutic for type 2 diabetes [81,82].

Fibroblast Growth Factor Receptors (FGFRs)

There are only 18 FGFR ligands for the FGF family. FGF homologous factors (FHFs), FGF11, FGF12, FGF13, and FGF14, do not bind with the FGF receptors [7]. FGF ligands carry out their diverse functions by binding and activating the FGFR family of tyrosine kinase receptors in an HSGAG-dependent manner. FGFs exert their physiological roles through binding to FGFR and regulate developmental pathways, controlling events such as mesoderm patterning in the early embryo till the development of multiple organ systems. There are four FGFR (FGFR1–FGFR4) that encode receptors consisting of three extracellular immunoglobulin domains (D1–D3), a single-pass transmembrane domain and a split cytoplasmic tyrosine kinase domain [83]. FGFRs are expressed on many different cell types and regulate key cell behaviors, such as proliferation, differentiation, and survival, which make FGF signaling susceptible to subversion by cancer cells [84].

FGFRs consist of an acid box that includes an acidic, serine-rich sequence in the linker between the D1 and D2 domain. D1 domain of FGFR is responsible for receptor autoinhibition. The base of D2 domain helps in the binding of each FGF (ligand) to FGF receptors on the cell surface. Each FGF molecule interacts with the D2 domain of a second receptor through a secondary receptor binding site, and mutation of ligand residues within this site reduces receptor dimerization and signaling without affecting ligand-receptor binding [13]. The D2-D3 fragment is important for ligand binding and specificity. An exon-skipping mechanism removes the D1 domain or acid box leading to various isoforms of the receptor (FGFR1-FGFR3) whereas an alternative splicing process in the second half of D3 domain of FGFR1–3 yields b (FGFR1b–3b)

and c (FGFR1c–3c) isoforms that have distinct FGF binding specificities and are primarily epithelial and mesenchymal, respectively. Except for FGF1, all the other FGFs bind to epithelial or mesenchymal FGFRs and activate both the spliced isoforms. Now, HSGAGs come into play and bind to the ligand (FGFs), FGFRs dimerize, which enables the cytoplasmic kinase domains, in turn, trans phosphorylating and activating the A-loop tyrosines (Fig. 4). A-loop phosphorylation is followed by phosphorylation of tyrosines in the C tail, kinase insert and juxtamembrane regions [64]. The two main intracellular substrates of FGFR are PLCγ substrate 1 (also known as FRS1) and FGFR substrate 2 (also known as FRS2). Phosphorylation of an FGFR-variant tyrosine (Y766 in FGFR1) at the C tail of FGFR creates a binding site for the SH2 domain of PLCγ and is required for PLCγ phosphorylation, and activation, whereas FRS2 associates constitutively with the juxtamembrane region of the FGFR [85]. Phosphorylation of FRS2 is essential for activation of the Ras-MAPK and PI3K-AKT signaling pathways.

FGFR-FGF binding interface

hFGF-FGFR binding interface studies report that hFGF1 makes contacts with Ig domains, D2 and D3, along with the D2-D3 linker [9]. D1 and the serine rich linker between D1 and D2 inhibits FGF binding to the receptor. Additional reports suggest that mutant receptor proteins lacking D1 have a higher binding affinity for the ligands. Of all the other FGFs, studies related to hFGF1 will be discussed here to stay relevant to the aims of this project. Detailed study on FGFR-FGF interaction reveals that hFGF1 residues interacting with D2 are more conserved than the residues binding with the D3 domain of FGFR. Out of 140 residues, 39 residues of hFGF1 are involved in receptor binding. None of these 39 residues are located in the heparin binding site [86]. Crystallographic studies have demonstrated that mostly hydrophobic residues of hFGF1 interact with the D2 domain of the receptor. This includes residues Y29, G34, F36,

Y108, L147, and L149 of hFGF1 binding to K164, L166, A168, V169, and P170 of the D2 domain. Apart from hydrophobic interactions, electrostatic interactions also take place between residues R49 and R51 of FGF1 and E163 and D247 of the D2 domain, respectively [65]. Moreover, interactions occurring in the D2-D3 linker region is a hydrogen bond interaction between N109 of FGF1 and R251 of the linker region. Interactions between hFGF1 and D3 domain of the receptor involves both electrostatic and hydrophobic interactions. An electrostatic interaction occurs between E101 of hFGF1 and R255 of the D3 domain, whereas hydrophobic interactions happens between I257 of D3 domain and L103 and H107 of hFGF1 [65].

Study of the 2:2 FGF1:FGFR2 complex (PDB 1DJS) in the absence of heparin reveals that the D2 and D3 domain of the FGFR make contacts with both the ipsilateral and contralateral FGF1 ligand yet no ligand-ligand contacts are reported. Heparin bound FGF-FGFR dimer structural complex can be symmetrical and asymmetrical. Study of the decasaccharide heparin bound FGF1:FGFR complex (PDB 1E0O) shows that heparin binds to hFGF1 (residues 126-142) through the heparin-binding region with further contacts between residues V175, H167, K164, T174, K176, R178, and K161 of the D2 domain of FGFR and heparin [86].

FGF-FGFR regulation and signaling pathway

HSGAG dependent FGF-FGFR binding leads to receptor dimerization and trans-autophosphorylation of the tyrosine receptor. During the receptor activation of the tyrosine kinase domain of FGFR1, the six tyrosine residues (Y653, Y583, Y463, Y766, Y585, and Y654) are phosphorylated [83]. As tyrosine's are phosphorylated, the receptor activity increases by many folds. The phosphorylation of Y653 increases activity by 50-100 folds. Followed by the phosphorylation of Y653. Other tyrosine residues (Y583, Y463, Y766, Y585, and Y654) are phosphorylated, resulting in an overall 500-1000 fold increase in the receptor kinase activity.

Phosphorylation of above six tyrosine residues accounts for the tyrosine kinase activity but not for the STAT3 and PLCγ binding. Therefore, phosphorylation of the two additional tyrosine residues - Y677 and Y766 are needed [85]. Activated FGFR initiates the major downstream intracellular signaling pathways such as RAS-MAPK, PI3K-AKT, PLCγ, and Signal Transducer and Activator of Transcription (STAT) [1]. Of these signaling pathways, activation of RAS-MAPK and PI3K-AKT pathways are mediated by phosphorylation of FGF receptor substrate 2α (FRS2α). Phosphorylation of Y463 and the presence of CRK Like Proto-Oncogene, Adaptor Protein (CRKL) facilitates the phosphorylation of FRS2α. Phosphorylated FRS2α also binds to the membrane-anchored adaptor protein, growth factor receptor-bound 2 (GRB2), and the SH2 domain-containing protein tyrosine phosphatase-2 (SHP2) [87]. This finally leads to activation of the RAS-MAPK and PI3K-AKT signaling pathway. RAS-MAPK signaling pathway stimulates expression of several genes through phosphorylation of E26 transformation-specific (ETS) transcription factors, which regulates the DNA interaction and gene expression [88] (Fig. 3). On the other side, PI3K-AKT pathway inhibits the function of forkhead box class transcription factor (FOXO1) and cytosolic tuberous sclerosis complex 2 (TSC2) [89]. PLCγ pathway, when activated by the FGFRs, leads to the hydrolysis of phosphatidylinositol 4,5-bisphosphate which produces inositol triphosphate (IP_3) and diacylglycerol (DAG). IP_3 subsequently regulates the subcellular calcium ion levels and DAG transduces the signal to the protein kinase C (PKC). FGF-FGFR interaction also phosphorylates STAT1, STAT3, and STAT5, to regulate the STAT pathway target gene expression (Fig. 4).

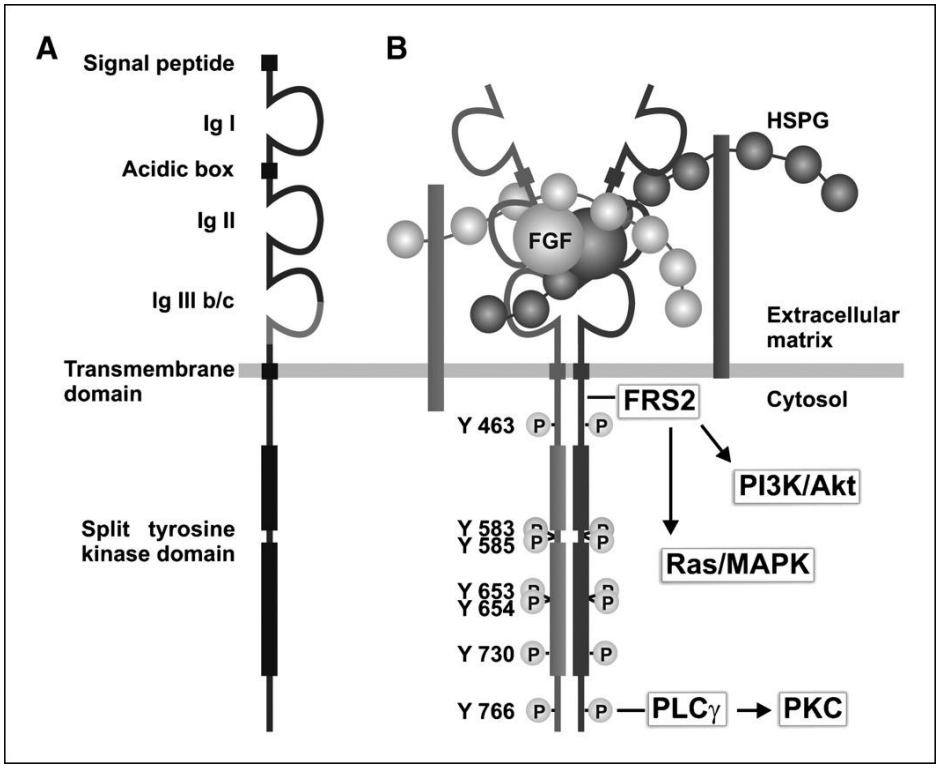

Fig. 4: (A) A cartoon representation of the FGFR structure. The splicing of the third Ig domain in FGFR1, FGFR2, and FGFR3 gives rise to Ig IIIb and Ig IIIc isoforms. (B) A schematic depiction of FGF-FGFR signaling cascade. Upon binding of HSGAGs to FGF, FGFRs are activated. Heparin promotes FGF signaling through the formation of a 2:2:2 and 2:2:1 (FGF: FGFR: HS) complex. This leads to receptor autophosphorylation and activation of downstream signaling pathways [88].

FGFR2 consists of three extracellular immunoglobulin (Ig)-like domains, a single transmembrane domain, and two tyrosine kinase domains in the cytoplasmic region. In particular, the formation of FGF2-FGFR2 complex involves two Ig-like ligand-binding domains (D2 and D3 domains) of FGFR2. Similar to FGFR1, autophosphorylation of receptor tyrosine residues in cytoplasmic domains contribute to the docking of the signaling molecules which include, Src homology2 (SH2) domain proteins. The binding of SH2 domain-containing proteins have been demonstrated in activation of MAPK pathways. Seven phosphorylation sites in the cytoplasmic domain including Y463, Y583, Y585, Y653, Y654, Y730, and Y766 have been identified in FGFR1 which are also well-conserved in FGFR2. Phosphorylation of FGFR2

occurs on serine 779 (S779) in response to FGF2 [90]. S779 is situated adjacent to the phospholipase Cγ binding Site, at Y766, and contributes to a putative binding site for the 14-3-3 phosphoserine-binding proteins. S779 is found to be essential for the potential activation of PI3K and Ras/MAPK pathways. Furthermore, it has been demonstrated that S779 signaling is also important for proliferation in both Ba/F3 (interleukin (IL)-3 dependent, hematopoietic) and BALB/c 3T3 fibroblast cells. GRB2 directs the regulation of receptor tyrosine kinase (RTK) FGFR2 and SHP2. A recent study by Ahmed *et al.,* suggested that FGFR2 cycles between its partially phosphorylated and its SHP2- dephosphorylated state(s) [91]. To determine the significance of the six conserved tyrosine molecules in intracellular domain of FGFR3 for signaling, activated mutant K650E-FGFR3 was constructed. It was found that K650E mutation renders constitutive kinase activation and regulates activation of various FGFR3 signaling cascades. Function of Y724 is also important for its role in phosphatidylinositol 3-kinase activation, and phosphorylation of SHP2, MAPK, STAT1, and STAT3 [92]. In addition, tyrosine phosphorylation of SH2-Bβ was observed when co-expressed with one weakly activated (N540K-FGFR3) and a strongly activated (K650E-FGR3) mutants. Two phosphorylation sites of FGFR3 are identified, Y724 and Y760, which are necessary for the binding of the SH2 domain(s) of SH2-Bβ. In this context, phosphorylation and nuclear translocation of STAT5, and activated FGFR3 promotes elevated expression of SH2-Bβ [93].

Aberrations of FGFR Signaling

Binding specificity of FGF-FGFR depends on the variability in the primary sequence of 18 FGFs and the 4 FGFRs. The different isoforms formed due to splicing display tissue specificity. For example, isoforms b and c are expressed usually in the epithelial tissue and mesenchymal tissue, respectively and the corresponding ligands trigger the receptors on the other

tissues. An exception to this is FGF1, which binds to both b and c isoforms of certain FGFRs. Anomalies in the binding specificity can lead to pathological or diseased conditions such as, cancer. Analyses of structural characteristics of FGF1, FGF2, FGF8, and FGF10 with their cognate FGFRs display variation at the β1 strand length of the N-terminal region and the alternatively spliced regions in D3 dictate their binding specificities [13]. Several evidences suggest that FGFR activating mutation, overexpression, and aberrant activation of the RTK signaling system can lead to excessive cell proliferation, angiogenesis, cancer, and other pathophysiological changes.

Factors Influencing Specific Aberrations in FGFR Signaling

Fusion of FGFR Genes

Fusion genes are formed by the rearrangement of two independent genes and can occur as a result of chromosomal translocation and inversion. FGFR gene fusions play an important role in lung squamous cell cancer, oral cancer, thyroid cancer, gall bladder cancer and glioblastoma with intact kinase domains. The FGF signaling is involved in cancer, resulting from hematological malignancies. N terminus of a transcription factor of FGFR chromosomal translocations in a fusion protein is fused to an FGFR kinase domain, leading to a kinase activation. Most of the FGFR1 fusion proteins are identified in patients with the myeloproliferative disorder stem cell leukemia/lymphoma syndrome (SCLL/8p11 myeloproliferative syndrome) [94]. Studies have shown that 3′ gene fusions of FGFR1 and FGFR3 are related to myeloproliferative disorder and peripheral T-cell lymphoma, respectively. 8p11 myeloproliferative syndrome (EMS), a hematopoietic stem cell disorder is related to chromosomal translocations of fusion genes, namely zinc finger 198-FGFR1. It has been demonstrated that zinc finger 198-FGFR1 induces EMS-like disease in mice, with

myeloproliferation and T lymphoma [95]. Recently, several fusion genes of FGFR1-3 along with transforming acidic coiled coil containing protein 1 (TACC1), Transforming acidic coiled coil containing protein 3 (TACC3), BAR/IMD Domain Containing Adaptor Protein 2 Like 1 (BAIAP2L1), *BicC* Family RNA Binding Protein *1* (BICC1), and adenosylhomocysteinase like 1 (AHCYL1) have been identified in multiple malignancies including glioblastoma, urothelial bladder and cholangiocarcinoma [96]. Singh *et al.,* reported that FGFR1 and FGFR3 gene fusions with TACC1 and TACC3 have been identified in approximately 3% of the tumor glioblastoma multiforme (GBM) [97]. It has been demonstrated that the abnormal localization of fusion protein to mitotic spindle poles induces mitotic and chromosomal segregation defects. FGFR3-TACC3 fusion gene was identified in a subset of bladder carcinomas [98].

Overexpression and Amplification of FGFR

Overexpression of FGFRs may lead to ligand independent FGFR signaling and is mainly caused by focal amplifications. Overexpression of FGFRs are associated with the development of several cancers such as lung cancer, brain cancer, prostate cancer, liver cancer, and MM along with angiogenesis around the tumor. Overexpression of FGFR may either be due to dysregulation of transcription or chromosomal amplification. Underlying mechanism of FGFRs overexpression in the development of cancer still remains elusive. FGFR1 is found to be amplified in approximately 18% of osteosarcoma, 7% to 20% of squamous non-small cell lung carcinoma, 6% of small cell lung carcinoma, and 14% of breast cancer in the chromosomal region 8p11-12 [99]. It has also been suggested that activation of FGFR1 in the non-transformed human mammary cell line resulted in cellular transformation which is evidenced by epidermal growth factor-independent cell growth, cell proliferation, loss of cell polarity, and epithelial-to-mesenchymal transition [100]. In the case of breast cancers, amplification of FGFR1and/or

11q12-14 has been identified in the chromosomal region containing cyclin D1 (CCND1) and amplification of several FGFs (FGF3, FGF4 and FGF19) have been found in 23% of hormone receptor-positive (HR+) breast cancer, 27% of human epidermal growth factor receptor 2 (HER2) breast cancer, and 7% of triple-negative breast cancer [101]. Triple negative breast cancer (TNBC) might carry amplification of FGFR2 in 6 out of 165 (3.6%) cases. This type of breast cancer is very aggressive and respond poorly to the conventional therapeutic measures. [102]. In addition, FGFR2 gene amplification and protein overexpression has been detected in 2/51 breast cell lines, out of which MFM223 and SUM52PE are the TNBCs. This amplification of FGFR2 exerts effect on the activation of PI3K-AKT downstream signaling pathway, resulting in inhibition of apoptosis. The FGFR2 amplification is hypersensitive to FGFR-targeted therapy and is detected in 3% to 25% of gastric cancers [103]. Many reports have demonstrated that overexpression of FGFR4 is associated in the development of several cancers including colon, liver and prostate. According to a study on the conditional knockout mouse, prostrate organogenesis and androgenic dependency and homeostasis depends largely on the presence of FGFR2. Studies have also shown that in early stages of prostate cancer, in particular when the prostatic intraepithelial neoplasia carcinoma is *in situ* of the prostate, there is an evidence of non-regulated FGF/FGFR signaling. Defective FGF/FGFR signaling has been implicated as a mechanism for the occurrence of epithelial carcinoma and prostate cancer. The growth and progression of gastric cancer requires the activation of the FGFR2 pathway with FGFR2 gene amplification reported both *in vitro* and *in vivo*. FGFR2 gene has two different isoforms; FGFR2b and FGFR2c. The gene undergoes alternative splicing in the third immunoglobulin domain resulting in those two isoforms with different FGF ligand binding. FGFR2b isoform has been specifically found to be overexpressed in FGFR2 induced gastric cancer. About 8% of

gastroesophageal cancers display amplification of FGFR2 gene. FGFR1 gene is over-amplified in lung cancer and estrogen receptor-positive breast cancer. The FGFR gene is also involved in different translocations in hematological malignancies like myeloid and lymphoid cancer wherein the immature cells never mature, consequently preventing proliferation. FGFR gene expression also induces sarcoma tumors such as Ewing's sarcoma, alveolar rhabdomyosarcoma, and angiosarcoma, and FGFR-3 causes multiple myeloma and T-cell lymphoma. Amplification in FGFR4 gene has been detected in approximately 7-8% of rhabdomyosarcoma patients [104]. Both FGF19 and FGFR4 are found to be overexpressed in the patients with hepatocellular carcinoma (HCC) and therapeutically potential inhibitor of FGF19/FGFR4 are considered to be effective for the patients suffering from HCC [105].

FGFR-activating Mutations

A number of FGFR activating point mutations are connected with various types of cancers such as: liver cancer, bladder cancer, renal cell carcinoma, prostate cancer, lung cancer, and breast cancer [106]. Specific aberrations in FGFR signaling have been identified which are summarized as below:

- Overexpression of FGFR due to gene amplification or post-transcriptional activation
- FGFR mutated form induce dimerization and thus produce receptors which are either constitutively active or exhibit an independent ligand binding for activation
- Chromosomal translocations resulting in expression of FGFR-fusion proteins with constitutive FGFR kinase activity
- Alternative splicing of FGFR and isoform switching changes the binding affinity with FGF ligands and as a consequence, it triggers the tumor growth of FGFs

- Elevated levels of FGF in cancer cells and substantial release of FGFs from the extracellular matrix, resulting in paracrine/autocrine activation

Studies reported on FGFR-activating mutations and the related diseases are summarized below:

FGFR1: According to the catalog of somatic mutations in cancer (COSMIC) data**,** five FGFR1 mutations are most commonly identified [107]. However, functions of only two mutations (N546K and K656E) are known. In addition, a proline to arginine mutation in IgII-IgIIIa linker is associated with mild Pfeiffer syndrome in FGFR1. The most notable FGFR1 mutated forms are Y99C and C277Y which have been detected in Kallmann syndrome [108]. Also, a constitutively active mutant of FGFR1 expression has been implicated in the development of prostate carcinoma lesion. The FGFR1 mutations are highly applicable in the drug-targeted development. Various other mutations of FGFRs have been detected in solid tumors related cancer cells.

FGFR2: FGFR2 mutations have been detected in 12 to 14% of endometrial cancer. According to the COSMIC data, 12 mutations have been identified. Among these mutations, 7 activating mutations are reported including P253R, N549K and S252W [109]. There are two particularly notable mutation sites in FGFR2. First, a cysteine to glycine mutation in IgIII domain causing apert and crouzon syndrome in FGFR2. Second, a conserved proline residue in the linker between the IgII and IgIII extracellular domain of FGFR2 frequently mutating to arginine and causing apert syndrome [110].

FGFR3: The first reported mutation of FGFR3 was Gly→Arg missense mutation (G380R) in its transmembrane domain, resulting in achondroplasia [111]. Naski *et al.,* reported that the mutated form (R248C) of FGFR3 in the extracellular domain or introduction of K650E substitution in the tyrosine kinase (TK) domain causes the autosomal dominant human skeletal disorders,

hypochondroplasia, achondroplasia and thanatophoric dysplasia. It has been demonstrated through the ligand-independent receptor tyrosine kinase phosphorylation and cell proliferation studies that R248C and K650E mutations activate the FGFR3 receptor [112]. Ser→Cys (S365C), a FGFR3-activating variant has been found to cause dwarfism. It has been observed that S365C mutation could lead to downregulation of expression of the Indian hedgehog and parathyroid hormone-related protein receptor genes, which ultimately reduces bone growth [113]. FGFR3 activating mutations have been identified in thanatophoric dysplasia. Among three FGFR3 mutations (G370C, S371C, and Y373C), the two common mutations are G370C and S371C. It has been observed that G370C and S371C induce receptor dimerization and activation [114]. FGFR3 activating mutations have also been identified in various urothelial cell carcinomas (UCC). The expression of K652E FGFR3 in normal urothelial cell results in constitutive phosphorylation. The role of K652E FGFR3 in the kinase domain is still unclear. Martino *et al.*, described that K652E mutation was not connected with the receptor dimerization as compared to the other two mutants. It might be essential for the physical interaction with some downstream signaling effector or for trans-phosphorylation of some tyrosine residues, such as Y762 [115]. A study by Ahmad *et al.*, suggests that K644E FGFR3 variant is not related to UCC [116]. The mutations in the kinase domain including N540S, K650E, K650M, K650N, K650Q, and K650T are rarer. FGFR3 gene mutations are also spotted in bladder cancer [117].

FGFR4: Different FGFR4 activating mutations in the kinase domain have been reported in 7-8% of rhabdomyosarcomas, associated with advanced stage cancer and poor survival. Two of them (N535K and V550E) occur at the auto-phosphorylation site, and thus induce constitutive activation of the receptor. FGFR4 gene mutations are spotted in sarcomas.

FGFRs mutations have been linked to various types of cancers. Correcting these mutations, plausibly through gene therapy, can be expected to be a reliable treatment for cancers ascribed to the FGFR mutations.

Therapeutic applications of FGF

Dysregulation of FGF signaling can lead to a variety of human conditions, such as cancer, ineffective wound healing, metabolic syndrome, chronic kidney disease, and cardiovascular diseases [118]. Tissue injury involves a complicated repairing process by which some organisms can lead to complete regeneration of tissues. In the case of mammals, injury to most tissues leads to scar formation [119]. Reparations and regeneration are demonstrated by a large number of cytokines and growth factors. FGFs are the most effective growth factors that control organogenesis and tissue homeostasis [120]. Since early 1980s, the US Wound Healing Society and European Wound Management Association recommended FGFs for the treatment of refractory ulcers. Some pharmaceutical companies such as Amgen, Merck, and Lilly have significantly invested in the development of FGF-based drugs. Amongst the FGF family, FGF1, FGF2, FGF7 (or keratinocyte growth factor 1 (KGF1)), and FGF10 (or keratinocyte growth factor 2 (KGF2)) are integral to cutaneous wound healing [2].

There is a wide range of developing clinical applications for many different FGFs; however, to stay relevant to the aims of this project, only those pertaining to hFGF1 will be examined. FGF1 serves as a mitogen for different cell types [84]. However, FGF1/FGF2 double-knockout mice do not exhibit any of the observable aberrations. These results suggest that the developmental and physiological roles of FGF1 are highly restricted [121]. Immunohistochemical methods showed that expression of the FGF1 protein was undetectable in intact skin, but it was mainly localized in higher amounts near the wound area and lesser at the

edges. Moreover, in skin wounds, healing proteins were found in vast quantities around the injury site and were produced by damaged inflammatory cells such as macrophages and non-inflammatory cells such as endothelial cells. However, it has been shown that addition of growth factors, including FGF1, to chronic wounds, can speed up the wound healing process and enhance wound closure [122]. FGF1 has been effectively used as a possible therapy in many cases that are characterized by damaged or diseased cells that require tissue regeneration such as skin, nerves, blood vessels, and bone tissue. FGF1 promotes the migration of fibroblast and keratinocyte cells to the wound area and accelerates the rate of angiogenesis, granulation, and epithelialization processes [123]. Improvement in the deep burn wound along with an acceleration in the healing time has been reported after applying recombinant human FGF1 (rh-FGF1) at the injured site [124]. In China, rh-FGF1 was marketed specifically to cure the deep second-degree burn wounds and chronic ulcers such as flat residual traumatic wounds, diabetic ulcers, vascular ulcers, and bedsores [125]. The efficacy of the topical rh-FGF1 for treatment of deep partial-thickness burn or skin graft donor sites was investigated by a randomized, multicenter, double-blind, and placebo-controlled clinical trial [125]. Results showed that the healing of burn wounds and skin graft donor sites treated by rh-FGF1 was significantly higher than that observed in the placebo. Also, the mean healing time of burn wounds and skin graft donor sites in the rh-FGF1 group was significantly shorter than that observed in the placebo group. FGF1 has been used as a potential therapeutic to treat spinal cord injury and to assist healing of deep burns or skin graft donor sites [125]. Several pharmacological and *in vitro* studies have suggested that FGF1 maintains the integrity/function of the myocardium by acting on the cardiomyocytes. Several pre-clinical studies have demonstrated that FGF1 is a promising therapeutic strategy to improve myocardial survival and cardiac function, but there are several

issues that complicate the clinical application of FGFs for acute myocardial infarction. One of the issues is its interaction with heparin; exogenous heparin treatment, either with unfractionated or low molecular weight (enoxaparin), is standard medical practice for patients with acute myocardial infarction (MI). Thus, findings by Huang *et al.*, demonstrate that FGF1 mutant with reduced heparin binding affinity may be a promising strategy for acute treatment of MI; yet, future studies are needed to address its long-term effects, post-MI [126]. FGF1 is also known to act as an anti-diabetic agent. High-calorie diet might lead to an increase in insulin resistance, and cause metabolic syndrome, obesity, type 2 diabetes mellitus (DM), and hypertension. However, aggravating metabolic conditions reduce the neurogenic potential of hypothalamic neuro progenitor cells, which contribute to a decreased central glucose sensing and peripheral glucose clearance. Potentially, FGF1 remedies the debilitated hypothalamic state in DM by restoring the number of glucose-sensing neurons, inducing neurogenesis, suppressing reactive astrocytes and restoring synaptic functionality, which ultimately leads to the observed restoration of normoglycemia. FGF1 with low mitogenic variants came up as an important candidate in restoring euglycemia and did not lead to any side effects. The peripheral administration of FGF1 need hours to reach the normal glucose levels without facing hypoglycemic risk [127].

FGFs are modified either by adsorption or encapsulation within materials to ensure elevated biological activity in a well-regulated manner. Several materials have been formulated to carry the FGF drug and reduce their therapeutic ability and bioavailability, still, there is an immense need to develop a more sustained and targeted drug delivery system.

Focus of this project

hFGF1 uniquely binds to all the four types of FGFRs and therefore it is often referred to as a universal ligand. hFGF1 enhances proliferation of fibroblasts and embryonic cells, thereby

regulating wound healing and angiogenesis. However, one of the disadvantages in using hFGF1 as a therapeutic agent is its low thermodynamic stability and short half-life *in vivo*. It is known that specific binding to negatively charged heparin sulfate proteoglycans (HSPGs) increases the stability of hFGF1. Nevertheless, the role of heparin in stabilization of hFGF1 and activation of FGF-FGFR induced cell signaling has been a subject of debate. There have been reports which show that heparin is essential for the cell proliferation activity of hFGF1 [26-29]. In marked contrast, there are studies which show that the role of heparin is only restricted to conferring stability to the growth factor. In this context, this project is divided into four distinct aims: 1) overexpression, purification and characterization of the hFGF1 variants leading to the design of a hyperstable and bioactive acidic fibroblast growth factor 2) design of a heparin independent human acidic fibroblast growth factor variant 3) characterization of the structural forces governing the reversibility of the unfolding of the human acidic fibroblast growth factor 4) stability of sFGF1 with respect to the fluctuating pH conditions, aliphatic alcohols, and cell culture media.

The first and second studies aim to enhance the inherent thermal stability, resistance to proteases, and mitogenic activity of wtFGF1 using site directed mutagenesis. These mutations were made on wtFGF1 as single, double, triple, quadruple, and penta mutants at positions 136, 126, 54, 61, and 107 (R136E, K126N, Q54P, S61L, and H107S). Two of these mutations (R136E and K126N) belong to the heparin binding pocket so it was predicted that introduction of negative charges in the heparin binding pocket would reduce the electrostatic interaction between the dense cluster of positive charges and lead us to better understand of the role of heparin in hFGF1 activation and cell signaling. Isothermal titration calorimetry and bioactivity assay results have concluded that heparin binding is not mandatory for hFGF1 to perform its biological

function. Heparin only aids in stabilization of the growth factor. These two studies lead to generation of a hyper stable and heparin independent hFGF1 variant (sFGF1). sFGF1 is anticipated to be more effective in treating variety of biomedical conditions, including wound healing.

The third study aims at comprehending the effects of single, double and triple variants (R136E, K126N, Q54P) on the conformational stability and reversible unfolding of hFGF1. Equilibrium unfolding process of hFGF1 is irreversible and is known to exist in partially unfolded state(s) close to physiological pH and temperature. This specific aim involves the use of biophysical techniques like circular dichroism and fluorescence spectroscopy, nuclear magnetic resonance, and molecular dynamics simulations to characterize the structural determinants involved in refolding of the triple variant of hFGF1. The results obtained from these studies could provide valuable clues in designing drugs against large number of amyloid diseases.

The last chapter focusses on studying sFGF1's ability to sustain conformational fluctuations at varied pH conditions, resistance to proteases in DMEM cell culture media, and stability in different aliphatic alcohols (ethanol, 2,2,2- trifluoroethanol (TFE), and acetonitrile). Results of these studies might be useful for many biomedical applications, including drug delivery and tissue engineering.

REFERENCES

[1] Itoh N, Ornitz DM. Fibroblast growth factors: from molecular evolution to roles in development, metabolism and disease. The Journal of Biochemistry. 2011 Feb 1;149(2):121-30.

[2] Hui Q, Jin Z, Li X, Liu C, Wang X. FGF family: from drug development to clinical application. International journal of molecular sciences. 2018 Jul;19(7):1875.

[3] Itoh N, Ornitz DM. Evolution of the Fgf and Fgfr gene families. TRENDS in Genetics. 2004 Nov 1;20(11):563-9.

[4] The Universal Protein Resource. The Universal Protein Resource for fibroblast growth factor-15 in mouse. Available at: https://www.uniprot.org/uniprot/O35622.

[5] Kerr R, Agrawal S, Maity S, Koppolu B, *et al*. Design of a thrombin resistant human acidic fibroblast growth factor (hFGF1) variant that exhibits enhanced cell proliferation activity. Biochemical and biophysical research communications. 2019 Oct 15;518(2):191-6.

[6] Davis JE, Alghanmi A, Gundampati RK, *et al*. Probing the role of proline− 135 on the structure, stability, and cell proliferation activity of human acidic fibroblast growth factor. Archives of biochemistry and biophysics. 2018 Sep 15;654:115-25.

[7] Ornitz DM, Itoh N. Fibroblast growth factors. Genome biology. 2001 Mar;2(3):reviews3005-1.

[8] Wang YC, Peterson SE, Loring JF. Protein post-translational modifications and regulation of pluripotency in human stem cells. Cell research. 2014 Feb;24(2):143-60.

[9] Ornitz DM, Itoh N. The fibroblast growth factor signaling pathway. Wiley Interdisciplinary Reviews: Developmental Biology. 2015 May;4(3):215-66.

[10] Olsnes S, Klingenberg O, Wie¸ dłocha A. Transport of exogenous growth factors and cytokines to the cytosol and to the nucleus. Physiological reviews. 2003 Jan 1;83(1):163-82.

[11] Planque N. Nuclear trafficking of secreted factors and cell-surface receptors: new pathways to regulate cell proliferation and differentiation, and involvement in cancers. Cell Communication and Signaling. 2006 Dec 1;4(1):7.

[12] Bouleau S, Grimal H, Rincheval V, Godefroy N, Mignotte B, Vayssiere JL, Renaud F. FGF1 inhibits p53-dependent apoptosis and cell cycle arrest via an intracrine pathway. Oncogene. 2005 Nov;24(53):7839-49.

[13] Beenken A, Mohammadi M. The FGF family: biology, pathophysiology and therapy. Nature reviews Drug discovery. 2009 Mar;8(3):235-53.

[14] Li Y, Sun C, Yates EA, Jiang C, Wilkinson MC, Fernig DG. Heparin binding preference and structures in the fibroblast growth factor family parallel their evolutionary diversification. Open biology. 2016 Mar 1;6(3):150275.

[15] Thallapuranam SK, Agarwal S, Gindampati RK, Jayanthi S, Wang T, Jones J, Kolenc O, Lam N, Niyonshuti I, Balachandran K, Quinn K, inventors. Engineered fgf1 and fgf2 compositions and methods of use thereof. United States patent application US 16/356,872. 2019 Sep 19.

[16] Abraham JA, Whang JL, Tumolo A, *et al*. Human basic fibroblast growth factor: nucleotide sequence and genomic organization. The EMBO Journal. 1986 Oct 1;5(10):2523-8.

[17] Bing M, Da-Sheng C, Zhao-Fan X, *et al*. Randomized, multicenter, double-blind, and placebo-controlled trial using topical recombinant human acidic fibroblast growth factor for deep partial-thickness burns and skin graft donor site. Wound repair and regeneration. 2007 Nov;15(6):795-9.

[18] Higgins CA, Petukhova L, Harel S, Ho YY, Drill E, Shapiro L, Wajid M, Christiano AM. FGF5 is a crucial regulator of hair length in humans. Proceedings of the National Academy of Sciences. 2014 Jul 22;111(29):10648-53.

[19] Kook SH, Jeon YM, Lim SS, Jang MJ, Cho ES, Lee SY, Choi KC, Kim JG, Lee JC. Fibroblast growth factor-4 enhances proliferation of mouse embryonic stem cells via activation of c-Jun signaling. PloS one. 2013 Aug 13;8(8):e71641.

[20] Suzuki S, Ota Y, Ozawa K, Imamura T. Dual-mode regulation of hair growth cycle by two Fgf-5 gene products. Journal of investigative dermatology. 2000 Mar 1;114(3):456-63.

[21] Armand AS, Laziz I, Chanoine C. FGF6 in myogenesis. Biochimica et Biophysica Acta (BBA)-Molecular Cell Research. 2006 Aug 1;1763(8):773-8.

[22] Zinkle A, Mohammadi M. Structural biology of the FGF7 subfamily. Frontiers in Genetics. 2019 Feb 12;10:102.

[23] Itoh N, Ornitz DM. Functional evolutionary history of the mouse Fgf gene family. Developmental dynamics: an official publication of the American Association of Anatomists. 2008 Jan;237(1):18-27.

[24] Rohmann E, Brunner HG, Kayserili H, Uyguner O, Nürnberg G, Lew ED, Dobbie A, Eswarakumar VP, Uzumcu A, Ulubil-Emeroglu M, Leroy JG. Mutations in different components of FGF signaling in LADD syndrome. Nature genetics. 2006 Apr;38(4):414-7.

[25] Osslund TD, Syed R, Singer E, Hsu EW, Nybo R, Harvey T, Arakawa T, Narhi LO, Chirino A, Morris CF, Chen BL. Correlation between the 1.6 Å crystal structure and mutational analysis of keratinocyte growth factor. Protein Science. 1998 Aug;7(8):1681-90.

[26] Friedl A, Chang Z, Tierney A, Rapraeger AC. Differential binding of fibroblast growth factor-2 and-7 to basement membrane heparan sulfate: comparison of normal and abnormal human tissues. The American journal of pathology. 1997 Apr;150(4):1443.

[27] Tsai SM, Wang WP. Expression and function of fibroblast growth factor (FGF) 7 during liver regeneration. Cellular Physiology and Biochemistry. 2011;27(6):641-52.

[28] Kim N, Yamamoto H, Pauling MH, Lorizio W, Vu TH. Ablation of lung epithelial cells deregulates FGF-10 expression and impairs lung branching morphogenesis. The Anatomical Record: Advances in Integrative Anatomy and Evolutionary Biology: Advances in Integrative Anatomy and Evolutionary Biology. 2009 Jan;292(1):123-30.

[29] Ware LB, Matthay MA. Keratinocyte and hepatocyte growth factors in the lung: roles in lung development, inflammation, and repair. American Journal of Physiology-Lung Cellular and Molecular Physiology. 2002 May 1;282(5):L924-40.

[30] Tong L, Zhou J, Rong L, *et al*. Fibroblast growth factor-10 (FGF-10) mobilizes lung-resident mesenchymal stem cells and protects against acute lung injury. Scientific reports. 2016 Feb 12;6(1):1-2.

[31] Terauchi A, Johnson-Venkatesh EM, Bullock B, Lehtinen MK, Umemori H. Retrograde fibroblast growth factor 22 (FGF22) signaling regulates insulin-like growth factor 2 (IGF2) expression for activity-dependent synapse stabilization in the mammalian brain. Elife. 2016 Apr 15;5:e12151.

[32] Boylan M, Anderson MJ, Ornitz DM, Lewandoski M. The Fgf8 subfamily (Fgf8, Fgf17 and Fgf18) is required for closure of the embryonic ventral body wall. Development. 2020 Nov 1;147(21).

[33] Falardeau J, Chung WC, Beenken A, Raivio T, Plummer L, Sidis Y, Jacobson-Dickman EE, Eliseenkova AV, Ma J, Dwyer A, Quinton R. Decreased FGF8 signaling causes deficiency of gonadotropin-releasing hormone in humans and mice. The Journal of clinical investigation. 2008 Aug 1;118(8):2822-31.

[34] Sunmonu NA, Li K, Li JY. Numerous isoforms of Fgf8 reflect its multiple roles in the developing brain. Journal of cellular physiology. 2011 Jul;226(7):1722-6.

[35] Olsen SK, Li JY, Bromleigh C, Eliseenkova AV, Ibrahimi OA, Lao Z, Zhang F, Linhardt RJ, Joyner AL, Mohammadi M. Structural basis by which alternative splicing modulates the organizer activity of FGF8 in the brain. Genes & development. 2006 Jan 15;20(2):185-98.

[36] Lewandoski M, Meyers EN, Martin GR. Analysis of Fgf8 gene function in vertebrate development. InCold Spring Harbor symposia on quantitative biology 1997 Jan 1 (Vol. 62, pp. 159-168). Cold Spring Harbor Laboratory Press.

[37] Cholfin JA, Rubenstein JL. Patterning of frontal cortex subdivisions by Fgf17. Proceedings of the National Academy of Sciences. 2007 May 1;104(18):7652-7.

[38] Ohbayashi N, Shibayama M, Kurotaki Y, Imanishi M, Fujimori T, Itoh N, Takada S. FGF18 is required for normal cell proliferation and differentiation during osteogenesis and chondrogenesis. Genes & development. 2002 Apr 1;16(7):870-9.

[39] Fon Tacer K, Bookout AL, Ding X, Kurosu H, John GB, Wang L, Goetz R, Mohammadi M, Kuro-o M, Mangelsdorf DJ, Kliewer SA. Research resource: comprehensive expression atlas of the fibroblast growth factor system in adult mouse. Molecular endocrinology. 2010 Oct 1;24(10):2050-64.

[40] Hotta Y, Sasaki S, Konishi M, Kinoshita H, Kuwahara K, Nakao K, Itoh N. Fgf16 is required for cardiomyocyte proliferation in the mouse embryonic heart. Developmental Dynamics. 2008 Oct;237(10):2947-54.

[41] Itoh N, Ohta H. Roles of FGF20 in dopaminergic neurons and Parkinson's disease. Frontiers in molecular neuroscience. 2013 May 31;6:15.

[42] Liu Y, Ma J, Beenken A, Srinivasan L, Eliseenkova AV, Mohammadi M. Regulation of receptor binding specificity of FGF9 by an autoinhibitory homodimerization. Structure. 2017 Sep 5;25(9):1325-36.

[43] Kalinina J, Byron SA, Makarenkova HP, Olsen SK, Eliseenkova AV, Larochelle WJ, Dhanabal M, Blais S, Ornitz DM, Day LA, Neubert TA. Homodimerization controls the fibroblast growth factor 9 subfamily's receptor binding and heparan sulfate-dependent diffusion in the extracellular matrix. Molecular and cellular biology. 2009 Sep 1;29(17):4663-78.

[44] Kharitonenkov A, Shiyanova TL, Koester A, *et al*. FGF-21 as a novel metabolic regulator. The Journal of clinical investigation. 2005 Jun 1;115(6):1627-35.

[45] Nishimura T, Nakatake Y, Konishi M, Itoh N. Identification of a novel FGF, FGF-21, preferentially expressed in the liver. Biochimica et Biophysica Acta (BBA)-Gene Structure and Expression. 2000 Jun 21;1492(1):203-6.

[46] Coskun T, Bina HA, Schneider MA, *et al*. Fibroblast growth factor 21 corrects obesity in mice. Endocrinology. 2008 Dec 1;149(12):6018-27.

[47] Holland WL, Adams AC, Brozinick JT, *et al*. An FGF21-adiponectin-ceramide axis controls energy expenditure and insulin action in mice. Cell metabolism. 2013 May 7;17(5):790-7.

[48] Chartoumpekis DV, Habeos IG, Ziros PG, Psyrogiannis AI, Kyriazopoulou VE, Papavassiliou AG. Brown adipose tissue responds to cold and adrenergic stimulation by induction of FGF21. Molecular medicine. 2011 Jul;17(7):736-40.

[49] Hanssen MJ, Broeders E, Samms RJ, *et al*. Serum FGF21 levels are associated with brown adipose tissue activity in humans. Scientific reports. 2015 May 18;5:10275.

[50] Itoh N. FGF21 as a hepatokine, adipokine, and myokine in metabolism and diseases. Frontiers in endocrinology. 2014 Jul 7;5:107.

[51] Staiger H, Keuper M, Berti L, Hrabě de Angelis M, Häring HU. Fibroblast growth factor 21—metabolic role in mice and men. Endocrine Reviews. 2017 Oct 1;38(5):468-88.

[52] Giralt M, Gavaldà-Navarro A, Villarroya F. Fibroblast growth factor-21, energy balance and obesity. Molecular and cellular endocrinology. 2015 Dec 15;418:66-73.

[53] Kilkenny DM, Rocheleau JV. The FGF21 receptor signaling complex: Klothoβ, FGFR1c, and other regulatory interactions. InVitamins & Hormones 2016 Jan 1 (Vol. 101, pp. 17-58). Academic Press.

[54] Fisher FM, Maratos-Flier E. Understanding the physiology of FGF21. Annual review of physiology. 2016 Feb 10;78:223-41.

[55] Shalhoub V, Shatzen EM, Ward SC, *et al*. FGF23 neutralization improves chronic kidney disease–associated hyperparathyroidism yet increases mortality. The Journal of clinical investigation. 2012 Jul 2;122(7):2543-53.

[56] Shimada T, Mizutani S, Muto T, *et al*. Cloning and characterization of FGF23 as a causative factor of tumor-induced osteomalacia. Proceedings of the National Academy of Sciences. 2001 May 22;98(11):6500-5.

[57] Shimada T, Hasegawa H, Yamazaki Y, *et al*. FGF-23 is a potent regulator of vitamin D metabolism and phosphate homeostasis. Journal of Bone and Mineral Research. 2004 Mar;19(3):429-35.

[58] Fukumoto S. Targeting fibroblast growth factor 23 signaling with antibodies and inhibitors, is there a rationale? Frontiers in endocrinology. 2018 Feb 20;9:48.

[59] Bernett MJ, Somasundaram T, Blaber M. An atomic resolution structure for human fibroblast growth factor 1. PROTEINS: Structure, Function, and Bioinformatics. 2004 Nov 15;57(3):626-34.

[60] Zhu X, Komiya H, Chirino A, Faham S, Fox GM, Arakawa T, Hsu BT, Rees DC. Three-dimensional structures of acidic and basic fibroblast growth factors. Science. 1991 Jan 4;251(4989):90-3.

[61] Sweet RM, Wright HT, Janin J, Chothia CH, Blow DA. Crystal structure of the complex of porcine trypsin with soybean trypsin inhibitor (Kunitz) at 2.6 Å resolution. Biochemistry. 1974 Sep 1;13(20):4212-28.

[62] Brych SR, Blaber SI, Logan TM, Blaber M. Structure and stability effects of mutations designed to increase the primary sequence symmetry within the core region of a β-trefoil. Protein Science. 2001 Dec;10(12):2587-99.

[63] Häcker U, Nybakken K, Perrimon N. Heparan sulphate proteoglycans: the sweet side of development. Nature reviews Molecular cell biology. 2005 Jul;6(7):530-41.

[64] Schlessinger J, Plotnikov AN, Ibrahimi OA, *et al*. Crystal structure of a ternary FGF-FGFR-heparin complex reveals a dual role for heparin in FGFR binding and dimerization. Molecular cell. 2000 Sep 1;6(3):743-50.

[65] Pellegrini L, Burke DF, von Delft F, Mulloy B, Blundell TL. Crystal structure of fibroblast growth factor receptor ectodomain bound to ligand and heparin. Nature. 2000 Oct;407(6807):1029-34.

[66] DiGabriele AD, Lax I, Chen DI, Svahn CM, Jaye M, Schlessinger J, Hendrickson WA. Structure of a heparin-linked biologically active dimer of fibroblast growth factor. Nature. 1998 Jun;393(6687):812-7.

[67] Raman R, Venkataraman G, Ernst S, Sasisekharan V, Sasisekharan R. Structural specificity of heparin binding in the fibroblast growth factor family of proteins. Proceedings of the National Academy of Sciences. 2003 Mar 4;100(5):2357-62.

[68] Harmer NJ. Insights into the role of heparan sulphate in fibroblast growth factor signalling. Biochemical Society Transactions. 2006 Jun 1;34(3):442-5.

[69] Arunkumar AI, Kumar TK, Kathir KM, Srisailam S, Wang HM, Leena PS, Chi YH, Chen HC, Wu CH, Wu RT, Chang GG. Oligomerization of acidic fibroblast growth factor is not a prerequisite for its cell proliferation activity. Protein science. 2002 May;11(5):1050-61.

[70] Angulo J, Hricovíni M, Gairi M, Guerrini M, De Paz JL, Ojeda R, Martín-Lomas M, Nieto PM. Dynamic properties of biologically active synthetic heparin-like hexasaccharides. Glycobiology. 2005 Oct 1;15(10):1008-15.

[71] Canales A, Lozano R, López-Méndez B, Angulo J, Ojeda R, Nieto PM, Martín-Lomas M, Giménez-Gallego G, Jiménez-Barbero J. Solution NMR structure of a human FGF-1 monomer, activated by a hexasaccharide heparin-analogue. The FEBS journal. 2006 Oct;273(20):4716-27.

[72] Chi YH, Kumar TK, Wang HM, Ho MC, Chiu IM, Yu C. Thermodynamic characterization of the human acidic fibroblast growth factor: Evidence for cold denaturation. Biochemistry. 2001 Jun 26;40(25):7746-53.

[73] Culajay JF, Blaber SI, Khurana A, Blaber M. Thermodynamic characterization of mutants of human fibroblast growth factor 1 with an increased physiological half-life. Biochemistry. 2000 Jun 20;39(24):7153-8.

[74] Zakrzewska M, Krowarsch D, Wiedlocha A, Otlewski J. Design of fully active FGF-1 variants with increased stability. Protein Engineering Design and Selection. 2004 Aug 1;17(8):603-11.

[75] Zakrzewska M, Krowarsch D, Wiedlocha A, Olsnes S, Otlewski J. Highly stable mutants of human fibroblast growth factor-1 exhibit prolonged biological action. Journal of molecular biology. 2005 Sep 30;352(4):860-75.

[76] Wong P, Hampton B, Szylobryt E, Gallagher AM, Jaye M, Burgess WH. Analysis of putative heparin-binding domains of fibroblast growth factor-1 using site-directed mutagenesis and peptide analogues. Journal of Biological Chemistry. 1995 Oct 27;270(43):25805-11.

[77] Zakrzewska M, Wiedlocha A, Szlachcic A, Krowarsch D, Otlewski J, Olsnes S. Increased protein stability of FGF1 can compensate for its reduced affinity for heparin. Journal of Biological Chemistry. 2009 Sep 11;284(37):25388-403.

[78] Dubey VK, Lee J, Somasundaram T, Blaber S, Blaber M. Spackling the crack: stabilizing human fibroblast growth factor-1 by targeting the N and C terminus β-strand interactions. Journal of molecular biology. 2007 Aug 3;371(1):256-68.

[79] Szlachcic, A., et al., Structure of a highly stable mutant of human fibroblast growth factor 1, Acta Cryst, 2009. D65: p. 67-73.

[80] Ortega, S., et al., Conversion of Cysteine to Serine Residues Alters the Activity, Stability, and Heparin Dependence of Acidic Fibroblast Growth Factor, J Biol Chem, 1991. 266(9): p. 5842-5846.

[81] Huang, Z., Tan, Y., Gu, J., Liu, Y., Song, L., Niu, J., Zhao, L., Srinivasan, L., Lin, Q., Deng, J. and Li, Y., 2017. Uncoupling the Mitogenic and Metabolic Functions of FGF1 by Tuning FGF1-FGF Receptor Dimer Stability. Cell reports, 20(7), pp.1717- 1728.

[82] Xia, X., Kumru, O. S., Blaber, S. I., Middaugh, C. R., Li, L., Ornitz, D. M., Suh, J. M., Atkins, A. R., Downes, M., Evans, R. M., Tenorio, C. A., Bienkiewicz, E., & Blaber, M. (2016). An S116R Phosphorylation Site Mutation in Human Fibroblast Growth Factor-1 Differentially Affects Mitogenic and Glucose-Lowering Activities. *Journal of pharmaceutical sciences*, *105*(12), 3507–3519.

[83] Lew ED, Furdui CM, Anderson KS, Schlessinger J. The precise sequence of FGF receptor autophosphorylation is kinetically driven and is disrupted by oncogenic mutations. Sci. Signal. 2009 Feb 17;2(58):ra6.

[84] Brewer JR, Mazot P, Soriano P. Genetic insights into the mechanisms of Fgf signaling. Genes & development. 2016 Apr 1;30(7):751-71.

[85] Bae JH, Boggon TJ, Tomé F, Mandiyan V, Lax I, Schlessinger J. Asymmetric receptor contact is required for tyrosine autophosphorylation of fibroblast growth factor receptor in living cells. Proceedings of the National Academy of Sciences. 2010 Feb 16;107(7):2866-71.

[86] Stauber DJ, DiGabriele AD, Hendrickson WA. Structural interactions of fibroblast growth factor receptor with its ligands. Proceedings of the National Academy of Sciences. 2000 Jan 4;97(1):49-54.

[87] Lin X, Zhang Y, Liu L, *et al*. FRS2α is essential for the fibroblast growth factor to regulate the mTOR pathway and autophagy in mouse embryonic fibroblasts. International journal of biological sciences. 2011;7(8):1114.

[88] Haugsten EM, Wiedlocha A, Olsnes S, Wesche J. Roles of fibroblast growth factor receptors in carcinogenesis. Molecular Cancer Research. 2010 Nov 1;8(11):1439-52.

[89] Manning BD, Cantley LC. AKT/PKB signaling: navigating downstream. Cell. 2007 Jun 29;129(7):1261-74.

[90] Lonic A, Barry EF, Quach C, Kobe B, Saunders N, Guthridge MA. Fibroblast growth factor receptor 2 phosphorylation on serine 779 couples to 14-3-3 and regulates cell survival and proliferation. Molecular and cellular biology. 2008 May 15;28(10):3372-85.

[91] Ahmed Z, Lin CC, Suen KM, *et al*. Grb2 controls phosphorylation of FGFR2 by inhibiting receptor kinase and Shp2 phosphatase activity. Journal of Cell Biology. 2013 Feb 18;200(4):493-504.

[92] Hart KC, Robertson SC, Donoghue DJ. Identification of tyrosine residues in constitutively activated fibroblast growth factor receptor 3 involved in mitogenesis, Stat activation, and phosphatidylinositol 3-kinase activation. Molecular biology of the cell. 2001 Apr 1;12(4):931-42.

[93] Kong M, Wang CS, Donoghue DJ. Interaction of Fibroblast Growth Factor Receptor 3 and the Adapter Protein SH2-B a role in stat5 activation. Journal of Biological Chemistry. 2002 May 3;277(18):15962-70.

[94] Jackson CC, Medeiros LJ, Miranda RN. 8p11 myeloproliferative syndrome: a review. Human pathology. 2010 Apr 1;41(4):461-76.

[95] Roumiantsev S, Krause DS, Neumann CA, Dimitri CA, Asiedu F, Cross NC, Van Etten RA. Distinct stem cell myeloproliferative/T lymphoma syndromes induced by ZNF198-FGFR1 and BCR-FGFR1 fusion genes from 8p11 translocations. Cancer cell. 2004 Mar 1;5(3):287-98.

[96] Wu YM, Su F, Kalyana-Sundaram S, Khazanov N, Ateeq B, Cao X, Lonigro RJ, Vats P, Wang R, Lin SF, Cheng AJ. Identification of targetable FGFR gene fusions in diverse cancers. Cancer discovery. 2013 Jun 1;3(6):636-47.

[97] Singh D, Chan JM, Zoppoli P, *et al*. Transforming fusions of FGFR and TACC genes in human glioblastoma. Science. 2012 Sep 7;337(6099):1231-5.

[98] Williams SV, Hurst CD, Knowles MA. Oncogenic FGFR3 gene fusions in bladder cancer. Human molecular genetics. 2013 Feb 15;22(4):795-803.

[99] Heist RS, Mino-Kenudson M, Sequist LV, *et al*. FGFR1 amplification in squamous cell carcinoma of the lung. Journal of thoracic oncology. 2012 Dec 1;7(12):1775-80.

[100] Xian W, Pappas L, Pandya D, *et al*. Fibroblast growth factor receptor 1–transformed mammary epithelial cells are dependent on RSK activity for growth and survival. Cancer research. 2009 Mar 15;69(6):2244-51.

[101] Sobhani N, Ianza A, D'Angelo A, *et al*. Current status of fibroblast growth factor receptor-targeted therapies in breast cancer. Cells. 2018 Jul;7(7):76.

[102] André F, Bachelot T, Campone M, *et al*. Targeting FGFR with dovitinib (TKI258): preclinical and clinical data in breast cancer. Clinical cancer research. 2013 Jul 1;19(13):3693-702.

[103] Turner N, Pearson A, Sharpe R, *et al*. FGFR1 amplification drives endocrine therapy resistance and is a therapeutic target in breast cancer. Cancer research. 2010 Mar 1;70(5):2085-94.

[104] Matsumoto K, Arao T, Hamaguchi T, *et al.* FGFR2 gene amplification and clinicopathological features in gastric cancer. British journal of cancer. 2012 Feb;106(4):727-32.

[105] Li SQ, Cheuk AT, Shern JF, *et al.* Targeting wild-type and mutationally activated FGFR4 in rhabdomyosarcoma with the inhibitor ponatinib (AP24534). PLoS One. 2013;8(10) e76551.

[106] Chae YK, Ranganath K, Hammerman PS, *et al.* Inhibition of the fibroblast growth factor receptor (FGFR) pathway: the current landscape and barriers to clinical application. Oncotarget. 2017 Feb 28;8(9):16052.

[107] Catalogue of Somatic Mutations in Cancer. Available at: http://cancer.sanger.ac.uk/cosmic.

[108] Dodé C, Levilliers J, Dupont JM, *et al.* Loss-of-function mutations in FGFR1 cause autosomal dominant Kallmann syndrome. Nature genetics. 2003 Apr;33(4):463-5.

[109] NIH Survillance epidemiology. Available at: https://seer.cancer.gov/statfacts/html/breast.html.

[110] Snyder-Warwick AK, Perlyn CA, Pan J, Yu K, Zhang L, Ornitz DM. Analysis of a gain-of-function FGFR2 Crouzon mutation provides evidence of loss of function activity in the etiology of cleft palate. Proceedings of the National Academy of Sciences. 2010 Feb 9;107(6):2515-20.

[111] Naski MC, Wang Q, Xu J, Ornitz DM. Graded activation of fibroblast growth factor receptor 3 by mutations causing achondroplasia and thanatophoric dysplasia. Nature genetics. 1996 Jun;13(2):233-7.

[112] Chen L, Li C, Qiao W, Xu X, Deng C. A Ser365→ Cys mutation of fibroblast growth factor receptor 3 in mouse downregulates Ihh/PTHrP signals and causes severe achondroplasia. Human molecular genetics. 2001 Mar 1;10(5):457-66.

[113] Adar R, Monsonego-Ornan E, David PE, Yayon A. Differential activation of cysteine-substitution mutants of fibroblast growth factor receptor 3 is determined by cysteine localization. Journal of Bone and Mineral Research. 2002 May;17(5):860-8.

[114] Di Martino E, L'hôte CG, Kennedy W, Tomlinson DC, Knowles MA. Mutant fibroblast growth factor receptor 3 induces intracellular signaling and cellular transformation in a cell type-and mutation-specific manner. Oncogene. 2009 Dec;28(48):4306-16.

[115] Ahmad I, Singh LB, Foth M, Morris CA, Taketo MM, Wu XR, Leung HY, Sansom OJ, Iwata T. K-Ras and β-catenin mutations cooperate with Fgfr3 mutations in mice to promote tumorigenesis in the skin and lung, but not in the bladder. Disease models & mechanisms. 2011 Jul 1;4(4):548-55.

[116] Munro NP, Knowles MA. Fibroblast growth factors and their receptors in transitional cell carcinoma. The Journal of urology. 2003 Feb 1;169(2):675-82.

[117] Vi JG, Cheuk AT, Tsang PS, *et al*. Identification of FGFR4-activating mutations in human rhabdomyosarcomas that promote metastasis in xenotransplanted models. The Journal of clinical investigation. 2009 Nov 2;119(11):3395-407.

[118] Zhang J, Li Y. Therapeutic uses of FGFs. InSeminars in cell & developmental biology 2016 May 1 (Vol. 53, pp. 144-154). Academic Press.

[119] Maddaluno L, Urwyler C, Werner S. Fibroblast growth factors: key players in regeneration and tissue repair. Development. 2017 Nov 15;144(22):4047-60.

[120] Tanaka EM. The molecular and cellular choreography of appendage regeneration. Cell. 2016 Jun 16;165(7):1598-608.

[121] Miller DL, Ortega S, Bashayan O, Basch R, Basilico C. Compensation by fibroblast growth factor 1 (FGF1) does not account for the mild phenotypic defects observed in FGF2 null mice. Molecular and cellular biology. 2000 Mar 15;20(6):2260-8.

[122] Abraham JA, Whang JL, Tumolo A, *et al*. Human basic fibroblast growth factor: nucleotide sequence and genomic organization. The EMBO Journal. 1986 Oct 1;5(10):2523-8.

[123] Weich HA, Iberg N, Klagsbrun M, Folkman J. Expression of acidic and basic fibroblast growth factors in human and bovine vascular smooth muscle cells. Growth Factors. 1990 Jan 1;2(4):313-20.

[124] Feige JJ, Baird A. Glycosylation of the basic fibroblast growth factor receptor. The contribution of carbohydrate to receptor function. Journal of Biological Chemistry. 1988 Oct 5;263(28):14023-9.

[125] Bing M, Da-Sheng C, Zhao-Fan X, *et al*. Randomized, multicenter, double-blind, and placebo-controlled trial using topical recombinant human acidic fibroblast growth factor for deep partial-thickness burns and skin graft donor site. Wound repair and regeneration. 2007 Nov;15(6):795-9.

[126] Huang C, Liu Y, Beenken A, *et al*. A novel fibroblast growth factor-1 ligand with reduced heparin binding protects the heart against ischemia-reperfusion injury in the presence of heparin co-administration. Cardiovascular research. 2017 Nov 1;113(13):1585-602.

[127] Gasser E, Moutos CP, Downes M, Evans RM. FGF1—a new weapon to control type 2 diabetes mellitus. Nature Reviews Endocrinology. 2017 Oct;13(10):599-609.

CHAPTER II

Overexpression, Purification and Characterization of the hFGF1 Variants Leading to the Design of a Hyperstable and Bioactive Acidic Fibroblast Growth Factor (sFGF1)

Abstract

Human acidic fibroblast growth factor (hFGF1) regulates key cellular processes such as cell proliferation, cell differentiation, angiogenesis, and tumor growth. hFGF1 is known to have low *in vivo* half-life and low melting temperature in the physiological range (T_m -37˚C). Binding of heparin to hFGF1 increases the stability of the growth factor. Moreover, it is believed that heparin is mandatory for the activation of FGF-FGFR complex formation and signaling. Thus, the main objective of this study is to build a hFGF1 variant which is entirely heparin independent yet possess elevated biological activity. In this context, successful expression, production, and purification of single, double, triple, and quadruple variants leading to the highly stable variant, superFGF1 (sFGF1) is achieved by introduction of mutations in wtFGF1. After obtaining the pure protein(s), all the variants are characterized using biophysical methods to monitor the overall structure, conformational stability, and backbone flexibility. The bioactivities of the designed variants are monitored using cell proliferation assay. The results of this study show that no major structural changes are caused due to the mutations leading to sFGF1. Additionally, limited enzymatic digestion and ANS binding experiments reveal that the mutations leading to sFGF1 render the growth factor more resistance to proteolytic enzymes and also results in decreasing the flexibility than the wtFGF1 molecule. Isothermal titration calorimetry data suggest that the heparin binding affinity is significantly decreased due to the introduction of R136E/K126N mutation. Thermal equilibrium unfolding data demonstrate that all mutations exhibit higher T_m in comparison to wtFGF1. Overall, the results of this study indicate that

introduction of specific mutations of R136E, K126N, S61L, H107S and Q54P into wtFGF1 causes hFGF1 variants (R136E/K126N, R136E/K126N/Q54P, R136E/K126N/S61L, R136E/K126N/H107S, R136E/K126N/Q54P/S61L, and R136E/K126N/Q54P/H107S) to lose its heparin binding affinity, enhance its thermal, chemical, and proteolytic stability, and gain mitogenic activity.

Introduction

Growth factors are a large class of biomolecules that promote cell growth, development, and differentiation. Fibroblast growth factors (FGFs) are a family of twenty-two related proteins that are involved in mitogenic and cell-survival activities. All members of the FGF family show strong mitogenic properties that are essential for proper growth and development [1-3]. FGFs play a vital role in many biological processes, including cell proliferation and angiogenesis [4]. One member of this family is the protein known as acidic fibroblast growth factor (FGF1). The human FGF1 (hFGF1) is a ~16kDa, positively charged, heparin-binding monomeric protein. The wild-type hFGF1 has a relatively short half-life of 5 minutes and low thermal stability in the body, with a melting temperature (T_m - 41°C) close to the physiological range [5].

The stability of hFGF1 increases as a consequence of binding to heparin, which also protects the protein against proteolytic digestion and denaturation via heat. Heparin is a negatively charged glycosaminoglycan of repeating disaccharide chains of L-iduronic acid and D-glucosamine, which binds to the cluster of positively charged amino acids on hFGF1, known as the heparin binding region [6]. It has been long debated whether heparin is essential for hFGF1 to bind to fibroblast growth factor receptors (FGFRs) since it plays an important role in stabilizing the protein. This added stability allows hFGF1 to have more time to interact with FGFRs, a family of receptor tyrosine kinases (RTKs), on the surface of cell membranes,

stimulating intracellular signaling pathways that lead to processes such as cell proliferation, cell differentiation, and cell migration. hFGF1's inherent instability stems from the repulsive electrostatic forces of positively charged amino acid residues in the heparin-binding region making hFGF1 to be more susceptible to proteolytic cleavage and degradation. The three-dimensional solution structure of hFGF1, determined using multidimensional nuclear magnetic resonance (NMR) technique demonstrates that hFGF1 consists of twelve β-strands arranged in an antiparallel fashion into a β-barrel structure [7-10].

One of the wild-type hFGF1 (wtFGF1) variant called R136E has been found to gain stability and enhanced bioactivity, which appears to be beneficial for potential pharmaceutical use in wound healing medications [11-15].

Most of these hFGF1 variants have been constructed based on the introduction of point mutations into the receptor binding site and heparin binding pocket of hFGF1; thus, increasing its stability. Prior work conducted in our lab demonstrated that mutations in the heparin binding pocket can modulate the stability and mitogenic activity, which is the basis of this project [16-19]. This chapter is focused on generating double, triple, and quadruple variant(s) of hFGF1 with four more mutations on R136E-FGF1 using site directed mutagenesis. The four mutations made on R136E are K126N, S61L, Q54P, and H107S (Fig. 1).

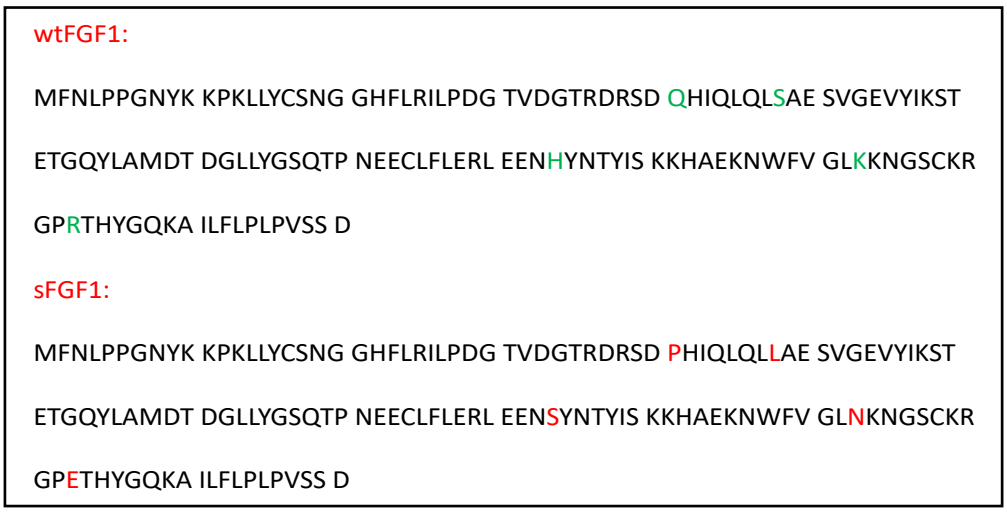

Fig. 1: Amino acid sequence of wtFGF1. The residues highlighted in green represent the amino acids that are mutated to construct sFGF1. Correspondingly, the residues in red represent the mutated residues in wtFGF1 (R136E, K126N, Q54P, S61L, and H107S).

R136E and K126N mutations were chosen because they are both located in hFGF1's heparin-binding region (Fig. 2). The R136E mutation replaced a polar positively charged amino acid with a polar negatively charged one [20]. The K126N mutation replaced a polar positively charged amino acid with a polar neutral amino acid. Replacement of the lysine residue with another negatively charged residue can potentially cause repulsion between the two negatively charged residues; therefore, we replaced lysine with a neutral amino acid (Asn). Since, trypsin cleaves at the C-terminal of arginine and lysine residues, mutating an Arg to Glu and a Lys to Asn will increase the variant hFGF1's resistance to trypsin digestion. Moreover, R136 is the secondary thrombin cleavage site in hFGF1. Mutating R136 to Glu will significantly reduce the chances of hFGF1 being cleaved by thrombin. There will also be less repulsion between the positively charged amino acid residues in the heparin-binding region, which can plausibly lead to increase the inherent stability of the hFGF1. Histidine at position 107 plays an important role in receptor binding and interacts with R251 and R255 of D2 and D3 domain of the FGFR. Both the positively charged amino acids (Arg and His) might repel at the receptor binding site; therefore,

we have substituted histidine with serine. S61 lies close to the hydrophobic pocket in the structure of hFGF1. So, the mutation of Ser, a polar amino acid to Leu, a non-polar amino acid is expected to increase the stability of hFGF1 by rendering it more compact [21-23]. Lastly, it has already been known that Pro rearranges the β-turn geometry and forms a short 3_{10}- helix [13]. This 3_{10}- helix is expected to form two continuous overlapping type I β-turns. Thus, substitution of Gln to Pro might provide more stability to hFGF1 by increasing the β-strand interactions.

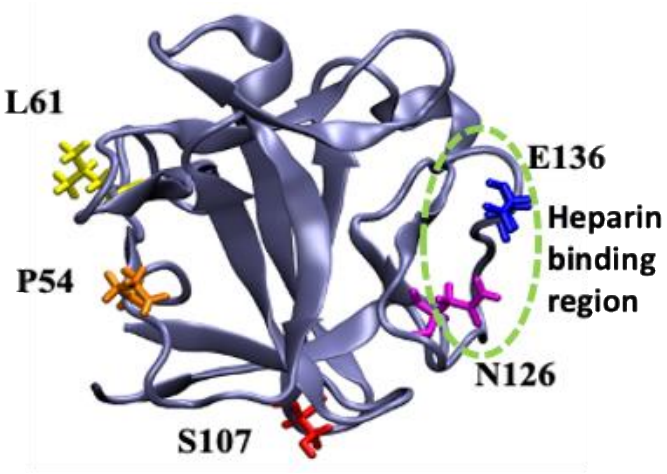

Fig. 2: Ribbon representation of hFGF-1 structure (PDB ID: 1RG8) showing the location of mutated residues.

The objective of this chapter is to shed light on the structural forces that contribute to high stability of these mutations. As altering the primary amino acid sequence can potentially alter the secondary and tertiary structure of the protein, measures were taken to ensure that the three-dimensional structure of the variants is not significantly altered. Structural analyses were conducted to study the role of the amino acid mutations on hFGF1 variants contributing to its higher stability and enhanced biological function. In summary, all the single, double, triple and quadruple variants have been found to have a higher inherent stability and a reduced affinity for heparin as compared to wtFGF1.

Results and discussion

Human acidic fibroblast growth factor (hFGF1) is a 155-amino acid, an all β-sheet protein. The heparin binding pocket (HBP) on hFGF1 constitutes the region between residues 124 and 140 (Fig. 2). The heparin binding site carries net positive charge attributed by the six polar, basic amino acids at physiological pH [24]. Previous studies on hFGF1 have shown that due to the repulsion between these positive residues in HBP, hFGF1 is unstable and it is unlikely that hFGF1 will complex with the FGF receptor. Therefore, binding of hFGF1 to the negatively charged heparin provides stability to the growth factor [25].

Construction and purification of pure wtFGF1 and its variants

The single (R136E), double (R136E/K126N), (R136E/S61L), (R136E/H107S), (R136E/Q54P), triple (R136E/K126N/S61L), (R136E/K126N/Q54P), (R136E/K126N/H107S), and quadruple (R136E/K126N/Q54P/S61L), (R136E/K126N/Q54P/H107S) variants were designed and transformed into the multiple cloning site of pET-20b vector. wtFGF1 and the variants were overexpressed in BL21-plysS cells in lysogeny broth (LB) media. As hFGF1 is a heparin binding protein, wtFGF1 and the designed variants were purified by heparin sepharose affinity column chromatography. The proteins were eluted using a stepwise salt (sodium chloride) gradient. Pure wtFGF1 was eluted with 1.5M sodium chloride concentration, whereas, R136E single variant and double variants (R136E/Q54P, R136E/S61L, and R136E/H107S) were eluted with 0.8M sodium chloride. However, R136E/K126N variant, and the triple and quadruple variants were eluted from the column using 10 mM phosphate buffer with 0 mM NaCl, suggesting no heparin binding affinity for hFGF1 (Fig. 3). Correspondingly, the binding affinity of the R136E/K126N variant, and the triple and quadruple variants is weaker than that of the non-heparin binding *E. coli* proteins, which non-specifically bind to the heparin beads.

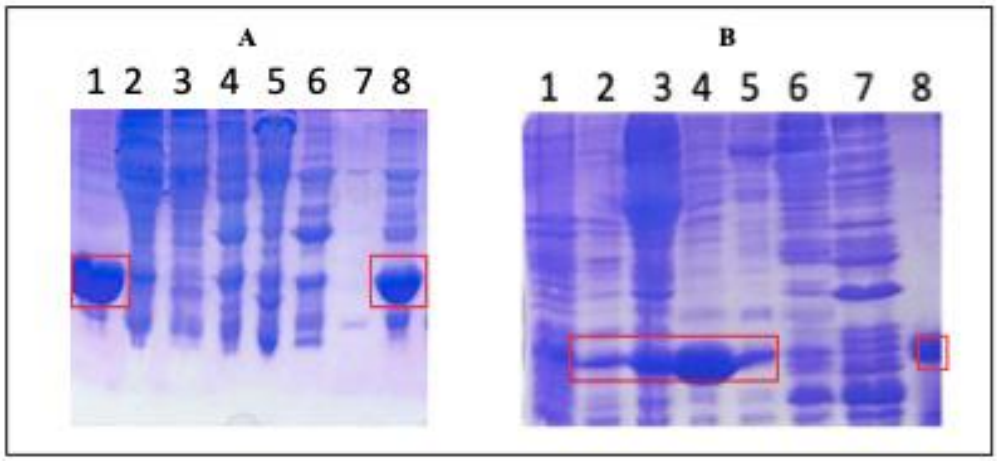

Fig. 3: SDS-PAGE analysis of proteins (A - wtFGF1 and B - R136E/K126N) eluted upon heparin sepharose chromatography at different concentrations of NaCl. Panel-A: Pure wtFGF1 (Lane-1); Supernatant (Lane-2); 10 mM PB + 0 mM NaCl (Lane-3); 10 mM PB + 100mM NaCl (Lane-4); 10 mM PB + 300 mM NaCl (Lane-5); 10 mM PB + 500 mM NaCl (Lane-6); 10 mM PB + 800 mM NaCl (Lane-7); 10 mM PB + 1500 mM NaCl (Lane-8). Panel-B: Supernatant (Lane-1); 10 mM PB + 0 mM NaCl (Lanes 2-5); 10 mM PB + 300 mM NaCl (Lane-6); 10 mM PB + 800 mM NaCl (Lane-7); Marker-pure wtFGF1 (Lane-8).

To remove minor bacterial impurities, R136E/K126N variant, the triple variants and quadruple variants were further subjected to S-75 size-exclusion column chromatography. The revealed three peaks – the first major peak comprised of high molecular weight *E.coli* contaminants followed by a middle peak corresponding to the molecular weight of hFGF1 variant, and a third peak corresponding to low molecular weight *E.coli* contaminants (Figs. 4 and 5).

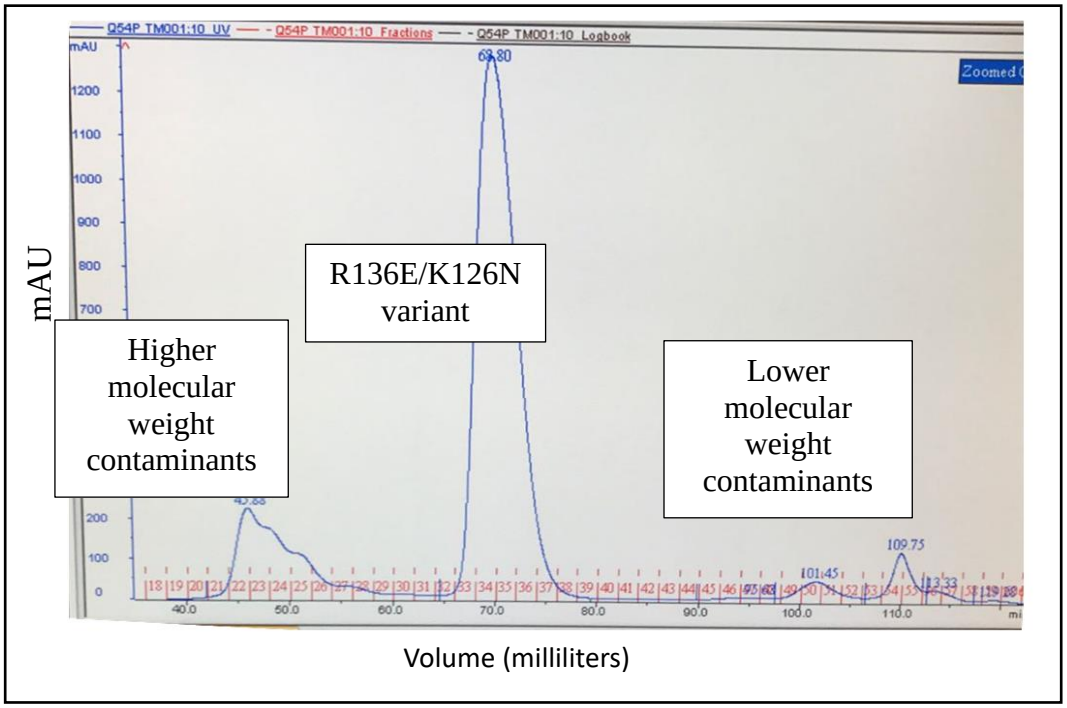

Fig. 4: Elution profile of the R136E/K126N variant (M.W- 15.9 kDa) from a S-75 size-exclusion column.

The yields of purified wtFGF1 and the variants were in the range of 25-30 mg/L of the bacterial culture (Table 1). The results of purification suggest a positive co-relation between the salt concentration at which hFGF1 elutes out of the heparin sepharose column and heparin binding affinity of hFGF1.

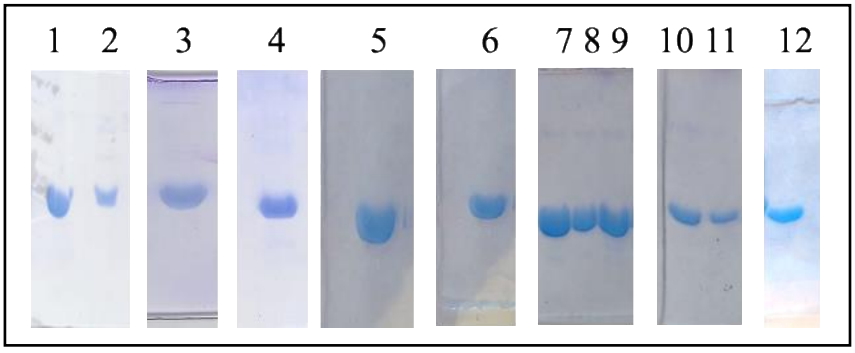

Fig. 5: Analysis of size-exclusion chromatographic profile by SDS-PAGE. wtFGF1 (Lane-1); sFGF1 (Lane-2); R136E (Lane-3); R136E/K126N (Lane-4); R136E/Q54P (Lane-5); R136E/S61L (Lane-6); R136E/H107S (Lane-7); R136E/K126N/Q54P (Lane-8); R136E/K126N/S61L (Lane-9); R136E/K126N/H107S (Lane-10); R136E/K126N/Q54P/S61L (Lane-11); 136E/K126N/Q54P/H107S (Lane-12).

Table 1: Protein yield of wtFGF1 and the variants.

hFGF1 variants	Protein yield (mg/L)
wtFGF1	29 ± 0.408
R136E	29.2 ± 0.510
R136E/K126N	27.14 ± 0.914
R136E/H107S	26.8 ± 1.54
R136E/S61L	27.6 ± 1.60
R136E/Q54P	27.93 ± 1.36
R136E/K126N/Q54P	25.8 ± 0.618
R136E/K126N/S61L	28.2 ± 0.338
R136E/K126N/H107S	27.7 ± 0.74
R136E/K126N/Q54P/S61L	26.81 ± 0.702
R136E/K126N/Q54P/H107S	27.92 ± 0.654

Mutations in hFGF1 does not cause significant structural change

wtFGF1 is known to contain one tryptophan (W121) and eight tyrosine residues. The fluorescence spectrum is analyzed by examining the presence or absence of peaks at 305 nm and 350 nm. hFGF-1's lone tryptophan residue is typically quenched by adjacent proline and lysine resides in the native state. Therefore, wtFGF1 shows an emission maximum at 305 nm corresponding to the eight tyrosine residues in the native protein. These quenching effects are completely relieved in the denatured state(s) of the protein, resulting in a significant increase in the fluorescence at 350 nm characteristic for tryptophan residues. Fig. 6 displays the overlay of intrinsic fluorescence spectra of wtFGF1 and its variants. The presence of tyrosine peak at 305 nm and absence of tryptophan peak at 350 nm indicates that the mutations did not alter the tertiary structure of wtFGF1. The broadening of peak at 340 nm corresponds to the emission of the previously quenched tryptophan residues.

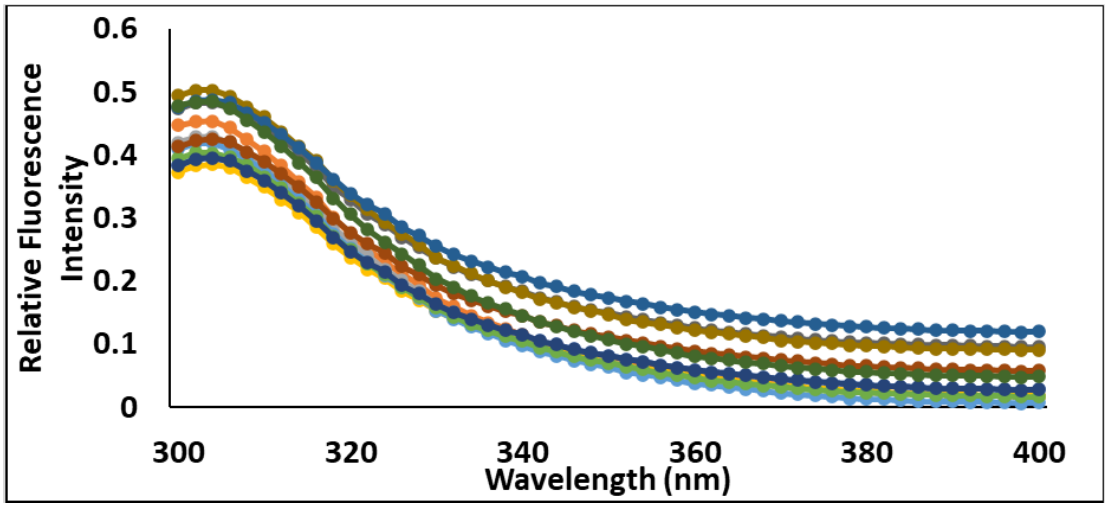

Fig. 6: Overlay of the Fluorescence spectra showing the similarity in the tertiary structure of wtFGF1 and the designed variants. wtFGF1 (pink), R136E (orange), K126N-DM (gray), Q54P-DM (yellow), S61L-DM (purple), H107S-DM (green), Q54P-TM (blue), S61L-TM (red), H107S-TM (dark green), H107S-QM (teal), and S61L-QM (brown).

Far-UV CD spectra is a valuable technique for examining the secondary structure of proteins in solution. The overlay of far-UV CD spectra of wtFGF1 and the variants shows no apparent changes in the overall secondary structure of the variant protein (Fig. 7). The negative peak at 210 nm (class II β-protein structure) and the positive peak at 228 nm (β-turns, loops and aromatic side chains) show that the characteristic secondary (β -trefoil) structure of wtFGF1 is preserved in all the variants.

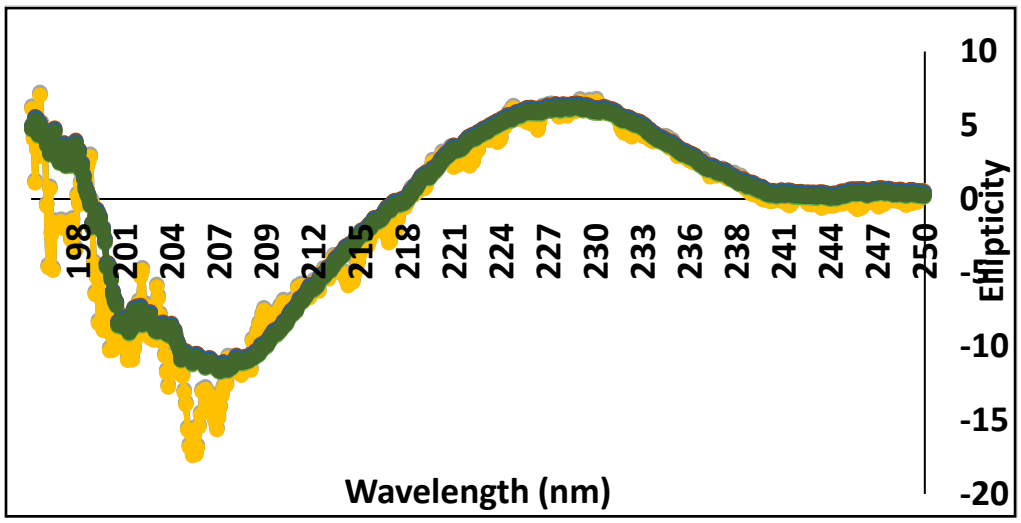

Fig. 7: Overlay of the Circular dichroism (CD) spectra of wtFGF1 and its variants. wtFGF1 (pink), R136E (orange), K126N-DM (gray), Q54P-DM (yellow), S61L-DM (purple), H107S-DM (green), Q54P-TM (blue), S61L-TM (red), H107S-TM (dark green), H107S-QM (teal), and S61L-QM (brown).

Introduction of the R136E mutation renders the hFGF1 molecule more compact

8-anilino-1-nathalenesulfonate (ANS) is a non-polar fluorescent dye that is widely used to determine the presence of solvent-exposed hydrophobic surfaces in proteins [26]. The data in Fig. 8 (Panel - A and B) depicts the binding of ANS to wtFGF1. The relative fluorescent intensity is directly proportional to the number of ANS molecules bound to the protein. Normally, hydrophobic residues are buried inside the protein core. Therefore, increase in the ANS fluorescence suggests exposure of these hydrophobic residues towards the surface of the protein. The plot from the ANS binding assay (Fig. 8) indicates that the solvent-exposure of non-polar surfaces in the structures of wtFGF1 and the variants do not vary significantly from each other. Also, this data indicates that the maximum solvent exposure of hydrophobic surface(s) is seen in wildtype in the absence of heparin. This suggests that wtFGF1, when not bound to heparin, is more flexible. On the other hand, R136E, R136E/S61L, R136E/Q54P, and R136E/H107S variants exhibit decreased flexibility and increased compactness compared to R136E/K126N, the triple variants and quadruple variants. The ANS fluorescence decreases for

R136E, R136E/S61L, R136E/Q54P, and R136E/H107S when exposed to heparin whereas, R136E/K126N, the triple variants and the quadruple variants do not show any difference in the ANS fluorescence when bound to heparin which infers that R136E, R136E/S61L, R136E/Q54P, and R136E/H107S variants are more stable upon binding to heparin. Overall, the results of ANS binding experiments suggest that R136E/K126N variant, the triple variants and quadruple variants possess fewer solvent-accessible non-polar surfaces as compared to wtFGF1.

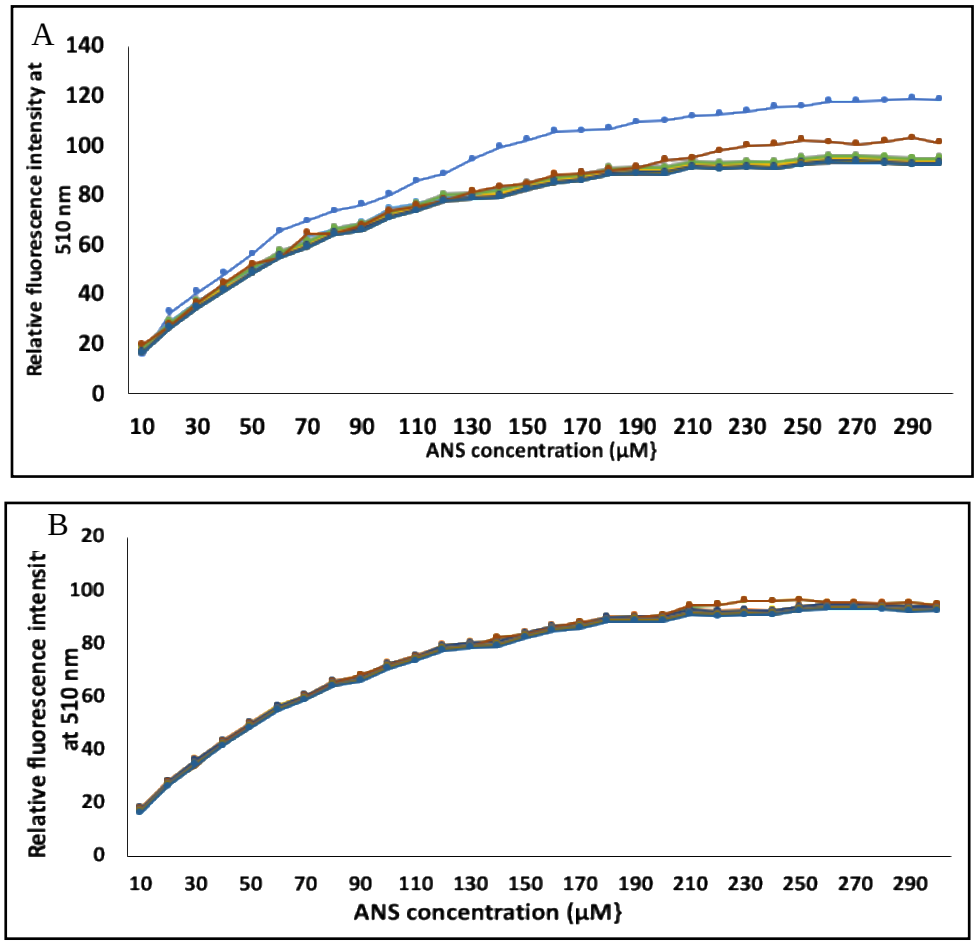

Fig. 8: ANS binding curves of wtFGF1 and the variants in the, absence (Panel-A) and presence of heparin (Panel-B). The presence of solvent-exposed hydrophobic regions in the proteins were monitored by changes in relative fluorescence intensity at 510 nm. wtFGF1 (blue), R136E (orange), K126N-DM (gray), Q54P-DM (yellow), S61L-DM (purple), H107S-DM (green), Q54P-TM (pink), S61L-TM (red), H107S-TM (dark green), H107S-QM (teal), and S61L-QM (brown).

Introduction of the R136E mutation makes the hFGF1 molecule resistant to the proteolytic action

Trypsin, a serine protease, specifically cleaves polypeptides at the carboxyl end of positively charged amino acids - lysine and arginine [27]. wtFGF1 contains three arginine and nine lysine residues. Therefore, limited trypsin cleavage is performed to understand if the conformational flexibility of the arginine and lysine residues are altered due to introduction of the mutations in wtFGF1; thereby, monitoring the conformational flexibility of the protein. It can be inferred from Fig. 9 that wtFGF1 (Panel-A) is susceptible to trypsin digestion and gets completely degraded in the first 20 minutes, whereas the R136E/K126N variant is resistant to the action of trypsin (Panel-B).

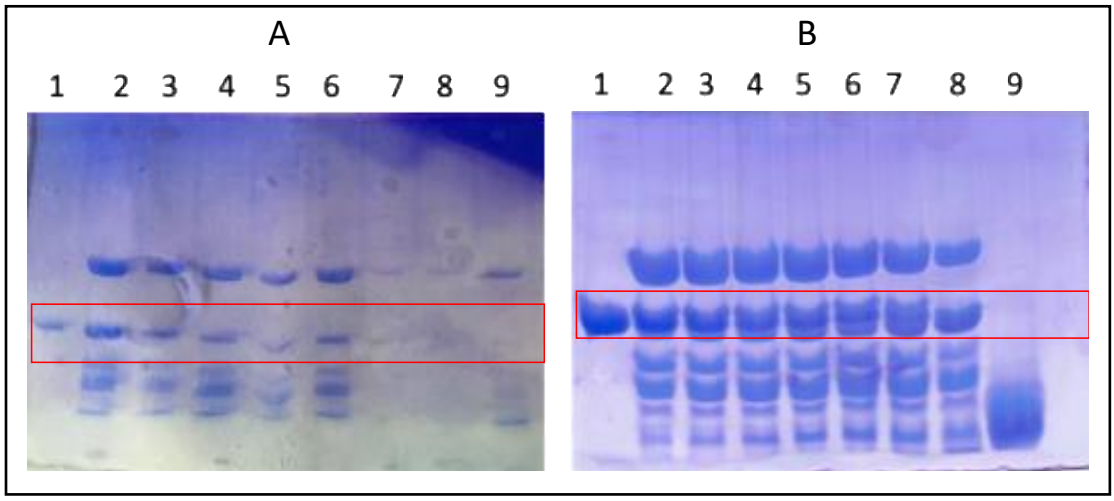

Fig. 9: SDS-PAGE analysis of limited trypsin digestion of wtFGF1 (Panel – A) and R136E/K126N (Panel-B) variant. 0.5 mg/mL of proteins (Lane-1); 4 minutes (Lane-2); 6 minutes (Lane-3); 10 minutes (Lane-4); 15 minutes (Lane-5); 30 minutes (Lane-6); 45 minutes (Lane-7); 60 minutes (Lane-8); 5 mg/mL of trypsin (Lane-9).

The densitometric analysis results suggest that all the variants (R136E, R136E/S61L, R136E/Q54P, R136E/H107S, R136E/K126N, R136E/K126N/S61L, R136E/K126N/Q54P, R136E/K126N/H107S, R136E/K126N/Q54P/S61L, and R136E/K126N/Q54P/H107S) showed complete resistance against trypsin whereas wtFGF1 was digested by 80% in the first 20 minutes

(Fig. 10). These results clearly indicate that the variants resulting from the manipulation of wtFGF1 decrease the backbone flexibility and consequently increase the resistance of protein to proteolytic digestion. This result corroborates the inference drawn from the ANS binding experiment.

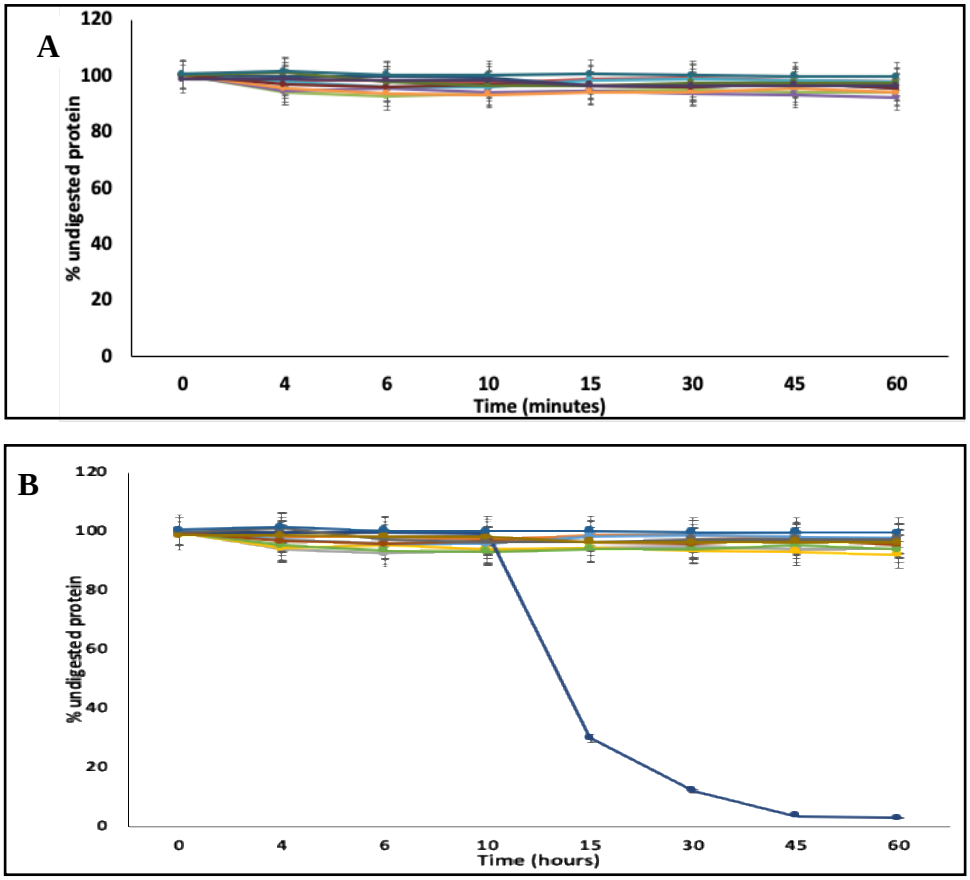

Fig. 10: Densitometric analysis of limited trypsin digestion of wtFGF1 and the designed variants as monitored by SDS-PAGE in the absence of heparin (Panel-A) and presence of heparin (Panel-B). wtFGF1 (blue), R136E (orange), K126N-DM (gray), Q54P-DM (yellow), S61L-DM (purple), H107S-DM (green), Q54P-TM (pink), S61L-TM (red), H107S-TM (dark green), H107S-QM (teal), and S61L-QM (brown).

Besides being present at the wound site to help in blood clot formation, thrombin is also known to cleave hFGF1 at R136 and make it biologically inactive. In this regard, resistance of hFGF1 to thrombin is imperative [28]. Limited thrombin experiment was performed to examine subtle changes in the flexibility of the protein backbone caused by the introduction of mutations

in wtFGF1. The data in Fig. 11 depicts the undigested proteins (wtFGF1 and the hFGF1 variants) after 72 hours of thrombin exposure. The densitometric analysis results elucidate that all the variants- R136E, R136E/S61L, R136E/Q54P, R136E/H107S, R136E/K126N, R136E/K126N/S61L, R136E/K126N/Q54P, R136E/K126N/H107S, R136E/K126N/Q54P/S61L, and R136E/K126N/Q54P/H107S show complete resistance against thrombin whereas wtFGF1 is completely degraded within the first 24 hours.

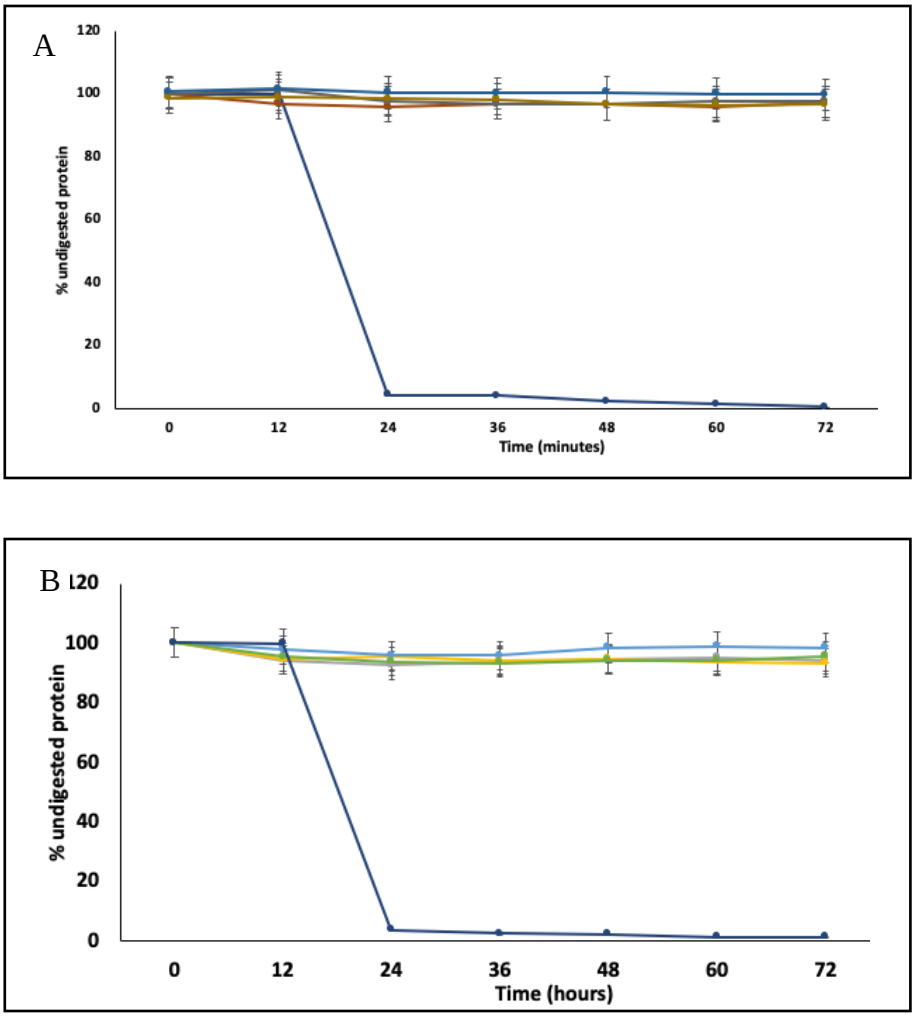

Fig. 11: Densitometric analysis of the limited thrombin digestion of R136E and the double variants (Panel - A), the triple and quadruple variants (Panel – B) over 72 hours at protein concentrations of 33 µM and 165 µM of thrombin. Panel – A: wtFGF1 (blue), R136E (brown), K126N-DM (red), Q54P-DM (teal), S61L-DM (green), H107S-DM (golden). Panel – B: wtFGF1 (blue), Q54P-TM (yellow), S61L-TM (red), H107S-TM (green), H107S-QM (teal), and S61L-QM (gray).

ANS binding and limited enzymatic digestion experiments lead us to an understanding that the designed variants of hFGF1 render decreased flexibility to the growth factor. The reversal of charge at position 136 (R136E) produces a counter-ion effect and aids in the partial nullification of the repulsions experienced by closely placed positive charges in the heparin binding pocket. The counterion effect introduced in the heparin binding pocket due to the introduction of R136E mutation not only decreases the flexibility of the heparin binding pocket, but also renders the FGF1 molecule more compact [12]. This aspect appears to make the potential trypsin cleavage sites in hFGF1 less accessible to the enzyme. Another reason for the increased resistance of the designed hFGF1 mutations might be due to the substitution of one of the three arginine residues to glutamic acid (arginine is one of the trypsin cleavage site). However, it is highly unlikely that substitution of just one Arg to Glu could decrease the susceptibility of the protein to trypsin so predominantly in hFGF1 variant than wtFGF1. So, it appears that the substitution of Arg to Glu changes the conformation flexibility by rendering the molecule more compact due to the plausible introduction of a new electrostatic interaction between E136 with a neighboring positively charged amino acid in the heparin binding pocket. On the other hand, reduced susceptibility of the R136E variant to the action of thrombin could be primarily because of the removal of secondary thrombin cleavage site (R136) caused by the replacement of arginine to glutamic acid. Therefore, out of the other four mutations (K126N, Q54P, S61L, H107S), R136E was chosen as the basis of the project. K126N mutation also lies in the heparin binding pocket. It appears that substitution of Lys with Asn at position 126 led to introduction of two new hydrogen bonds (N126-S130 and G129-N126). Thus, introduction of new interactions happens to make the potential trypsin cleavage site in hFGF1 less accessible to trypsin [29].

Introduction of R136E/K126N/Q54P/S61L mutation increases the thermal stability of hFGF1

The unfolding of the proteins under increasing temperature were monitored by the change in intrinsic fluorescence intensity at 305 nm/350 nm. The intrinsic fluorescence spectrum of properly folded wtFGF1 shows an emission maximum at around 305 nm, characteristic for the eight tyrosine residues. The signal from the single tryptophan residue (Trp121) is completely quenched by the surrounding lysine and proline residues. Upon unfolding, the tertiary structure becomes more relaxed and the quenching effect is weakened (the nearby proline and lysine residues move away from the indole ring or Trp), resulting in a significant increase in the fluorescence at 350 nm, characteristic for tryptophan residues.

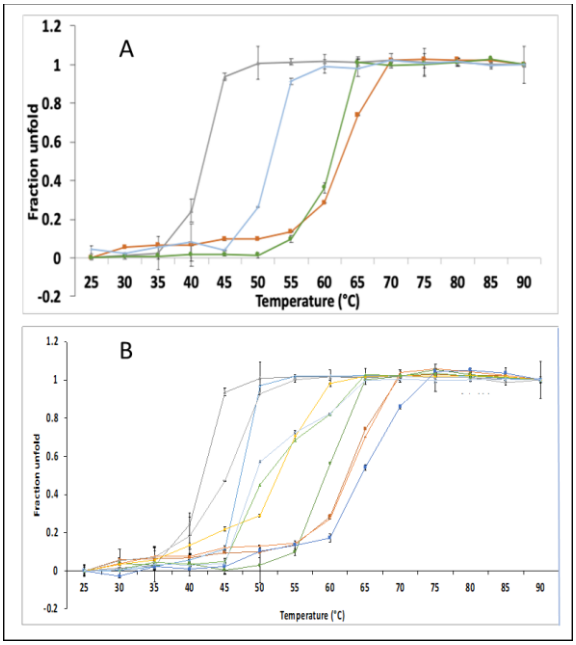

Fig. 12: Thermal stability analysis of the R136E (Panel – A) and double variants (Panel – B) in the presence and absence of heparin. Panel – A: wtFGF1 with hep (orange), wtFGF1 without hep (gray), R136E with hep (green), and R136E without hep (blue). Panel – B: wtFGF1 with hep (red), wtFGF1 without hep (gray), H107S-DM with hep (dark green), H107S-DM without hep (blue), S61L-DM with hep (orange), S61L-DM without hep (graphite), Q54P-DM with hep (teal), Q54P-DM without hep (yellow), K126N-DM without hep (aqua), and K126N-DM with hep (light green).

The thermal stability data reveal that the R136E/K126N/Q54P/S61L mutation is the most stable design of all the hFGF1 variants, with the T_m being 62 ± 0.23˚C in the absence of heparin and 63 ± 0.36˚C in the presence of heparin (Fig. 13D).

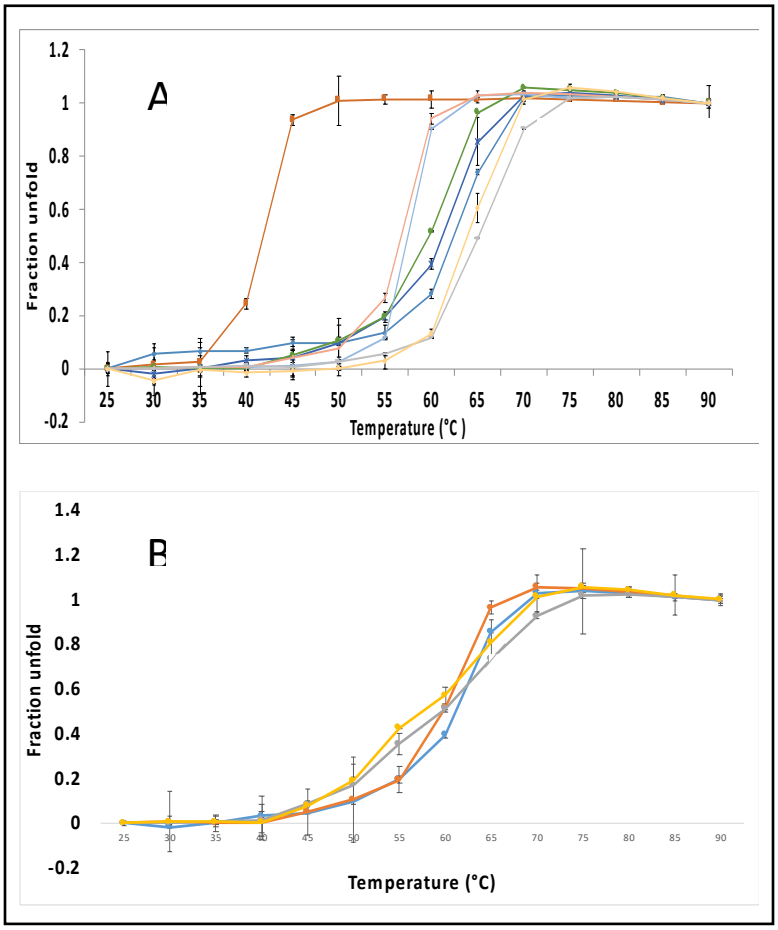

Fig. 13: Thermal stability analysis of the triple variants (Panel -A) and quadruple variants (Panel – B) in the presence and absence of heparin. Panel – A: wtFGF1 without hep (red), wtFGF1 with hep (blue), Q54P-TM with hep (teal), Q54P-TM without hep (green), H107S-TM with hep (aqua), H107S-TM without hep (orange), S61L-TM with hep (gray), and S61L-TM without hep (yellow). Panel – B: S61L-QM with hep (blue), S61L-QM without hep (orange), H107S-QM with hep (gray), and H107S-QM without hep (yellow).

It has also been shown in Table 2 that unlike the other variants tested, the thermal stability of R136E/K126N (ΔT_m - 2 ± 0.16˚C), the triple [R136E/K126N/S61L (ΔT_m - 1 ± 0.02˚C), R136E/K126N/Q54P (ΔT_m - 1 ± 0.15˚C), and R136E/K126N/H107S (ΔT_m - 1 ± 0.05˚C)] and the quadruple variants [R136E/K126N/Q54P/S61L (ΔT_m - 1 ± 0.13˚C),

R136E/K126N/Q54P/H107S (ΔT_m - 2 ± 0.04˚C)], is independent of heparin whereas the thermal stability of the other double variants [R136E/S61L (ΔT_m - 17 ± 0.05 ˚C), R136E/H107S (ΔT_m - 12 ± 0.23 ˚C), and R136E/Q54P (ΔT_m - 10 ± 0.11 ˚C)] and the R136E variant (ΔT_m - 9 ± 0.18 ˚C) still depends on heparin, in fact, it increases in the presence of heparin (Figs. 12 and 13).

T_m is the denaturation temperature at which 50% of the protein population exists in the denatured state(s). ΔT_m (T_m with heparin - T_m without heparin) analysis of wtFGF1 shows that heparin protects wtFGF1 from degrading at higher temperatures. Higher ΔT_m value indicates higher dependency of the growth factor on heparin. Of the four double variants (R136E/S61L, R136E/H107S, R136E/Q54P, and R136E/K126N), R136E/K126N is the only variant, wherein the ΔT_m value was observed to drop by ~ 2˚C. This implies that the R136E/K126N variant of hFGF1 has a higher inherent stability than the wtFGF1 alone. As R136E/K126N double variant was the basis for the triple and the quadruple variant, it is reasonable to expect that these variants do not exhibit heparin binding affinity.

Table 2: Comparison of the thermal stability of the wtFGF1 and the designed variants.

hFGF1 variants	**T_m without heparin (Celsius)**	**T_m with heparin (Celsius)**	**Δ T_m (Celsius)**
wtFGF1	42 ± 0.05	63 ± 0.08	21 ± 0.03
R136E	52 ± 0.60	61 ± 0.42	9 ± 0.18
R136E/K126N	49 ± 0.25	51 ± 0.41	2 ± 0.16
R136E/H107S	46 ± 0.59	58 ± 0.82	12 ± 0.23
R136E/S61L	43 ± 0.04	60 ± 0.09	17 ± 0.05
R136E/Q54P	52.5 ± 0.12	62.5 ± 0.23	10 ± 0.11
R136E/K126N/Q54P	58.5 ± 0.17	59.5 ± 0.32	1 ± 0.15
R136E/K126N/S61L	63 ± 0.6	64 ± 0.62	1 ± 0.02
R136E/K126N/H107S	55 ± 0.26	56 ± 0.31	1 ± 0.05
R136E/K126N/Q54P/S61L	62 ± 0.23	63 ± 0.36	1 ± 0.13
R136E/K126N/Q54P/H107S	58 ± 0.17	60 ± 0.21	2 ± 0.04

Overall, the thermal equilibrium unfolding data indicate that substituting Arg with Glu at position 136, Lys by Asn at position 126, Gln by Pro at position 54, Ser by Leu at position 61, and His by Ser at position 107 helped in stabilizing the growth factor. Out of all the variant combinations, the highest thermal stability is exhibited by the quadruple variant (R136E/K126N/Q54P/S61L) where the T_m without heparin is 62˚C, which is nearly 67% more when compared to wtFGF1 in the absence of heparin (T_m - 42˚C). The thermal stability has a positive relation with the half-life of a protein. It appears that K126N eliminates the heparin binding affinity and S61L mutation confers higher thermal stability because replacement of serine, a polar amino acid with leucine, a non-polar amino acid appears make the hFGF1 structure more compact. This compactness might strengthen the interactions (H-bond and salt bridges) inside the protein core and stabilize the protein against thermal and enzymatic degradation. These conclusions are consistent with the conclusions drawn from the limited proteolytic digestion data.

The R136E/K126N variant causes complete loss of heparin binding affinity

Isothermal titration calorimetry (ITC) was used to directly determine the heparin binding affinity of wtFGF1 and its variants. The binding affinities, reported as K_d values, are derived from the ITC data (Fig. 14). A small K_d value indicates a high binding affinity, while a large K_d value indicates a low binding affinity. Fig 14 depicts that the heparin binding affinity of R136E (K_d - 4.2 µM), R136E/S61L (K_d - 4.5 µM), R136E/H107S (K_d - 4.6 µM), R136E/Q54P (K_d - 3.1 µM) is lower than that of wtFGF-1 (K_d - 1.6 µM). This infers that the hFGF1 variants exhibit weaker heparin binding affinity than wtFGF1. Contrastingly, the R136E/K126N (K_d - could not be determined) variant lacks the ability to bind to heparin suggesting that R136 and K126 are critical for the heparin binding of hFGF1. The unusual heat changes in the isothermograms are

due to the electrostatic interactions between the charged heparin molecules and some of the charged components present in the buffer. Furthermore, as R136E/K126N was the basis for the third mutation, all the triple and quadruple variants lacked heparin binding affinity as shown in Table 3. This data clearly suggests that the charge reversal at position 136 (R136E) and charge neutralization at position 126 (K126N) are important residues for the heparin interaction.

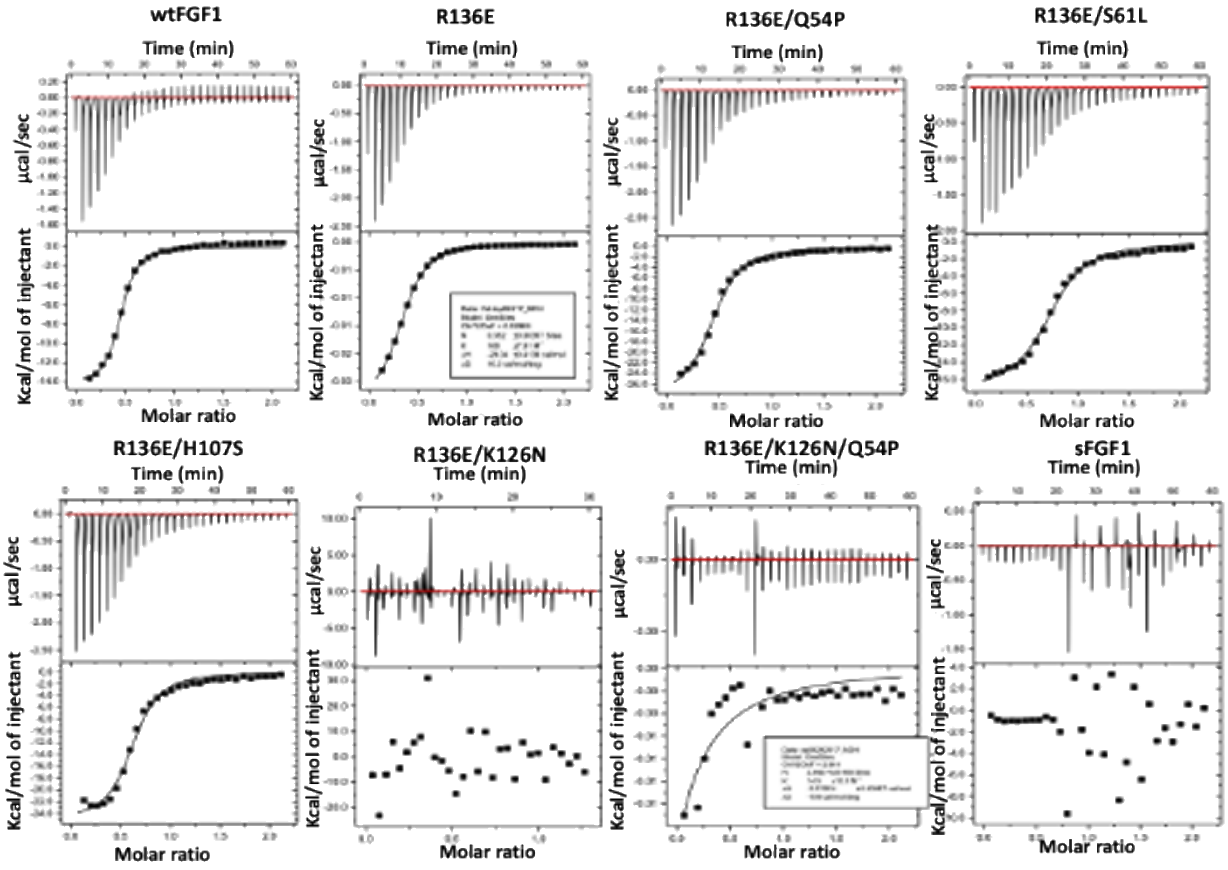

Fig 14: Isothermograms representing titration of wtFGF1 and all the designed variants with heparin.

Table 3: Heparin binding affinity of wtFGF1 and its variants.

hFGF1 variants	K_d (μM)
wtFGF1	1.6
R136E	4.2
R136E/K126N	No binding
R136E/H107S	4.6
R136E/S61L	3.1
R136E/Q54P	4.5
R136E/K126N/Q54P	No binding
R136E/K126N/S61L	No binding
R136E/K126N/H107S	No binding
R136E/K126N/Q54P/ S61L	No binding
R136E/K126N/Q54P/ H107S	No binding

The complete loss of heparin binding affinity observed for the R136E/K126N variant but not for R136E variant is probably due to the knockout of two positively charges residues in the heparin binding region (Table 3). Examination of the X-ray crystal structure of acidic hFGF shows that the region from residues 105-128 contains eight basic amino acids, making it conducive for heparin binding. Perhaps, most significantly, the crystal structure of hFGF1 suggests that heparin interacts with K132, K126, and R136 [31]. Therefore, R136E variant appears to decrease the heparin binding affinity by 2.5 times but could not knock down the ability of hFGF1 to bind to heparin completely. On the other hand, substitution of two of the three residues (K126N and R136E) located in the core heparin binding triad (K132, K126, and R136) might lead to the complete knock down of hFGF1's ability to bind to heparin. This is expected because introduction of a negative charge and a neutral amino acid in the heparin

binding pocket of hFGF1 could plausibly reduce the repulsion between the positively charged amino acids. The reduction in the charge-charge repulsion in the heparin binding region might have led to a heparin independent hFGF1 variant (R136E/K126N). The distance between the Cα atoms of R136 from Cα atom of R133 (located in the middle of the heparin binding pocket) in the absence of heparin is 7.15 Å and the distance between the Cα atoms of K126 from Cα atom of R133 is 13.24 Å. In the presence of heparin, R136 and K126 shift moderately closer to R133 (~5.15 Å and 9.57 Å, respectively). Surprisingly, the distance of residues E136 and N126, irrespective of the presence of heparin, is quite similar to the wtFGF1 in the presence of heparin (E136 - 9.68 Å and N126 - 5.16 Å). This indicates that introduction of these two mutations (R136E and K126N) bring conformational changes in the heparin binding region making the hFGF1 molecule more compact and heparin independent.

Introduction of R136E variant enhances the bioactivity of hFGF1

hFGF1 is a heparin binding protein capable of stimulating mitogenic and angiogenic responses in a variety of cell types. There have been several studies which suggest that heparin is mandatory for the activation of the FGF receptor. In this context, decrease in heparin binding affinity of hFGF1 variants to heparin can be expected to decrease the ability of the growth factor variants to promote cell proliferation activity. However, comparison of the cell proliferation activity of wtFGF1 with those observed for the different variants clearly show that lack of heparin binding affinity of hFGF1 does not significantly affect their cell proliferation activity. Out of all, only R136E, R136E/H107S, R136E/S61L, and R136E/Q54P are the hFGF1 variants which exhibit reduced heparin binding affinity. The other variants (R136E/K126N, R136E/K126N/Q54P, R136E/K126N/S61L, R136E/K126N/H107S, R136E/K126N/Q54P/S61L, and R136E/K126N/Q54P/H107S) do not bind to heparin. Fig. 15A indicates that at all the

concentrations of hFGF1, R136E exhibits higher cell proliferation activity than wtFGF1 although, the heparin binding affinity is lower than that of wtFGF1. Figs. 15 and 16 shows that all the hFGF1 variants display higher mitogenic activity than wtFGF1 irrespective of their heparin binding affinity.

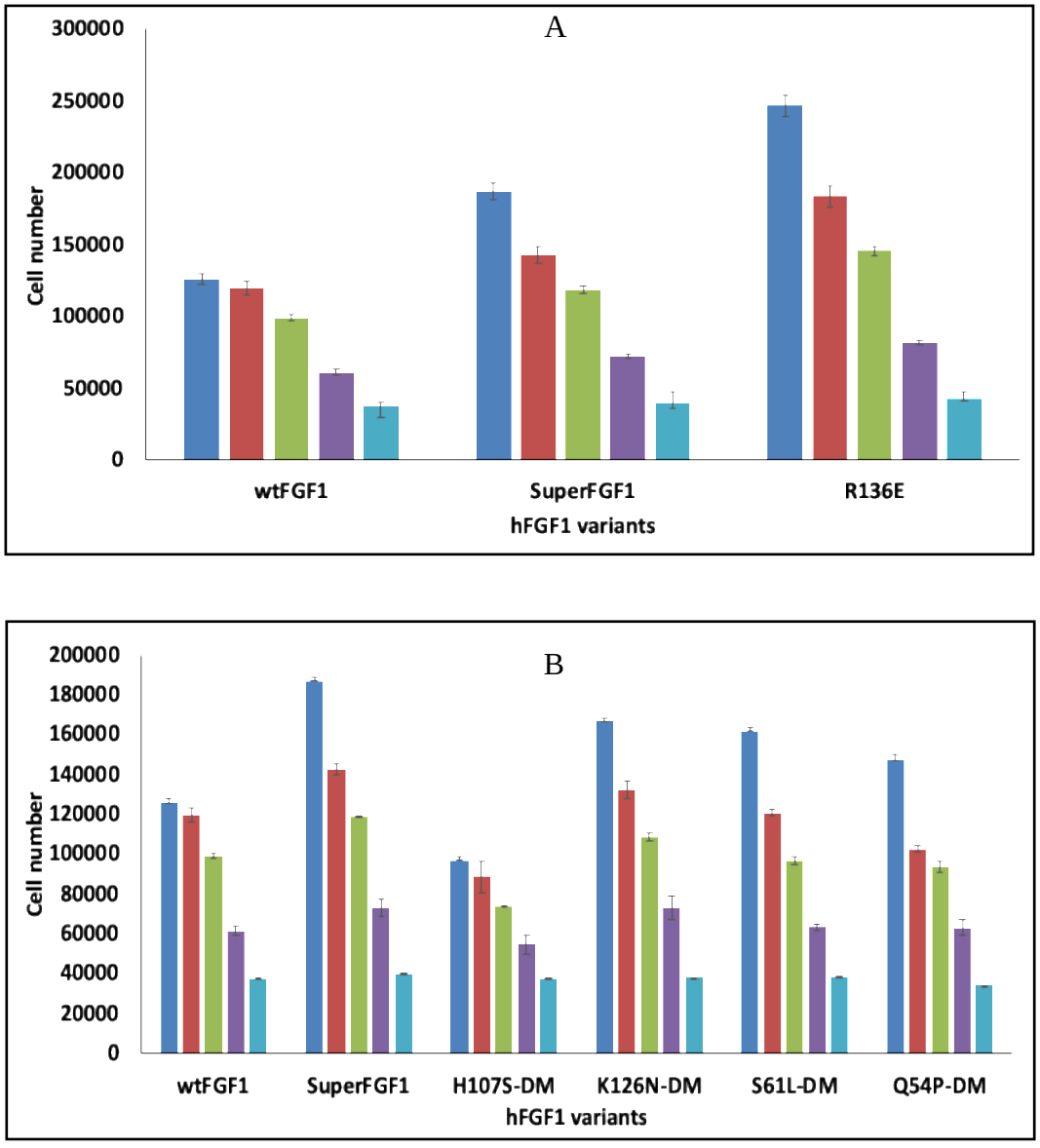

Fig. 15: Cell proliferation activity of NIH 3T3 cells treated with wtFGF1 and R136E (Panel – A) and wtFGF1 and double variants (Panel – B). 50 ng/mL (blue), 10 ng/mL (red), 2 ng/mL (green), 0.4 ng/mL (purple), and 0 ng/mL (aqua).

Overall, this data suggests that there is no positive correlation between the heparin binding affinity and the cell proliferation activity. There have been several reports which suggest that heparin dependent hFGF1 activity is necessary for the receptor activation. Contrastingly, there are other groups which demonstrate that the former is not true. Moscatelli *et al.*, have reported in their study that human FGF2 interacts with its receptor even when hFGF2 is not bound to heparin [32]. Several site-directed mutagenesis reports on hFGF1 are working on improving the proteolytic and enzymatic stability. A study by Ortega *et al.*, where they substitute the cysteine residues by serine (C30S, C131S, C97S) led to decreased heparin binding affinity, yet the variants exhibited longer physiological half-life and increased mitogenic activity [14]. Similar observation was made by other groups, which showed that heparin binding is not essential for the FGFR activation and inducing downstream signaling pathways [15, 33]. The K132E mutation was observed to exhibit significantly lower heparin dependency as compared to that of wthFGF1 [18, 33]. Additionally, Brych *et al.*, reported that higher stability is directly related to the higher bioactivity irrespective of heparin binding [15].

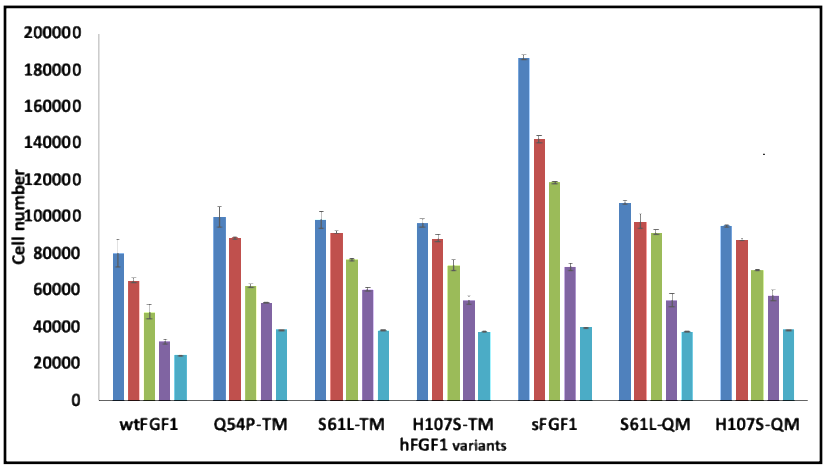

Fig. 16: Cell proliferation activity of NIH 3T3 cells treated with wtFGF1, triple and quadruple variants. 50 ng/mL (blue), 10 ng/mL (red), 2 ng/mL (green), 0.4 ng/mL (purple), and 0 ng/mL (aqua).

Zakrzewska *et al.*, examined the biological and biophysical properties of 17 variants of hFGF1 which include single mutation of lysine residues (at positions 126 and 132), double mutations of the same lysine residues and a few multiple variants where in along with lysine mutation they included different combinations of Q54P, S61I, and H107G [13, 29]. It was observed that the single mutation (K126N and K132E) exhibit reduced heparin affinity but yet displayed higher mitogenic activity than wtFGF1. In case of the double substitution (K132E/K126N), the variant exhibits strongly reduced affinity for heparin but did not show any difference in the mitogenic activity in the presence or absence of heparin. However, K126N/Q54P/S61I/H107G, a quadruple variant exhibited reduced heparin binding ability and showed two-folds higher mitogenic activity than wtFGF1 in absence of heparin [16, 29]. In conclusion, almost all the mutations exhibited reduced heparin binding affinity and prolonged mitogenic activity in comparison to wtFGF1 [16, 17]. Most of the mutations were known to increase the T_m up to 64°C. Thus, our results are in good agreement with many hFGF1 and hFGF2 studies, which state~~s~~ that the FGF-FGFR complex can still be formed in the absence of heparin and can lead to activation of the signaling complex.

Conclusions

The hFGF1-heparin complex is the most extensively studied protein-glycosaminoglycan complex. There have been two opposing arguments regarding the role of heparin in the biological function of hFGF1. X-ray crystal structure studies have established the fact that heparin plays a critical role in the receptor activation of hFGF1. On the contrary, there have been reports that demonstrate that heparin only improves the stability of hFGF1 through electrostatic interactions. The results of the current study show that heparin appears to influence the stability of the growth factor but has very little effect on the cell proliferation activity of the protein.

Isothermal titration calorimetric results from this study show that the R136 and K126 positions are critical for the heparin binding ability of hFGF1. The cell proliferation assay results were one of the most important outcomes for the future application of this research, which concluded that all the heparin-independent variants of hFGF1 show higher mitogenic activity than wtFGF1. Overall, the results obtained in the current chapter suggest that introduction of specific mutations of R136E, K126N, S61L, H107S and Q54P into wtFGF1 causes hFGF1 to lose its heparin binding affinity, gain cell proliferation activity and enhance its thermal, chemical, and proteolytic stability when compared to wtFGF1.

Materials and methods

Materials

Agilent was the producer for the site directed mutagenesis kit and the competent cells (XL-gold, BL 21 plysS, BL 21 star). The plasmid isolation kit was obtained from Qiagen Inc., USA. Lysogeny broth was purchased from IBI Scientific, USA. Heparin sepharose resin was obtained from GE Healthcare, USA. VWR Scientific., USA supplied the buffer components (Na_2HPO_4, NaH_2PO_4, NaCl). Low molecular weight (~3000 Da) heparin sodium salt was obtained from Sigma and MP Biomedicals LLC. NIH 3T3 cells were obtained from ATCC and all the cell culture reagents including, DMEM media, fetal bovine serum (FBS) and penicillin streptomycin were purchased from Thermo Fisher Scientific (Waltham, MA). All other chemicals and materials were of high-quality analytical grade. Due to the polydisperse nature of high molecular weight of heparin, we have used low molecular weight heparin (M.wt ~ 3000 Da) for this study. Unless otherwise stated, samples were made in 10 mM phosphate buffer saline (pH 7.2) and incubated at 37 ºC.

Construction and Purification of hFGF1 and the variants

Site-directed mutagenesis was employed to construct the mutations (R136E, K126N, Q54P, S61L, and H107S) (Fig. 17, Table 4). For expression of hFGF1, BL-21star cells were grown to an Optical Density of 0.6–8.0 at Abs of 600 and incubated with 1 mM isopropyl β-D-thiogalactoside for 2.5 hours. Cells were harvested and resuspended in 10 mM phosphate buffer (PB). Cells were sonicated for 30 cycles with 20 second on/off pulses. Supernatant was separated from the cell debris using centrifugation at 19,000 rpm for 30 minutes and subsequently passed over heparin Sepharose affinity column that was then washed extensively with equilibration buffer (10 mM phosphate buffer). The proteins were purified using step-wise sodium chloride gradient. Certain variants were further purified using gel filtration chromatography. The hFGF1 variants were loaded onto a Superdex 75(S-75) column (GE Healthcare, Pittsburgh, PA) equilibrated in 10 mM phosphate buffer and 100 mM NaCl, pH 7.2 on an AKTA FPLC and ran at a flow rate of 1 milliliter per minute. The elution volume was monitored by absorbance at 280 nm. Fractions were collected and the purity of proteins were verified using 15% Sodium Dodecyl Sulfate Poly Acrylamide Gel Electrophoresis (SDS-PAGE) followed by staining with Coomasie brilliant blue. The concentration of the protein was quantified using the Bradford method [24,25].

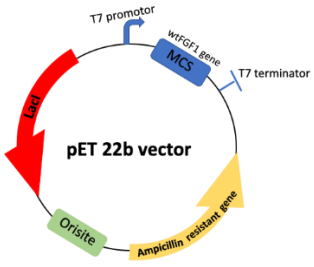

Fig. 17: pET20 expression vector with recombinant wtFGF1 gene and ampicillin resistant gene.

Table 4: Codon changes in *E.coli* corresponding to the mutations.

Amino acid change	Codon present in wtFGF1	Codon present in sFGF1
Arg to Glu	CGG	GAG
Lys to Asn	AAG	AAC
Ser to Leu	AGT	CTT
Gln to Pro	CAG	CCG
His to Ser	CAT	AGT

Circular Dichroism and fluorescence spectroscopy

Using a combo circular dichroism / fluorescence Jasco J-1500 Spectrophotometer dual results of the CD and fluorescence spectra were obtained to determine the secondary and tertiary structural changes of wtFGF1 and hFGF1 in the presence and absence of heparin. Circular dichroism is used to determine the secondary structural changes in the protein. For analysis, 13µM of protein was added to 10 mM PB + 100 mM NaCl and loaded into a 0.1 cm path length quartz cell. The wavelength of the spectrophotometer was set in a range of 190 - 250nm at 25ºC, and the scanning speed was 20 nm/min. The data of CD was collected as an average of three scans. The resultant CD data was expressed in terms of molar ellipticity.

Intrinsic fluorescence spectroscopy was used to examine any alternation in the tertiary structure and folding of protein by combining 13 µM protein with 10 mM phosphate buffer (PB). The excitation wavelength for the fluorescence measurements was 280 nm and the emission were recorded from 300 – 450 nm. Intrinsic fluorescence was done at these wavelengths to study if there were any changes among tyrosine and tryptophan residues, which fluoresce at 308 and 340 nm, respectively. A buffer subtraction was made to correct any background noise.

8-Anilino-1-napthalenesulfonic acid (ANS) binding assay

ANS binding assay measurements were made using a Fluorescence Spectrophotometer F-2500 (Hitachi) with a slit width set to 2.5nm. Protein concentrations of 33 µM in phosphate buffer containing 100 mM NaCl, pH 7.2 were placed in a quartz cuvette. Titrations using an ANS stock were made by addition of 10 µM increments of ANS followed with mixing and incubation for 2 minutes preceding each reading at 25ºC. Fluorescence intensity was determined with an excitation at 380nm and emission intensity was recorded at 510nm.

Limited Trypsin and thrombin digestion

Limited trypsin digestion of hFGF1 and the variants was performed in phosphate buffer containing 100 mM NaCl, pH 7.2. The initial reaction tube contained 50 µM of protein and 0.5 µg of enzyme. The trypsin and thrombin containing samples were incubated at room temperature (25 °C) and 37 °C respectively. Digested samples were removed at specific intervals as noted in the results section and then the reaction was stopped by the addition of 10% trichloroacetic acid and the samples were resolved on a 15% sodium dodecyl sulfate-polyacrylamide gel electrophoresis (SDS− PAGE) gel and subsequently stained using Coomassie brilliant blue. The percentage of enzymatic digestion was identified from the band intensity, on the SDS PAGE gel, using UN-ScanIT densiometric software (Silk Scientific Inc.). hFGF1 samples which were not subjected to the enzymatic digestion was considered as the control representing 100% undigested hFGF1.

Equilibrium unfolding

Intrinsic fluorescence using the Jasco J-1500 Spectrophotometer was used to monitor the unfolding nature of hFGF1 and the variants at increasing thermal intervals. The protein concentration used was 50 µM in 10 mM phosphate buffer and 100 mM NaCl (pH 7.2). A

temperature probe was inserted into the sample cell to heat the sample. Fraction of protein unfolded was calculated from the ratio of the wavelength of emission maxima (305/350 nm) observed during chemical denaturant titration. Thermal denaturation as probed by fluorescence was carried by heating of samples at 5-degree increments for 5 minutes.

Isothermal titration calorimetry

The binding affinity of hFGF1 and the variants with heparin were measured using a Microcal VP-ITC Micro Calorimeter. The wtFGF1 and the designed variants were prepared at a concentration of 100 mM. Heparin in the syringe was at a concentration of 1000 mM (to maintain a 1:10 protein: ligand ratio). All samples were degassed before loading. The volume of heparin injections was 6 mL and a total of 49 titrations were performed at 25 °C. The data was analyzed using Origin scientific plotting software.

Bioactivity Assay

3T3 fibroblast cells obtained from ATCC (Manassas, VA) were cultured in media consisting of DMEM supplemented with 10% bovine calf serum. Cells were grown and were incubated overnight at 37 °C. The bioactivity of FGF1 was determined by quantifying the cell number increase after the cells were incubated with hFGF1. Starved 3T3 fibroblasts were collected and seeded in a well plate at a seeding density of 10,000 cells/well. The bioactivity assays were performed five times under the same condition. 3T3 cell proliferation was assessed by the Cell Titer-Glo (Promega, Madison, WI) cell proliferation assay after 24 hours.

REFERENCES

[1] Brewer JR, Mazot P, Soriano P. Genetic insights into the mechanisms of Fgf signaling. Genes & development. 2016 Apr 1;30(7):751-71.

[2] Hui Q, Jin Z, Li X, Liu C, Wang X. FGF family: from drug development to clinical application. International journal of molecular sciences. 2018 Jul;19(7):1875.

[3] Ornitz DM, Itoh N. Fibroblast growth factors. Genome biology. 2001 Mar;2(3):reviews3005-1.

[4] Itoh N, Ornitz DM. Fibroblast growth factors: from molecular evolution to roles in development, metabolism and disease. The Journal of Biochemistry. 2011 Feb 1;149(2):121-30.

[5] Arunkumar AI, Srisailam S, Kumar TK, Kathir KM, Chi YH, Wang HM, Chang GG, Chiu M, Yu C. Structure and stability of an acidic fibroblast growth factor from Notophthalmus viridescens. Journal of Biological Chemistry. 2002 Nov 29;277(48):46424-32.

[6] Davis JE, Alghanmi A, Gundampati RK, Jayanthi S, Fields E, Armstrong M, Weidling V, Shah V, Agrawal S, prasanth Koppolu B, Zaharoff DA. Probing the role of proline− 135 on the structure, stability, and cell proliferation activity of human acidic fibroblast growth factor. Archives of biochemistry and biophysics. 2018 Sep 15;654:115-25.

[7] Itoh N, Ornitz DM. Evolution of the Fgf and Fgfr gene families. TRENDS in Genetics. 2004 Nov 1;20(11):563-9.

[8] Häcker U, Nybakken K, Perrimon N. Heparan sulphate proteoglycans: the sweet side of development. Nature reviews Molecular cell biology. 2005 Jul;6(7):530-41.

[9] Copeland RA, Ji H, Halfpenny AJ, Williams RW, Thompson KC, Herber WK, Thomas KA, Bruner MW, Ryan JA, Marquis-Omer D, Sanyal G. The structure of human acidic fibroblast growth factor and its interaction with heparin. Archives of biochemistry and biophysics. 1991 Aug 15;289(1):53-61.

[10] Eswarakumar VP, Lax I, Schlessinger J. Cellular signaling by fibroblast growth factor receptors. Cytokine & growth factor reviews. 2005 Apr 1;16(2):139-49.

[11] Lee J, Blaber M. The interaction between thermodynamic stability and buried free cysteines in regulating the functional half-life of fibroblast growth factor-1. Journal of molecular biology. 2009 Oct 16;393(1):113-27.

[12] Kerr R, Agrawal S, Maity S, Koppolu B, Jayanthi S, Kumar GS, Gundampati RK, McNabb DS, Zaharoff DA, Kumar TK. Design of a thrombin resistant human acidic

fibroblast growth factor (hFGF1) variant that exhibits enhanced cell proliferation activity. Biochemical and Biophysical Research Communications. 2019 Oct 15;518(2):191-6.

[13] Szlachcic A, Zakrzewska M, Krowarsch D, Os V, Helland R, Smalås AO, Otlewski J. Structure of a highly stable mutant of human fibroblast growth factor 1. Acta Crystallographica Section D: Biological Crystallography. 2009 Jan 1;65(1):67-73.

[14] Ortega S, Schaeffer MT, Soderman D, DiSalvo J, Linemeyer DL, Gimenez-Gallego G, Thomas KA. Conversion of cysteine to serine residues alters the activity, stability, and heparin dependence of acidic fibroblast growth factor. Journal of Biological Chemistry. 1991 Mar 25;266(9):5842-6.

[15] Brych SR, Blaber SI, Logan TM, Blaber M. Structure and stability effects of mutations designed to increase the primary sequence symmetry within the core region of a β-trefoil. Protein Science. 2001 Dec;10(12):2587-99.

[16] Zakrzewska M, Krowarsch D, Wiedlocha A, Olsnes S, Otlewski J. Highly stable mutants of human fibroblast growth factor-1 exhibit prolonged biological action. Journal of molecular biology. 2005 Sep 30;352(4):860-75.

[17] Zakrzewska M, Krowarsch D, Wiedlocha A, Otlewski J. Design of fully active FGF-1 variants with increased stability. Protein Engineering Design and Selection. 2004 Aug 1;17(8):603-11.

[18] Huang Z, Tan Y, Gu J, Liu Y, Song L, Niu J, Zhao L, Srinivasan L, Lin Q, Deng J, Li Y. Uncoupling the mitogenic and metabolic functions of FGF1 by tuning FGF1-FGF receptor dimer stability. Cell reports. 2017 Aug 15;20(7):1717-28.

[19] Xia X, Kumru OS, Blaber SI, Middaugh CR, Li L, Ornitz DM, Suh JM, Atkins AR, Downes M, Evans RM, Tenorio CA. An S116R phosphorylation site mutation in human fibroblast growth factor-1 differentially affects mitogenic and glucose-lowering activities. Journal of pharmaceutical sciences. 2016 Dec 1;105(12):3507-19.

[20] Thallapuranam SK, Agarwal S, Gindampati RK, Jayanthi S, Wang T, Jones J, Kolenc O, Lam N, Niyonshuti I, Balachandran K, Quinn K, inventors. Engineered fgf1 and fgf2 compositions and methods of use thereof. United States patent application US 16/356,872. 2019 Sep 19.

[21] Kimura S, Kanaya S, Nakamura H. Thermostabilization of Escherichia coli ribonuclease HI by replacing left-handed helical Lys95 with Gly or Asn. Journal of Biological Chemistry. 1992 Nov 5;267(31):22014-7.

[22] Stites WE, Meeker AK, Shortle D. Evidence for strained interactions between side-chains and the polypeptide backbone. Journal of molecular biology. 1994 Jan 7;235(1):27-32.

[23] Takano K, Yamagata Y, Yutani K. Role of amino acid residues in left-handed helical conformation for the conformational stability of a protein. Proteins: Structure, Function, and Bioinformatics. 2001 Nov 15;45(3):274-80.

[24] Hung KW, Kumar TK, Kathir KM, Xu P, Ni F, Ji HH, Chen MC, Yang CC, Lin FP, Chiu IM, Yu C. Solution structure of the ligand binding domain of the fibroblast growth factor receptor: role of heparin in the activation of the receptor. Biochemistry. 2005 Dec 6;44(48):15787-98.

[25] Powers CJ, McLeskey SW, Wellstein A. Fibroblast growth factors, their receptors and signaling. Endocrine-related cancer. 2000 Sep 1;7(3):165-97.

[26] Gasymov OK, Glasgow BJ. ANS fluorescence: potential to augment the identification of the external binding sites of proteins. Biochimica et Biophysica Acta (BBA)-Proteins and Proteomics. 2007 Mar 1;1774(3):403-11.

[27] Leiros HK, Brandsdal BO, Andersen OA, Os V, Leiros I, Helland R, Otlewski J, Willassen NP, Smalås AO. Trypsin specificity as elucidated by LIE calculations, X-ray structures, and association constant measurements. Protein science. 2004 Apr;13(4):1056-70.

[28] Göbel K, Eichler S, Wiendl H, Chavakis T, Kleinschnitz C, Meuth SG. The coagulation factors fibrinogen, thrombin, and factor XII in inflammatory disorders—a systematic review. Frontiers in immunology. 2018 Jul 26;9:1731.

[29] Zakrzewska M, Wiedlocha A, Szlachcic A, Krowarsch D, Otlewski J, Olsnes S. Increased protein stability of FGF1 can compensate for its reduced affinity for heparin. Journal of Biological Chemistry. 2009 Sep 11;284(37):25388-403.

[30] O'Brien R, Markova N, Holdgate GA. Thermodynamics in drug discovery. Applied biophysics for drug discovery. 2017 Aug 10:7-28.

[31] Volkin DB, Tsai PK, Dabora JM, Gress JO, Burke CJ, Linhardt RJ, Middaugh CR. Physical stabilization of acidic fibroblast growth factor by polyanions. Archives of biochemistry and biophysics. 1993 Jan 1;300(1):30-41.

[32] Rifkin DB, Moscatelli D. Recent developments in the cell biology of basic fibroblast growth factor. The Journal of cell biology. 1989 Jul;109(1):1-6.

[33] Wong P, Hampton B, Szylobryt E, Gallagher AM, Jaye M, Burgess WH. Analysis of putative heparin-binding domains of fibroblast growth factor-1 using site-directed mutagenesis and peptide analogues. Journal of Biological Chemistry. 1995 Oct 27;270(43):25805-11.

CHAPTER III

Design of a Human Acidic Fibroblast Growth Factor (hFGF1) Variant that has no Heparin Binding Affinity

Abstract

Human acidic fibroblast growth factor (hFGF1) is a member of a family of polypeptides that are involved in cell proliferation, cell differentiation, angiogenesis and wound healing. hFGF1 is known to exhibit low half-life *in vivo* and has poor thermal and proteolytic stability (T_m -37˚C). Binding of heparan sulfate, a glycosaminoglycan, stabilizes the protein and aids in activation of the biological response. However, heparin binding affinity of hFGF1 can be a significant disadvantage in healing topical wounds. In general, it is believed that high binding affinity of both hFGF1 and thrombin to heparin potentially increases the probability of thrombin to gain access to hFGF1 and render it inactive. In this context, generation of a bioactive hFGF1 variant that exhibits poor heparin binding may significantly decrease its susceptibility to thrombin cleavage. Surprisingly, results of the current study show that super FGF1 (sFGF1) exhibits enhanced cell proliferation activity, lacks heparin binding affinity, and shows an increased activation of Erk and Akt pathways when compared to wtFGF1. Limited enzymatic digestion and ANS binding experiments show that in comparison to wtFGF1, sFGF1 render less flexibility and less susceptibility of hFGF1 to the action of trypsin and thrombin. Thermal and urea equilibrium unfolding data suggest that sFGF1 exhibits significantly higher T_m (68˚C) and C_m (3.6 M) when compared to wtFGF1 (T_m -37˚C and C_m -1.2 M). Isothermal titration calorimetry data reveal that sFGF1 is the only known mutation till date which completely lacks heparin binding affinity. Overall, the results for hyperthermal stability, resistance to the action of

proteases, and enhanced heparin-independent bioactivity infer that sFGF1 can be used as a viable target for wound healing.

Introduction

Human acidic fibroblast growth factor (hFGF1) is a 16kDa mitogen that is characterized by its high affinity for heparin. It is one of the twenty-three different types of FGFs, all of which are involved in crucial cell-survival activities [1-3]. FGFs are vital for embryonic and fetal development, wound healing, bone fracture healing, neuroprotection, and tumor development and progression [4,5]. Fibroblast growth factor (FGF) signals cellular processes by activating the specific tyrosine kinase fibroblast growth factor receptors (FGFRs). Activated FGFRs in-turn induce downstream signaling through some common pathways such as: mitogen activated protein kinase (MAPK), phosphoinositide-3-kinase/AKT, and phospholipase-Cλ pathways [6]. hFGF1 uniquely binds to all the four types of FGFRs; therefore, it is often referred to as a universal ligand [7].

hFGF1 has an intrinsically low thermodynamic stability, and almost half of the wild type hFGF1 population is unfolded at physiological pH and temperature [8-10]. FGFs have high affinity for cell-surface proteoglycans, such as heparin sulfate (HSPGs) HSPGs are essential for the protein regulation especially in signal transmission and chemical recruitment [11]. Heparin-hFGF1 interaction mediates specific binding to the cell surface tyrosine kinase receptors, fibroblast growth factor receptors (FGFRs) and as a result mediates FGFs' biological response [12]. Heparin is a highly sulfated glycosaminoglycan made up of 2-O-sulfated iduronic acid and 6-O-sulfated, N-sulfated glucosamine, IdoA(2S)-GlcNS(6S), linked by α-(1→4) glycosidic linkages. Binding of heparin to hFGF1 ensures stability and confers better interaction of hFGF1 to its receptor [13-15]. X-ray crystal and solution NMR structures of heparin-hFGF1 complex

shows that the negatively charged heparin binds to the positively charged heparin binding region located at the C-terminal of hFGF1 [20]. Heparin-binding site (HBS) in hFGF1 spans residues between ß strands 1/2 and extends from the loop between β strands 9/10 to the loop between β strands 11/12 [21]. Crystal structure data on FGF-FGFR-HS ternary complex revealed that heparin promotes FGF signaling through the formation of a 2:2:2 or 2:2:1 (FGF: FGFR: HS) complexes [22]. The cluster of positively charged amino acids in the heparin binding region is accountable for the thermal and proteolytic instability of hFGF1 [9, 23, 24]. Therefore, it is believed that the binding of heparin to hFGF1 increases the stability of the protein [25]. However, there is significant debate whether or not heparin is mandatory for effective functioning of hFGF1. There have been reports which show that heparin is essential for the cell proliferation activity of hFGF1 [26-29]. In marked contrast, there are also studies which show that the role of heparin is only restricted to conferring stability to the growth factor [4, 8, 9-11, 30]. Interestingly, K132E mutation, in the heparin binding region has been shown to diminish the heparin binding affinity of hFGF1 and exhibit significant loss of cell proliferation activity [39].

hFGF1 has also been shown to be susceptible to thrombin cleavage [16,1]. Although hFGF1 lacks the primary thrombin cleavage site (-LVPRGS-), the enzyme has been known to specifically cleave hFGF1 at position R136 and render it biologically inactive. In this context, there have been several attempts to design hFGF1 variants that exhibit increased resistance to the action of thrombin [17]. Thus, all the three molecules, (hFGF1 (for its cell proliferation activity), thrombin (aid in blood clot formation), and heparin (to stabilize hFGF1 and act as an anticoagulant) are present at wound site. Studies have shown that the relationship of heparin with thrombin and hFGF1 at the wound site is competitive. Therefore, design of a heparin

independent hFGF1 variant might decrease the competition and consequently increase the wound healing potential of hFGF1 [1, 18].

Kerr *et al.*, has designed an hFGF1 variant, R136E, which has higher thermal stability, is more resistant to proteolytic degradation, and enhanced cell proliferation activity when compared to wtFGF1. However, R136E variant exhibits heparin binding affinity. In this context, the main objective of this chapter is to introduce mutations on R136E variant to further enhance its stability and cell proliferation activity in a heparin independent manner. This study also aims to understand the structural basis for the extraordinary properties introduced due to four additional mutations (K126N, S61L, H107S, and Q54P) on R136E (Fig. 1) [19]. In this context, due to its extraordinary stability and cell proliferation activity, we believe that it would be apt to name the penta mutant of hFGF1 as super-hFGF1 (sFGF1).

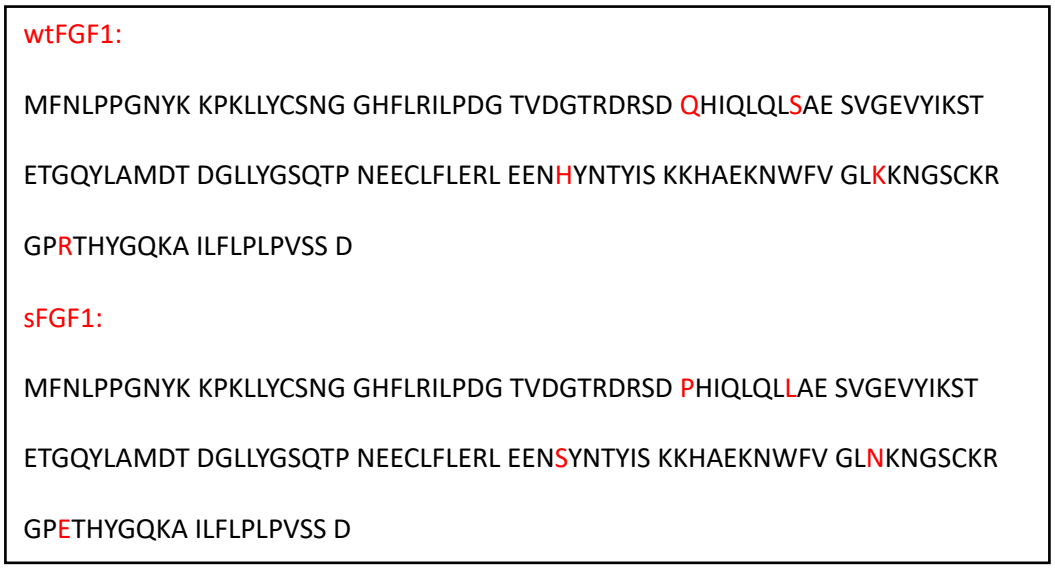

Fig. 1: Amino acid sequence of wtFGF1. The residues highlighted in red represent the mutated residues in wtFGF1 (R136E, K126N, Q54P, S61L, and H107S).

In order to accomplish this, mutational studies as well as various biophysical techniques and molecular dynamic simulations have been performed. Results of this study indicate that in

spite of significant differences in the stability, resistance to proteases, and enhanced cell proliferation activity, overall structure of hFGF1 was not found to be substantially perturbed due to introduction of the mutations. Amongst all other hFGF1 variants known so far, R136E/K126N/Q54P/S61L/H107S variant demonstrates zero heparin binding affinity. Results of the current study also indicate that introduction of five mutations led to formation of new electrostatic interactions and hydrogen bonds that are plausibly responsible for higher stability and enhanced cell proliferation activity of hFGF1.

Results and discussion

Spatial proximity of the penta mutations (Q54P, S61L, H107S, K126N, and R136E) in the structure of hFGF1

The crystal structure analysis of heparin-hFGF1 binary complex reveals that heparin is sandwiched between two FGF1 monomers. Heparin binding pocket (HBP) spans from residue N120 to H138 towards the C-terminal domain of hFGF1 [20,33]. Basic and polar amino acids of HBP (N32, K126, K127, N128, K132, Q141, K142) bind to the negatively charged heparin decasaccharide through electrostatic interactions [1]. These positively charged residues are primarily located in the flexible loops between beta strands X, XI, and XII. K127, K132, G134, and R136 are well conserved among different isoforms of FGF. Interestingly, alignment of amino acid sequences of FGF1 isolated from different species shows that residues in the heparin-binding pocket, including residues 132 to 137, are highly conserved. The well-conserved R136 and K126 residues are located in the heparin binding region. As mentioned above, HBP consists of positively charged residues, therefore, mutating a polar positively charged amino acid with a polar negatively charged residue (R136E) and substituting a polar positively charged amino acid with a polar neutral residue (K126N) can potentially decrease the repulsion between the closely

packed positively charged residues [1, 19]. Additionally, thrombin cleaves hFGF1 at R136, hence mutating Arg to Glu at position 136 will reduce the probability of thrombin induced FGF1 degradation [1]. Q54 is located within a turn between β-strands III and IV. Studies have shown that presence of proline in a β-turn rearranges the β-turn geometry and forms a short 3_{10}- helix. Therefore, Gln was mutated to Pro [19, 24]. H107 is located in the turn spanning β8/ β9 and is also involved in receptor binding. At the receptor binding site, His interacts with Arg at positions 251 and 255 of the D2 and D3 domain of the receptor [24]. To prevent the repulsion between His107 and Arg251 and 255, His was replaced with Ser. S61 is located in the middle of β-strand IV, which is close to the hydrophobic pocket in the hFGF1 structure. Thus, mutation of Ser to Leu (S61L) is predicted to increase the stability of the growth factor by rendering it more compact (Fig. 2) [1, 30].

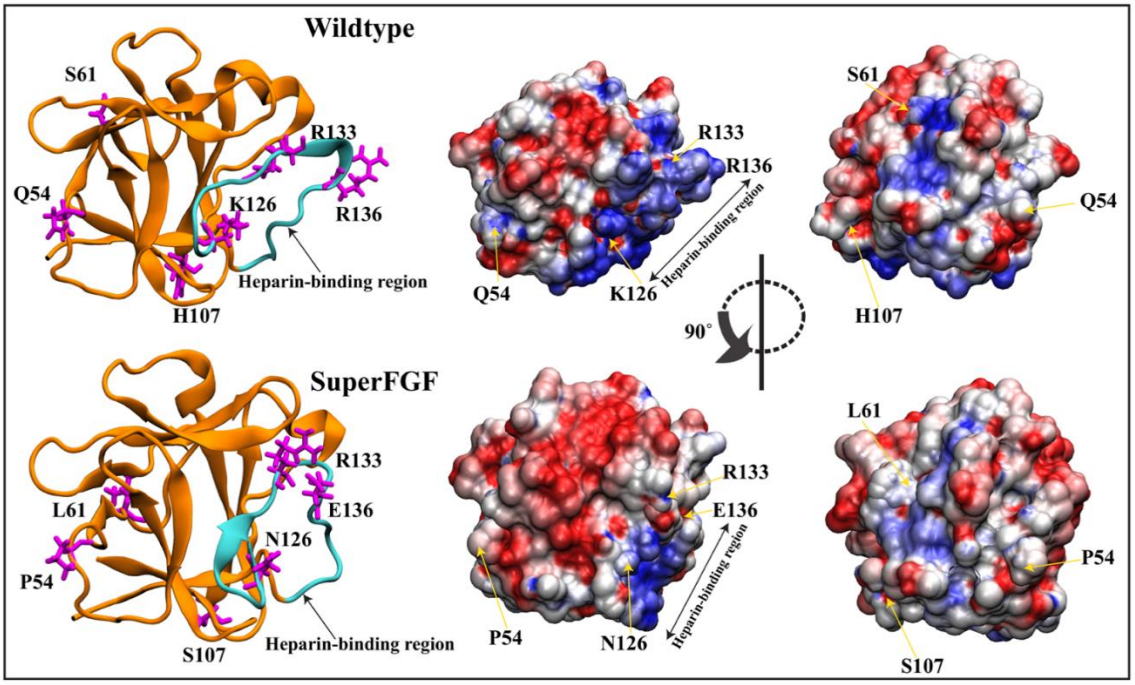

Fig. 2: Ribbon representation of wtFGF1 illustrating mutation sites and electrostatic potential map showing that the heparin binding region in wtFGF1 is flexible and extends outwards (Top panel). Ribbon representation and electrostatic potential map of sFGF1 showing that the heparin binding region is less flexible upon introduction of mutations (Bottom panel).

Construction and purification of pure wtFGF1 and super FGF1 (sFGF1)

wtFGF1 and sFGF1 were overexpressed in BL21-PlysS cells in LB medium. They were purified to homogeneity on a heparin sepharose matrix using affinity column chromatography. The proteins were eluted using a stepwise sodium chloride gradient. wtFGF1 exhibited strong heparin binding affinity and was eluted in 1.5 M sodium chloride concentration. In contrast, sFGF1 eluted from the column, along with some bacterial contaminants, in 10mM phosphate buffer with 0 mM NaCl. These results suggest that sFGF1, unlike wtFGF1, has no or very insignificant heparin binding affinity. sFGF1 was re-purified using gel filtration chromatography to obtain the pure protein (approximately 98% pure). The yields of purified wtFGF1 and sFGF1 were in the range of 35-40 mg/L of the bacterial culture. SDS-PAGE gels were analyzed using pure wtFGF1, purified and characterized previously, as a protein marker. Analysis of the results of SDS PAGE data shows that wtFGF1 elutes out in the 1500 mM NaCl fraction whereas sFGF1 elutes in the buffer wash (Fig. 3 A and B).

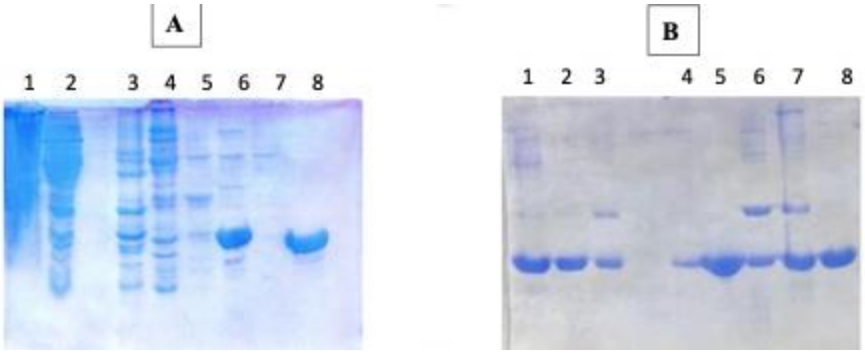

Fig. 3: SDS-PAGE analysis of protein fractions (A- wtFGF1 and B- sFGF1) eluted upon heparin sepharose chromatography at different concentrations of NaCl. Panel -A: Supernatant (Lane-1); 10 mM PB + 0 mM NaCl (Lane-2); 10 mM PB + 100mM NaCl (Lane-3); 10 mM PB + 300 mM NaCl (Lane-4); 10 mM PB + 500 mM NaCl (Lane-5); 10 mM PB + 1500 mM NaCl (Lane-6); and Pure wtFGF1 as a marker (Lane - 8). Panel-B: Supernatant (Lane-1); 10 mM PB + 0 mM NaCl (Lanes 2-5); 10 mM PB + 100 mM NaCl (Lanes 6 and 7); Pure wtFGF1 as a marker (Lane-8).

The sFGF1 fraction obtained from heparin sepharose chromatography was subjected to S-75 column, size-exclusion chromatography. The size-exclusion chromatography profile showed 4 peaks (Fig. 4A). The first peak corresponds to high molecular weight *E. coli* contaminants, the middle peak represents a fraction that contains pure sFGF1 protein (Fig. 4B), and the third and fourth peaks comprise of low molecular weight *E. coli* contaminants.

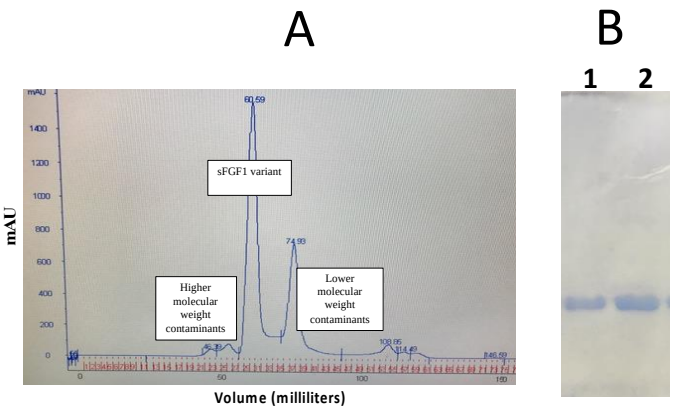

Fig. 4: Elution profile of sFGF1 (M.W- 15.9 kDa) from a S-75 size-exclusion column (Panel-A). Analysis of size-exclusion chromatographic profile by SDS-PAGE. wtFGF1 (Lane-1); sFGF1 (Lane-2) (Panel-B).

Mutations in sFGF1 does not cause substantial structural change

wtFGF1 contains eight tyrosine residues and a lone tryptophan at position 121 (Trp^{121}) [1]. Intrinsic fluorescence spectrum of native wtFGF1 shows only tyrosine fluorescence at 308 nm. In the native state, fluorescence of the tryptophan residue is completely quenched by the amine/imine groups of lysine and proline residues, which are located in close spatial proximity to Trp^{121}. However, when exposed to a denaturant, such as chemical or temperature, position of indole ring of tryptophan is shifted away from the lysine and proline residues, exposing tryptophan to the polar environment. This is manifested by the fluorescence spectrum which has an emission maximum at 350 nm. Intrinsic fluorescence spectra of wtFGF1 and sFGF1 completely overlap with the emission maxima at 308 nm (Fig. 5). These results suggest that

incorporated mutations, in sFGF1, did not significantly perturb the tertiary structure of the protein.

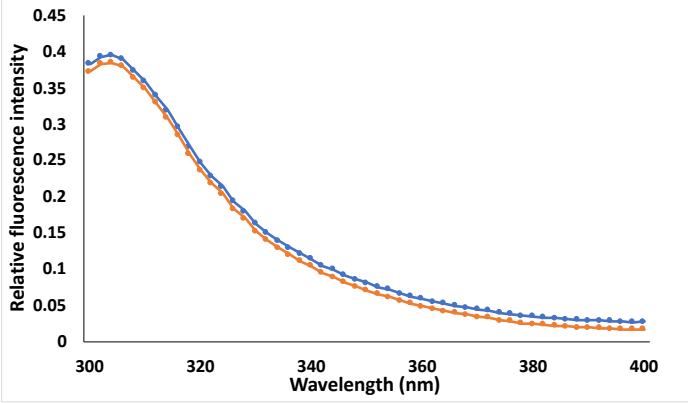

Fig. 5: Overlay of the Fluorescence spectra of wtFGF1 (blue) and sFGF1 (orange).

Far-UV circular dichroism (CD) spectra (190 nm – 250 nm) is an excellent technique to determine alterations in the secondary structures of proteins. Far UV-CD spectrum of wtFGF1 overlays well with that of sFGF1, suggesting no major secondary structural changes occur due to the mutations in sFGF1 (Fig. 6). These spectral features (characteristic positive ellipticity band in the wavelength ranging from 220-230 nm and a negative band in the region of 210 ~ 200 nm) indicate that the protein still maintains its native β-trefoil conformation upon introduction of five mutations.

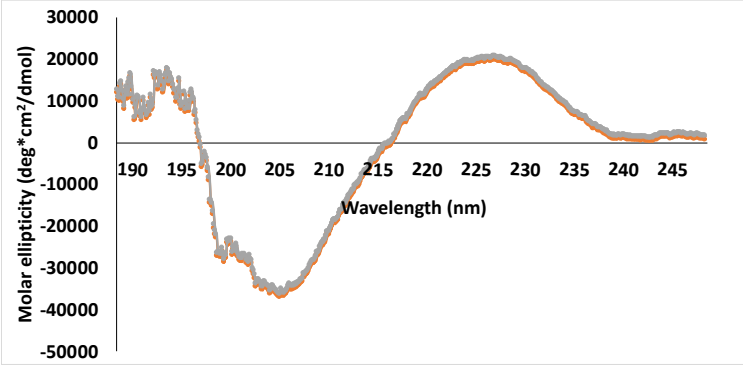

Fig. 6: Overlay of far-UV Circular dichroism (CD) spectra of wtFGF1 (gray) and sFGF1 (orange).

To investigate the interactions that stabilized the structure of hFGF1, we also performed molecular dynamic (MD) simulation analyses on wtFGF1 and sFGF1. Molecular dynamics simulations were performed on wtFGF1 and sFGF1 to supplement the experimental data. Simulations were run on the crystal structure of protein in the absence (1RG8) and presence of heparin. Hexasaccharide heparin from a dimeric hFGF1 crystal structure (2AXM) was added to monomeric hFGF1 to build the heparin-bound systems. Root mean square fluctuations (RMSF) of the Cα atoms and root mean square deviations (RMSD), in the presence and absence of heparin, of sFGF1 were compared to wtFGF1.

In the absence of heparin, wtFGF1 remains stable upto 2μs with a RMSD value of 1Å. However, after 2μs (Fig. 7) the RMSD abruptly changes to and remains around 3Å for the rest of the simulation, indicating that a conformational transition has occurred. In the contrary, heparin-free and heparin-bound sFGF1 show significant fluctuations in the RMSD value when compared to wtFGF1. Both the forms of sFGF1 stay stable throughout the 4.8 μs time period. Unlike wtFGF1, sFGF1 does not undergo any conformational transition. These results suggest that heparin-free wtFGF1 is more flexible than the heparin-bound wtFGF1. The heparin-bound wtFGF1 curve overlays well with the curves of both the forms of sFGF1 (heparin-free and heparin-bound).

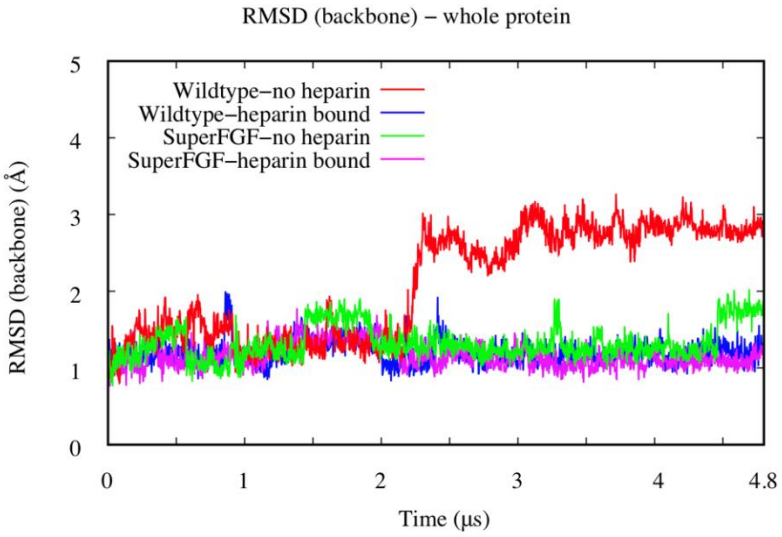

Fig. 7: Overlay of root mean square deviation curves of wtFGF1 and sFGF1 in absence and presence of heparin.

Heparin stabilizes the structure of hFGF1 by decreasing repulsion(s) between the positively charged residues located in the heparin binding pocket. The fact that heparin bound wtFGF1 overlays well with heparin-free and heparin-bound sFGF1 provides insight the extraordinary stability of sFGF1. This means that introduction of mutations, especially the ones involved in the heparin binding (R136E and K126N), might have increased electrostatic interaction in the residues; which in turn, increased the inherent stability of hFGF1. Similar trend in the fluctuation of the RMSD values were observed for the heparin binding region (Fig. 8). Heparin-free wtFGF1 showed higher flexibility than heparin bound wtFGF1 and both the forms of sFGF1.

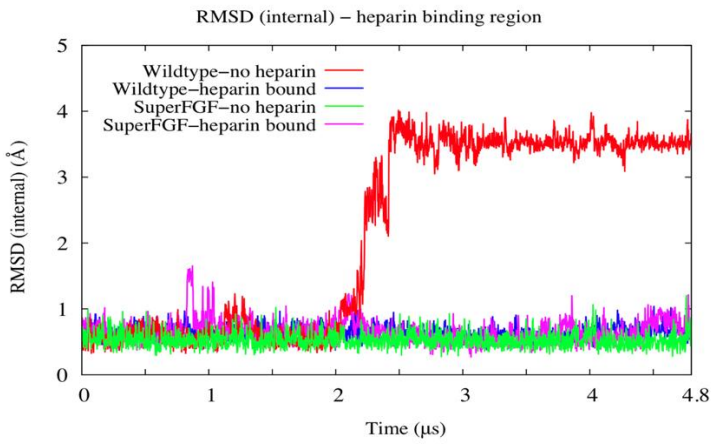

Fig. 8: Overlay of root mean square deviation curves of the heparin binding region (residues 127 – 143) of wtFGF1 and sFGF1 in absence and presence of heparin.

RMSD results are further supported by the RMSF results. Heparin bound and heparin free forms of wtFGF1 and sFGF1 showed similar trends in their fluctuations in the entire protein except for the heparin binding region (Fig. 9). The heparin binding region of the heparin-free wtFGF1 is more flexible than in the other systems. The heparin binding region spans residues 126-142 in hFGF1. This data along with the RMSD measurements support the conclusions drawn from structural flexibility experiments that sFGF1 renders more compactness to hFGF1.

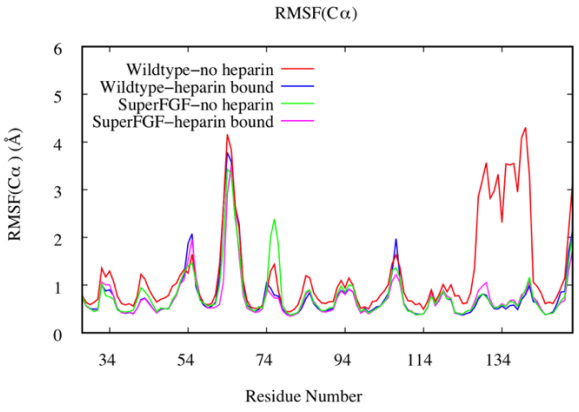

Fig. 9: Overlay of root mean square fluctuation curves of wtFGF1 and sFGF1 in absence and presence of heparin.

Introductions of mutations leads to electrostatic interactions in the structure of hFGF1

Analysis of the salt bridge interactions revealed two additional salt bridges which are not found in wtFGF1. One salt bridge that is observed is between the carboxylic acid group of E136 and epsilon amino group of K132 (Fig. 10). This interaction occurs within the heparin binding region and stays stable at around 6Å (weak salt bridge) for 4.8μs. Another salt bridge occurs between the carboxylate group of E136 and guanidinium head group of R133 (Fig. 11). This interaction is also present in the heparin binding region. Both salt bridges are observed in the sFGF1 in the presence and absence of heparin but not in wtFGF1. Thus, extra stability of sFGF1 over wtFGF1 appears to be due to these additional salt bridges. The introduction of the mutations plausibly promotes these new salt bridges in the heparin binding region (R136E and K126N). These mutations also could have lowered the repulsion between closely packed basic amino acids in the heparin binding region. The salt bridges present exclusively in wtFGF1 in the absence of heparin have been described in Chapter-IV.

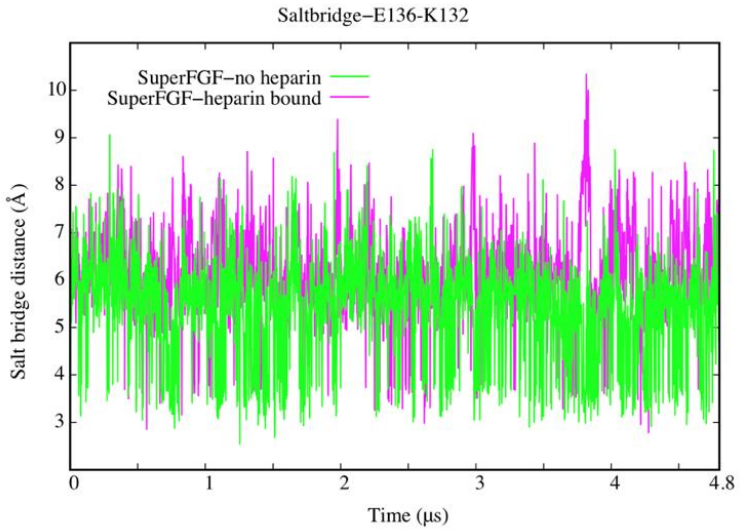

Fig. 10: Time series of the E136-K132 donor-acceptor salt bridge distance in the sFGF1 structure.

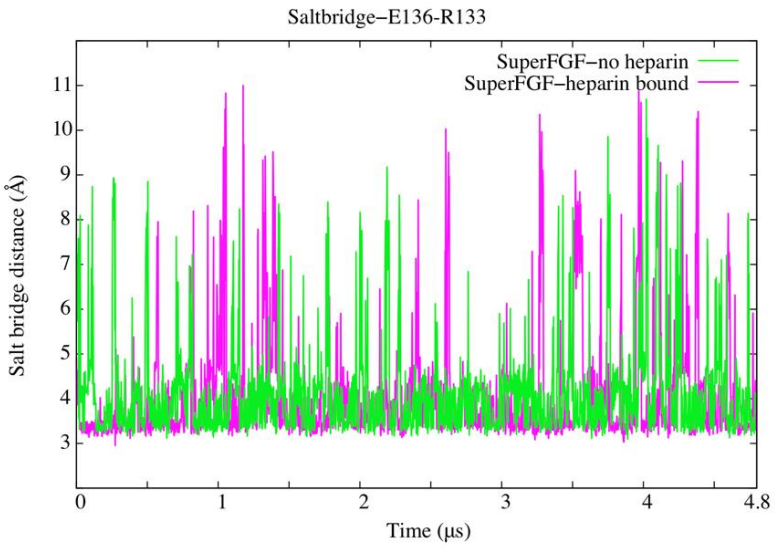

Fig. 11: Time series of the E136-R133 donor-acceptor salt bridge distance in the sFGF1 structure

The number of transient H-bond interactions (including those that do not satisfy the occupancy criteria; mentioned in the methods section) over the course of the simulation is nearly same for wtFGF1 and sFGF1. In heparin-free wtFGF1, only 1 out of 65 H-bonds (that satisfy the occupancy criteria) involves the heparin binding region (L145-K142 which is a backbone-backbone H-bond). All the 65 interactions observed in wtFGF1 also occur in sFGF1 with similar occupancies. 7 stable hydrogen bonds were identified in the heparin binding region of sFGF1(Table 1) that do not qualify as hydrogen bonds in heparin-free wtFGF1 (Table 1) based on the occupancy criteria defined in the methods section. Five of these interactions involved variant residues (N126 and E136) and are unique to sFGF1 (Table 1). It should be noted that equivalent interactions in both sFGF1 models and heparin-bound wtFGF1 have similar occupancies (Table 1), thus recapitulating the results of the RMSD and RMSF analyses.

Table 1: Comparison of electrostatic interactions involved in the heparin-binding region of wtFGF1 and sFGF1.

Donor	Acceptor	wtFGF1 w/o hep	wtFGF1 with hep	sFGF1 with hep	sFGF1 w/o hep
K126 (B)	S130 (B)	44	97	N/A	N/A
Q141 (S)	R136 (B)	31	80	N/A	N/A
G129 (B)	K126 (B)	33	79	N/A	N/A
R136 (B)	R133 (B)	37	76	N/A	N/A
T137 (S)	G134 (B)	35	70	67	67
H138 (B)	Q141 (S)	22	54	55	51
G129 (B)	N126 (B)	N/A	N/A	74	72
N126 (B)	S130 (B)	N/A	N/A	98	97
Q141 (S)	E136 (B)	N/A	N/A	62	57
E136 (B)	R133 (B)	N/A	N/A	68	64
R133 (S)	E136 (S)	N/A	N/A	150	158

Introduction of the mutations did not significantly perturb the hFGF1 structure

Changes in the structure of wtFGF1 and sFGF1 were determined using ^{1}H ^{15}N HSQC multidimensional NMR spectroscopy. NMR structure of wtFGF1 has been solved earlier and a complete set of assigned resonances is available. ^{1}H ^{15}N chemical shift perturbations were monitored based on chemical shifts assignments published by our group and others [17, 38]. The ^{1}H ^{15}N chemical shift perturbation of individual residues were calculated using the formula, ($\sqrt{[(2\Delta\delta NH)^2 + (\Delta\delta N)^2]}$). Our results are in good agreement with the published assignments. Superimposition of ^{1}H ^{15}N HSQC spectra of wtFGF1 and sFGF1 reveals modest chemical shift perturbations. The calculated ^{1}H ^{15}N chemical shift perturbations indicate that there were significant perturbations in the position of amino acids which are in proximity to the mutation sites (E136, G134, K132, and S107). E136, G134, and K132 are located in the heparin binding region. Spatially, S107 is positioned very close to the heparin binding pocket. E136 and S107 are the mutated residues. G134 is located very close to E136, and R133 and is involved in an

electrostatic interaction with the hydroxyl side chain of Thr at position 137 in wtFGF1 as well as sFGF1.

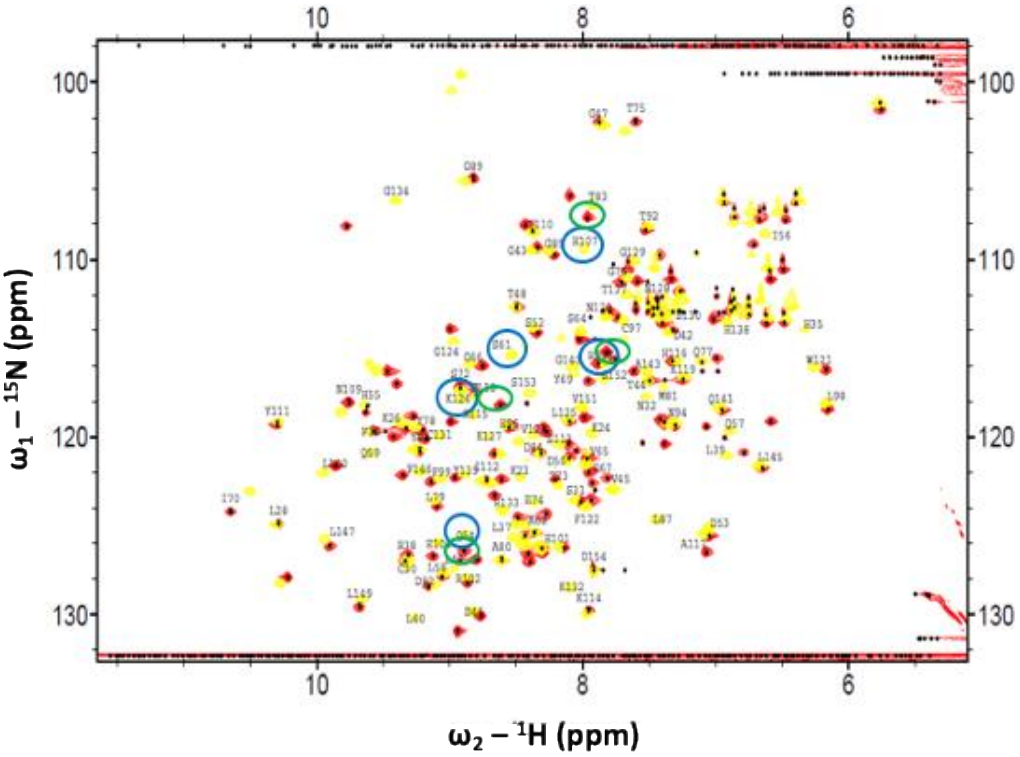

Fig. 13: Overlay of the ^{1}H ^{15}N HSQC of the wtFGF1 (yellow) and sFGF1 (red). The blue circles represent the amino acids in the wtFGF1 (R136, K126, Q54, S61, and H107). The green circles are predicted location of the amino acid after the mutation.

Introductions of mutations renders hFGF1 to be more compact, thus increasing the thermal, chemical and proteolytic stability of hFGF1. It also leads to complete loss of heparin binding affinity of hFGF1. Overall, results of the ^{1}H ^{15}N HSQC data suggest that engineered mutations, generating sFGF1, did not significantly alter the gross three-dimensional structure of the protein (Fig. 13).

Introduction of the mutations renders the hFGF1 molecule more compact

8-anilinonaphthalene-1-sulfonate (ANS) is a non-polar dye that is widely used to detect the presence of solvent-exposed hydrophobic region(s) in proteins. Results of ANS binding experiments shed light on the structural flexibility of the proteins. As hydrophobic residues are

typically buried in the interior of the protein core, an increase in ANS fluorescence suggests greater exposure of solvent-accessible hydrophobic region(s) [2]. Hydrophobic properties of proteins can be crucial as a driving force towards proper folding as well as protein-protein interactions. ANS binding curve for sFGF1 is quite similar to that of wtFGF1 (Fig. 14), indicating that the mutations did not lead to any significant tertiary structural changes. wtFGF1 without heparin exhibits maximum relative fluorescence intensity which indicates that wtFGF1 is structurally more flexible than sFGF1 with/without heparin and wtFGF1 with heparin. Unlike wtFGF1, sFGF1 does not show any difference in the ANS fluorescence in presence of heparin which indicates that heparin does not significantly affect the tertiary structure of sFGF1. On the other hand, the structure of wtFGF1 becomes more compact upon binding to heparin.

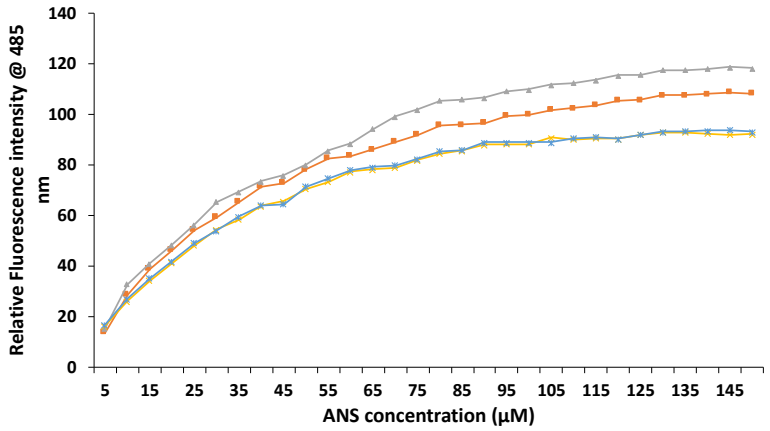

Fig. 14: ANS binding curves of wtFGF1 and sFGF1 in the presence and absence of heparin. wtFGF1 without heparin (gray), wtFGF1 with heparin (orange), sFGF1 without heparin (blue), and sFGF1 with heparin (yellow).

sFGF1 mutations is more resistant to the action of proteolytic enzymes

Trypsin, a serine protease, specifically cleaves proteins at the C-terminal end of lysine and arginine residues. hFGF1 contains three arginine and nine lysine residues. We performed limited trypsin digestion (LTD) assay on wtFGF1 and sFGF1, to determine effects of the mutations on the conformational flexibility of hFGF1. The percentage of hFGF1 digested after

different time periods of incubation with trypsin was measured by densitometric analysis based on the change(s) in intensity of the ~16 kDa hFGF1 band on Coomassie blue stained SDS-PAGE gels (Fig. 15).

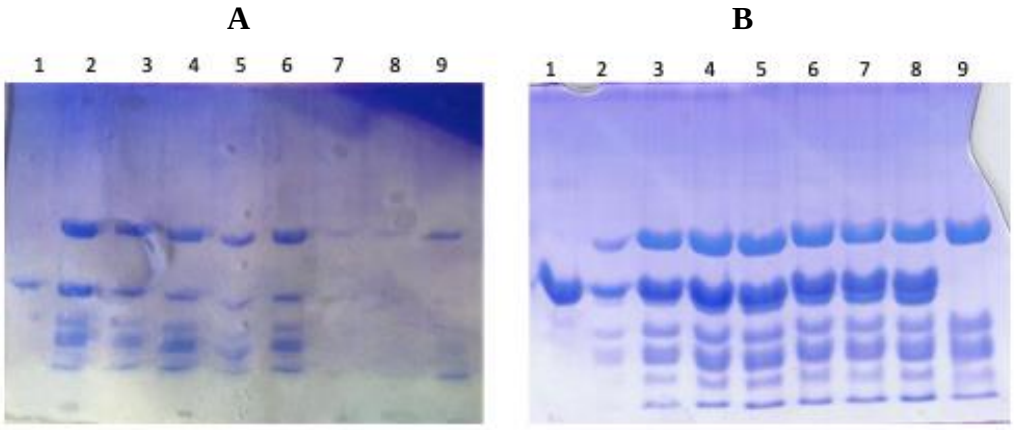

Fig. 15: SDS-PAGE analysis of limited trypsin digestion of wtFGF1 (Panel – A) and sFGF1 (Panel-B). 0.5 mg/mL of proteins (Lane-1); 4 minutes (Lane-2); 6 minutes (Lane-3); 10 minutes (Lane-4); 15 minutes (Lane-5); 30 minutes (Lane-6); 45 minutes (Lane-7); 60 minutes (Lane-8); 5 mg/mL of trypsin (Lane-9).

Densitometric analysis of SDS PAGE gels reveal the rate of digestion of wtFGF1 and sFGF1 by trypsin. Fig. 16 showed that after 20 minutes of incubation with the enzyme, approximately 80% of wtFGF1 was digested. Contrastingly, sFGF1, after 20 minutes of incubation with trypsin, remains almost completely undigested. In fact, sFGF1 remains stable for 24 hours when treated with trypsin (Fig. 16 B). These results indicate that sFGF1 is a highly compact molecule with significantly diminished backbone flexibility. In addition, results of the LTD experiments corroborate well with ANS binding data.

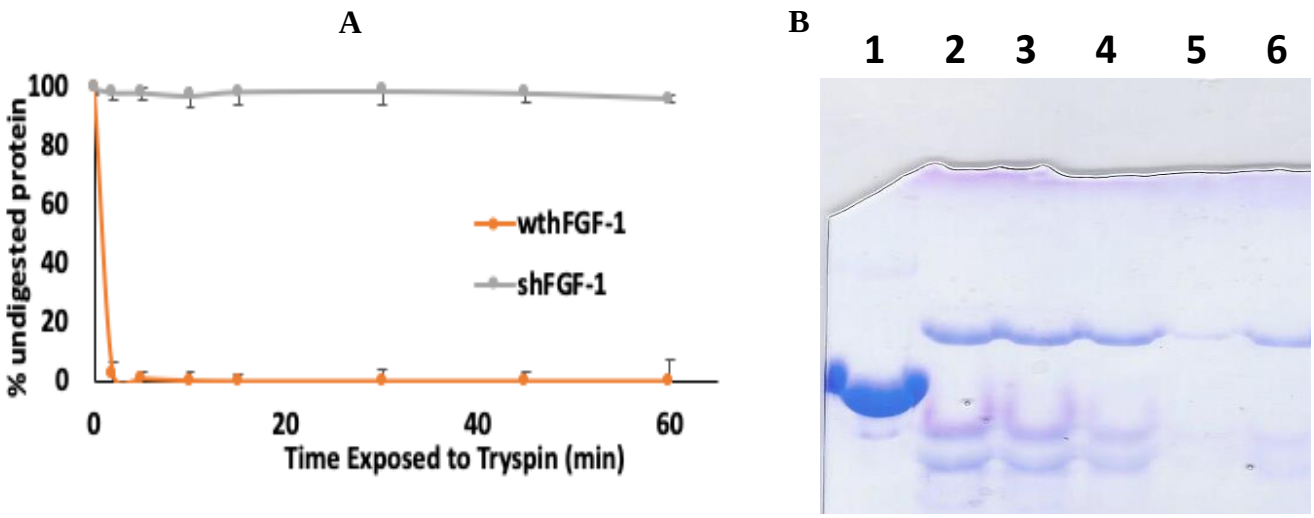

Fig. 16: Densitometric analysis of limited trypsin digestion of wtFGF1 and sFGF1 as monitored by SDS-PAGE (Panel-A). SDS-PAGE analysis of limited trypsin digestion of sFGF1 (Panel-B). 0.5 mg/mL of proteins (Lane-1); 1 hour (Lane-2); 4 hours (Lane-3); 8 hours (Lane-4); 16 hours (Lane-5); 24 hours (Lane-6).

Thrombin is another serine protease which is mainly present at the wound site and converts fibrinogen to fibrin. This conversion creates a matrix which includes cytokines (growth factor) and heparin. The primary thrombin cleavage site is -LVPRGS-. Slowly, the matrix is dissolved, and growth factors including hFGF1 are released at the site of wound. hFGF1 has a secondary thrombin cleavage site between R136 and T137. It has been reported earlier that thrombin degrades wtFGF1 at the wound site and renders it biologically inactive [40, 41]. In this context, limited thrombin experiments were performed to examine if substitution of secondary cleavage site (Arg at position 136 by Glu) in the structure of hFGF1 can enable thrombin resistant hFGF1 variant. Densitometric analysis of the rate of digestion of wtFGF1 and sFGF1 by thrombin shows that intensity of the 16 kDa band does not change for sFGF1 after 48 hours. On the contrary, the 16 kDa band intensity is completely lost/faded for wtFGF1 in about 24 hours

(Figs. 17 and 18). Thus, it can be inferred that sFGF1 is resistant to the action of thrombin for 48 hours whereas wtFGF1 is completely degraded within the first 24 hours (Fig. 17).

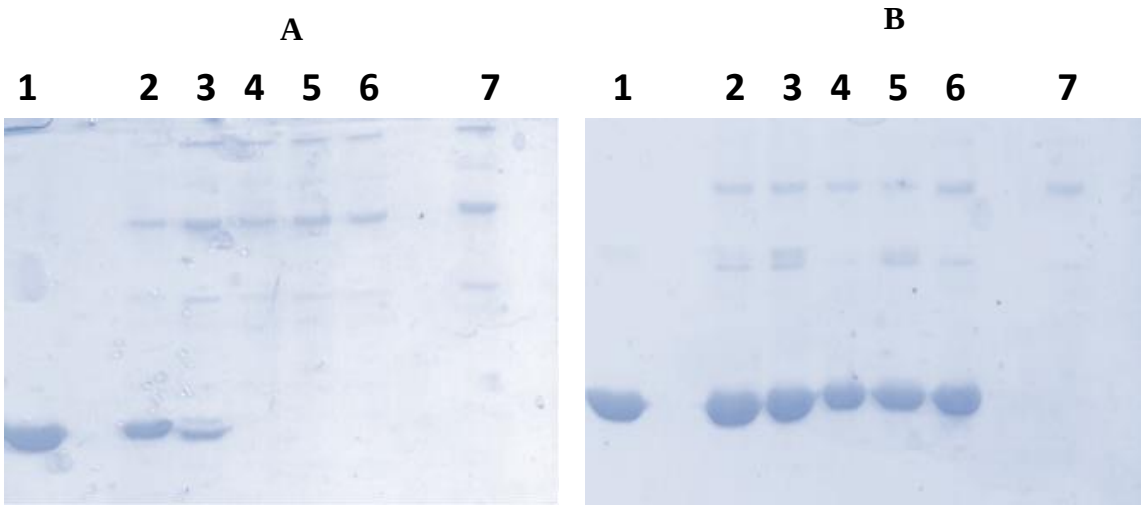

Fig. 17: SDS-PAGE analysis of limited thrombin digestion of wtFGF1 (Panel-A) and sFGF1 (Panel-B). 33 µM of proteins (Lane-1); 12 hours (Lane-2); 24 hours (Lane-3); 36 hours (Lane-4); 48 hours (Lane-5); 60 hours (Lane-6); 165 µM of thrombin (Lane-7).

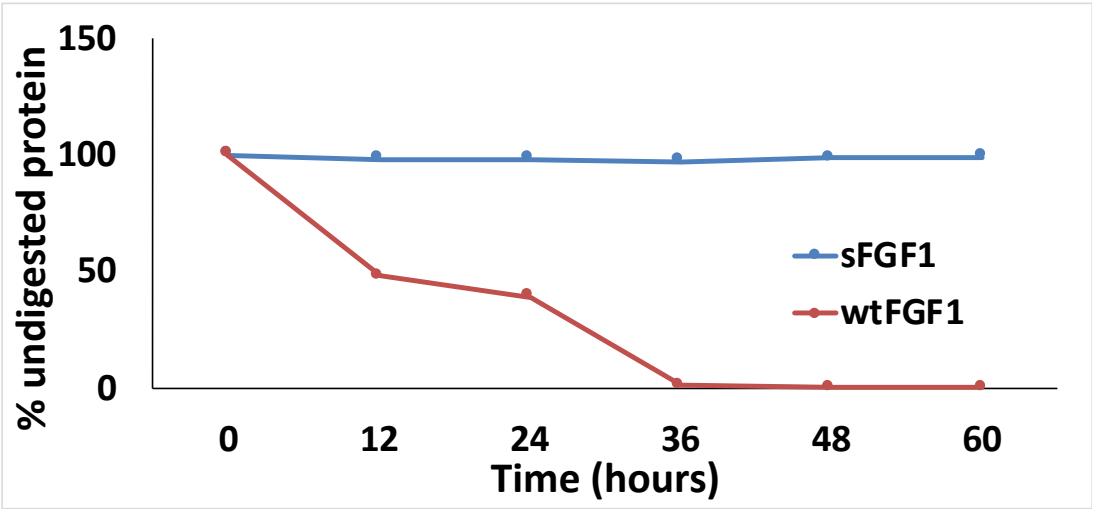

Fig. 18: Densitometric analysis of limited thrombin digestion of wtFGF1 and sFGF1 as monitored by SDS-PAGE.

Introduction of the mutations increases the stability of hFGF1

The thermal stability of wtFGF1 and sFGF1 were examined by monitoring the changes in the intrinsic fluorescence intensity ratio at 308 nm and 350 nm. The data in Fig. 19 depicts

unfolding curves of wtFGF1 and sFGF1 when exposed to increasing temperature, with and without heparin in solution.

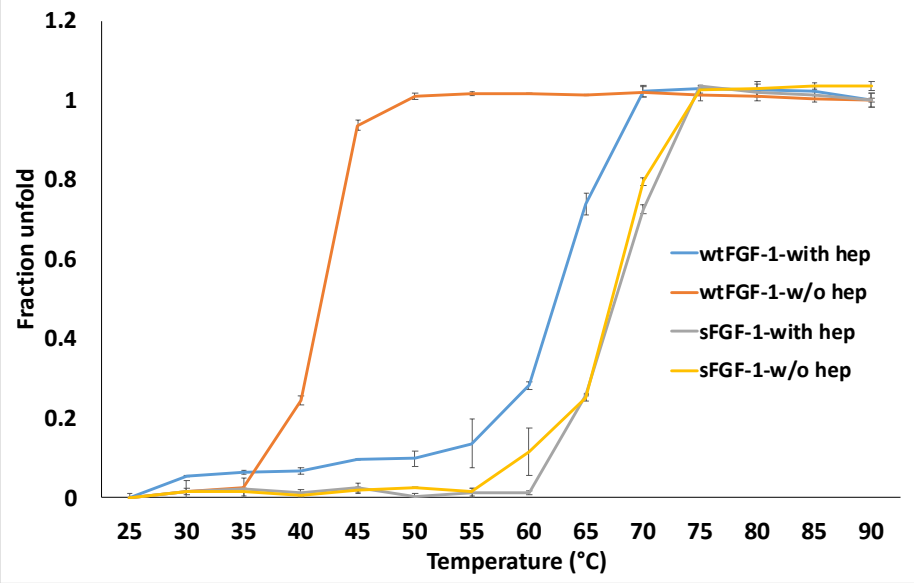

Fig. 19: Thermal stability analysis of wtFGF1 and sFGF1 in the presence and absence of heparin.

Table 2. Comparison of the thermal stability of wtFGF1 and sFGF1.

T_m Values (°C)	sFGF1	wtFGF1
With Heparin	68 ± 0.012	62 ± 0.012
Without Heparin	67 ± 0.023	41 ± 0.047
ΔT_m	1 ± 0.026	21 ± 0.049

Analysis of the denaturation temperature, T_m (the temperature at which 50% of the protein population exists in unfolded state(s)), revealed that presence of heparin significantly increases ability of wtFGF1 to resist the denaturation by increase in temperature. The presence of heparin accounts for 21°C of thermal resistance by wtFGF1. Also, heparin independent nature of sFGF1 is evident from the data, T_m remains 67.5˚C for sFGF1 with and without heparin, thus showing that addition of heparin doesn't significantly affect the thermal stability of sFGF1 (Table 2).

Unfolding of the proteins under increasing urea concentration was also monitored by the change in intrinsic fluorescence intensity at 305 nm/350 nm. Urea-induced unfolding curves of wtFGF1 and sFGF1 shows that both the forms of sFGF1 (with and without heparin), is more stable at higher urea concentrations than wtFGF1 without heparin, as shown in Fig 20. wtFGF1 has C_m value (the concentration value where 50% of the protein population remains in unfolded state (s)) of 3.8 ± 0.051 M and 1.2 ± 0.02 M with and without heparin, respectively. Contrastingly, sFGF1 exhibits C_m values of 3.65 ± 0.12 M with heparin and 3.66 ± 0.054 M without heparin. C_m values displayed by sFGF1 are approximately three times higher than that exhibited by wtFGF1 without heparin. Thus, data from the urea denaturation experiment suggest that sFGF1 has a higher inherent stability than wtFGF1.

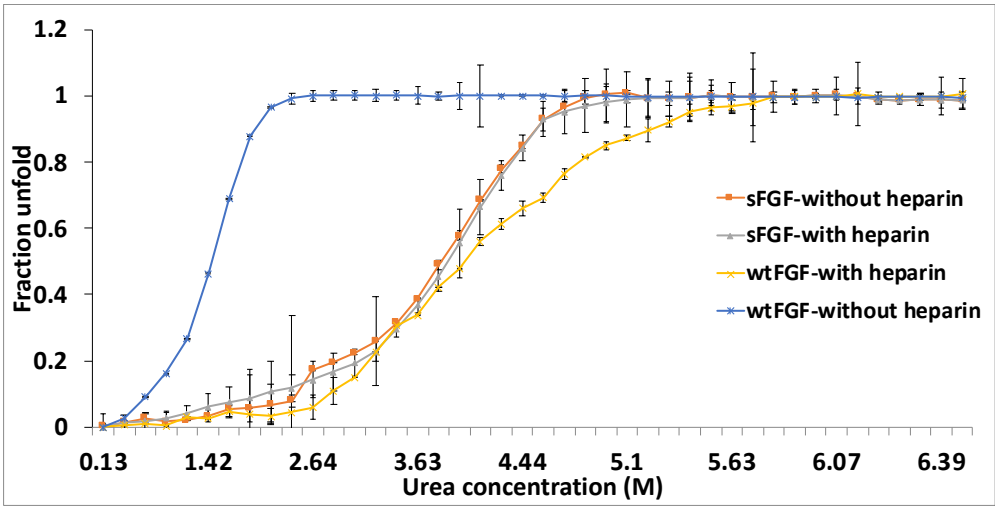

Fig. 20: Urea stability analysis of wtFGF1 and sFGF1 in the presence and absence of heparin.

Table 3. Comparison of urea stability of wtFGF1 and sFGF1.

C_m Values (M)	**sFGF1**	**wtFGF1**
With Heparin	3.65 ± 0.12	3.8 ± 0.02
Without Heparin	3.66 ± 0.054	1.2 ± 0.051
ΔC_m	0.01 ± 0.087	2.6 ± 0.0355

Overall, the thermal and urea equilibrium unfolding data indicate that introduction of mutations aid in stabilizing the growth factor. Stability against temperature and urea can be directly related to half-life of the protein, hence molecules exhibiting higher T_m and C_m values are expected to exhibit higher biological activity at physiological temperature for an extended period of time. sFGF1 exhibited much higher thermal stability (T_m~ 68°C) in comparison to wtFGF1, both in absence and presence of heparin. A similar trend was observed even in case of urea-induced denaturation. This may be due to the reduction of charge-charge repulsion in the heparin binding pocket caused because of the substitution of Lys by Asn and Arg by Glu at positions 126 and 136, respectively. Furthermore, Q54P and S61L mutations might have led to increase in β-sheet propensity and decrease in entropy, consequently enhancing the stability of sFGF1. Additionally, introduction of H107S mutation appears to significantly increase the hydrogen bonding network (G129-N126, N126-S130, Q141-E136, and E136-R133) in the vicinity of heparin binding site. These conclusions are in good agreement with the conclusions drawn from the structural flexibility data.

Introduction of a negative and a neutral charge in the heparin binding pocket leads to complete loss of heparin binding affinity

Isothermal titration calorimetry (ITC) is a valuable technique to determine the thermodynamic binding parameters of interactions in solution. The dissociation constant, K_d, has an inverse relationship with the binding affinity. Thus, more the K_d, less is the binding affinity of the protein to the ligand. Comparison of the K_d values between wtFGF1 (K_d = 1.6μM) and sFGF1 (K_d value can't be determined) reveals that wtFGF1 exhibits significantly more heparin binding affinity than sFGF1. The unusual heat changes in the isothermograms are due to the electrostatic interactions between the charged heparin molecules and some of the charged

components present in the buffer. From Fig. 21 and table 4, it can be concluded that sFGF1 clearly exhibits zero heparin binding affinity indicating that integrity of the heparin binding pocket is reliant on the presence of the positively charges residues.

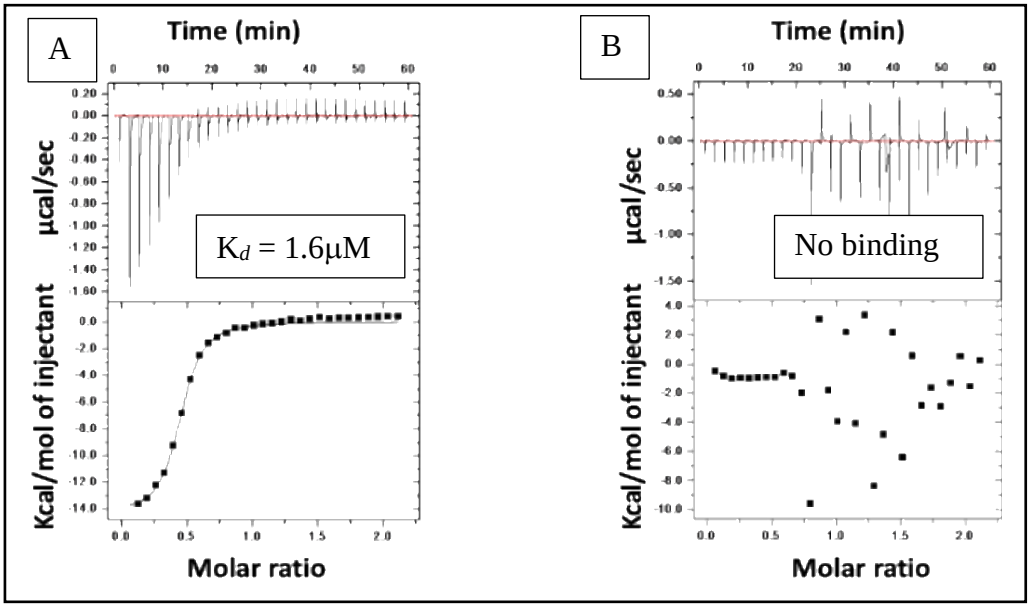

Fig. 21: Isothermograms representing titration of wtFGF1 (Panel - A) and sFGF1 (Panel - B) with heparin.

Table 4: Heparin binding affinity of wtFGF1 and sFGF1.

hFGF1 variants	**K_d (µM)**
wtFGF1	1.6
sFGF1	No binding

X-ray crystal structure of hFGF1 indicates that R136, K132, and K126 form a triad and facilitate binding of hFGF1 to heparin. Mutating two of these three residues might lead to significant reduction in the repulsion between positively charged amino acids in the heparin binding pocket. Using the crystal structures of hFGF1 in presence (PDB 2ERM) and absence of heparin (PDB 1RG8), distance of all the mutated residues were measured with respect to R133

(which lies in the middle of the heparin binding pocket) [20, 33]. The distance between the two residues was calculated using a combination of the following commands in VMD – measure center, vecsub, and veclength. In absence of heparin, the residues in wtFGF1 (R136, K126, Q54, S61, and H107) are located ~7.15 Å, ~13.24 Å, ~27.75 Å, ~26.32 Å, and ~25.6 Å, respectively, away from the critical heparin binding residue R133 (PDB 1RG8) whereas in the presence of hexasaccharide heparin (PDB 2ERM), R136 is shifted significantly closer to R133 (~9.57 Å) whereas K126, Q54, S61, and H107 are moderately positioned ~9.57 Å, ~24.41 Å, ~24.17 Å, and ~24.8 Å near R133. On the contrary, the distance between the mutated residues and R133 in sFGF1 (E136, N126, P54, L61, and S107) remains nearly the same, irrespective of the presence of heparin (Table 5). Thus, modification of Arg with Glu at position 136, Lys with Asn at position 126, Gln with Pro at position 54, Ser with Leu at position 61, and His with Ser at position 107 seems to compact the overall hFGF1 structure including the heparin binding pocket (HBP). Although out of all the five substitutions, R136E and K126N appears to bring drastic conformational changes in the heparin binding region making sFGF1 heparin independent.

Table 5: Distance of residues in wtFGF1 and sFGF1 from the middle of the heparin binding pocket (R133).

	Distance between (Å)				
Proteins	**K/N126 - R133**	**R/E136 - R133**	**S/L61 – R133**	**Q/P54 - R133**	**H/S107 - R133**
wtFGF1 w/o heparin	13.24	7.15	26.32	27.75	25.6
wtFGF1 with heparin	9.57	5.15	24.17	24.41	24.8
sFGF1 w/o heparin	9.7	5.16	23.46	23.97	23.9
sFGF1 with heparin	9.68	5.18	23	25	23.78

Introduction of the mutations enhances the mitogenic activity of hFGF1

The final step in analysis of viability of sFGF1 in a clinical setting is the understanding of its proliferative activity. Heparin is considered to be a crucial player in the hFGF1-FGFR interaction and activation. On that basis, decrease in the heparin binding affinity of the growth factor would lead to decrease in the mitogenic activity. In this context, cell proliferation assay was conducted using different concentrations of wtFGF1 and sFGF1. Fig. 22 displays that sFGF1 enhances the cell proliferation activity of the FGF1 protein as compared to wtFGF1. This result is nearly 70% more effective than wtFGF1 at the highest concentration (Fig. 22). Increased mitogenic activity is possibly due to the increased structural stability as measured by the equilibrium unfolding experiments. Isothermal titration calorimetric results suggest that sFGF1 is a heparin independent protein. Since sFGF1 is shown to demonstrate high cell proliferative ability despite having no heparin binding affinity, the data here shows that heparin binding is not mandatory to initiate cell proliferation.

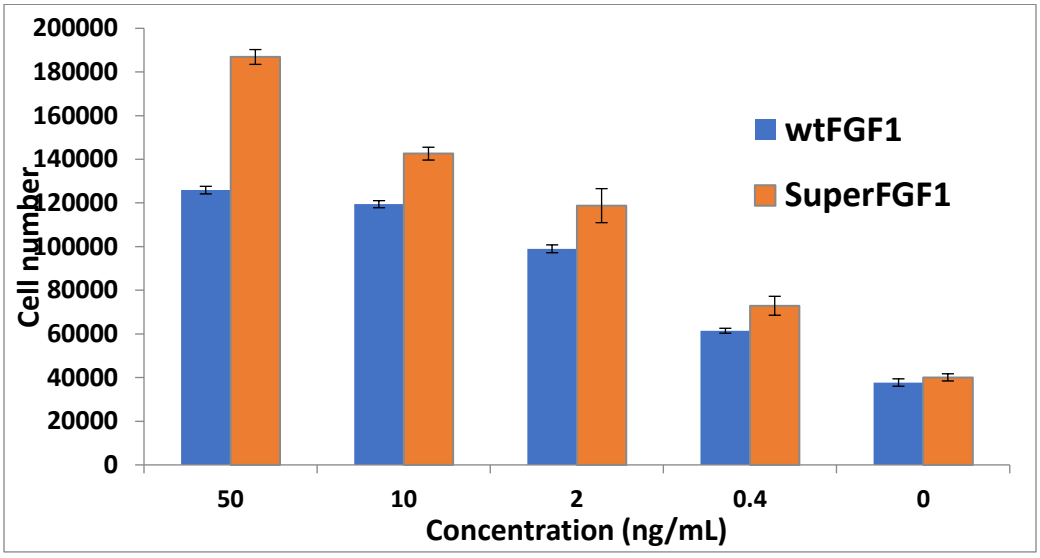

Fig. 22: Cell proliferation activity of NIH 3T3 cells treated with wtFGF1 and sFGF1

The notion that heparin is not mandatory for hFGF1 activation of cell surface receptors has been previously reported [4,8,10,11]. Culajay *et al.,* reported that substitution of the three cysteine residues (C30S, C131S, C97S) with serine decreased the heparin binding affinity of hFGF1 but increased the physiological half-life of hFGF1 and also enhanced the mitogenic activity of hFGF1 [9]. Additionally, combination of mutations L58F, H35Y, H116Y, and F122Y demonstrated an increase in the thermal stability, even in the absence of heparin, without causing significant loss in the bio activity of hFGF1 [9]. Further introduction of mutations at multiple sites on the quadruple mutant (L58F/H35Y/H116Y/F122Y) led to generation of a septuplet mutant (H35Y/Q54P/L58F/S61I/H107G/H116Y/F122Y). Surprisingly, this septuplet mutant was found to exhibit six-fold higher cell proliferation activity than wtFGF1 in the absence of heparin [24]. In this context, results of this study clearly show that heparin is not a pre-requisite for the cell proliferation activity of hFGF1. Heparin, present on the cell surface, possibly regulates the FGF protein level in the extracellular matrix (ECM), and also confers protection to FGFs against thermal denaturation and proteolytic degradation. In addition to facilitating the FGF-FGFR binding, HS also acts as a storage reservoir for ligand and determines the radius of ligand diffusion by controlling the gradients of paracrine FGFs in ECM [38].

Introduction of mutations enhances the ability of sFGF1 to activate ERK and Akt pathways

FGF ligands carry out their diverse functions by binding and activating the FGFR family of tyrosine kinase receptors in an HSGAG-dependent manner. FGFs exert their physiological roles through binding to the FGFR and regulate downstream signaling pathways such as, RAS/MAPK, PI3K/AKT, and PLCγ pathways. In this context, receptor activation assay was conducted to study the effects of wtFGF1 and sFGF1 on Valve interstitial cells (VICs). We used

western blotting to detect the expression of phosphorylated Erk1/2 and Akt in cultured valve interstitial cells treated with different doses of wtFGF1 and sFGF1. Results in Fig. 23 indicate that sFGF1 significant increases the activation of both these pathways (Erk1/2 and Akt) specifically, that of Erk1/2 pathway when compared to wtFGF1.

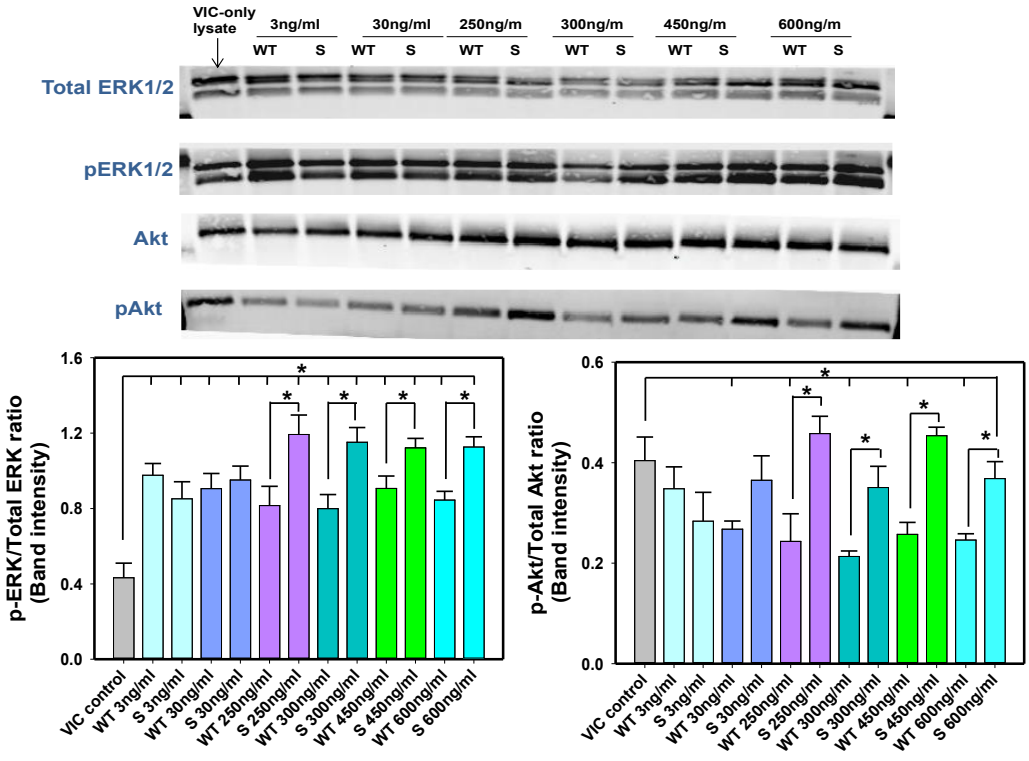

Fig. 23: Receptor activation assay of serum starved valve interstitial cells (VICs) treated with different concentrations of wtFGF1 and sFGF1. Cell lysates were resolved on SDS-PAGE followed with western blotting to detect ability of wtFGF1 and sFGF1 to activate ERK and Akt signaling pathways.

In spite of many years of research, the role of heparin in hFGF1-induced cell signalling is still controversial. Several studies have demonstrated that presence of heparin on the cell surface is mandatory for the receptor dimerization and augments the mitogenic response stimulated by hFGF1. In contrast, there have been reports indicating that heparin is not mandatory for the activation of FGF-FGFR cell signaling. In this context, results of this study show that sFGF1 can interact with the FGFR and trigger phosphorylation of Erk and Akt pathways even in the absence

of heparin. This is an important finding since activation of the Erk 1/2 pathway is known to be involved in wound healing mechanism [42].

Conclusions

Amino acid sequence of the FGFs, including hFGF1, folds into a β-trefoil conformation. This group of cytokines exhibits a wide array of activities such as, mitogenic activity, angiogenic activity, wound healing, and bone growth. There has been a long-standing debate on the role of heparin in determining the biological function of hFGF1. Initially there existed a general belief within literature that heparin is critical for binding of hFGF1 to its receptors. In contrast, there have been studies which demonstrated that heparin is not mandatory for the cell proliferation activity of hFGF1. In this study, we were able to demonstrate that heparin only stabilizes the structure of hFGF1 by decreasing the repulsion(s) between the positively charged residues located in the heparin binding pocket. Limited enzymatic digestion data suggest that sFGF1 substantially increases the resistance of hFGF1 to trypsin and thrombin. Thermal and urea induced unfolding results demonstrate that sFGF1 is significantly more stable than wtFGF1 with a T_m of around 68 °C and C_m of approximately 3.6 M. Isothermal titration calorimetry data indicate that the positively charged residues (K126 and R136) are significant in determining affinity of hFGF1 to heparin. Molecular dynamic (MD) simulation analyses suggest the introduced mutations in sFGF1 lowers the flexibility to the heparin binding region and consequently increases the stability of the growth factor by forming stable electrostatic interactions (salt bridges and hydrogen bonds). ^{1}H-^{15}N HSQC NMR experiment show that sFGF1 does not significantly affect the three-dimensional structure of the growth factor. Cell proliferation experiments indicate that sFGF1 exhibits a heparin-independent cell proliferation activity which is higher than that exhibited by wtFGF1. Receptor activation assay demonstrates

that sFGF1 exhibits substantial increase in activation of Erk and Akt pathways, which is known to be crucial for the wound healing. In conclusion, the hyperstability, resistance to the action of proteases, and enhanced heparin-independent bioactivity and activation of FGFR qualifies sFGF1 as a promising biotherapeutic to promote wound healing.

Materials and methods

Materials

The Quikchange lightning multi-site directed mutagenesis kit was from Agilent and the DNA plasmid isolation kit was from Qiagen Inc., USA. XL-Gold, PlysS, and BL-21(DE3) competent cells were obtained from Agilent and Novagen Inc., USA respectively. Lysogeny broth was purchased from IBI Scientific, USA. Heparin sepharose resin was from GE Healthcare, USA. Buffer components (Na_2HPO_4, NaH_2PO_4, NaCl) were supplied from VWR Scientific., USA. Low molecular weight (~3000 Da) heparin sodium salt was obtained from Sigma and MP Biomedicals LLC. NIH 3T3 cells were obtained from ATCC and all the cell culture reagents including, DMEM media, fetal bovine serum (FBS) and penicillin streptomycin were purchased from Thermo Fisher Scientific (Waltham, MA). All other chemicals and materials were of high-quality analytical grade. Unless otherwise stated, samples were made in 10 mM phosphate buffer saline (pH 7.2) and incubated at 37 ºC.

In this study, we have used low molecular weight heparin (M.wt~ 3000 Da) because the high molecular weight heparin is a polydispersed glycosaminoglycan. The high polydispersity imposes a serious challenge to accurately determine the binding affinity of the ligand to the growth factor [32]. Furthermore, the low molecular weight (M.wt~ 3000 Da) heparin used has been estimated to be 8 to 12 units long and multiple studies have shown that heparin with a chain

length of 8-units has been shown to be sufficient to facilitate optimal FGF-1 induced cell signaling [33, 34].

Construction and purification of pure wtFGF1 and sFGF1

For all the experiments, a truncated version of hFGF1 (residue number, 15-154) was inserted into a pET20b expression vector. Primers were designed using an online agilent primer design program and were ordered from IDT DNA Inc., USA. Site-directed mutagenesis (SDM) was performed using a QuickChange lightning kit followed by polymerase chain reaction (PCR) as per the protocol provided by the manufacturer. This project specifically utilizes *Escherichia coli* cells (BL21 *E. coli*). The plasmid was then transformed into XL-gold competent cells and sequencing of the plasmid was performed at the University of Arkansas Medical Science (UAMS) – DNA core sequencing facility. After verification of the plasmid sequence, sFGF1 was overexpressed in BL-21(pLysS) Escherichia coli cells cultured in lysogeny broth (LB) and then placed in New Brunswick Science Innova 4330 Refrigerated Incubator Shaker at 37 °C with agitation speed of 250 rpm. All transfers and inoculations were done in a Labconco Purifier Class II Biosafety Cabinet rinsed with 70% ethanol prior to work. After the overexpression, bacterial cells were lysed via ultra-sonication using a Branson Sonifier 150 at a 32% amplitude and the released proteins were separated from the cell debris by centrifugation for 20 minutes at 19,000 rpm. wtFGF1 and sFGF1 were then purified on a pre-equilibrated heparin-sepharose column with increasing sodium chloride gradient in 10 mM PB at speed of approximately 1.5 mL/min. SDS-PAGE was then used to determine the purity of the protein. The protein bands were visualized by staining the gels with Coomassie brilliant blue and the protein concentrations were determined by Bradford assay using a Hitachi F-2500 fluorimeter.

Fluorescence and Circular Dichroism Spectroscopy

Circular dichroism and intrinsic fluorescence data were acquired using a Jasco J-1500 Spectrophotometer. 33 µM protein was added to 10 mM PB + 100 mM NaCl and loaded into a 0.1 cm path length quartz cuvette. CD machine was kept at a constant temperature at 25ºC. The wavelength of the spectrophotometer was set over the range of 190-250 nm and the spectrum were scanned at 20nm/min speed. To obtain the intrinsic fluorescence spectrum, the excitation wavelength was set to 280 nm and the emission spectra was set for a range of 300 to 450 nm. The fluorescence data sheds light on the tertiary folding of the protein based on the naturally fluorescent tryptophan and tyrosine residues, which have an emission wavelength of approximately at around 350 nm and 305 nm, respectively.

^{1}H ^{15}N HSQC multidimensional NMR spectroscopy

^{1}H-^{15}N HSQC experiments were conducted on a Bruker Avance DMX-700 MHz spectrometer equipped with a 5 mm inverse cryoprobe at 25°C. wtFGF1 and the sFGF1 were grown in M9 medium with $^{15}NH_4Cl$ used as the sole nitrogen source. ^{15}N labeled protein samples (1 mM) were prepared in 90% H_2O + 10% D_2O solution containing 10 mM phosphate buffer containing 100 mM NaCl and 25 mM $(NH_4)_2SO_4$ (pH 6.5). Data were analyzed using XWINNMR 3.5 software supplied by Bruker.

ANS Binding

ANS (8-anilinonaphthalene-1-sulfonate) binding experiments were performed to provide further information regarding the protein's tertiary structure. ANSs an extrinsic fluorophore that fluoresces when it binds to solvent exposed hydrophobic regions of a protein. ANS binding experiments were performed by addition of increasing concentrations (10 µM addition) of ANS to 33 µM of wtFGF1. Relative fluorescence intensity was determined with an excitation at 380

nm and emission intensity was recorded at 510 nm. These experiments were repeated with sFGF1 samples in the presence and absence of heparin.

Limited Trypsin Digestion

Proteolytic trypsin digestion was performed to determine the structural flexibility of the wild-type and sFGF1. Trypsin is a proteolytic enzyme that cleaves peptide bonds at the C-terminal end of lysine and arginine amino acids, except when either are followed by a proline.10 µL of 330 mM trypsin was added to 10 µL of 33 µM of protein and 90 µL of 10 mM PB + 100 mM NaCl. The samples were immediately incubated in a hot water bath at 37ºC for 0, 4, 6, 10, 15, 30, 45, and 60 minutes. TCA preparation was performed on each sample immediately after being removed from the hot water bath to stop the trypsin reaction. The results were assessed using SDS-PAGE analysis along with UN-SCAN-IT gel software. The intensity of the bands in the gel was compared to control bands containing only wtFGF1. This study was repeated with sFGF1 samples.

Limited Thrombin Digestion

Proteolytic thrombin digestion was performed to determine the structural flexibility of the wild-type and the mutant protein. Thrombin recognizes the specific amino acid sequence LVPRGS and cleaves between the arginine (R) and glycine (G) residues. In hFGF1, thrombin cleaves between the Arg at position 136 and Thr at position 137. Thrombin cleavage was performed using 33 µM of wtFGF1 and sFGF1 protein, 165 µM of bovine thrombin, and 10 mM PB + 100 mM NaCl. The samples were incubated at 37º C in a rotator and collected at 3, 6, 18, 24, 36, and 48 hours. TCA preparation was performed on each sample immediately after being removed from the rotator to stop the thrombin reaction. The results were assessed using SDS

PAGE analysis along with UN-SCAN-IT gel software. The intensity of the bands in the gel was compared to control bands containing only protein.

Equilibrium unfolding experiments

Thermal denaturation studies were performed on the JASCO-1500 spectrofluorometer using intrinsic fluorescence emission scans to reveal how temperature affects the stability of wtFGF1 and sFGF1 with and without heparin. 33 μM protein in 10 mM PB + 100 mM NaCl were added to a cuvette and a temperature probe was inserted to monitor the temperature. Data on the samples were collected at 5º C intervals over a temperature range of 25 ºC – 90 ºC. The fraction of the unfolded protein was calculated using the ratio of tyrosine to tryptophan emission fluorescence measurements at 305 nm and 340 nm, respectively.

For the chemical denaturation studies, 8 M urea was used to induce protein denaturation. This process was monitored using intrinsic fluorescence emission scans using a JASCO-1500 spectrophotometer. Data of samples of 33 μM protein in 10 mM PB + 100 mM NaCl (wtFGF1 and sFGF1) were each collected over a urea concentration of 0-6 M. The fraction of unfolded protein was calculated using the ratio of tyrosine to tryptophan emission fluorescence measurements at 305 and 340 nm.

Isothermal titration calorimetry

Isothermal titration calorimetry (ITC) was used to calculate the binding affinity of wtFGF1 and sFGF1 to heparin. ITC measures the molar ratio of bound ligand to protein at specified aliquots of titrant, which in this case is heparin. Within an adiabatic chamber, a series of 30 titrations were performed at 25°C with a stir speed of 750 rpm. Protein samples were prepared with 10 mM sodium phosphate buffer containing 100 mM NaCl and 25 mM $(NH_4)_2SO_4$

pH 7.2. A 1:10 ratio of protein to ligand (100 μM protein: 1 mM heparin) was used on a GE MicroCal iTC-200 in which heparin was titrated into hFGF1 samples. The detected thermal change from the binding of heparin to hFGF1 is then measured by a small sensor and compared to a reference cell. The data for wtFGF1 and sFGF1 were best-fit to one set of sites and any excess heats of dilution given from heparin were appropriately subtracted out.

Cell Proliferation Activity

The cell proliferation assay measures the biological activity of a growth factor. 3T3 fibroblast cells obtained from ATCC (Manassas, VA) were cultured in complete media consisting of DMEM supplemented with 10% FBS and 1% penicillin/streptomycin. Cells were grown to 80-90% confluency and were incubated overnight at 37°C with 5% CO_2 in serum free media before further use. The cell proliferation activity of hFGF1 was determined by quantifying the increase in cell number after the cells had been incubated with wtFGF1/sFGF1 at varying concentrations. Starved 3T3 fibroblasts were collected and seeded in a 96-well plate at a seeding density of 10,000 cells/well. Cells were then co-incubated individually with wild type and sFGF1 at concentrations of 0, 0.4, 2, 10, and 50 ng/mL. After 24 hours of incubation, 3T3 cell proliferation was assessed by the CellTiter-Glo (Promega, Madison, WI) cell proliferation assay.

Receptor activation assay

Valve interstitial cells (VICs) were isolated from porcine heart and used at passage 2-7. VICs were allowed to reach about 80% confluence before they were serum starved for 24 hours prior to treatment. 6 different doses of wild-type (WT) and super (S) FGF were used, including 3ng/ml, 30ng/ml 250ng/ml, 300ng/ml, 450ng/ml and 600ng/ml. 10 minutes after treatment, cells were lysed with RIPA lysis buffer (Santa Cruz Biotech). Cell lysate was centrifuged at 10,000 rpm, 4^0C and the supernatant was collected and quantified by BCA assay (Thermo Scientific).

Control samples had VICs only, no treatment with either wild-type or mutant FGF. For western blotting, cell lysate was mixed with 4X Laemmli buffer (Bio-Rad) in the presence of reducing condition β-mercaptoethanol (Bio-Rad) and equally loaded to each lane of 4-15% polyacrylamide gel (Bio-Rad). Electrophoresis was run for 1 hour at room temperature before the protein was transferred to polyvinyldifluoride (PVDF) membrane (Immobilon-FL), blocked in Licor blocking buffer (Li-Cor, Lincoln NE) for 1 hour before probing with total mouse ERK1/2 (Cell signaling 1:50) and rabbit p-ERK1/2 (Cell signaling 1:500). For Akt detection, membranes were probed with rabbit p-Akt (Cell signaling 1:100) prior to stripping and reprobing with rabbit Akt (Cell signaling, 1:200). The membranes were kept at 4^0C overnight. The next day, appropriate secondary antibodies (Li-Cor, 1:15,000) were added to the membranes and incubated for 1 hour before the membranes were washed and scanned using a Licor Odyssey scanner. Relative expression of p-ERK1/2 and p-Akt were quantified by comparing the band intensity obtained for the phosphorylated proteins and normalizing it with the intensity obtained for the corresponding total proteins.

REFERENCES

[1] Kerr R, Agrawal S, Maity S, Koppolu B, Jayanthi S, Kumar GS, Gundampati RK, McNabb DS, Zaharoff DA, Kumar TK. Design of a thrombin resistant human acidic fibroblast growth factor (hFGF1) variant that exhibits enhanced cell proliferation activity. Biochemical and biophysical research communications. 2019 Oct 15;518(2):191-6.

[2] Davis JE, Alghanmi A, Gundampati RK, Jayanthi S, Fields E, Armstrong M, Weidling V, Shah V, Agrawal S, prasanth Koppolu B, Zaharoff DA. Probing the role of proline− 135 on the structure, stability, and cell proliferation activity of human acidic fibroblast growth factor. Archives of biochemistry and biophysics. 2018 Sep 15;654:115-25.

[3] Ornitz DM, Itoh N. Fibroblast growth factors. Genome biology. 2001 Mar;2(3):1-2.

[4] Zakrzewska M, Wiedlocha A, Szlachcic A, Krowarsch D, Otlewski J, Olsnes S. Increased protein stability of FGF1 can compensate for its reduced affinity for heparin. Journal of Biological Chemistry. 2009 Sep 11;284(37):25388-403.

[5] Ogura K, Nagata K, Hatanaka H, Habuchi H, Kimata K, Tate SI, Ravera MW, Jaye M, Schlessinger J, Inagaki F. Solution structure of human acidic fibroblast growth factor and interaction with heparin-derived hexasaccharide. Journal of biomolecular NMR. 1999 Jan 1;13(1):11-24.

[6] Miller DL, Ortega S, Bashayan O, Basch R, Basilico C. Compensation by fibroblast growth factor 1 (FGF1) does not account for the mild phenotypic defects observed in FGF2 null mice. Molecular and cellular biology. 2000 Mar 15;20(6):2260-8.

[7] Beenken A, Eliseenkova AV, Ibrahimi OA, Olsen SK, Mohammadi M. Plasticity in interactions of fibroblast growth factor 1 (FGF1) N terminus with FGF receptors underlies promiscuity of FGF1. Journal of Biological Chemistry. 2012 Jan 27;287(5):3067-78.

[8] Brych SR, Blaber SI, Logan TM, Blaber M. Structure and stability effects of mutations designed to increase the primary sequence symmetry within the core region of a β-trefoil. Protein Science. 2001 Dec;10(12):2587-99.

[9] Culajay JF, Blaber SI, Khurana A, Blaber M. Thermodynamic characterization of mutants of human fibroblast growth factor 1 with an increased physiological half-life. Biochemistry. 2000 Jun 20;39(24):7153-8.

[10] Zakrzewska M, Krowarsch D, Wiedlocha A, Otlewski J. Design of fully active FGF-1 variants with increased stability. Protein Engineering Design and Selection. 2004 Aug 1;17(8):603-11.

[11] Zakrzewska M, Marcinkowska E, Wiedlocha A. FGF-1: from biology through engineering to potential medical applications. Critical reviews in clinical laboratory sciences. 2008 Jan 1;45(1):91-135.

[12] Beenken A, Mohammadi M. The FGF family: biology, pathophysiology and therapy. Nature reviews Drug discovery. 2009 Mar;8(3):235-53.

[13] Blaber SI, Culajay JF, Khurana A, Blaber M. Reversible thermal denaturation of human FGF-1 induced by low concentrations of guanidine hydrochloride. Biophysical journal. 1999 Jul 1;77(1):470-7.

[14] Alsenaidy MA, Wang T, Kim JH, Joshi SB, Lee J, Blaber M, Volkin DB, Middaugh CR. An empirical phase diagram approach to investigate conformational stability of "second-generation" functional mutants of acidic fibroblast growth factor-1. Protein Science. 2012 Mar;21(3):418-32.

[15] Powers CJ, McLeskey SW, Wellstein A. Fibroblast growth factors, their receptors and signaling. Endocrine-related cancer. 2000 Sep 1;7(3):165-97.

[16] Erzurum VZ, Bian JF, Husak VA, Ellinger J, Xue L, Burgess WH, Greisler HP. R136K fibroblast growth factor-1 mutant induces heparin-independent migration of endothelial cells through fibrin glue. Journal of vascular surgery. 2003 May 1;37(5):1075-81.

[17] Xia X, Babcock JP, Blaber SI, Harper KM, Blaber M. Pharmacokinetic Properties of 2 nd-Generation Fibroblast Growth Factor-1 Mutants for Therapeutic Application. PloS one. 2012 Nov 1;7(11):e48210.

[18] Kumar TK, Zaharoff DA, Jayanthi S, Koppolu B, Kerr R, Balachandran K, McNabb DS. Engineered FGF compositions and methods of use thereof.

[19] Thallapuranam SK, Agarwal S, Gindampati RK, Jayanthi S, Wang T, Jones J, Kolenc O, Lam N, Niyonshuti I, Balachandran K, Quinn K, inventors. Engineered fgf1 and fgf2 compositions and methods of use thereof. United States patent application US 16/356,872. 2019 Sep 19.

[20] Canales A, Lozano R, López-Méndez B, Angulo J, Ojeda R, Nieto PM, Martín-Lomas M, Giménez-Gallego G, Jiménez-Barbero J. Solution NMR structure of a human FGF-1 monomer, activated by a hexasaccharide heparin-analogue. The FEBS journal. 2006 Oct;273(20):4716-27.

[21] Beenken A, Mohammadi M. The structural biology of the FGF19 subfamily. InEndocrine FGFs and Klothos 2012 (pp. 1-24). Springer, New York, NY.

[22] Schlessinger J, Plotnikov AN, Ibrahimi OA, Eliseenkova AV, Yeh BK, Yayon A, Linhardt RJ, Mohammadi M. Crystal structure of a ternary FGF-FGFR-heparin

complex reveals a dual role for heparin in FGFR binding and dimerization. Molecular cell. 2000 Sep 1;6(3):743-50.

[23] Dubey VK, Lee J, Somasundaram T, Blaber S, Blaber M. Spackling the crack: stabilizing human fibroblast growth factor-1 by targeting the N and C terminus β-strand interactions. Journal of molecular biology. 2007 Aug 3;371(1):256-68.

[24] Zakrzewska M, Krowarsch D, Wiedlocha A, Olsnes S, Otlewski J. Highly stable mutants of human fibroblast growth factor-1 exhibit prolonged biological action. Journal of molecular biology. 2005 Sep 30;352(4):860-75.

[25] Goetz R, Mohammadi M. Exploring mechanisms of FGF signalling through the lens of structural biology. Nature reviews Molecular cell biology. 2013 Mar;14(3):166-80.

[26] Pellegrini L, Burke DF, von Delft F, Mulloy B, Blundell TL. Crystal structure of fibroblast growth factor receptor ectodomain bound to ligand and heparin. Nature. 2000 Oct;407(6807):1029-34.

[27] de Paz JL, Angulo J, Lassaletta JM, Nieto PM, Redondo-Horcajo M, Lozano RM, Giménez-Gallego G, Martín-Lomas M. The activation of fibroblast growth factors by heparin: Synthesis, structure, and biological activity of heparin-like oligosaccharides. ChemBioChem. 2001 Sep 3;2(9):673-85.

[28] Pellegrini L. Role of heparan sulfate in fibroblast growth factor signalling: a structural view. Current opinion in structural biology. 2001 Sep 1;11(5):629-34.

[29] Harmer NJ. Insights into the role of heparan sulphate in fibroblast growth factor signalling. Biochemical Society Transactions. 2006 Jun 1;34(3):442-5.

[30] Szlachcic A, Zakrzewska M, Krowarsch D, Os V, Helland R, Smalås AO, Otlewski J. Structure of a highly stable mutant of human fibroblast growth factor 1. Acta Crystallographica Section D: Biological Crystallography. 2009 Jan 1;65(1):67-73.

[31] Kimura H, Okubo N, Chosa N, Kyakumoto S, Kamo M, Miura H, Ishisaki A. EGF positively regulates the proliferation and migration, and negatively regulates the myofibroblast differentiation of periodontal ligament-derived endothelial progenitor cells through MEK/ERK-and JNK-dependent signals. Cellular Physiology and Biochemistry. 2013;32(4):899-914.

[32] Arunkumar AI, Srisailam S, Kumar TK, Kathir KM, Chi YH, Wang HM, Chang GG, Chiu M, Yu C. Structure and stability of an acidic fibroblast growth factor from Notophthalmus viridescens. Journal of Biological Chemistry. 2002 Nov 29;277(48):46424-32.

[33] Fu L, Zhang F, Li G, Onishi A, Bhaskar U, Sun P, Linhardt RJ. Structure and activity of a new low-molecular-weight heparin produced by enzymatic ultrafiltration. Journal of pharmaceutical sciences. 2014 May;103(5):1375-83.

[34] Robinson CJ, Harmer NJ, Goodger SJ, Blundell TL, Gallagher JT. Cooperative dimerization of fibroblast growth factor 1 (FGF1) upon a single heparin saccharide may drive the formation of 2: 2: 1 FGF1· FGFR2c· heparin ternary complexes. Journal of biological chemistry. 2005 Dec 23;280(51):42274-82.

[35] Kimura S, Kanaya S, Nakamura H. Thermostabilization of Escherichia coli ribonuclease HI by replacing left-handed helical Lys95 with Gly or Asn. Journal of Biological Chemistry. 1992 Nov 5;267(31):22014-7.

[36] Stites WE, Meeker AK, Shortle D. Evidence for strained interactions between side-chains and the polypeptide backbone. Journal of molecular biology. 1994 Jan 7;235(1):27-32.

[37] Takano K, Yamagata Y, Yutani K. Role of amino acid residues in left-handed helical conformation for the conformational stability of a protein. Proteins: Structure, Function, and Bioinformatics. 2001 Nov 15;45(3):274-80.

[38] Häcker U, Nybakken K, Perrimon N. Heparan sulphate proteoglycans: the sweet side of development. Nature reviews Molecular cell biology. 2005 Jul;6(7):530-41.

[39] Huang Z, Tan Y, Gu J, Liu Y, Song L, Niu J, Zhao L, Srinivasan L, Lin Q, Deng J, Li Y. Uncoupling the mitogenic and metabolic functions of FGF1 by tuning FGF1-FGF receptor dimer stability. Cell reports. 2017 Aug 15;20(7):1717-28.

[40] Shireman PK, Xue L, Maddox E, Burgess WH, Greisler HP. The S130K fibroblast growth factor–1 mutant induces heparin-independent proliferation and is resistant to thrombin degradation in fibrin glue. Journal of vascular surgery. 2000 Feb 1;31(2):382-90.

[41] Erzurum VZ, Bian JF, Husak VA, Ellinger J, Xue L, Burgess WH, Greisler HP. R136K fibroblast growth factor-1 mutant induces heparin-independent migration of endothelial cells through fibrin glue. Journal of vascular surgery. 2003 May 1;37(5):1075-81.

[42] Hou B, Cai W, Chen T, Zhang Z, Gong H, Yang W, Qiu L. Vaccarin hastens wound healing by promoting angiogenesis via activation of MAPK/ERK and PI3K/AKT signaling pathways in vivo. Acta Cirurgica Brasileira. 2019;34(12).

CHAPTER IV

Characterization of the Structural Forces Governing the Reversibility of the Thermal Unfolding of the Human Acidic Fibroblast Growth Factor

Abstract

Human acidic fibroblast growth factor (hFGF1) ~16 kDa is an all beta-sheet protein that is involved in the regulation of key cellular processes including cell proliferation, cell differentiation, angiogenesis, and wound healing. hFGF1 is known to be an unstable protein and has been shown to aggregate when subjected to thermal unfolding. In this study, we investigate the equilibrium unfolding of hFGF1 using a wide array of biophysical and biochemical techniques including multidimensional NMR spectroscopy. Systematic analyses of the thermal and chemical denaturation data on seven different designed variants (Q54P, K126N, R136E, K126N/R136E, Q54P/K126N, Q54P/R136E, and Q54P/K126N/R136E) of hFGF1 indicate that nullification of charges in the heparin binding pocket can significantly increase the thermal stability of the protein. The triple variant (Q54P/K126N/R136E) was found to be the most stable of all the hFGF1 variants studied. Its T_m value is about ~ 20°C higher than the wild type protein. GdnHCl/urea-induced equilibrium unfolding of wtFGF1 and the other designed variants of hFGF1 are reversible. However, with the exception of the triple variant, the thermal unfolding of wtFGF1 and the other designed hFGF1 is irreversible. However, renaturation of the triple variant from its thermal denatured state(s) shows hysteresis behavior. Two-dimensional ^{1}H-^{15}N HSQC and cell proliferation data clearly show that the triple variant of hFGF1 regains its biologically active conformation upon refolding from its thermal denatured state(s). Results from microsecond-level molecular dynamics (MD) simulations show that a network of hydrogen bonds and salt bridges linked to the Q54P, K126N, and R136E mutations, are responsible for the

high thermal stability and reversibility of the thermal unfolding of the triple variant of hFGF1. In our opinion, the findings of the study provide valuable clues for the rational design of a stable hFGF1 variant that exhibits potent wound healing properties.

Introduction

Protein folding is a fascinating puzzle that has attracted the attention of researchers for a long time [1]. The mechanism by which a nascent polypeptide chain folds into a unique three-dimensional structure has largely remained enigmatic. However, useful knowledge about the plausible structural events that occur during the folding of proteins from their denatured state(s) has been gained [2,3]. Stable intermediate state(s) that populate the equilibrium/kinetic folding/unfolding pathways of several proteins have been characterized and their significance in directing a protein to fold to its native conformation have been reported [4,5]. It is widely believed that the folding polypeptide is partitioned between productive intra-chain interactions leading to the formation of the native conformation and non-productive inter-chain interactions that result in misfolding and consequently aggregation of the protein [6,7]. Aggregates formed can range from amorphous structures without order to highly structured fibrils as observed in dilapidating amyloid diseases such as Alzheimer's disease, Parkinson's disease, serum amyloid-A (SAA), dialysis-related amyloidosis, cystic fibrosis, Creutzfeldt-Jakob disease, Huntington disease, and type-II diabetes [8-10]. In several cases, the propensity to aggregate is attributed to inter-chain interactions between solvent-exposed hydrophobic surfaces present in obligatory and non-obligatory partially structured intermediates that populate the kinetic or equilibrium folding/unfolding pathways of proteins [11]. In this context, understanding the structural determinants governing protein aggregation is critical for the rational design of drugs against the multitude of amyloid diseases [12].

The folding/unfolding pathways of single and multidomain proteins have been extensively studied [13,14]. However, most of these proteins are predominantly helical [15]. Studies examining the kinetics of all helical proteins such as myoglobin and cytochrome-c have indicated that α-helical proteins refold from their denatured state(s) very rapidly on a millisecond timescale [16]. The higher rate of refolding of all-helical single domain proteins is believed to be due to the ease of formation of intra-strand backbone hydrogen bonds in helical conformations. Interestingly, very little information exists on the kinetics of folding of all beta-sheet proteins. A detailed knowledge of the kinetic events in the folding of all-beta-sheet proteins will likely provide valuable information on the structural forces that trigger aggregation or fibril formation which mostly involves organization of the polypeptide backbone into an array of beta-sheets [17,18].

Human acidic fibroblast growth factor (hFGF1) is a ~16 kDa heparin binding protein. hFGF1 is an all beta-sheet protein and its backbone is organized into a beta-trefoil architecture [19, 20]. hFGF1 plays crucial role(s) in the regulation of key cellular processes such as cell proliferation, cell differentiation, angiogenesis, tumor metastasis, and wound healing [21-23]. hFGF1 has a low half -life *in vivo* [24]. Interestingly, a significant population of hFGF1 has been shown to exist in partially unfolded states at temperatures which are marginally higher than the physiological temperature [25]. Previous studies have demonstrated that the denaturant-induced equilibrium unfolding/refolding of hFGF1 does not occur *via* a two-state mechanism. Samuel *et al.,* showed that guanidium hydrochloride (GdnHCl)-induced equilibrium unfolding of hFGF1 proceeds through the formation of an obligatory intermediate [26]. Similarly, Alsenaidy *et al.,* have shown that hFGF1 is highly prone to aggregation when subjected to heat beyond its T_m (< 40°C) value or when subjected to minor changes in pH or ionic strength [27]. Blaber and

coworkers elucidated that the thermal unfolding of hFGF1 can only be reversed by the addition of low concentrations of GdnHCl [28]. It is believed that addition of low concentrations of the denaturant potentially destabilizes the stable obligatory intermediate that accumulates in the GdnHCl-induced equilibrium unfolding pathway of hFGF1 [26]. The propensity of hFGF1 to heavily aggregate has been a significant impediment in realizing its strong wound healing potential. In this context, there has been an increased interest in devising new wound healing formulations that could stabilize hFGF1 against heat-induced aggregation. In this context, in this study, we have designed a novel triple variant (TM) (Fig.1, Q54P, K126N, R136E) of hFGF1 that not only exhibits significantly higher thermal stability but also exhibits reversible thermal unfolding by resisting the formation of aggregates. We believe that the findings of this study provide valuable insights into the interplay of structural forces that confer reversible unfolding behavior to the protein and also provide useful clues for the rational design of hFGF1-based therapeutics to manage chronic wounds.

Results and discussion

Rationale for the designed mutations

As mentioned previously, hFGF1 is an all beta sheet protein with 12 beta strands organized into a β-trefoil structure. The flexible heparin binding pocket contains a high density of positively charged residues and is located between β-strands 10 and 12 (Fig. 1). We recently demonstrated that a charge reversal mutation (R136E) in the heparin binding pocket marginally decreases the heparin binding affinity but enhances both the thermodynamic stability and cell proliferation activity of hFGF1 [19]. hFGF1 is known to be inherently unstable molecule at temperatures just above the physiological temperature [20]. It is believed that the instability of hFGF1 largely stems from the charge repulsions between the closely placed positively charged

residues in the heparin binding pocket [19]. In this context, introduction of a negative charge in the heparin binding pocket is postulated to provide a counter-ion effect and consequently stabilize the growth factor molecule. K126 is located in the periphery of the heparin binding pocket and has been shown to contribute significantly to the heparin binding affinity [19]. Therefore, we expect that neutralization of the charge via the K126N mutation would not only decrease the heparin binding affinity but also increase the stability of hFGF1. Contribution of two negative charges in the cationic heparin binding pocket is expected to significantly stabilize the structure of hFGF1. Thus, introduction of Glu, Asn, and Pro residues at positions 54, 126, and 136, could plausibly induce a stable conformation by improving the interactions (salt bridges) in the protein core and stabilize the growth factor against temperature and chemical denaturants. Q54 is lodged on the loop connecting beta-strands -3 and 4. This β-turn falls under the category of type I or type IV turns. In either of these β-turns, proline is 4.3 times more favored than Gln [40]. In this context, substitution of Q54 with proline is expected to make the molecule more compact and consequently promote and stabilize additional interactions in the protein core. Zakrzewska *et al.*, showed that Q54P mutation significantly increases both the stability and cell proliferation activity of hFGF1 [40]. Substitution of glutamine with proline is believed to significantly decrease the local backbone flexibility and render the hFGF1 molecule more compact [40]. In addition, secondary structural analyses of wtFGF1 also revealed presence of short 3_{10}-helices. Again, Pro is a favored amino acid in 3_{10}-helix type of secondary structure. Matthews *et al.*, and Mateos *et al.*, observed that proline mutations decrease the conformational entropy of the unfolded state of proteins [41,42]. Thus, introduction of Q54P, K126N, and R136E plausibly aids in minimizing the exposure of hydrophobic regions to the surface and restricts the conformational fluctuations occurring in the heparin binding region, thereby leading

to refolding and higher stability of the growth factor. In this context, seven (Q54P, K126N, R136E, Q54P/R136E, Q54P/K126N, K126N/R136E and Q54P/K126N/R136E) different variants were designed to specifically delineate their effects on the structure, stability, heparin binding affinity, and cell proliferation activity of hFGF1.

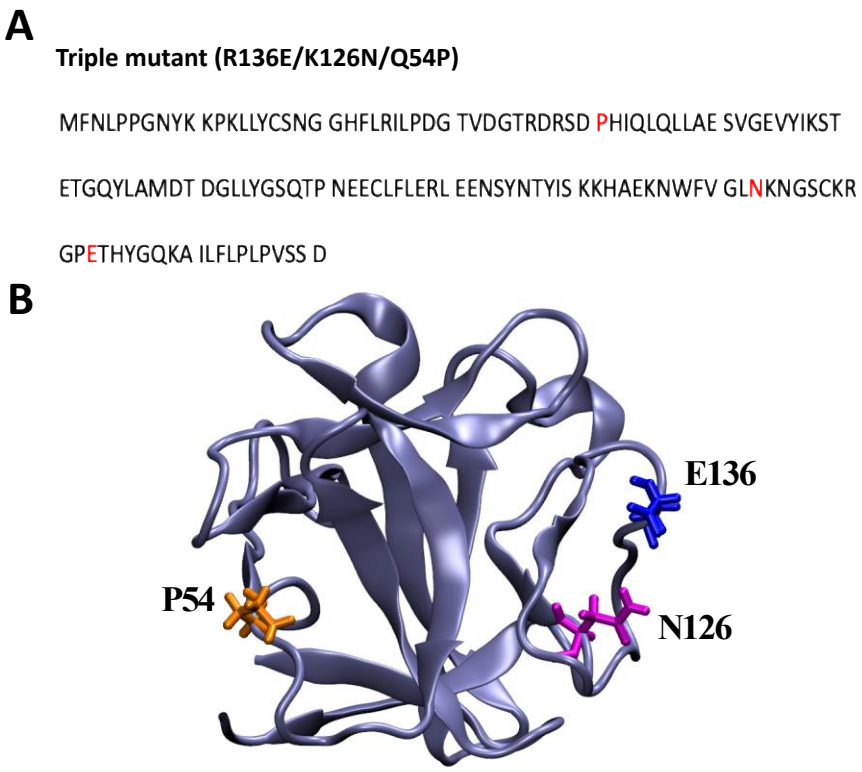

Fig. 1: Amino acid sequence of the triple variant of hFGF1. The residues highlighted in red represent the mutated residues in wtFGF1 (Q54P, K126N, and R136E) (Panel – A). Cartoon representation of hFGF1 structure (PDB ID: 1RG8) showing the mutation sites (Panel – B).

Mutations do not alter the structure of hFGF1

Human acidic fibroblast growth factor (wtFGF1) and the designed variants (R136E, K126N, Q54P, Q54P/R136E, Q54P/K126N, K126N/R136E and Q54P/K126N/R136E) were purified to homogeneity using affinity and gel filtration column chromatography (Fig. 2).

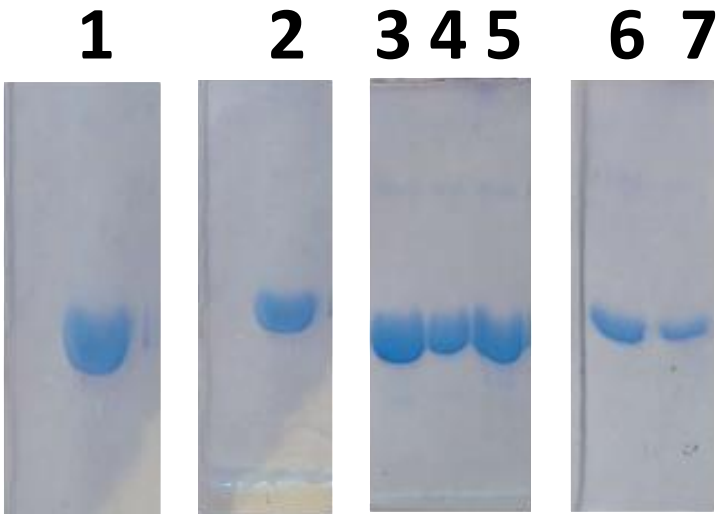

Fig. 2: SDS-PAGE analysis of proteins eluted upon heparin sepharose and gel filtration chromatography. wtFGF1 (Lane - 1), R136E (Lane – 2), K126N (Lane – 3), Q54P (Lane – 4), R136E/K126N (Lane – 5), R136E/Q54P (Lane – 6), and K126N/Q54P (Lane - 7).

It is important to verify if the introduction of mutations in the seven different variants significantly perturbed the structure of hFGF1. In this context, we used far-UV circular dichroism (CD) spectroscopy and intrinsic fluorescence spectroscopy to monitor the structural changes that could potentially occur as a consequence of the introduced mutations. Far-UV CD spectrum (190 nm – 250 nm) of the wtFGF1 shows positive and negative ellipticity bands centered at around 228 nm and 205 nm, respectively (Fig. 3A). These structural features are consistent with the β-trefoil structure of hFGF1. Interestingly, the far-UV CD spectra of the 7 designed hFGF1 variants superimpose quite well with that of the wild type protein suggesting that the secondary structure of the protein is not perturbed due to the designed mutations.

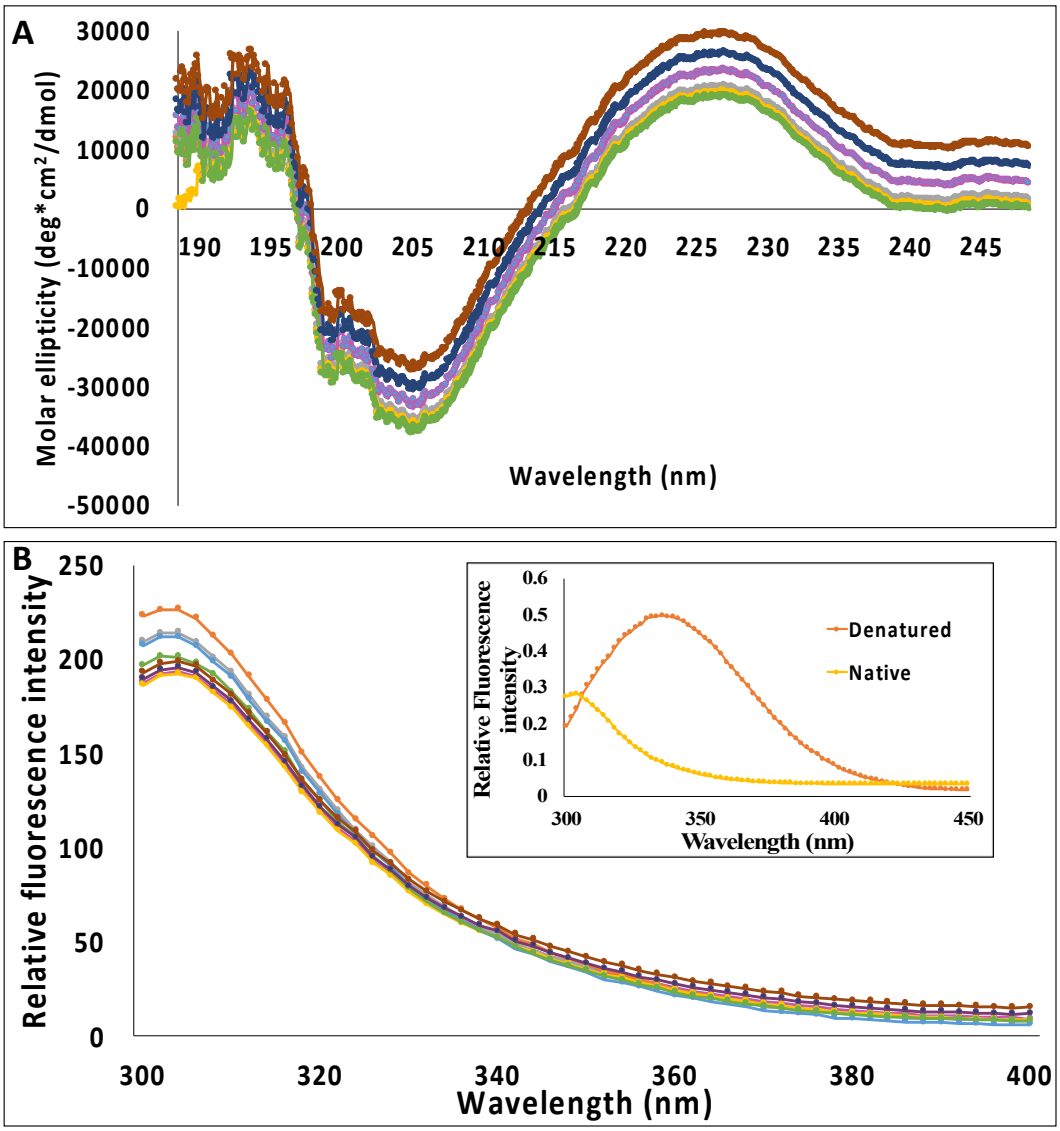

Fig. 3: Overlay of the far-UV CD spectra of wtFGF1 and the designed variants (Panel – A). Overlay of the fluorescence spectra showing the similarity in the tertiary structure of wtFGF1 and the designed variants (Panel – B). The inset figures represent a cartoon representation of the intrinsic fluorescence spectra of hFGF1 in its native and denatured state(s). Concentration of protein used was 0.5 mg/mL in 10mM phosphate buffer, pH 7.2 containing 100mM NaCl. wtFGF1 (pink), R136E (orange), K126N (gray), Q54P (yellow), K126N/R136E (purple), Q54P/R136E (green), Q54P/K126N (blue), and Q54P/K126N/R136E (brown).

hFGF1 contains eight tyrosine residues and a lone tryptophan residue (Trp121, Fig. 1A). Intrinsic fluorescence of a single tryptophan residue in the properly folded conformation is significantly quenched by the surrounding amine groups of lysine and proline residues [19]. As a consequence, intrinsic fluorescence spectrum of wtFGF1 in its native state shows an emission

maximum at 308 nm corresponding to the tyrosine fluorescence (Fig. 3B). However, the quenching effect of tryptophan is completely relieved in the unfolded state(s) and shows a characteristic emission maximum at around 350 nm (Fig. 3B, inset). Therefore, monitoring changes in the intrinsic fluorescence provides a reliable measure of the tertiary structural changes that could plausibly occur in the protein. Overlay of the intrinsic fluorescence spectra of the designed variants of hFGF1 revealed little or no significant differences indicating that the tertiary structural contacts in the protein mostly remain unperturbed after the introduction of the designed mutations in the protein (Fig. 3B). Results of intrinsic fluorescence and far-UV CD data analyzed in conjunction conclusively suggest that the designed mutations did not significantly perturb the native three-dimensional structure of wtFGF1.

Effect (s) of mutation on the thermal stability of hFGF1 variants

As mentioned previously, hFGF1 is an unstable molecule [T_m ~ 41 °C, T_m is the temperature at which 50% of the protein population exists in denatured state(s)] and is known to exist in partially folded state(s) around physiological temperatures (Table-1) [28]. The protein is known to aggregate when subjected to thermal unfolding at temperatures above its T_m [43]. In addition, thermal unfolding of hFGF1 is known to be irreversible and consequently the calculated T_m (apparent) value is only a qualitative measure of the thermal stability of the protein [43]. More recently, Blaber and coworkers showed that the thermal unfolding of hFGF1 can be reversed in the presence of low concentrations of GdnHCl [28]. The low thermal stability and the problems associated with irreversibility of the thermal unfolding have significantly impeded the development of hFGF1 based therapeutics for chronic wound care. In this context, we investigate the stability of wtFGF1 and its designed 7 variants by monitoring the changes in the intrinsic fluorescence intensity ratio at 308 nm and 350 nm (Fig. 4).

Table 1: Comparison of the stability of wtFGF1 and the designed variants.

Proteins	T_m value (°C)	C_m value (M Urea)	C_m value (M GdnHCl)
wtFGF1	41.5 ± 0.1	1.9 ± 0.4	1.0 ± 0.8
R136E	52 ± 0.2	2.25 ± 0.1	1.82 ± 0.4
K126N	54 ± 0.1	2.3 ± 0.3	1.87 ± 0.3
Q54P	43 ± 0.1	1.52 ± 0.3	1.44 ± 0.5
Q54P/R136E	53 ± 0.1	1.53 ± 0.2	1.53 ± 0.6
Q54P/K126N	56 ± 0.5	1.55 ± 0.1	1.43 ± 0.1
K126N/R136E	49 ± 0.1	1.70 ± 0.1	1.74 ± 0.2
Q54P/K126N/R136E	60 ± 0.1	3.97 ± 0.1	2.35 ± 0.1

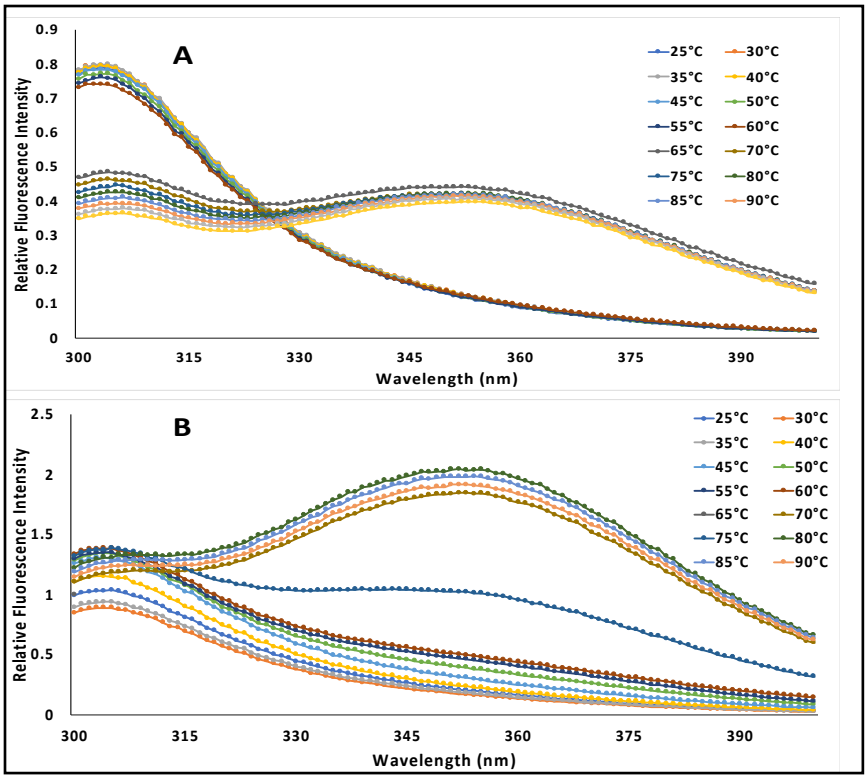

Fig. 4: Intrinsic fluorescence spectra of thermal unfolding of wtFGF1 (Panel – A) and triple variant of hFGF1 (Panel – B).

The thermal unfolding data suggests that wtFGF1 ($T_{m\ (apparent)}$ - 41 °C) exhibits the lowest thermal stability (Table-1). Replacement of Q54 with proline appears to have a marginal effect ($T_{m\ (apparent)}$ = ~ 43 °C, Fig. 5, Table-1)) on the stability of the protein. Interestingly, single point mutations (K126N and R136E) in the heparin binding pocket appear to have a more profound

effect (~ 10 °C – 12°C) on the thermal stability of the protein (Table-1 & Fig. 5). These results suggest that the charge repulsions between the closely placed residues in the heparin binding pocket are primarily responsible for the inherent instability of hFGF1. The K126N mutation not only decreases the repulsions between positively charged residues in the heparin binding pocket but also appears to facilitate forging of a backbone to side-chain hydrogen bonding between N126 and S130. It is believed that introduction of a negative charge *via* the R136E mutation induces a counter-ion effect in the heparin binding pocket which consequently partially screens the charge repulsions between the cationic residues located in the heparin binding pocket. Surprisingly, the double mutation (K126N/R136E) in the heparin binding pocket shows a noticeably lower ($T_{m\ (apparent)}$ ~ 49 °C, Table-1 & Fig. 6) stability than the corresponding individual single-point mutations (K126N and R136E).

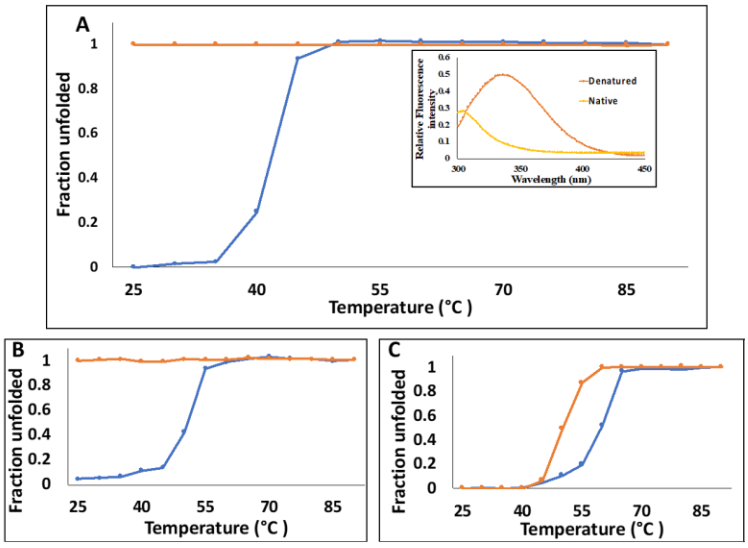

Fig. 5: Thermal unfolding and refolding curves of wtFGF1 (Panel-A; unfolding- blue, refolding- orange), R136E hFGF1 variant (Panel-B; unfolding- blue, refolding- orange), and TM-variant of hFGF1 (Panel-C; unfolding- blue, refolding- orange). The thermal unfolding and refolding of wtFGF1 and its variants was monitored by changes in the ratio of intrinsic fluorescence intensities at 308 nm to 350 nm. Insert figure in Panel-A depicts the intrinsic fluorescence spectra of hFGF1 in its native and denatured states. Concentration of protein used was 0.5 mg/mL in 10mM phosphate buffer, pH 7.2 containing 100mM NaCl.

Although it is not clear why simultaneous replacement of both K126 and R136 causes the observed decrease in stability, this is interesting considering the fact that these individual mutations distinctly stabilize the protein. It appears that the individual stabilizing forces that come into play in the heparin binding pocket (due to the incorporation of K126N and R136E mutations) mutually weaken each other leading to a net decrease in the stability of the protein. On the other hand, the K126N and R136E mutations when individually combined with the Q54P mutation, to yield the double variants (Q54P/K126N and Q54P/R136E), confers significant stability to the protein (Fig. 6, Table -1). These results once again confirm that maximum effects on the stability of the protein are caused by nullification or reversal of charges in the heparin binding pocket. Very interestingly, the Q54P mutation appears to compensate for the mutually destabilizing effects of the K126N and R136E mutations. This is obvious from the high $T_{m(\text{apparent})}$ value of the triple variant, Q54P/K126N/R136E (Fig. 6, Table-1). Although the Q54P site is located remotely from the mutation sites in the heparin binding pocket, the structural kink introduced by proline appears to be transmitted through a network of interactions to the heparin binding pocket and consequently enables the two mutations (K126N and R136E) to synergistically produce a stabilizing effect on the protein.

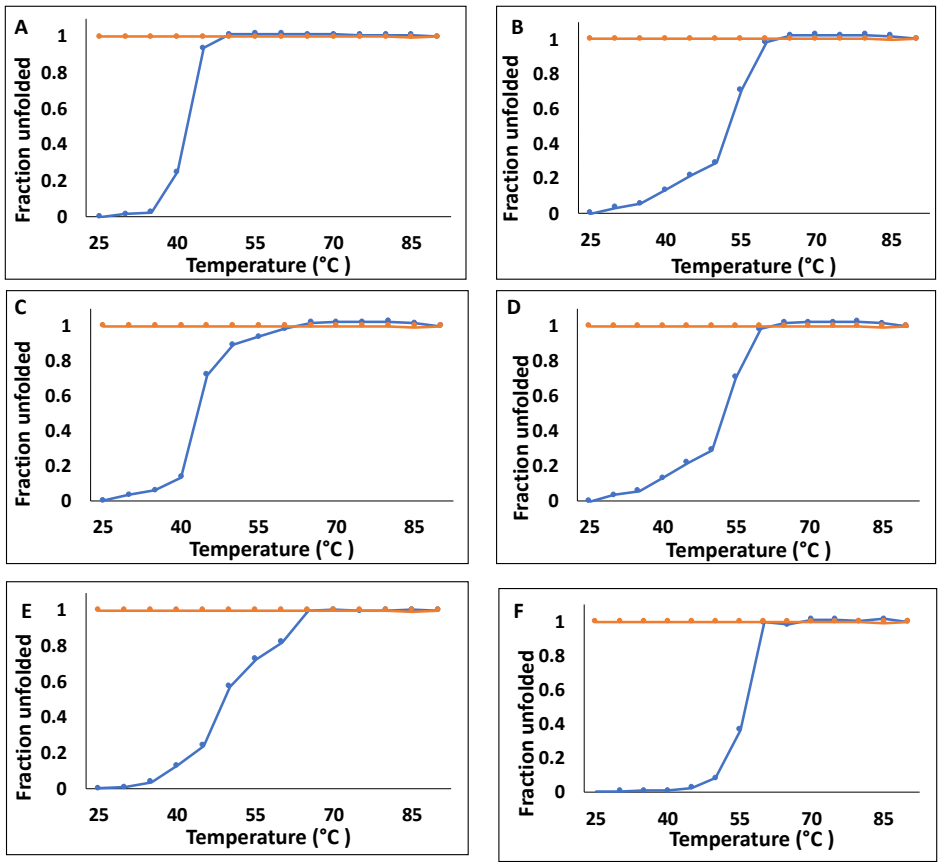

Fig. 6: Thermal unfolding and refolding curves of wtFGF1 (Panel-A; unfolding- blue, refolding- orange), K126N hFGF1 variant (Panel-B; unfolding- blue, refolding- orange), Q54P hFGF1 variant (Panel-C; unfolding- blue, refolding- orange), Q54P/R136E hFGF1 variant (Panel-D; unfolding- blue, refolding- orange), K126N/R136E hFGF1 variant (Panel-E; unfolding- blue, refolding- orange), and Q54P/K126N hFGF1 variant (Panel-F; unfolding- blue, refolding- orange). The thermal unfolding of wtFGF1 and its variants was monitored by changes in the ratio of intrinsic fluorescence intensities at 308 nm to 350 nm.

Mutations in the heparin binding pocket also affect stability of hFGF1 to chemical denaturants

Chemical denaturant–induced isothermic equilibrium unfolding of hFGF1 was examined to study the effects of the designed mutations on the stability of hFGF1 using intrinsic fluorescence spectroscopy (Figs. 7 and 8). Urea-induced equilibrium unfolding of wtFGF1 at pH 7.2 (Fig. 7) shows that it is a relatively unstable molecule [C_m ~ 1.9 M, C_m is the concentration of the denaturant wherein 50% of the protein population exists in the denatured state(s)] (Table-1).

Similar to the thermal unfolding data, single point mutations (K126N and R136E) in the heparin binding pocket increase the resistance of the protein to the denaturation induced by urea. However, unlike the thermal denaturation data, urea-induced unfolding data suggests that Q54P does not contribute to the stability of the protein. In fact, the Q54P mutation marginally decreases the C_m (C_m ~1.5 M). Interestingly, the double variants (Q54P/K126N and Q54P/R136E) which increased the thermal stability of the protein, did not confer extra stability against urea denaturation. In fact, the C_m (C_m ~1.5 M) values of these double variants were in the similar range to that of wtFGF1. However, the triple variant (Q54P/K126N/R136E) was most resistant to urea-induce equilibrium unfolding. These results clearly indicate that the interplay of structural forces during thermal unfolding is subtly different than thin urea-induced unfolding of the protein. The results discussed above also suggest that caution needs to be exercised when designing proteins based on denaturation data obtained from one-set of conditions.

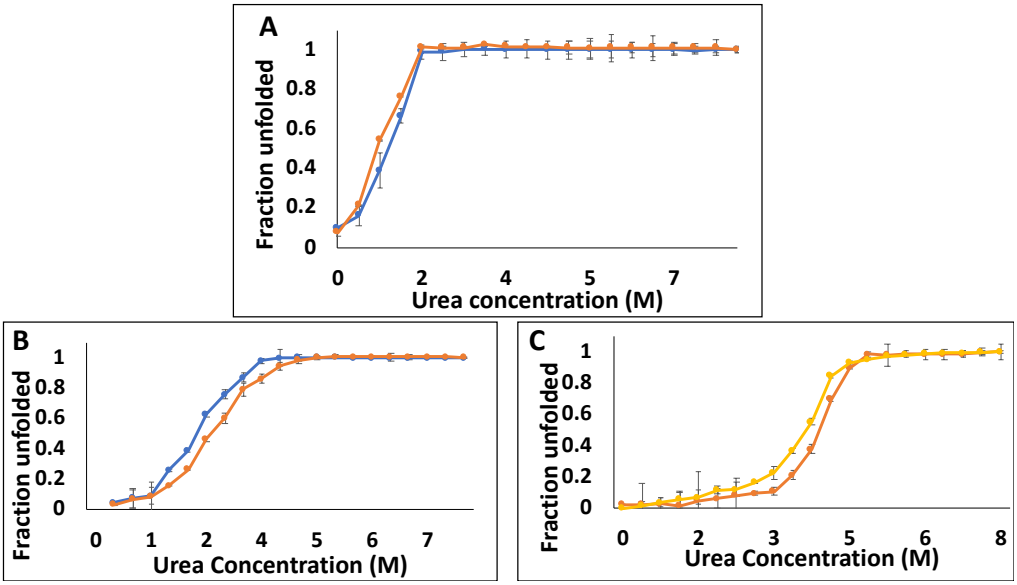

Fig. 7: Urea-induced equilibrium unfolding and refolding curves of wtFGF1 (Panel-A; unfolding – blue, refolding - orange), R136E hFGF1 variant (Panel-B; unfolding – orange, refolding- blue), and TM-variant of hFGF1 (Panel-C; unfolding – yellow, refolding - orange). The urea-induced equilibrium unfolding/refolding of wtFGF1 and its variants was monitored by changes in the ratio of intrinsic fluorescence intensities at 308 nm to 350 nm. Concentration of protein used was 0.5 mg/mL in 10mM phosphate buffer, pH 7.2 containing 100mM NaCl.

GdnHCl is an ionic denaturant and is known to efficiently disrupt both hydrogen bonds and electrostatic interactions in proteins. We examined the GdnHCl-induced equilibrium unfolding of hFGF1 to understand if the trend in the relative stability of the different designed variants is similar to that observed in the presence of a neutral denaturant such as urea. GdnHCl-induced equilibrium unfolding of hFGF1 was studied previously under different buffer conditions and a stable obligate intermediate was found to be populated at around 0.96 M GdnHCl[29]. The partially folded obligatory intermediate was shown to have characteristics resembling that of a molten-globule-like state. In this study, we find that the C_m of wtFGF1 is 1 M (Table-1, Fig. 8) and is very close to the one reported earlier [44]. All the seven variants of hFGF1 investigated herein showed higher stability than the wild type protein. This trend in the C_m values is slightly different from those calculated from the urea-induced unfolding profiles. Interestingly, the double mutants (Q54P/K126N, Q54P/R136E and K126N/R136E) seem to exhibit slightly lower stability than the single point mutants (Table-2). These results once again emphasize that the relative stabilities of hFGF1 appear to vary depending on the nature of the denaturant used. However, one aspect that can be consistently inferred from all the denaturation experiments is the extremely high stability of the triple (Q54P/K126N/R136E) variant of hFGF1.

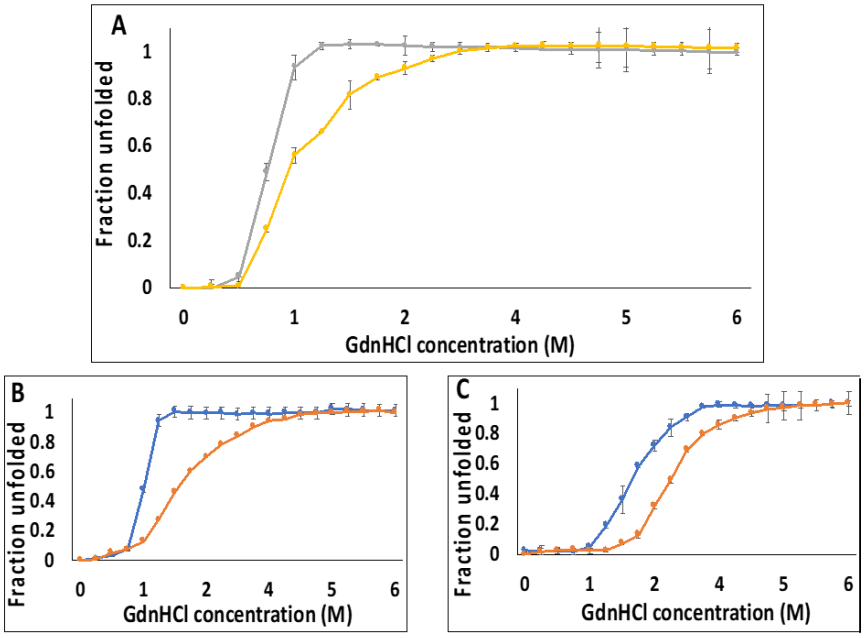

Fig. 8: GdnHCl-induced equilibrium unfolding and refolding curves of wtFGF1 (Panel-A; unfolding- yellow, refolding- gray), R136E hFGF1 variant (Panel-B; unfolding- orange, refolding- blue), and TM-variant of hFGF1 (Panel-C; unfolding- orange, refolding- blue). The GdnHCl-induced equilibrium unfolding/refolding of wtFGF1 and its variants was monitored by changes in the ratio of intrinsic fluorescence intensities at 308 nm to 350 nm. Concentration of protein used was 1 mg/mL in 10mM phosphate buffer, pH 7.2 containing 100mM NaCl.

Reversibility of the thermal unfolding of hFGF1

The thermal unfolding of hFGF1 is not reversible. Heating hFGF1 beyond its T_m causes aggregation of the protein. In fact, several reports show that wtFGF1 aggregates at temperatures beyond 50°C (Fig. 5) [19]. There has been increased interest in designing novel variants of hFGF1 which show increased stability and enhanced cell proliferation activity. In this context, we examined the reversibility of the temperature-induced unfolding of hFGF1 and its variants by monitoring intrinsic fluorescence changes at 308 nm and 350 nm. wtFGF1 completely unfolds at temperatures beyond 50°C. Refolding of the protein was attempted by slow cooling from 75°C to 25°C and the results clearly show that the protein remained in the unfolded state(s) (Fig. 5). This is obvious from the low 308 nm /350 nm intrinsic ratio. Attempts to refold wtFGF1 and its variants from a lower temperature (55°C to 25°C) also did not help the proteins regain their

native conformations. hFGF1 variants, which showed significantly higher $T_{m(\text{apparent})}$ (K126N, R136E, Q54P/K126N, and Q54P/R136E) than the wild type protein, also did not refold to their native conformations upon cooling from 85°C to 25°C. Interestingly, heat-induced denaturation of the triple variant (Q54P/K126N/R136E) is completely reversible (Fig. 5). The intrinsic fluorescence spectrum of the refolded protein at 25°C overlaid quite well with the protein that was not subjected to thermal denaturation at 75 °C (Fig. 9).

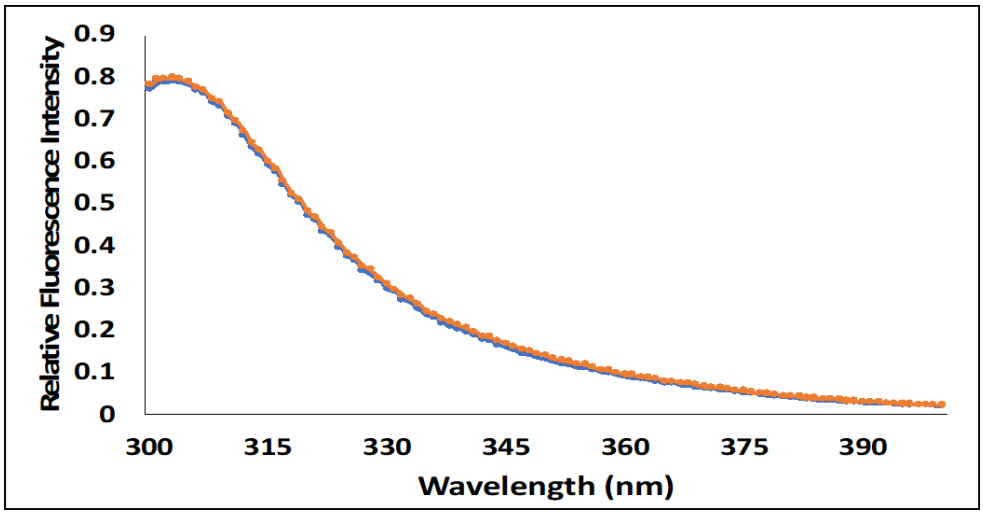

Fig. 9: Overlay of the intrinsic fluorescence spectrum of the refolded triple variant at 25°C (orange) and the triple variant during thermal denaturation at 75 °C (blue).

^{1}H-^{15}N HSQC spectrum provides atomic level information on the backbone conformation of a protein. Each crosspeak in the spectrum represents an amino acid in a particular backbone conformation. In this context, ^{1}H-^{15}N HSQC spectra of the triple variant (Q54P/K126N/R136E) were acquired before heat treatment and after refolding upon cooling from its heat denatured state(s). Superimposition of the ^{1}H-^{15}N HSQC spectra shows that most of the crosspeaks overlap quite well suggesting that the triple variant is capable of refolding back to its native conformation from the heat denatured state(s) (Fig. 10).

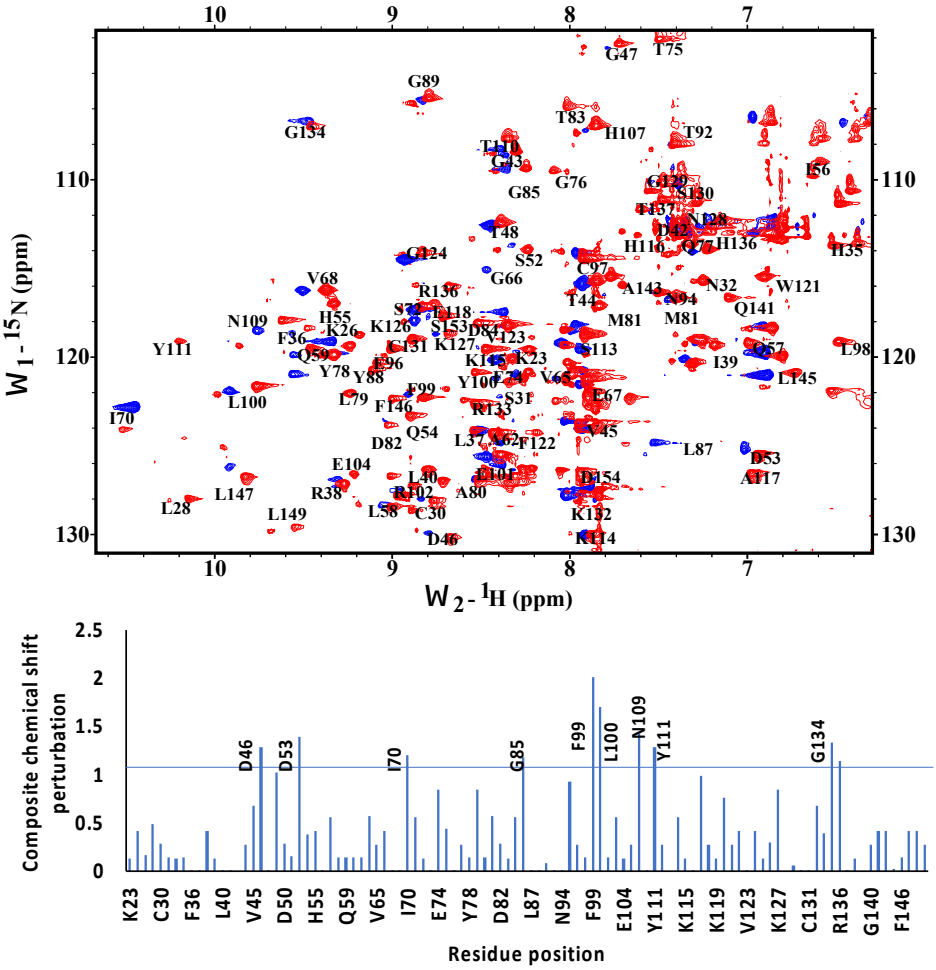

Fig. 10: Overlay of the $^{1}H–^{15}N$ HSQC of Q54P-TM without heat treatment (red) and the Q54P-TM after heat treatment (blue) (Panel-A). $^{1}H–^{15}N$ chemical shift perturbation observed due to the temperature effect (Panel-B). The horizontal line represents the arbitrary threshold above which the $^{1}H–^{15}N$ chemical shift perturbation(s) was considered as significant. The $^{1}H–^{15}N$ chemical shift perturbation of individual residues were calculated using the formula, ($\sqrt{[(2\Delta\delta_{NH})^2 + (\Delta\delta_N)^2]}$).

hFGF1 is a mitogen and exhibits potent cell proliferation activity. Therefore, the effect(s) of the untreated and refolded triple variant (Q54P/K126N/R136E) forms on the proliferation of NIH3T3 cells, were compared to examine if the refolded protein is biologically active. As expected, wtFGF1 promotes proliferation of NIH3T3 cells and the number of cells almost tripled compared to the control cells which were not treated with wtFGF1 (Fig. 11). Interestingly, the triple variant exhibits higher cell proliferation activity than the wild type which is mostly

consistent with its higher structural stability (Fig. 11). The triple variant which was refolded from its heat denatured state(s) is also biologically active albeit with a lower potency (Fig. 11). The moderately lower activity exhibited by the refolded triple variant protein could be either due to lower stability of the refolded protein in the cell culture medium or due to the presence of a small population of biologically inactive soluble oligomers. However, it should be mentioned that no visible aggregates were detected in the refolded triple variant protein. These results suggest that the triple variant can successfully regain its native conformation from its heat-denatured state(s). To our knowledge, this is the only hFGF1 variant that has been unequivocally shown to refold to its unique biologically active conformation from its heat denatured state(s).

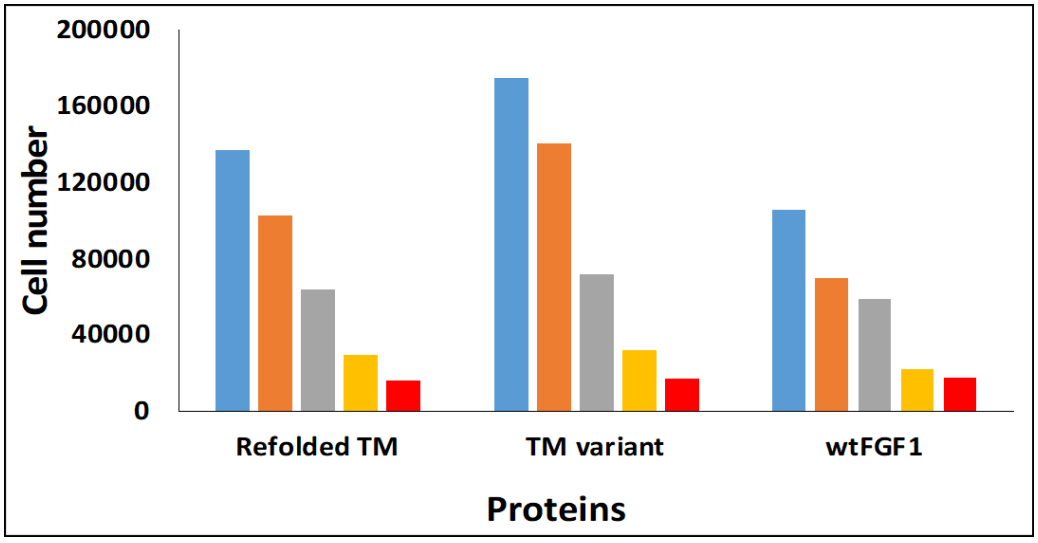

Fig. 11: Cell proliferation activity of the wtFGF1 and the triple variant (with and without heat treatment). 50 ng/mL (blue), 10 ng/mL (orange), 2 ng/mL (gray), 0.4 ng/mL (yellow), and 0 ng/mL (red).

The triple variant of hFGF1 exhibits hysteresis during refolding from its heat denatured state(s)

Thermal unfolding of the triple variant (Q54P/K126N/R136E) of hFGF1 is reversible but a closer look at the thermal unfolding and refolding curves shows that they don't superimpose

well (Fig. 12). The T_m values characterizing the unfolding (60 ± 0.07 °C) and refolding (50 ± 0.09 °C) processes do not match. Typically, if the structural transitions that occur during heat-induced denaturation and renaturation from the heat denatured state(s) to the native conformation are the same, then one would expect the denaturation and renaturation profiles to superimpose quite well with nearly similar T_m values. The mismatch in the T_m values, characterizing the thermal unfolding and refolding processes, is clearly indicative of hystersis. The observation of hysteresis is rare but not unprecedented [45]. Hysteresis has been observed in multidomain and multimeric proteins [45-50]. Hysteresis observed in the multidomain proteins is largely attributed to disparities in the folding transition ensembles, which probably stem from the fact that unfolding of these proteins is governed by domain transition whereas refolding events occur more cooperatively [50]. However, hysteresis in single domain proteins such as collagen is believed to be due to mismatch in the structural events that occur in unfolding and refolding of the protein. Refolding of collagen is believed to occur *via* slow structural rearrangement of the loop regions whereas unfolding has been shown to be more cooperative requiring the disruption of few structural interactions that are important for stability [47]. Another plausible explanation for the observed hysteresis in the thermal unfolding and refolding of the triple variant of hFGF1 may be ascribed to slow *cis-trans* isomeriztion of the proline introduced at position 54 via the Q54P mutation. Verification of this proposal would require in-depth site–directed mutation studies which are beyond the scope of this study. In addition, in some cases hysteresis has also been attributed to transient association between protein molecules during the process of protein folding/unfolding [51]. As protein association is a multimolecular reaction, the hysteresis behavior ascribed to protein association should be dependent on the protein concentration. In this context, we compared the thermal unfolding of the triple variant at two different protein

concentrations (0.5 mg/mL and 0.2 mg/ml). Thermal unfolding and refolding curves obtained at these concentrations were nearly identical suggesting that the hysteresis phenomenon observed in the triple variant of hFGF1 is not related to protein association events (Figs. 12A and 12C). In some cases, hysteresis observed during thermal unfolding-refolding is believed to be due to steep temperature gradients used during the renaturation process [49]. To verify this, we examined thermal unfolding/refolding of the triple variant of hFGF1 under two temperature gradient conditions, 5°C and 2°C temperature intervals (Figs. 12A and 12B). The results obtained suggest that the hysteresis observed during the thermal unfolding-refolding of the hFGF1 triple variant is independent of the temperature gradients used in the experiment (Fig. 12).

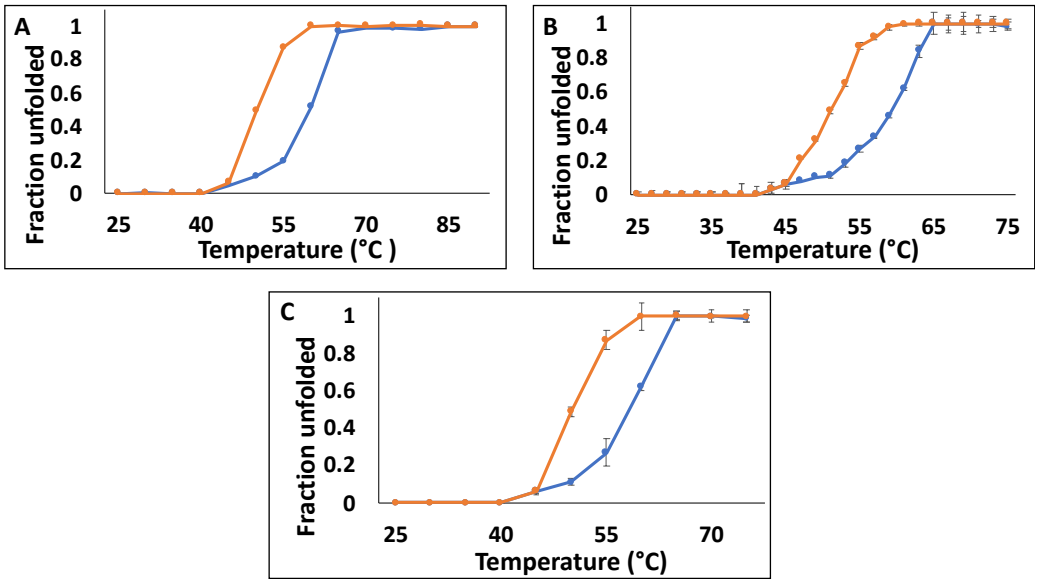

Fig. 12: Thermal unfolding and refolding curves of the triple variant at a concentration of 0.5 mg/mL and temperature interval of 5°C (Panel – A; unfolding (blue), refolding (orange)), 0.5 mg/mL and temperature interval of 2°C (Panel – B; unfolding (blue), refolding (orange)), and 0.2 mg/mL and temperature interval of 5°C (Panel – C; unfolding (blue), refolding (orange)).

Chemical denaturant-induced equilibrium unfolding-refolding of the triple variant of hFGF1 was examined to understand if the hysteresis behavior is dependent on the conditions used for protein unfolding/refolding. Overlay of the urea- and GdnHCl-induced equilibrium

unfolding/refolding profiles separately shows no signs of hysteresis under these conditions. The C_m values for the chemical-induced equilibrium unfolding and refolding processes appear to be in agreement within the limits of experimental error (Figs. 7C and 8C). Interestingly, these results appear to suggest that hysteresis behavior depends significantly on the conditions used for protein unfolding/refolding. Hysteresis behavior appears to be discernably controlled by the nature of structural intermediates that populate a particular unfolding pathway. In the theoretical sense, it appears that the roughness of the protein folding funnel/terrain is denaturant-dependent.

Structural interactions contribute to the stability and reversible thermal unfolding of the triple variant

The structural interactions that contribute to the enhanced stability and reversible thermal unfolding behavior of the triple variant of hFGF1 were investigated using two-dimensional NMR spectroscopy and MD simulations. Superimposition of the ^{1}H-^{15}N HSQC spectra of Q54P/K126N/R136E on wtFGF1 and analysis of the ^{1}H-^{15}N chemical shift perturbation plot (Figs. 13A and B) indicate that introduction of mutations at positions 54, 126, and 136, induces only a minor shift of the cross peaks corresponding to residues located in the spatial vicinity of the mutation site (R136, G134, and K132). These three residues are located in the heparin-binding pocket. R136 is one of the mutated sites and K132 and G134 are involved in the formation of stronger electrostatic interactions (E136-K132, G134-G85) in the triple variant. G134 is in close proximity to R136 and R133 (located in the center of the heparin binding pocket). Thus, introduction of Q54P, K126N, and R136E appears to have contributed to formation of new electrostatic interactions in the heparin binding pocket. These new interactions could plausibly have increased the compactness of the hFGF1 structure and consequently decreased the flexibility of the heparin binding loop.

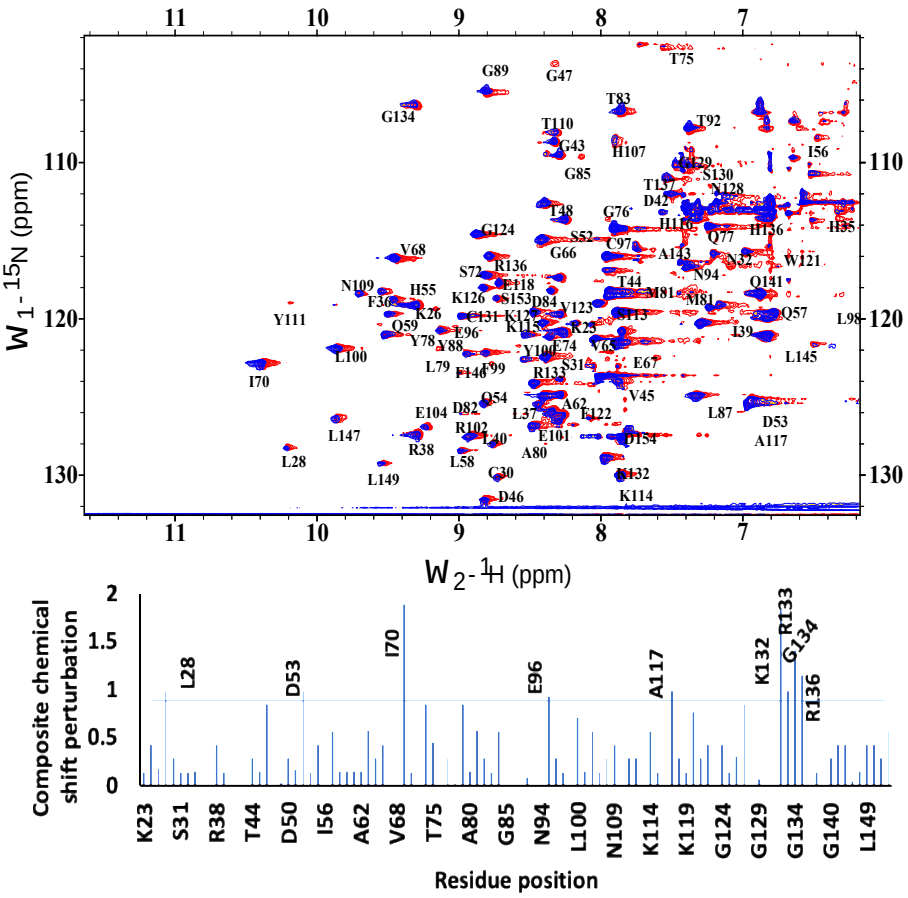

Fig. 13: Overlay of the $^{1}H–^{15}N$ HSQC of wtFGF1(blue) and the Q54P-TM (red) (Panel-A). $^{1}H–^{15}N$ chemical shift perturbation observed due to the R136E/K126N/Q54P mutation in hFGF1 (Panel-B). The horizontal line represents the arbitrary threshold above which the $^{1}H–^{15}N$ chemical shift perturbation(s) was considered as significant. The $^{1}H–^{15}N$ chemical shift perturbation of individual residues were calculated using the formula, $(\sqrt{[(2\Delta\delta_{NH})^2 + (\Delta\delta_N)^2]})$.

We have also performed microsecond-level equilibrium MD simulations of wtFGF1[38] and the triple variant, based on the X-ray crystal structure of the hFGF1 monomer (PDB ID: 1RG8) [29]. wtFGF1 is fairly stable initially, with RMSD values remaining around 1 Å for approximately 2 μs [38]. However, it undergoes a conformational change quite abruptly after about 2 μs and reaches an RMSD value of nearly 3 Å [38]. When compared with wtFGF1, the triple variant (Q54P/K126N/R136E) does not exhibit any sudden conformational changes and remains relatively stable for 4.8 μs with an RMSD of around 2 Å (Figure 14B). The differential

behavior of wtFGF1 and the triple variant is more clearly reflected in the RMSD time series of the heparin-binding region (residues 126-142), wherein wtFGF1 behaves significantly differently from the triple variant (Fig. 14C). The heparin-binding region in wtFGF1 is initially stable below 1Å but undergoes an abrupt conformational transition (Fig. 14A, 14C) at around 2 μs and stays at 3.5Å for the rest of the simulation, whereas the heparin-binding region of the triple variant remains stable around 2Å for 4.8 μs [38]. A visual inspection of the simulation trajectories clearly reveals that the heparin-binding region of wtFGF1 moves away from the core of the protein after the 2 μs timepoint, while no major change is observed for the triple variant (Fig. 14A) [38].

These results are further corroborated by the root-mean-square fluctuation (RMSF) analysis for wtFGF1 and the triple variant, wherein both systems show similar trends in their fluctuations for different regions with the exception of the heparin-binding region in wtFGF1 (Fig. 14D) [38]. Experimental results of intrinsic fluorescence and far-UV CD spectroscopy data are in good agreement with the MD simulation data suggesting that the designed mutations do not significantly perturb the beta-trefoil core structure of wtFGF1.

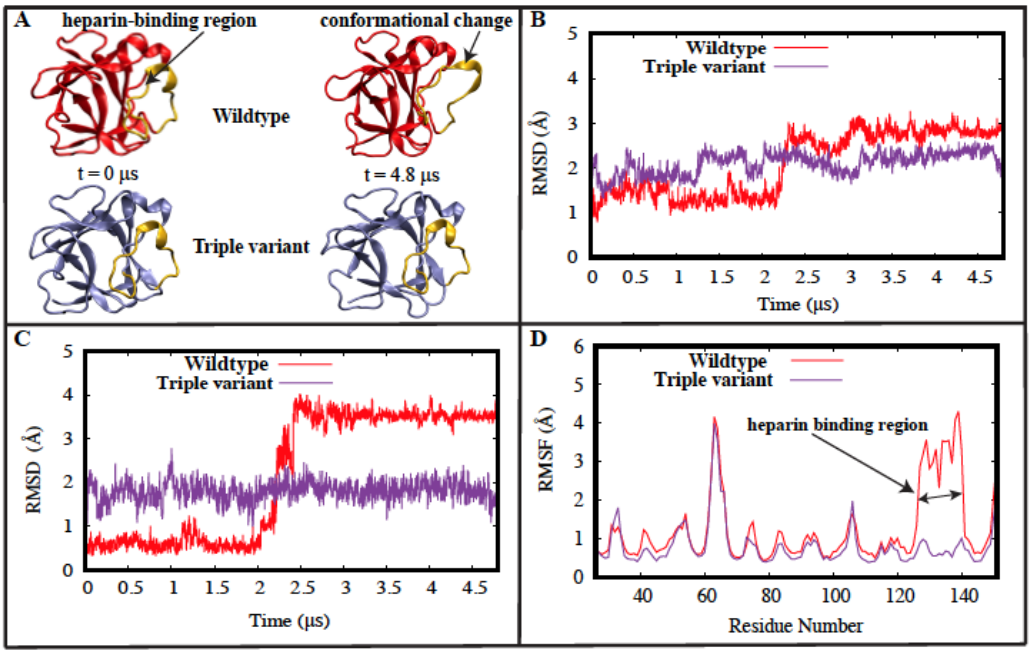

Fig. 14: A) Visual representation of wtFGF1 (red) before and after the conformational change. The heparin-binding region (gold) moves away from the beta-trefoil core of the protein. No major conformational change occurs in the triple variant (purple). The heparin-binding region (gold) maintains the same conformation for 4.8 μs. B) RMSD time series for wtFGF1 (red) and the triple variant (purple). C) RMSD time series for the heparin-binding region of wtFGF1 (red) and the triple variant (purple). D) Root mean square fluctuation (RMSF) estimations for the wtFGF1 (red) and the triple variant (purple).

Based on the criteria defined in the methods section, 65 stable hydrogen bonds were identified in wtFGF1. Only one interaction out of 65 involves the heparin-binding region – L145-K142 (84%) which is a backbone-backbone hydrogen bond. All 65 interactions observed in wtFGF1 also occur in the triple variant with similar occupancies. 6 stable hydrogen bonds were observed in the triple variant involving the heparin binding region (Table 2) that do not qualify as stable hydrogen bonds in wtFGF1 based on the criteria defined in the methods section (Table 2). Two of these six interactions involved variant residues (N126 and E136) (Table 2 in bold).

Table 2: Electrostatic interactions involved in the heparin binding region in the triple variant.

Salt bridge/hydrogen bond Interaction	Occupancy (%)	
	triple variant	wildtype
R133 – E136	**98**	**0**
N126 – S130	**79**	**0**
G134 – G85	79	35
T137 – G134	62	35
K132 – G124	62	28
Y139 – E104	54	13

Both interactions involving variant residues have very high occupancies. R133-E136 is a strong salt-bridge interaction, indicating that the R136E mutation might play a key role in conferring stability to the protein and in reversing the unfolding process of wtFGF1 (Fig. 15A). A weaker salt bridge involving E136 (E136-K132) (Fig. 15B) was also identified. Both these salt-bridges occur only in the triple variant.

Two unique salt-bridges were also identified in wtFGF1 – D84-K132 (Fig. 15C) and D46-K127 (Fig. 15D) [38]. Electrostatic interactions between positively charged residues in the heparin binding region and negatively charged residues in the beta-trefoil core, help stabilize the heparin-binding region after the conformational change that occurs in wtFGF1 [38]. D84 of the beta-trefoil core interacts with K132 of the heparin binding region, while D46 of the beta-trefoil core interacts with K127 of the heparin binding region [38]. The absence of the D84-K132 interaction in the triple variant (Figure 15C) indicates that K132 interacts more favorably with E136 (Figure 15B) than with D84. Therefore, the R136E mutation potentially causes a transition from a relatively weak long-range interaction to a stronger short-range interaction, thus stabilizing the triple variant.

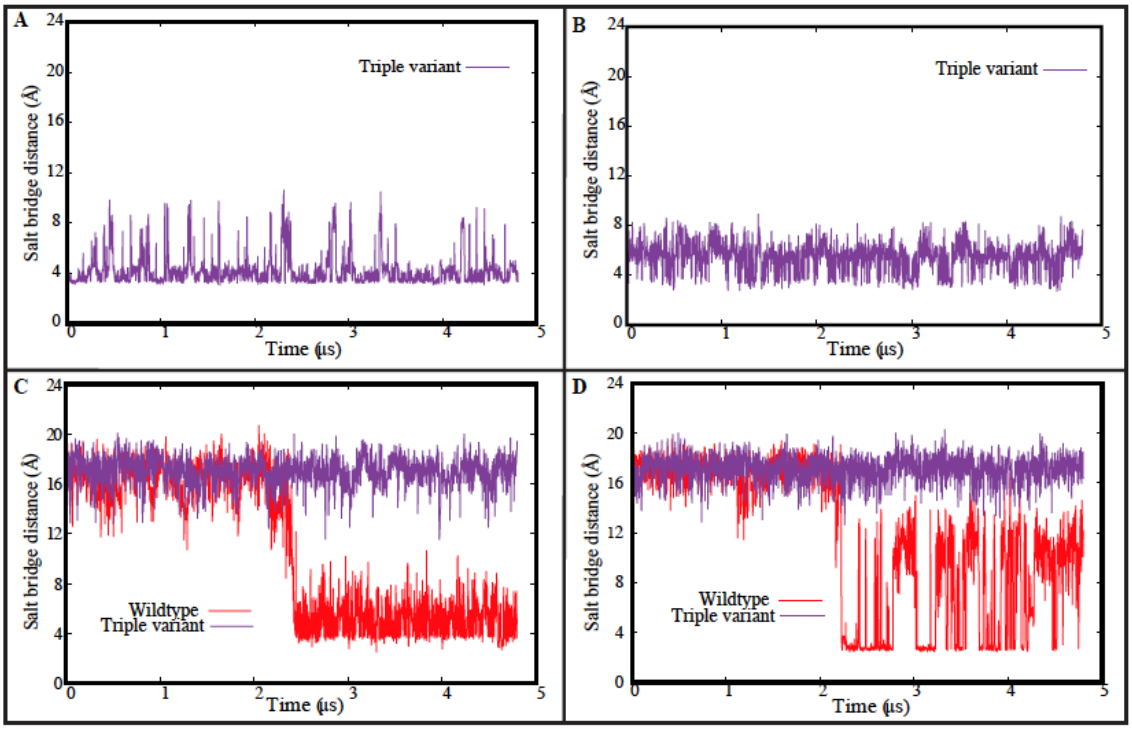

Fig. 15: A, B) Time series of the E136-R133 (A) and E136-K132 (B) donor-acceptor salt bridge distance in the triple variant structure. C, D) Time series of the D84-K132 (C) and D46-K127 (D) donor-acceptor salt bridge distances in wtFGF1 (red) and the triple variant (purple).

Two out of the three mutations (K126N and R136E) in the triple variant structure are located in the heparin binding region. RMSD, RMSF and electrostatic interaction analyses suggest that these mutations are the driving force behind the relative conformational stability of the triple variant. These results are further supported by solvent accessible surface area (SASA) calculations for the heparin binding region. SASA of the wildtype heparin-binding region increases significantly after 2 μs while there is no significant change during the triple variant simulation (Figure 16) [38].

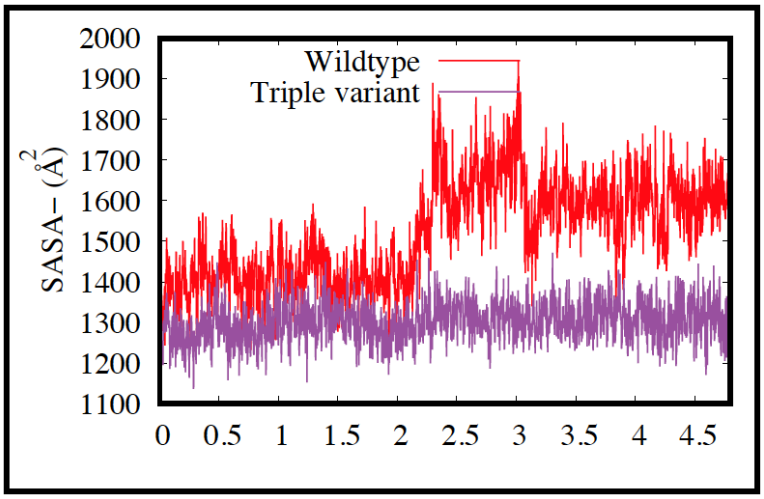

Fig. 16: Comparison of the SASA time series of the heparin-binding region of wtFGF1 and the triple variant.

The MD simulations reveal that although wtFGF1 is relatively stable within 2 microseconds (which could be misleading if one uses typical sub-microsecond-level simulations), it undergoes a rapid conformational transition after 2 microseconds [38]. Absence of this conformational change in the triple variant indicates that the mutations in the heparin binding region have led to an increase in stability of the protein. While microsecond-level MD simulations cannot provide a complete characterization of the unfolding and folding process, they do give us unique insights into the conformational dynamics of wildtype and triple variant hFGF1. The computational data is generally in agreement with the experimental data, showing that these mutations contribute to the structural forces responsible for the reversibility of unfolding of the triple variant.

Conclusions

In the present study, we show that nullification or reversal of charge of amino acids in the heparin binding pocket of hFGF1, increases protein stability without significant perturbation of the three-dimensional structure of the protein. The triple variant (Q54P/K126N/R136E) exhibits ~ 20°C higher stability than the wild type protein. With the exception of the triple variant, the thermal unfolding of wt-hFGF1 and designed variants is irreversible. Two-dimensional NMR

and cell proliferation activity data clearly show that the thermally denatured triple variant fully regains its biologically active native conformation upon cooling. The refolding of the triple mutant, from its thermally denatured state(s), exhibits a hysteresis behavior with a mismatch in the Tm values of the unfolding and refolding process. In addition, comparison of the thermal-, urea-, and GdnHCl-induced unfolding data suggest that the relative stabilities of hFGF1 and its variants vary depending on the nature of the denaturant used. MD simulation studies reveal that the triple variant mutations reduce the flexibility of the heparin binding region and enhance the stability of hFGF1 by forming a network of stable electrostatic interactions such as R133-E136 and N126-S130. These interactions in the triple variant also appear to play a critical role in the reversible thermal unfolding of the protein. To the best of our knowledge, this is the first study wherein a hFGF1 variant with increased stability and reversible protein folding behavior is reported. The findings of this study, in our opinion, can be expected to provide valuable leads for the design of an efficient FGF-based therapy for chronic wound care.

Materials and methods

Materials

DNA plasmid isolation kits were purchased from Qiagen, USA and Quikchange II XL mutagenesis kits were obtained from Agilent. Competent cells (DH5α and BL-21(DE3)) were sourced from Novagen Inc., USA. Lysogeny broth (LB) was obtained from EMD Millipore, USA. Heparin sepharose was obtained from GE Healthcare, USA. VWR Scientific Inc, USA was the supplier for all buffer components including Na_2HPO4, NaH_2PO4 and NaCl. NIH 3T3 cells were obtained from ATCC and all the cell culture reagents including, DMEM media, fetal bovine serum (FBS) and penicillin-streptomycin were purchased from Thermo Fisher Scientific (Waltham, MA).

Construction and availability of pure wtFGF1 and hFGF1 variant (s)

For all site-directed mutagenesis experiments, a truncated form of the hFGF1 gene (residue number, 15-154) was inserted into a pET20b expression vector. Primers were designed using an Agilent primer design program and were ordered from IDT DNA Inc., USA. Site-directed mutagenesis (SDM) was performed using a QuikChange lightning kit followed by polymerase chain reaction (PCR) as per the protocol provided by the vendor (Agilent Technologies). The plasmid was then transformed into XL-gold competent cells and plasmid sequencing was carried out by the DNA core sequencing facility at the University of Arkansas Medical Science (UAMS). Each hFGF1 variant was overexpressed in BL-21(pLysS) *Escherichia coli* cells cultured in lysogeny broth (LB) at 37 °C with agitation at 250 rpm. After overexpression, bacterial cells were lysed by ultra-sonication and the released proteins were separated from the cell debris by centrifugation for 20 minutes at 19,000 rpm. All the hFGF1 variant proteins were then purified on a heparin-sepharose column using a stepwise salt gradient (100 – 1500 mM NaCl) in 10 mM sodium phosphate buffer (pH 7.2). SDS-PAGE was used to determine the purity of the protein. The protein bands were visualized by staining the gels with Coomassie brilliant blue and the protein concentrations were determined by Bradford assay using a Hitachi F-2500 fluorimeter.

Circular dichroism (CD) spectroscopy

Far-UV circular dichroism (CD) measurements were performed on a JASCO-1500 spectropolarimeter using a quartz cell of 1 mm path length. Each spectrum was an average of 3 scans and the wavelength range used was from 190-250 nm. The concentration of the protein used was 33 μM in 10 mM sodium phosphate buffer (pH 7.2) containing 100 mM NaCl at 25 °C. All the data points were normalized using necessary background corrections and smoothened

using the Savitzky-Golay algorithm. The final spectra were obtained after necessary blank corrections with 10 mM sodium phosphate buffer (pH 7.2) containing 100 mM NaCl.

Fluorescence spectroscopy

All intrinsic fluorescence measurements were performed on a Hitachi F-2500 spectrophotometer at 25 °C and a 10 mm quartz cuvette. The excitation and emission slit widths were each set at 2.5 nm. All the experiments were performed with protein concentration of 33 μM in 10 mM sodium phosphate buffer (pH 7.2) containing 100 mM NaCl. wtFGF1 and all the variant proteins were excited at a wavelength of 280 nm and the emission spectra were recorded from 300 nm to 400 nm.

Equilibrium unfolding

Thermal, urea and GdnHCl unfolding of wtFGF1 and all the hFGF1 variants were performed on a Jasco-1500 spectrophotometer using the fluorescence and circular dichroism spectroscopy. Equilibrium unfolding experiments were performed using a protein concentration of 33 μM in 10 mM sodium phosphate buffer (pH 7.2) containing 100 mM NaCl. Spectra were collected every 5 degrees from 25 to 90 °C. Each set of data was fit using excel graphing tools. The proteins were excited at a wavelength of 280 nm and the emission spectra were recorded from 300 nm to 400 nm and the fraction unfolded was plotted as a function of temperature. The denaturation temperature (T_m) was determined as the temperature at which 50% of the protein population was denatured. Urea and GdnHCl-induced equilibrium unfolding experiments were conducted at a protein concentration of 33 μM. Urea and GdnHCl was titrated in consistent volumes into the sample up to a concentration of 8 M and 6 M, respectively. Protein unfolding was monitored by fluorescence and the fraction unfolded was determined using the ratio of the fluorescence 308/350 nm intrinsic fluorescence. Spectra were collected as an average of 3 scans.

Nuclear magnetic spectroscopy

^{1}H-^{15}N HSQC experiments were conducted on a Bruker Avance DMX-700 MHz spectrometer equipped with a 5 mm inverse cryoprobe at 25°C. wtFGF1 and the Q54P/K126N/R136E-TM were grown in M9 medium with $^{15}NH_4Cl$ used as the sole nitrogen source. For the heat treated Q54P/K126N/R136E-TM NMR sample, the protein was heated to 75°C using the water bath for 3 minutes and then cooled down at room temperature for 5 minutes. The sample was then centrifuged to remove any visible aggregates. ^{15}N labeled protein samples (1 mM) were prepared in 90% H_2O + 10% D_2O solution containing 10 mM sodium phosphate buffer (pH 7.2) containing 100 mM NaCl and 25 mM $(NH_4)_2SO_4$. Spectra were recorded using 48 scans and 256 data points in XY dimension. Data were analyzed using XWINNMR 3.5 software supplied by Bruker.

Cell proliferation activity

3T3 fibroblast cells obtained from ATCC (Manassas, VA) were cultured in complete media consisting of DMEM supplemented with 10% FBS and 1% penicillin/streptomycin. Cells were grown to 80–90% confluency and were incubated overnight at 37 °C with 5% CO_2 in serum free media. Cells were then centrifuged for 2 min at 6000 rpm and then washed twice with hyclone buffer to remove any remaining trace of enzyme and were transferred to incomplete media (DMEM media without 10% FBS). The cell proliferation activity of hFGF1 was determined by quantifying the increase in cell number after the cells had been incubated with hFGF1 at varying concentrations. Starved 3T3 fibroblasts were collected and seeded in a 96-well plate at a seeding density of 10,000 cells/well. Cells were then co-incubated individually with wild type and variant hFGF1 at concentrations of 0, 0.4, 2, 10, and 50 ng/mL. After 24 h of incubation, 3T3 cell proliferation was assessed by the CellTiter-Glo (Promega, Madison, WI) cell proliferation assay.

All-atom equilibrium MD simulation

An all-atom equilibrium MD simulation of the triple variant (Q54P, K126N, R136E) was performed based on the X-ray crystal structure of the hFGF1 monomer (PDB ID: 1RG8 – Resolution: 1.1 angstroms) [29]. CHARMM-GUI was used to generate the initial simulation model [30,31]. Residues 12-137 from the crystal structure correspond to residues 26-151 in the experimental sequence. The first 12 residues were not used experimentally because they are part of a random coil. The heparin-binding region spans residues 126-142 (in the experimental sequence). The initial part of simulation was performed with the NAMD 2.13 simulation package and the CHARMM36 all-atom additive force field [32,33]. The input files were generated using CHARMM-GUI's QuickMD Simulator plugin [31]. The model was solvated in a rectangular TIP3P water box and 150 mM of NaCl ions were inserted into the system using the Monte-Carlo ion placing method [31]. The system consisted of approximately 25,000 atoms. Initially, we energy-minimized the system for 10,000 steps using the conjugate gradient algorithm [34]. Then, the system was relaxed by releasing the restraints in a stepwise manner (for a total of ~1 ns) using the standard CHARMM-GUI equilibration protocol [30,31]. The initial relaxation was performed in an NVT ensemble while the rest of the simulation was performed in an NPT ensemble at 300 K using a Langevin integrator with a time step of 2 fs and damping coefficient of 0.5 ps^{-1}. The pressure was maintained at 1 *atm* using the Nosé–Hoover Langevin piston method [34,35]. The smoothed cut-off distance for non-bonded interactions was set to 10−12 Å, and long-range electrostatic interactions were computed with the particle mesh Ewald (PME) method [36]. The initial equilibration run lasted 15 nanoseconds. The production run was then extended on the Anton2 supercomputer for 4.8 microseconds, with a timestep of 2.5 fs. The pressure was maintained at 1 atm semi-isotropically, using the MTK barostat, while the

temperature was maintained at 300 K, using the Nosé–Hoover thermostat. The long-range electrostatic interactions were computed using the fast Fourier transform (FFT) method [37]. Conformations were collected every 240 picoseconds. Data from an all-atom equilibrium MD simulation of wildtype hFGF1 that we had performed previously using identical conditions, was compared with data from the triple variant simulation described above [38].

The RMSD trajectory tool of VMD was used to calculate the RMSD and C_α atoms were considered for these calculations [39]. For RMSD calculations, we aligned the region of interest against its own initial configuration and calculated RMSD with respect to this configuration. RMSF of individual residues was calculated using the C_α atoms by aligning the trajectory against the crystal structure. The salt bridge plugin of VMD was used to calculate the distance between the two salt bridge residues over the course of the simulation, which is the distance between the oxygen atom of the participating acidic residue and the nitrogen atom of the basic residue. The VMD HBond plugin was used for hydrogen bond analysis [39]. Salt bridges were defined as interactions with an oxygen-nitrogen cut-off distance below 4 Angstroms for at least 50% of the total simulation time [39]. Hydrogen bonds were defined as interactions between two residues with a hydrogen donor and a hydrogen acceptor with an angle cutoff of 35 degrees between the donor, hydrogen, and acceptor and a donor-acceptor distance cutoff of 4 angstroms. A stable hydrogen bond was defined as a hydrogen bond with an occupancy of 50% or more over the course of the simulation. SASA was calculated using the internal SASA measurement method of VMD [39].

REFERENCES

[1] Englander SW, Mayne L. The case for defined protein folding pathways. Proceedings of the National Academy of Sciences. 2017 Aug 1;114(31):8253-8.

[2] Cieplak AS. Protein folding, misfolding and aggregation: The importance of two-electron stabilizing interactions. PloS one. 2017 Sep 18;12(9):e0180905.

[3] Hsieh HC, Kumar TK, Chiu CC, Yu C. Equilibrium unfolding of an oligomeric protein involves formation of a multimeric intermediate state (s). Biochemical and biophysical research communications. 2004 Dec 31;326(1):108-14.

[4] Ebo JS, Guthertz N, Radford SE, Brockwell DJ. Using protein engineering to understand and modulate aggregation. Current opinion in structural biology. 2020 Feb 1;60:157-66.

[5] Wu S, Du L. Protein Aggregation in the Pathogenesis of Ischemic Stroke. Cellular and Molecular Neurobiology. 2020 Jun 11:1-2.

[6] Díaz-Villanueva JF, Díaz-Molina R, García-González V. Protein folding and mechanisms of proteostasis. International journal of molecular sciences. 2015 Aug;16(8):17193-230.

[7] Balchin D, Hayer-Hartl M, Hartl FU. In vivo aspects of protein folding and quality control. Science. 2016 Jul 1;353(6294).

[8] Soto C, Pritzkow S. Protein misfolding, aggregation, and conformational strains in neurodegenerative diseases. Nature neuroscience. 2018 Oct;21(10):1332-40.

[9] Mukherjee A, Soto C. Prion-like protein aggregates and type 2 diabetes. Cold Spring Harbor perspectives in medicine. 2017 May 1;7(5):a024315.

[10] Wang W, Khatua P, Hansmann UH. Cleavage, Downregulation, and Aggregation of Serum Amyloid A. The Journal of Physical Chemistry B. 2020 Jan 20;124(6):1009-19.

[11] Wang W, Roberts CJ. Protein aggregation–mechanisms, detection, and control. International Journal of Pharmaceutics. 2018 Oct 25;550(1-2):251-68.

[12] Sarkar S, Gulati K, Kairamkonda M, Mishra A, Poluri KM. Elucidating protein-protein interactions through computational approaches and designing small molecule inhibitors against them for various diseases. Current topics in medicinal chemistry. 2018 Aug 1;18(20):1719-36.

[13] Guinn EJ, Tian P, Shin M, Best RB, Marqusee S. A small single-domain protein folds through the same pathway on and off the ribosome. Proceedings of the National Academy of Sciences. 2018 Nov 27;115(48):12206-11.

[14] Kantaev R, Riven I, Goldenzweig A, Barak Y, Dym O, Peleg Y, Albeck S, Fleishman SJ, Haran G. Manipulating the folding landscape of a multidomain protein. The Journal of Physical Chemistry B. 2018 Aug 8;122(49):11030-8.

[15] Iglesias-Bexiga M, Szczepaniak M, Sanchez de Medina C, Cobos ES, Godoy-Ruiz R, Martinez JC, Muñoz V, Luque I. Protein Folding Cooperativity and Thermodynamic Barriers of the Simplest β-Sheet Fold: A Survey of WW Domains. The Journal of Physical Chemistry B. 2018 Jul 9;122(49):11058-71.

[16] Chen EH, Lu TT, Hsu JC, Tseng YJ, Lim TS, Chen RP. Directly monitor protein rearrangement on a nanosecond-to-millisecond time-scale. Scientific reports. 2017 Aug 18;7(1):1-1.

[17] Nowick JS. Exploring β-sheet structure and interactions with chemical model systems. Accounts of chemical research. 2008 Oct 21;41(10):1319-30.

[18] Kumar TK, Jayaraman G, Lee CS, Sivaraman T, Lin WY, Yu C. Identification of" molten globule"-like state in an all β-sheet protein. Biochemical and biophysical research communications. 1995 Feb 15;207(2):536-43.

[19] Kerr R, Agrawal S, Maity S, Koppolu B, Jayanthi S, Kumar GS, Gundampati RK, McNabb DS, Zaharoff DA, Kumar TK. Design of a thrombin resistant human acidic fibroblast growth factor (hFGF1) variant that exhibits enhanced cell proliferation activity. Biochemical and Biophysical Research Communications. 2019 Oct 15;518(2):191-6.

[20] Davis JE, Alghanmi A, Gundampati RK, Jayanthi S, Fields E, Armstrong M, Weidling V, Shah V, Agrawal S, prasanth Koppolu B, Zaharoff DA. Probing the role of proline− 135 on the structure, stability, and cell proliferation activity of human acidic fibroblast growth factor. Archives of biochemistry and biophysics. 2018 Sep 15;654:115-25.

[21] Davis JE, Gundampati RK, Jayanthi S, Anderson J, Pickhardt A, prasanth Koppolu B, Zaharoff DA, Kumar TK. Effect of extension of the heparin binding pocket on the structure, stability, and cell proliferation activity of the human acidic fibroblast growth factor. Biochemistry and biophysics reports. 2018 Mar 1;13:45-57.

[22] Huang Z, Tan Y, Gu J, Liu Y, Song L, Niu J, Zhao L, Srinivasan L, Lin Q, Deng J, Li Y. Uncoupling the mitogenic and metabolic functions of FGF1 by tuning FGF1-FGF receptor dimer stability. Cell reports. 2017 Aug 15;20(7):1717-28.

[23] Szlachcic A, Sochacka M, Czyrek A, Opalinski L, Krowarsch D, Otlewski J, Zakrzewska M. Low Stability of Integrin-Binding Deficient Mutant of FGF1 Restricts Its Biological Activity. Cells. 2019 Aug;8(8):899.

[24] Xia X, Kumru OS, Blaber SI, Middaugh CR, Li L, Ornitz DM, Suh JM, Atkins AR, Downes M, Evans RM, Tenorio CA. An S116R phosphorylation site mutation in human

fibroblast growth factor-1 differentially affects mitogenic and glucose-lowering activities. Journal of pharmaceutical sciences. 2016 Dec 1;105(12):3507-19.

[25] Thallapuranam SK, Agarwal S, Gindampati RK, Jayanthi S, Wang T, Jones J, Kolenc O, Lam N, Niyonshuti I, Balachandran K, Quinn K, inventors. Engineered fgf1 and fgf2 compositions and methods of use thereof. United States patent application US 16/356,872. 2019 Sep 19.

[26] Samuel D, Kumar TK, Balamurugan K, Lin WY, Chin DH, Yu C. Structural events during the refolding of an all β-sheet protein. Journal of Biological Chemistry. 2001 Feb 9;276(6):4134-41.

[27] Alsenaidy MA, Jain NK, Kim JH, Middaugh CR, Volkin DB. Protein comparability assessments and potential applicability of high throughput biophysical methods and data visualization tools to compare physical stability profiles. Frontiers in Pharmacology. 2014 Mar 12;5:39.

[28] Blaber SI, Culajay JF, Khurana A, Blaber M. Reversible thermal denaturation of human FGF-1 induced by low concentrations of guanidine hydrochloride. Biophysical journal. 1999 Jul 1;77(1):470-7.

[29] Bernett MJ, Somasundaram T, Blaber M. An atomic resolution structure for human fibroblast growth factor 1. PROTEINS: Structure, Function, and Bioinformatics. 2004 Nov 15;57(3):626-34.

[30] Jo S, Kim T, Im W. Automated builder and database of protein/membrane complexes for molecular dynamics simulations. PloS one. 2007 Sep 12;2(9):e880.

[31] Lee J, Cheng X, Swails JM, Yeom MS, Eastman PK, Lemkul JA, Wei S, Buckner J, Jeong JC, Qi Y, Jo S. CHARMM-GUI input generator for NAMD, GROMACS, AMBER, OpenMM, and CHARMM/OpenMM simulations using the CHARMM36 additive force field. Journal of chemical theory and computation. 2016 Jan 12;12(1):405-13.

[32] Phillips JC, Braun R, Wang W, Gumbart J, Tajkhorshid E, Villa E, Chipot C, Skeel RD, Kale L, Schulten K. Scalable molecular dynamics with NAMD. Journal of computational chemistry. 2005 Dec;26(16):1781-802.

[33] Best RB, Zhu X, Shim J, Lopes PE, Mittal J, Feig M, MacKerell Jr AD. Optimization of the additive CHARMM all-atom protein force field targeting improved sampling of the backbone ϕ, ψ and side-chain χ1 and χ2 dihedral angles. Journal of chemical theory and computation. 2012 Sep 11;8(9):3257-73.

[34] Parlett BN. Large Sparse Sets of Linear Equations (JK Reid, ed.); Sparse Matrices and Their Applications (Donald J. Rose and Ralph A. Willoughby, ed.). SIAM Review. 1974 Jul;16(3):396-8.

[35] Martyna GJ, Tobias DJ, Klein ML. Constant pressure molecular dynamics algorithms. The Journal of chemical physics. 1994 Sep 1;101(5):4177-89.

[36] Darden T, York D, Pedersen L. Particle mesh Ewald: An N· log (N) method for Ewald sums in large systems. The Journal of chemical physics. 1993 Jun 15;98(12):10089-92.

[37] Young C, Bank JA, Dror RO, Grossman JP, Salmon JK, Shaw DE. A 32x32x32, spatially distributed 3D FFT in four microseconds on Anton. InProceedings of the Conference on High Performance Computing Networking, Storage and Analysis 2009 Nov 14 (pp. 1-11). IEEE.

[38] Kumar VG, Agrawal S, Kumar TK, Moradi M. Mechanistic Picture for Monomeric Human Fibroblast Growth Factor 1 Stabilization by Heparin Binding. bioRxiv. 2020 Jan 1.

[39] Humphrey W, Dalke A, Schulten K. VMD: visual molecular dynamics. Journal of molecular graphics. 1996 Feb 1;14(1):33-8.

[40] Zakrzewska M, Krowarsch D, Wiedlocha A, Olsnes S, Otlewski J. Highly stable mutants of human fibroblast growth factor-1 exhibit prolonged biological action. Journal of molecular biology. 2005 Sep 30;352(4):860-75.

[41] Matthews BW, Nicholson H, Becktel WJ. Enhanced protein thermostability from site-directed mutations that decrease the entropy of unfolding. Proceedings of the National Academy of Sciences. 1987 Oct 1;84(19):6663-7.

[42] Mateos B, Conrad-Billroth C, Schiavina M, Beier A, Kontaxis G, Konrat R, Felli IC, Pierattelli R. The ambivalent role of proline residues in an intrinsically disordered protein: from disorder promoters to compaction facilitators. Journal of molecular biology. 2020 Apr 17;432(9):3093-111.

[43] Longo LM, Gao Y, Tenorio CA, Wang G, Paravastu AK, Blaber M. Folding nucleus structure persists in thermally-aggregated FGF-1. Protein Science. 2018 Feb;27(2):431-40.

[44] Srimathi T, Kumar TK, Kathir KM, Chi YH, Srisailam S, Lin WY, Chiu M, Yu C. Structurally homologous all β-barrel proteins adopt different mechanisms of folding. Biophysical journal. 2003 Jul 1;85(1):459-72.

[45] Singh S, Zlotnick A. Observed hysteresis of virus capsid disassembly is implicit in kinetic models of assembly. Journal of Biological Chemistry. 2003 May 16;278(20):18249-55.

[46] Minajeva A, Kulke M, Fernandez JM, Linke WA. Unfolding of titin domains explains the viscoelastic behavior of skeletal myofibrils. Biophysical journal. 2001 Mar 1;80(3):1442-51.

[47] Minajeva A, Kulke M, Fernandez JM, Linke WA. Unfolding of titin domains explains the viscoelastic behavior of skeletal myofibrils. Biophysical journal. 2001 Mar 1;80(3):1442-51.

[48] Davis JM, Bächinger HP. Hysteresis in the triple helix-coil transition of type III collagen. Journal of Biological Chemistry. 1993 Dec 5;268(34):25965-72.

[49] Benítez-Cardoza CG, Rojo-Domínguez A, Hernández-Arana A. Temperature-induced denaturation and renaturation of triosephosphate isomerase from Saccharomyces cerevisiae: evidence of dimerization coupled to refolding of the thermally unfolded protein. Biochemistry. 2001 Jul 31;40(30):9049-58.

[50] Kellermayer MS, Smith SB, Bustamante C, Granzier HL. Complete unfolding of the titin molecule under external force. Journal of structural biology. 1998 Jan 1;122(1-2):197-205.

[51] Andrews BT, Capraro DT, Sulkowska JI, Onuchic JN, Jennings PA. Hysteresis as a marker for complex, overlapping landscapes in proteins. The journal of physical chemistry letters. 2013 Jan 3;4(1):180-8.

CHAPTER V

Stability of sFGF1 with respect to the Fluctuating pH Conditions, Aliphatic Alcohols, and Cell Culture Media

Abstract

Human acidic fibroblast growth factor (hFGF1), a 16 kDa heparin binding protein is ubiquitously expressed and is a powerful mitogen which is involved in various crucial cell-survival activities. Besides the cell survival activities, this protein is also involved in treatment of disorders such as diabetes, myocardial infarction, neuroprotection, bone fracture healing, and wound healing. The major disadvantage of using hFGF1 as a wound healing agent is that the apparent melting temperature (T_m -37˚C) of the growth factor lies in the physiological range. A negatively charged glycosaminoglycan, heparin, when bound to wtFGF1 increases the stability of the growth factor. Using a wide range of biophysical techniques, we determine that super FGF1 (sFGF1) considerably increases resistance of the growth factor to a broader range of pH range (2.5-11) and stabilizes hFGF1 in different aliphatic alcohols, and DMEM cell culture media. Intrinsic fluorescence spectroscopy data suggest that sFGF1 can sustain the conformational fluctuations over a broader range of pH (2.0 -11), whereas wtFGF1 is only stable from pH 4.0 - 9.5. The stability of sFGF1 in all the three aliphatic alcohols (ethanol, TFE and acetonitrile) is more than double of that exhibited by wtFGF1. Results of differential scanning calorimetry experiments suggest that unlike wtFGF1, sFGF1 is thermally reversible from pH 4.0 - 9.0. Results from SDS-PAGE show that sFGF1 increases resistance of the growth factor to the action of proteases present in DMEM cell culture media. sFGF1 due to its ability to sustain varying pH conditions and enhanced stability in cell culture media is believed to help in the efficient growth of different

types of mammalian cells. Further, the stability of sFGF1 under diverse conditions may be useful to design a more versatile wound healing therapeutic(s).

Introduction

Fibroblast growth factors (FGFs) constitute a family of heparin binding proteins involved in the regulation of cell growth and differentiation, and angiogenesis [1]. Several fibroblast growth factors (FGFs) have been found to be vital for embryonic and fetal development, wound healing, bone fracture healing, neuroprotection, and tumor development and progression, and they also protect against radiation-induced intestinal damage, myocardial infarction, and diabetes mellitus [2-9]. Out of all the FGFs, hFGF1 is unique in a way that it can activate all four known tyrosine kinase fibroblast growth factor receptors (FGFRs) [10]. FGFs' activities, therefore, could be harnessed to treat disorders that result from these types of insufficiencies - diseases characterized by ischemia such as, peripheral arterial disease, coronary ischemia, diabetic ulcers, and bed sores. Previously, our group has reported that a mutated form of hFGF1 (sFGF1) showed an increased activation of the ERK1/2 pathway, which is known to be critical for wound healing [11, 21]. Therefore, sFGF1 may exert the most potent effect on the treatment of wounds.

Crystallographic analyses of hFGF1 proteins depict a β trefoil structure containing twelve beta sheet strands, organized into a central domain, five of these sheets form a hairpin binding structure. The beta-sheets are arranged in an anti-parallel direction and are well conserved [14,15]. hFGF1 has an intrinsically low thermal, pH and proteolytic stability, and almost half of the wild type hFGF1 population is denatured at physiological temperature (T_m -37˚C). Stability of wtFGF1 increases as a consequence of its binding to heparin. As the low stability of hFGF1 limits its potential for practical use, several studies have been conducted on improving the stability of hFGF1 and consequently facilitate its long-term storage [12,13].

Several hFGF1 variants have been generated to increase its thermodynamic and proteolytic stability [12,16]. Among such hFGF1 variants, R133E, R136E, K126N, K132E, Q40P, S47I, H93G, and cysteine variants (C131S, C97S, C31S) were identified as strong stabilizing substitutions [8,20]. Compared to individual point mutations (K126N, K132E, S61I, H107G, and Q54P), combinations of single mutations (K126/K132E), (K132E/S61I/Q54P/H107G), (K126/K132E/S61I/Q54P/H107G), and (K126N/S61I/Q54P/H107G) were able to enhance the thermal stability of hFGF1. Previously reported hFGF1 variant, also known as sFGF1 (R136E/K126N/Q54P/S61L/H107S) has been suggested to be the most stable variant of hFGF1 so far [11]. In particular, the denaturation temperature (T_m) of sFGF1 increased up to 68˚C when compared with that of wild type hFGF1 (wtFGF1), T_m - 37˚C. Furthermore, R136E/K126N/Q54P/S61L/H107S exhibited the longest half-life and the lowest proteolytic susceptibility among all the other hFGF1 variants reported in the literature. sFGF1 is a heparin-independent variant. This has been evidenced by cell proliferation experiments which show 70% increased mitogenic activity in sFGF1 than wtFGF1.

This chapter aims at studying sFGF1's ability to sustain varying pH conditions, stability in different aliphatic alcohols (ethanol, 2,2,2- trifluoroethanol (TFE), and acetonitrile), and DMEM cell culture media. The results of this study demonstrate that sFGF1 can sustain the conformational fluctuations in both, acidic and basic environments. Being able to resist the change in pH is an important finding for many biomedical applications, including drug delivery and tissue engineering. Owing to its ability to resist the action of cellular proteases, results of this study strongly suggest that sFGF1 can effectively regulate pluripotency and cell differentiation in human embryonic stem cells. Lastly, the extraordinary stability by sFGF1 in aliphatic alcohols

implies that it can be stored under sterile conditions in alcohols, thereby minimizing potential microbial infections.

Results and discussion

Effect of pH on the stability of wtFGF1 and sFGF1

Nearly every biological process is pH dependent reflecting the importance of local pH on all processes in the cell. Ionizable amino acid residues have been shown to have a large influence on protein structure, stability and solubility [37, 38]. The types of interactions the side chains have with their environment depend on their protonation state. As a consequence of the change in protonation of the ionizable residues, the stability of proteins is pH dependent. Changes in intracellular pH have been shown to regulate essential processes such as cell proliferation and apoptosis [39, 40]. However, our understanding on the effects of environmental pH on proteins is limited.

The process of wound healing involves various cellular events, including angiogenesis. pH within the wound environment directly and indirectly influences all cellular events [41]. It has been shown that the surface pH of any wound plays an important role in wound healing as it helps in controlling infection and increasing antibacterial and antifungal activity, oxygen release, and protease activity [42]. During the wound healing process, the wound site advances from an alkaline state to a neutral state and lastly to an acidic state. Therefore, alterations in pH can affect the regular cellular events in wound healing and to work as an efficient wound healing therapeutic, FGF with a wider range of pH stability is desired [44].

In this context, the stability of wtFGF1 and sFGF1 were monitored using fluorescence spectroscopy. Fluorescence spectroscopy is an excellent method to determine changes in the tertiary structure of the protein. wtFGF1 contains one tryptophan and eight tyrosine residues. In

the native state, fluorescence of a tryptophan residue is quenched by the lysine and proline residues located in the vicinity of the indole ring. The quenching effect diminishes the expected 350 nm tryptophan peak and therefore, only 305 nm emission peak from the eight tyrosine residues is observed in the native conformation of the protein. The intrinsic fluorescence spectra of wtFGF1 and sFGF1 at pH 3.5 and 7.0 are displayed in Fig. 1. The spectra from wtFGF1 and sFGF1 at pH 7.0 have an emission maximum at 305 nm, which corresponds to the emission of tyrosine residues. Contrastingly, the spectra at pH 3.5 show a major peak at 305 nm for sFGF1, but a 350 nm peak for wtFGF1 corresponding to the emission of a Trp residue. This infers that sFGF1 is stable even at pH 3.5. Absence of the 350 nm emission peak at pH 3.5 suggests that the native tertiary structural interactions in sFGF1 are mostly intact.

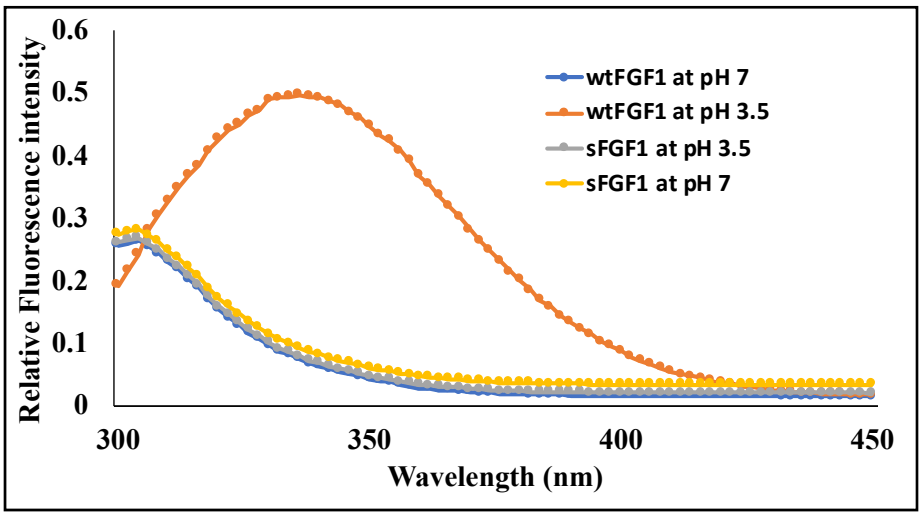

Fig. 1: Overlay of the fluorescence spectra of wtFGF1 and sFGF1 at pH 3.5 and 7.

The ratio of fluorescence intensity at 305 nm and 350 nm (305/350) has been established to examine the changes in tertiary structure of hFGF1 as a function of temperature, pH or a chemical denaturant. A greater intensity ratio denotes that the protein is in its properly folded tertiary structure. On the other hand, a lower value of 305/350 nm indicates perturbed tertiary structure. Hence, the intensity ratio has been calculated and plotted as a function of pH to

observe the alteration in the tertiary structure of wtFGF1 and sFGF1 (Fig. 2). 305/350 nm intensity ratio for wtFGF1 started at ~1 and increased steadily up to ~5. At pH 1.0, 1.5, 2.0, 2.5, 3.0, and 3.5, the intensity ratio was found to be at ~1, suggesting that the tertiary structure of wtFGF1 is altered from pH 1.0 - 3.5. In contrast, 305/350 nm ratio for pH 4.0 and 4.5 was found to gradually increase from ~1 to ~5, indicating minor structural perturbations. Fluorescent intensity ratio was found to be stable at ~5, from pH 5.0 to 7.5, suggesting that the tertiary structure of wtFGF1 is properly folded. 305/350 nm ratio decreases from pH 7.5 to pH 10, signifying structural changes in wtFGF1. Intensity ratio stays below 1 from pH 10 to 13, implying that the native tertiary structure of wtFGF1 is completely altered. On the other hand, fluorescence intensity ratio for sFGF1 initiates at 1 and gradually increases with an increase in pH, indicating that the tertiary structure is altered from pH 1.0 to 2.0 and there are some minor structural changes from pH 2.5 to 4.5. Fluorescence intensity ratio is found to be maximum (~6) from pH 4.5 to 9.5. This indicates that there is no significant alteration in the tertiary structure of sFGF1. However, intensity ratio stays below 1 from pH 11.5 to 13, implying that the native tertiary structure of sFGF1 is significantly altered.

It has been observed that both acute and chronic wounds have a lower healing rate with an alkaline pH when compared with an acidic pH [43]. Therefore, maintaining the protein stability under acidic conditions is critical in the biomedical applications, including wound healing [22,23]. There have been several studies that have examined different approaches to achieve this stability; including protein engineering and chemical modifications [24,25]. Heparin binding pocket comprises of positively charged amino acids. These amino acids repel each other and cause instability of wtFGF1. Two of these positively charged residues in heparin binding pocket of sFGF1 have been mutated to a negative and neutral amino acid (R136E and K126N).

These mutations aid in minimizing the repulsions between closely packed basic amino acids. Moreover, serine to leucine substitution at position 61 might help in rearrangement of the hydrogen bonds in sFGF1, thereby stabilizing the protein against conformational changes in different pH. Results from Chapter IV indicate that the thermal stability of the triple variant (R136E/K126N/Q54P) was found to be 18 °C higher than wtFGF1. The reason for enhanced stability of the triple variant could be attributed to formation of stable electrostatic interactions (R133-E136 and N126-S130) involving the mutated residues. It has also been demonstrated that Q54P mutation leads to the formation of a short 3_{10} helix which increases the β-sheet propensity of the growth factor [17]. Analyses of main-chain dihedral angles indicates that Ser at position 61 in wtFGF1 was located much closer to the surface ($\psi = 149°$ and $\psi = 143°$) whereas Ile in the triple variant structure was positioned in a region favorable for β-strand conformation ($\psi = -113°$ and $\psi = 124°$) [17]. H107 residue forms a type I β-turn in wtFGF1. However, glycine is preferred over His in type I β-turn. Therefore, substitution of His by Gly reduced the steric strain between the backbone and side-chain C-alpha atoms. Thus, it appears that introduction of R136E, K126N, Q54P, S61L, and H107S aid in stabilizing hFGF1 against the conformational fluctuations in pH, thereby qualifying sFGF1 as a better wound healing agent.

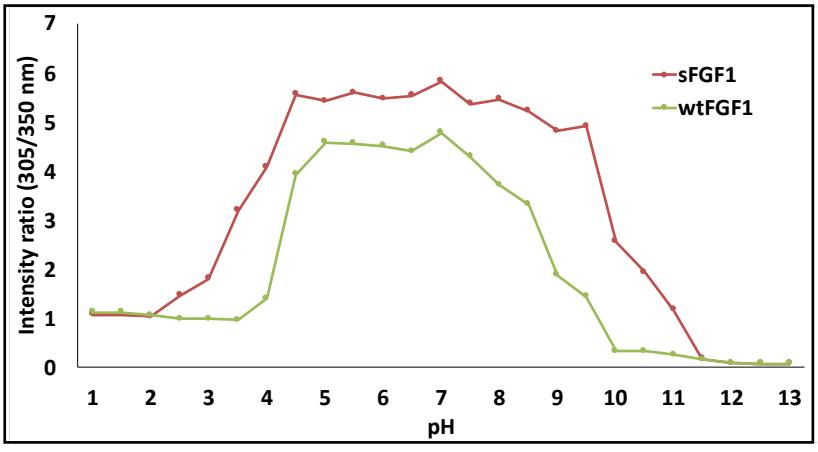

Fig. 2: Effect of pH on the stability of wtFGF1 and sFGF1

Effect of pH on the reversibility of thermal unfolding of hFGF1

Differential Scanning Calorimetry (DSC) is a useful tool for thermal analyses of proteins using changes in heat capacity due to exothermic or endothermic reactions. We examined the thermal stability and refolding of sFGF1 using DSC (Fig. 3). It can be inferred from the thermograms that fluctuations in pH significantly affect the refolding capacity of sFGF1. It should be noted that T_m (temperature at which 50% of the protein population exists in denatured state(s)) of unfolded and refolded sFGF1 from pH 4.0 - 9.0 is found to be ~68°C, indicating that sFGF1 is stable in a pH range of 4.0 -9.0. On the contrary, T_m of refolded sFGF1 at pH 2.0, 3.0, and 10 shifts from 68°C to ~50°C (Fig. 4). This signifies that some of the interactions that are present in sFGF1 (unfolded/native state) are disrupted during the refolding process at pH's 2.0, 3.0, and 10. Moreover, the DSC thermogram at pH 2.0, 3.0 and 10 are broad indicating that the protein exists in multiple conformations including a population of conformations which resemble the native state.

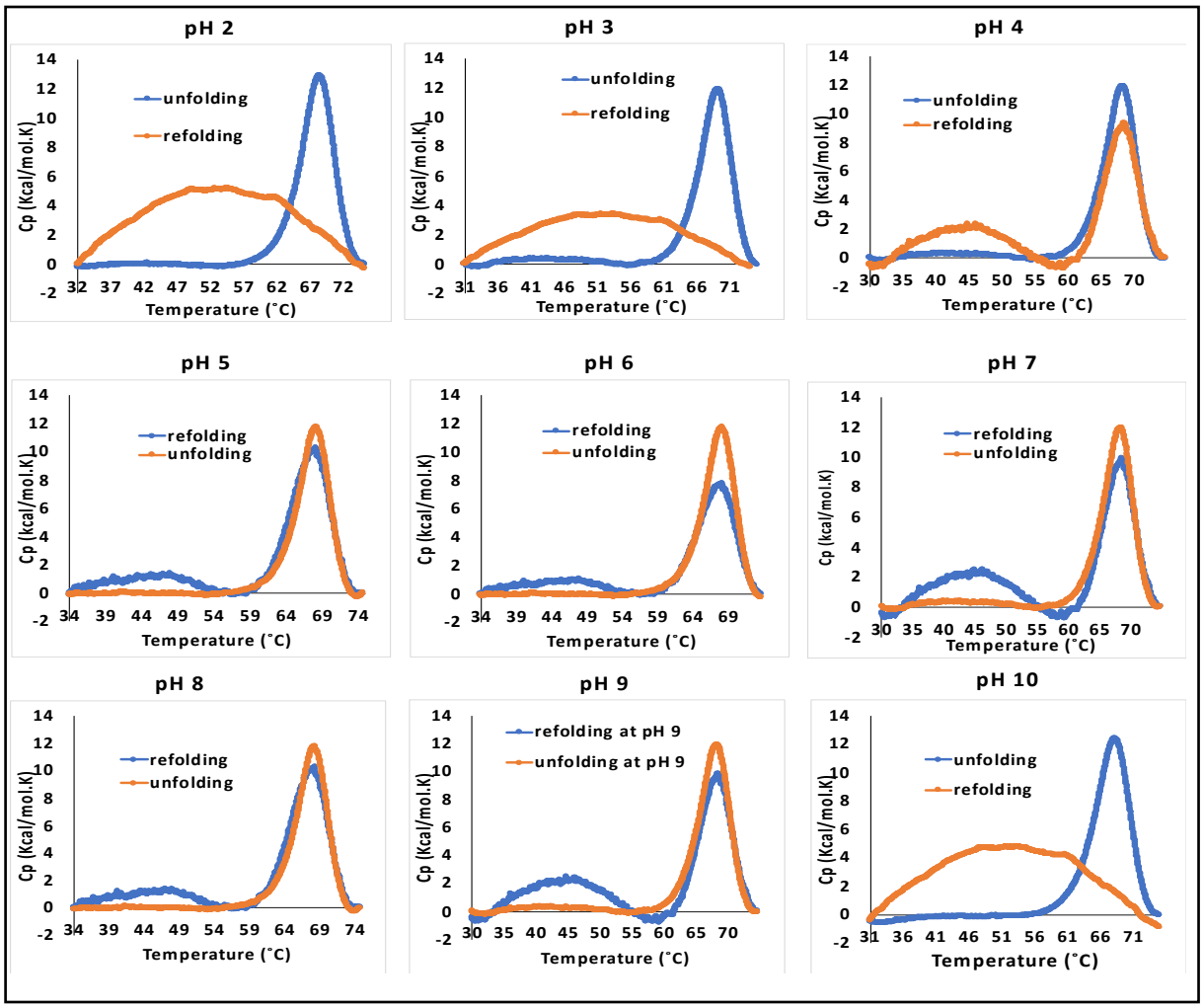

Fig. 3: Effect of pH on the reversibility of the thermal unfolding of sFGF1

The decrease in T_m of the refolded sFGF1 at pH's 2.0, 3.0, and 10 could presumably be due to the loss of stabilizing interactions (salt bridges (R133 and E136) and H-bonding (G129-N126, N126-S130, Q141-E136, and E136-R133)) present in the unfolded (native) sFGF1. It might also be plausible that time period for which the protein is cooled during the refolding process is not sufficient to form the interactions. Therefore, T_m of unfolded and refolded sFGF1 does not match at pH's 2.0, 3.0, and 10.

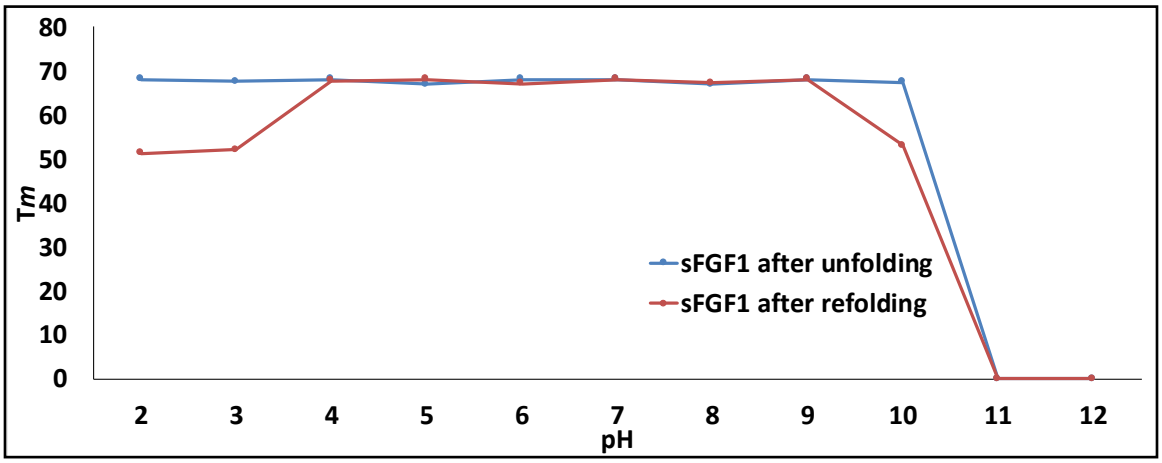

Fig. 4: T_m of the unfolded and refolded sFGF1 at different pH values.

SDS-PAGE was run on the thermally unfolded wtFGF1 and sFGF1 to examine the percentage of active protein in each sample (Figs. 5 and 6). Panel A of Figs. 5 and 6 represents DSC profile of unfolding of wtFGF1 and sFGF1. After the unfolding of hFGF1, samples were aliquoted for SDS-PAGE (Panel B of Figs. 5 and 6). Densitometric analysis of SDS-PAGE gel shows that only 5% of wtFGF1 was found in the supernatant (aggregated molecules settle at the bottom after centrifugation) in comparison to 75% of sFGF1 (Panel C of Figs. 5 and 6). The fully folded sample before loading into DSC was considered to be 100% unaggregated protein. Aggregation of wtFGF1 (70%) was evidently visible after centrifugation whereas sFGF1 did not show any visible aggregates (only 10%). Moreover, lower Cp as observed in DSC thermograms for the refolding process of sFGF1 could be due to formation of some aggregates (Fig. 3).

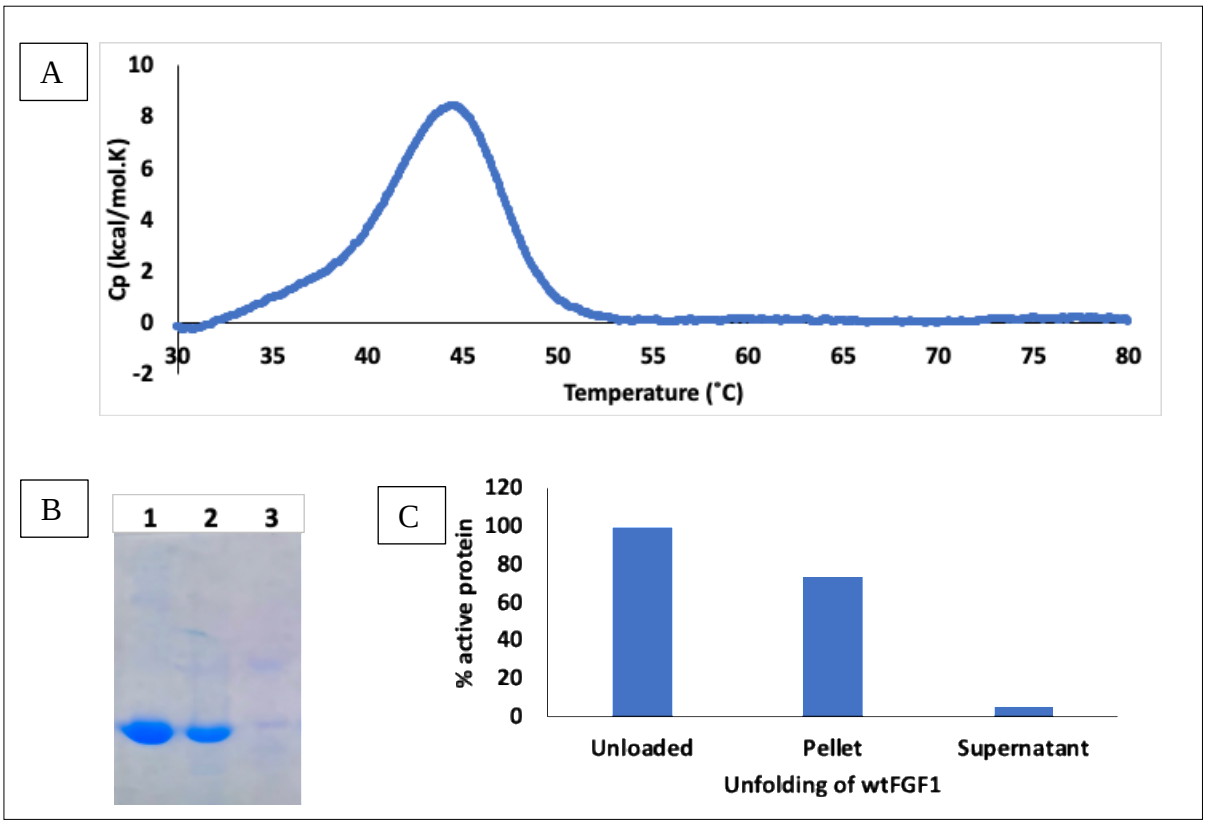

Fig 5: Thermal unfolding of wtFGF1 measured by DSC (Panel - A). SDS-PAGE gel showing aggregation of wtFGF1 during thermal unfolding by DSC (Panel - B). Unloaded protein (Lane-1); Pellet (Lane-2); Supernatant (Lane-3). Densitometric analysis of the SDS PAGE gel showing the protein aggregated during the thermal unfolding of wtFGF1 (Panel - C).

Overall, the results of thermal unfolding and refolding by DSC indicate that sFGF1 is not only more stable than wtFGF1, but it also refolds back. Introduction of mutations (R136E, K126N, Q54P, S61L, and H107S) appear to stabilize sFGF1 by forming new interactions. These interactions seem to strengthen hydrogen bonds and increase the β-sheet propensity. According to the statistical analysis, proline is the most preferred amino acid in type I β-turn and leucine and isoleucine are most preferred amino acids in the formation of β-sheet. Q54 is located within a turn between β3 and β4 strands. Therefore, replacing Gln with Pro at position 54 is expected to

enhance the tendency of growth factor to form β-sheets. It was also found that replacing Gln with Pro leads to formation of 3_{10} helix (two overlapping β-turns). S61 is located in the middle of β-strand IV. Szlachcic *et al.,* observed that substitution of serine by isoleucine aids in rearrangement of hydrogen bonds [17]. Heparin binding region in hFGF1 (ranging from residues 119-142) consists of positively charged amino acids. Two of the five mutations in sFGF1, R136E and K126N, belong to heparin binding pocket (HBP). Substitution of Arg by Glu and Lys by Asn produces a counter-ion and charge neutralization effect which reduces repulsion between the closely packed basic amino acids in HBP.

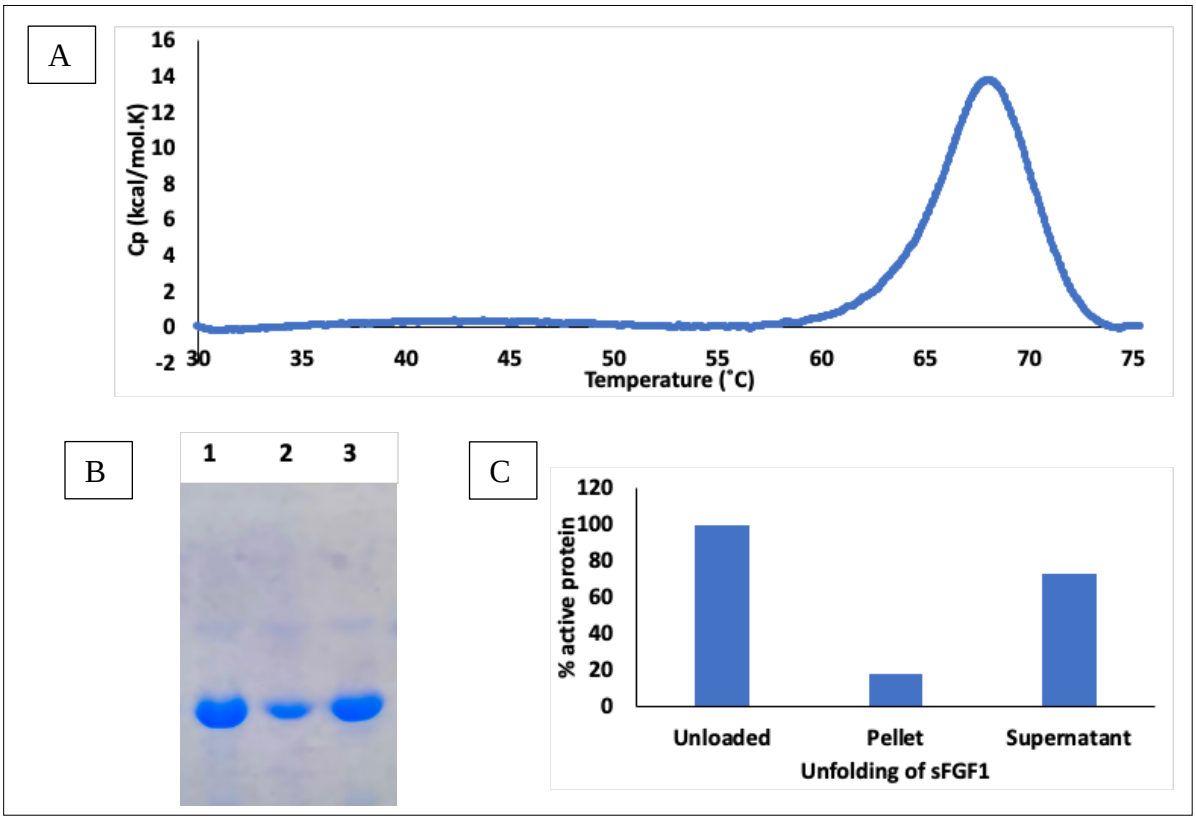

Fig 6: Thermal unfolding of sFGF1 by DSC (Panel - A). SDS-PAGE gel showing minimal aggregation of sFGF1 during thermal unfolding by DSC (Panel - B). Unloaded protein (Lane-1); Pellet (Lane-2); Supernatant (Lane-3). Densitometric analysis of the SDS PAGE gel showing the unaggregated protein during the thermal unfolding of sFGF1 (Panel - C).

Stability of wtFGF1 and sFGF1 in Aliphatic Alcohols

Alcohols have been used as co-solvents to study the hydrophobic effect of solvent on the structure and stability of proteins [28-30]. Addition of alcohols weaken nonlocal hydrophobic interactions and enhances local polar interactions [29-31]. This results in destabilization of the protein's native hydrophobic core and increased formation of local hydrogen bonds resulting in extended secondary structures.

Effects of alcohols on the tertiary structure of wtFGF1 and sFGF1 were monitored using intrinsic fluorescence spectroscopy. It is well known that intrinsic fluorescence of proteins relies upon microenvironment of three aromatic amino acids, tryptophan (Trp), tyrosine (Tyr) and phenylalanine (Phe). hFGF1 has eight tyrosine and one tryptophan residues. In native wtFGF1, intrinsic fluorescence from a tryptophan residue is quenched by adjacent lysine and proline residues. Therefore, wtFGF1 shows an emission maximum at 305 nm, resulting from the eight tyrosine residues. These quenching effects are completely alleviated in the denatured state of wtFGF1, resulting in a significant increase in fluorescence at 350 nm corresponding to the tryptophan residues. Here, two fluorescence parameters, emission wavelength maximum (λ_{max}) and fluorescence intensity ratio (305/350 nm), were used to obtain information on the tertiary structure of hFGF1.

Fig. 7 displays changes in the fluorescence emission spectrum of wtFGF1 and sFGF1 with the addition of different concentrations of 2,2,2- trifluorethanol (TFE). Fluorinated alcohols such as TFE is extensively used to study conformation of proteins or peptides in monomeric state [45]. Aqueous TFE solutions are known to induce helix formation in polypeptides and proteins [46]. However, TFE can induce β-sheet conformation under certain conditions [47]. λ_{max} of wtFGF1 changes from 308 nm to 350 nm when incrementing the TFE concentration from 0 to 10% v/v (Fig. 7A). However, λ_{max} again drops down to 308 nm with a small peak at 350 nm at

35% v/v TFE concentration. On the contrary, λ_{max} of sFGF1 changes from 308 nm to 350 nm when the TFE concentration increases from 0 to 20% v/v. However, sFGF1 behaves in the same way as wtFGF1 at 35% v/v TFE concentration. An altered λ_{max} suggests that microenvironment of the Trp residue changes upon addition of TFE. Initial increase in TFE concentration led to the shift of tryptophan residue from hydrophobic core to hydrophilic surface (solvent exposed). This red shift suggests the possibility of conformational changes in the structure of wtFGF1 and sFGF1. However, the fluorescence emission results of wtFGF1 and sFGF1, in the presence of TFE, indicate that the decrease in λ_{max} might be due to the strong hydrogen bond formation of TFE with the proteins.

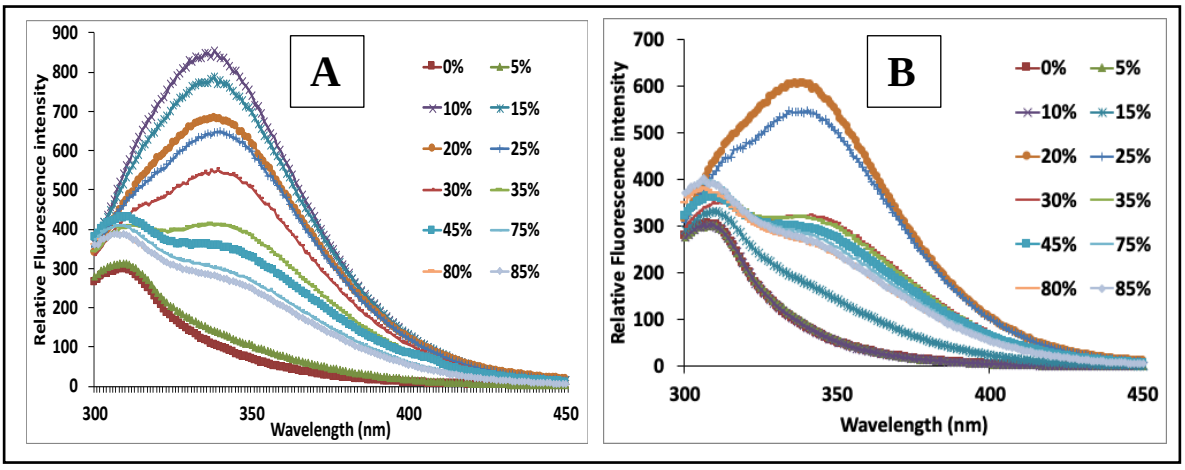

Fig. 7: Fluorescence emission spectra of wtFGF1 (Panel – A) and sFGF1 (Panel – B) at different concentrations of 2,2,2- trifluoroethanol (TFE) (0–85%, v/v).

The fluorescence intensity ratio is high when Trp residue is buried inside the hydrophobic core of protein, while the ratio is low when Trp residue is exposed to the hydrophobic environment. Fig. 8 displays changes in the fluorescence intensity ratio of wtFGF1 and sFGF1 at different TFE concentrations. It can be inferred from the graph that sFGF1 is more stable at varying concentrations of TFE than wtFGF1. In case of wtFGF1, 305/350 ratio decreases to

almost 0 upon addition of 10% v/v TFE, whereas the intensity ratio remains high for sFGF1 up to 20% v/v TFE concentration. This indicates that tryptophan is exposed to hydrophilic surface upon addition of 25% v/v TFE concentration or higher in both wtFGF1 and sFGF1.

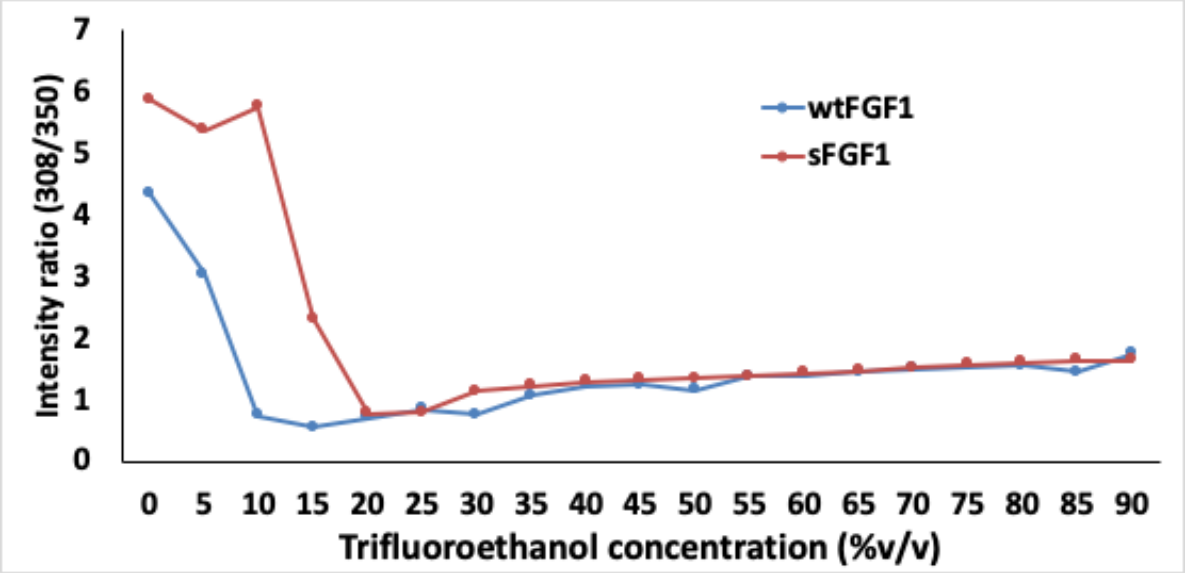

Fig. 8: TFE-induced unfolding of wtFGF1 (blue) and sFGF1 (red) as monitored by the ratio of emission intensities at 308 nm to 350 nm.

Similar to TFE, intrinsic fluorescence of wtFGF1 and sFGF1 was measured in presence of various concentrations of ethanol. It has been reported that ethanol can affect intermolecular electrostatic attractions, hydrogen bonds, and hydrophobic interactions, resulting in alteration of protein conformations [48]. Fig. 9 indicates changes in the fluorescence emission spectrum of wtFGF1 and sFGF1 as a function of ethanol content. As expected, λ_{max} of wtFGF1 and sFGF1 shifts from 305 nm to 350 nm (Figs. 9 A and B) accompanied by decrease in fluorescence intensity ratio (Fig. 10) when incrementing the ethanol concentration from 5 to 90% v/v. As discussed in case of TFE, the red shift in λ_{max} and lower intensity ratio (305/350 nm) indicate that polarity of the microenvironment of Trp residue is increased.

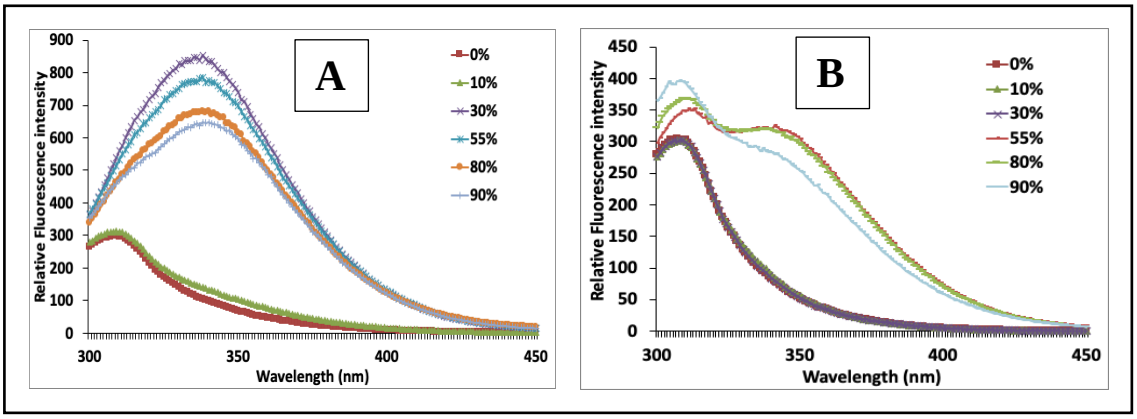

Fig. 9: Fluorescence emission spectra of wtFGF1 (Panel – A) and sFGF1 (Panel – B) at different concentrations of ethanol (0–90%, v/v).

Fig. 9A displays that λ_{max} of wtFGF1 (305 nm) did not change when the concentration of ethanol was increased up to 20% (v/v), but λ_{max} increases to 350 nm upon further addition of ethanol up to 90% v/v. On the contrary, λ_{max} of sFGF1 (305 nm) did not change as the concentration of ethanol was increased up to 80% (v/v), but λ_{max} increases to 350 nm upon further addition of ethanol up to 90% (v/v) (Fig. 9B). These results demonstrate that addition of ethanol perturbs the native tertiary structure of wtFGF1 (20% v/v) at a fairly low concentration when compared to sFGF1 (80% v/v), indicating that wtFGF1 cannot resist the conformational changes induced by ethanol.

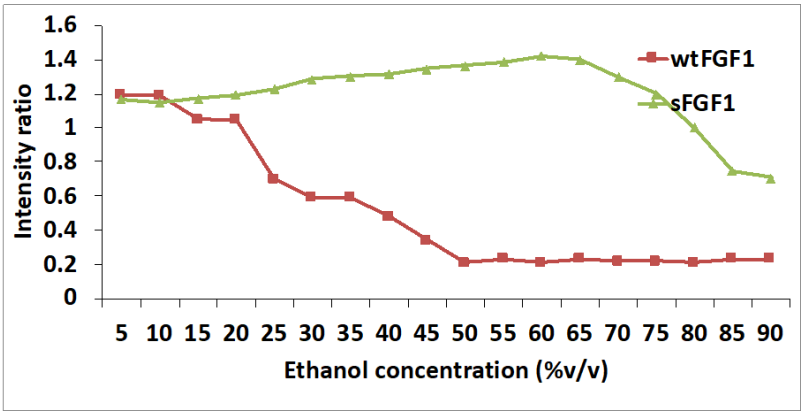

Fig. 10: Ethanol-induced unfolding of wtFGF1 (red) and sFGF1 (green) as monitored by the ratio of emission intensities at 308 nm to 350 nm.

It has been reported that acetonitrile can induce protein denaturation by altering the tertiary structure through hydrophobic interactions [50]. In this context, the intrinsic fluorescence of wtFGF1 and sFGF1 was measured in the presence of various concentrations of acetonitrile. Fig. 11 shows the changes in the fluorescence emission spectra of wtFGF1 and sFGF1 with increasing acetonitrile content. When increasing the acetonitrile concentration from 5 to 90 % v/v, λ_{max} of wtFGF1 and sFGF1 shifts from 305 nm to 350 nm (Figs. 11 A and B) and is associated with decrease in fluorescence intensity ratio (305/350 nm) (Fig. 12). This indicates that polarity of the microenvironment of Trp residue is increased.

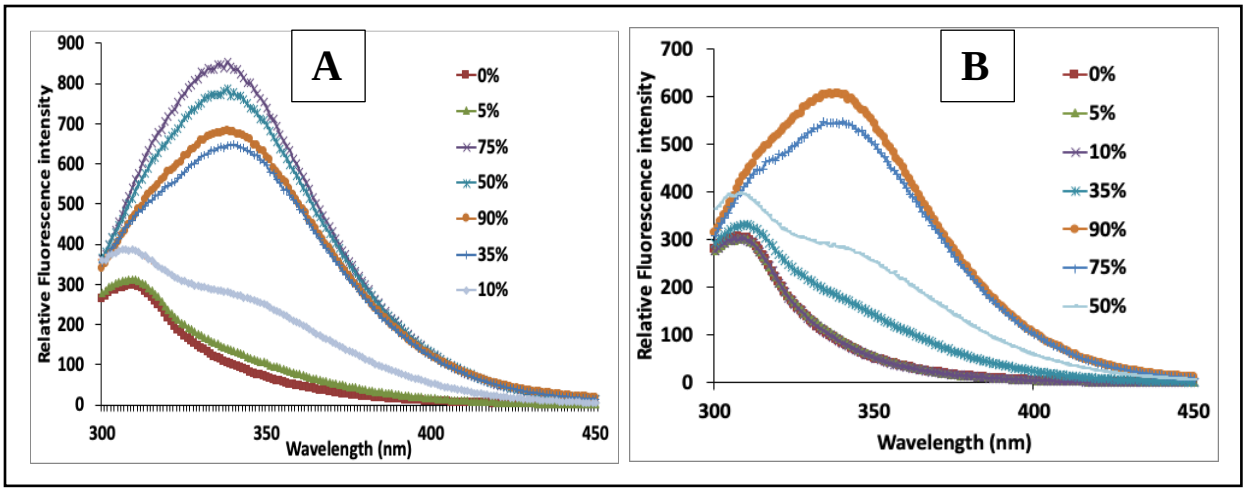

Fig. 11: Fluorescence emission spectra of wtFGF1 (Panel – A) and sFGF1 (Panel – B) at different concentrations of acetonitrile (0–90%, v/v)

Fig. 11B shows that λ_{max} of sFGF1 did not change as the concentration of acetonitrile was increased up to 50% v/v, but a decrease in intensity ratio (Fig. 12) was observed. An unaltered λ_{max} at 308 nm suggests that the tertiary structure of sFGF1 was not significantly perturbed upon addition of 50% v/v acetonitrile concentration. Under these conditions, the Trp residue could be buried within the protein core, thereby preventing the exposure of Trp residue to the solvent environment. On the other hand, λ_{max} of wtFGF1 was shifted to 350 nm upon addition of 15% v/v acetonitrile. The observed red shift suggests that conformational change in wtFGF1 and

sFGF1 causes an increased solvent-exposure of the Trp residue. It should be noted that sFGF1 is able to resist the change in conformation even at 50% v/v acetonitrile concentration, whereas wtFGF1 is only stable until 15% v/v acetonitrile concentration.

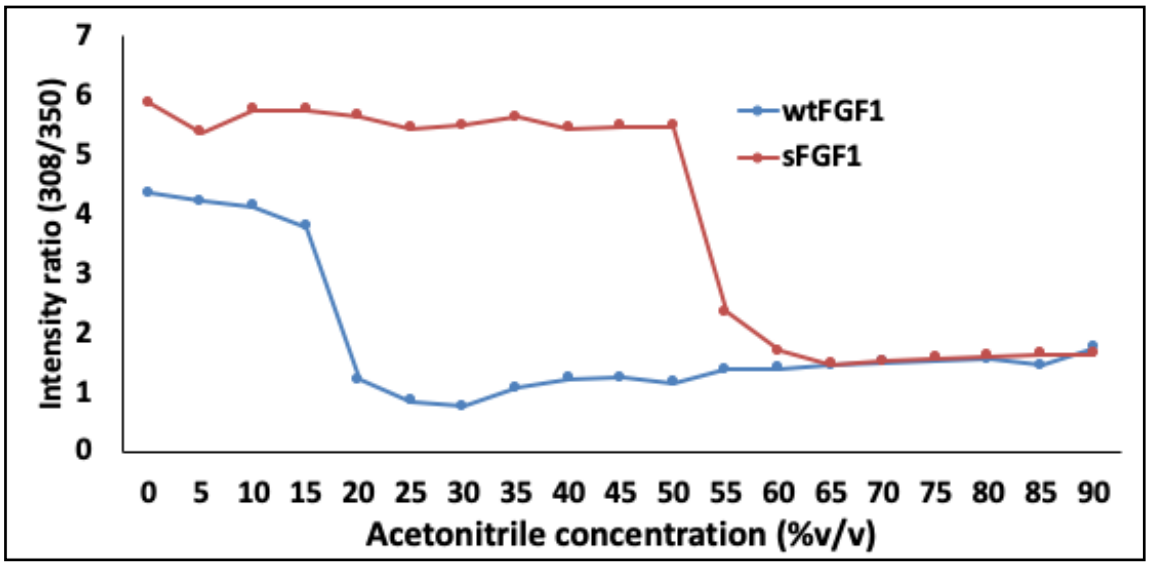

Fig. 12: Acetonitrile-induced unfolding of wtFGF1 (blue) and sFGF1 (red) as monitored by the ratio of emission intensities at 308 nm to 350 nm.

Overall, intrinsic fluorescence experiment reveals that substituting Arg with Glu at position 136, Lys by Asn at position 126, Gln by Pro at position 54, Ser by Leu at position 61, and His by Ser at position 107 helped in stabilizing sFGF1. It has been demonstrated that low levels of alcohols, in general, are often used in multi-dose protein formulations and drug delivery systems to prevent microbial growth [32]. However, these alcohols have been shown to induce protein aggregation [33]. Singh *et al.,* reported that the fundamental physical mechanism underlying such alcohol-induced protein aggregation is partial unfolding of local protein regions. Therefore, stabilizing such local regions through site-specific mutations could help in reducing protein aggregation. In hFGF1, one such conformationally unstable region is heparin binding pocket which consists of closely placed cluster of positively charged residues. These positively charged amino acids repel each other leading to hFGF1's instability. Two of these positively

charged heparin binding residues in wtFGF1 are substituted by a negative and a neutral amino acid (R136E and K126N) in sFGF1. R136E and K126N mutations might reduce the repulsion between the basic amino acids in the heparin binding region, thus conferring extra stability to sFGF1. Structurally, S61L mutation is expected to make the hFGF1 molecule more compact by strengthening the hydrogen bonds. Based on molecular dynamic simulation data (Chapter - III), four new hydrogen bonds (G129-N126, N126-S130, Q141-E136, and E136-R133) and one stable salt bridge (R133-E136) were identified in sFGF1. These new interactions likely stabilize the protein against the effect of aliphatic alcohols.

Stability of wtFGF1 and sFGF1 in the cell culture media

Acidic fibroblast growth factor (FGF1) plays an important role in a variety of biological processes, including embryonic development, morphogenesis, tissue repair, endothelial cell migration and proliferation. hFGF1 has been shown to be unstable under physiological conditions, with a half-life of approximately five hours in standard mammalian cell culture conditions (37°C, 5% CO_2). hFGF1 is also known to be degraded by proteolytic enzymes (metalloproteinase and collagenase) present in the DMEM cell culture medium. At this rate of decay, hFGF1 activity levels drop substantially after 48 hours at 37 °C [49]. Susceptibility of hFGF1 to enzymatic digestion might pose a significant challenge for the use of hFGF1 in cell culture, often requiring higher growth factor concentrations or daily media changes or FGF1 supplementation. In this context, stability of wtFGF1 and sFGF1 in culture medium was examined. Fig. 13 shows that wtFGF1 was found to be completely degraded at 37°C after 24 hours of incubation in the growth medium. On the other hand, sFGF1 showed insignificant degradation. Based on SDS-PAGE gel results, it was found that wtFGF1 band in lane 2 (1 day/ 24 hours) decreases by almost 80% of its original concentration as compared to the protein

(wtFGF1) which was not incubated in the culture medium. These results suggest that wtFGF1 is susceptible to the action of proteolytic enzymes present in the culture medium. In marked contrast, the concentration of the band corresponding to sFGF1 remains mostly unaltered implying that sFGF1 is significantly more stable in the culture medium conditions than wtFGF1.

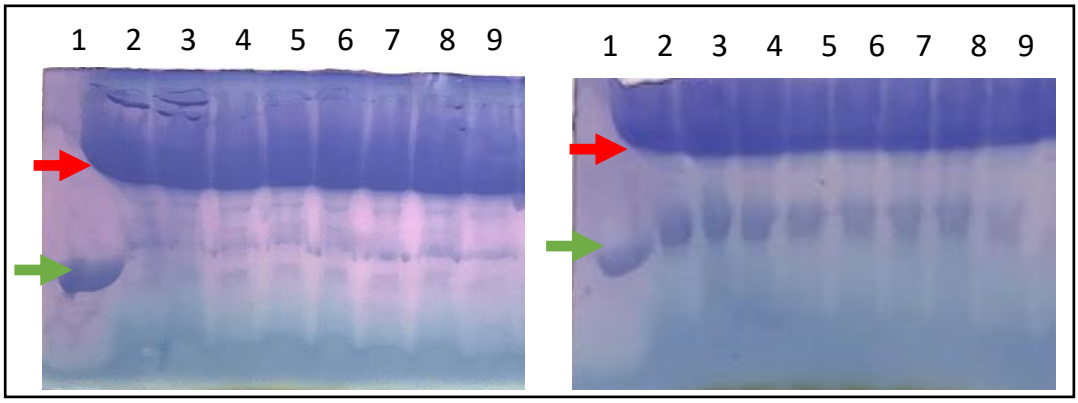

Fig. 13: SDS-PAGE analysis of stability of wtFGF1 (Panel – A) and sFGF1 (Panel-B) in cell culture medium. 50 ng/mL of proteins (Lane-1); 1 day (Lane-2); 2 days (Lane-3); 3 days (Lane-4); 4 days (Lane-5); 5 days (Lane-6); 6 days (Lane-7); 7 days (Lane-8); 14 days (Lane-9). The top red arrow represents the band corresponding to serum albumin whereas the bottom green arrow represents the hFGF1 protein band.

Densitometric analysis of the SDS PAGE gels suggest that sFGF1 is mostly resistant to the action of proteases present in cell culture medium. On the other hand, about 80% of wtFGF1 is digested within 24 hours under similar conditions (Fig. 14). These results clearly indicate that introduction of mutations in wtFGF1 has increased the resistance of protein to proteolytic digestion.

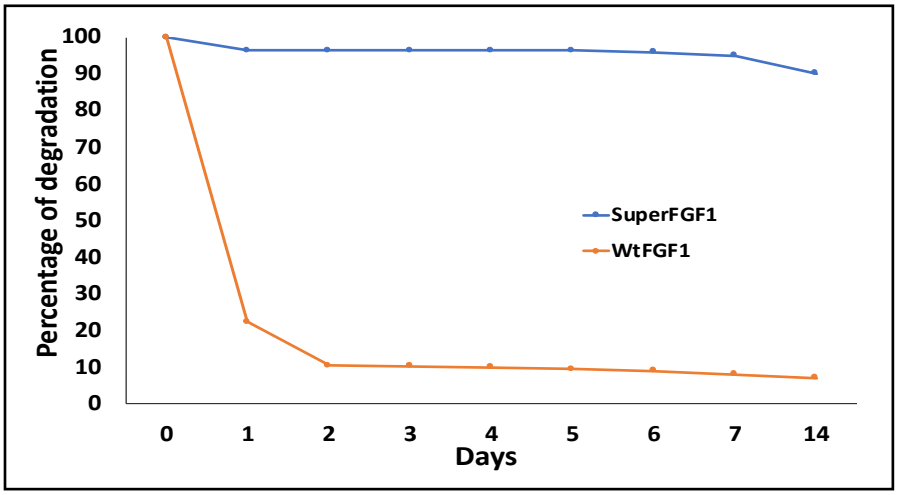

Fig. 14: Densitometric analysis to assess the stability of wtFGF1 and sFGF1 in cell culture medium as monitored by SDS-PAGE.

Chen *et al.*, reported that the thermal instability of FGF2 is because of the heparin binding region. Thus, they mutated one of the heparin binding residue (K128) to a neutral, polar amino acid (N). Surprisingly, they found that the mutation (K128N) helped hFGF2 maintain its activity in the cell culture medium at 37°C incubation [35]. Similarly, the stability provided by sFGF1 in DMEM cell culture media appears to be due to the presence of two mutations in the heparin binding pocket (R136E and K126N). Replacement of Arg with Glu and Lys with Asn could have plausibly reduced the repulsion between the positively charged residues in the heparin binding region.

Conclusions

Acidic fibroblast growth factor exhibits a wide array of activities such as, mitogenic activity, angiogenic activity, wound healing, and bone growth. However, there are some limitations to its use due to the thermal instability of hFGF1. Introduction of mutations in hFGF1 led to new interactions (hydrogen bonds and salt bridges) which increased its inherent structural stability. Results of the present study show that sFGF1 is more resistant in a broader pH range than wtFGF1. Unlike wtFGF1, sFGF1 is stable at higher concentration of aliphatic alcohols

(acetonitrile, TFE, and ethanol). wtFGF1 is only stable upto 10% v/v TFE, 20% v/v ethanol, and 15% v/v acetonitrile concentrations. Contrastingly, sFGF1 is stable upto 20% v/v TFE, 80% v/v ethanol, and 50% v/v acetonitrile concentrations. Native wtFGF1 is highly unstable under normal cell culture conditions, with a half-life of approximately 5 hours. Findings of this study demonstrate that wtFGF1 is susceptible to the action of proteases in cell culture media and degrades in 24 hours. On the other hand, sFGF1, highly stable human acidic fibroblast growth factor, exhibits increased stability in the cell culture medium up to 14 days. As, sFGF1 stays biologically active for a longer period than wtFGF1 in standard cell culture conditions, it may be now possible to design cost effective cell culture medium and also design new FGF1 based therapeutic formulations for chronic wound care.

Materials and methods

Materials

The site-directed mutagenesis kit (QuikChange lightning kit) was from Agilent, and the DNA plasmid isolation kit was from Qiagen. *Escherichia coli* strain BL21(DE3)pLysS was from New England Biolabs. Heparin-Sepharose affinity resin was from Amersham Biosciences. The basic components of culture media were purchased from IBI Scientific. Complete protease inhibitor mixture was from Roche Applied Science. The buffer components were from VWR Scientific. NIH 3T3 cells were purchased from ATCC and all the cell culture reagents including, DMEM media, fetal bovine serum (FBS) and penicillin, streptomycin were obtained from Thermo Fisher Scientific. All other chemicals were purchased from Sigma and were of high-quality grade.

Purification of wtFGF1 and sFGF1

A construct comprising a truncated form (residues, 21–154) of human FGF1 in the pET-20b expression vector was used. Mutagenesis and protein expression were performed as reported

previously [36]. wtFGF1 and sFGF1 were expressed at 37 °C in *E. coli* BL21(DE3)pLysS strain and were cultured at 37 °C to an A600 of 0.5 and induced with 1 mM isopropyl-L-thio- □ -D-galactopyranoside (IPTG) for 3.5 h. The cells were then lysed using the sonicator, and the soluble proteins were purified on a heparin-Sepharose affinity column, followed by size-exclusion chromatography on Superdex-75 using AKTA Explorer system (Amersham Biosciences). Protein purity was confirmed by Coomasie blue-stained SDS-PAGE. The purity of wtFGF1 and sFGF1 was estimated to be >98% based on SDS-PAGE analysis. The conformational changes in wtFGF1 and sFGF1 were examined by circular dichroism and fluorescence spectra measurements. The numbering system used to identify amino acids in hFGF1 has been reported previously [36]. Purified hFGF1C protein was stored at -80°C until further use.

SDS-PAGE was also performed to validate the thermal refolding and unfolding of wtFGF1 and sFGF1. After the thermal unfolding of proteins, the protein samples were pipetted out of the DSC machine and centrifuged at 13000 rpm for 3 minutes. The supernatant (active protein sample) was separated from the pellet (aggregated protein sample) into a different Eppendorf tube. TCA preparation was performed on each sample (aggregated and soluble wtFGF1 and sFGF1) immediately after the centrifugation. The results were assessed using SDS-PAGE analysis. The percentage of unaggregated protein was measured by comparing the band intensities in lane 1, 2 and 3 using UN-SCAN-IT software. The native protein (unfolded) was considered as 100% unaggregated protein (lane -1), the pellet and supernatant after the unfolding of proteins were considered as lane 2 and 3, respectively. After obtaining the values from the UN-SCAN-IT software, Microsoft excel was employed to obtain the graph of percentage active protein versus the protein samples.

Fluorescence and Circular Dichroism spectroscopy

Circular dichroism and intrinsic fluorescence spectra were measured using a Jasco J-1500 Spectrophotometer. Circular dichroism provides the information regarding the secondary structural changes whereas fluorescence spectroscopy determines the tertiary structural changes between wtFGF1 and sFGF1. All measurements were carried out at a protein concentration of 33 µM in a 10 mm quartz cuvette. CD spectra were recorded in the wavelength range 195–250 nm in 10 mM phosphate buffer with 100 mM NaCl (pH 7.2) at 25ºC with a scan speed of 20 nm/min, slit width set to 2 nm and a response time of 1 second. To acquire intrinsic fluorescence spectra, an excitation wavelength of 280 nm was used, and emission spectra were collected from 300 to 450 nm in a 1 cm quartz cuvette.

Differential Scanning Calorimetry

The protein samples of wtFGF1 and sFGF1 at a concentration of 0.5 mg/ml in 10 mM phosphate buffer containing 100 mM NaCl, pH 7.2 was used to determine the thermal denaturation on a N-DSC III Differential Scanning calorimeter. Prior to loading, all samples were subjected to degassing at 25°C for 15 minutes and after loading, the cells were equilibrated for 10 minutes at the same temperature. Scans were performed from 10 to 90 °C with a 1 C/min ramping temperature and variable pH solutions. To obtain a stable baseline, buffer blanks experiments were conducted before running the protein scans. Data obtained was processed using CpCalc Version 2.2.0.10 software provided by the manufacturer.

15% of sFGF1 protein was found to be aggregated. As it was difficult to remove the aggregates due to the process of unfolding, thermograms provided by DSC showed lower intensities for the refolded sFGF1. Therefore, normalization of protein concentration was done (multiplied the refolded intensities by a factor of 7.5 because 75% of sFGF1 was found to be active as shown in Fig. 6C) using Microsoft excel.

Cell culture experiments

The NIH 3T3 fibroblast cell line was obtained from ATCC (Manassas, VA). NIH 3T3 cells were grown in complete media consisting of Dulbecco's modified Eagle's medium supplemented with 10% FBS and 1% penicillin/streptomycin. Cells were grown to 80-90% confluency and were incubated overnight at 37°C with 5% CO_2 in serum free media before further use. Cells were seeded into tissue culture plates the day preceding the start of the experiments. Cells were then co-incubated individually with wtFGF1 and sFGF1 at concentrations of 50 ng/mL for 1, 2, 3, 4, 5, 6, 7, and 14 days. TCA preparation was performed on each sample immediately after being removed from the culture plate. The results were assessed using SDS-PAGE analysis along with UN-SCAN-IT gel software. The proteins (wtFGF1 and sFGF1) were loaded in the first lane on SDS-PAGE (without media) to identify hFGF1 out of all the other proteins in culture media.

REFERENCES

[1] Presta M, Dell'Era P, Mitola S, Moroni E, Ronca R, Rusnati M. Fibroblast growth factor/fibroblast growth factor receptor system in angiogenesis. Cytokine Growth Factor Rev. 2005;16:159–178.

[2] Okunieff P, Mester M, Wang J, et al. In vivo radioprotective effects of angiogenic growth factors on the small bowel of C3H mice. Radiat Res 1998;150:204-211.

[3] Hagiwara A, Nakayama F, Motomura K, et al. Comparison of expression profiles of several fibroblast growth factor receptors in the mouse jejunum: suggestive evidence for a differential radioprotective effect among major FGF family members and the potency of FGF1. Radiat Res 2009;172:58-65.

[4] Abraham JA, Whang JL, Tumolo A, *et al*. Human basic fibroblast growth factor: nucleotide sequence and genomic organization. The EMBO Journal. 1986 Oct 1;5(10):2523-8.

[5] Weich HA, Iberg N, Klagsbrun M, Folkman J. Expression of acidic and basic fibroblast growth factors in human and bovine vascular smooth muscle cells. Growth Factors. 1990 Jan 1;2(4):313-20.

[6] Feige JJ, Baird A. Glycosylation of the basic fibroblast growth factor receptor. The contribution of carbohydrate to receptor function. Journal of Biological Chemistry. 1988 Oct 5;263(28):14023-9.

[7] Bing M, Da-Sheng C, Zhao-Fan X, *et al*. Randomized, multicenter, double-blind, and placebo-controlled trial using topical recombinant human acidic fibroblast growth factor for deep partial-thickness burns and skin graft donor site. Wound repair and regeneration. 2007 Nov;15(6):795-9.

[8] Huang C, Liu Y, Beenken A, *et al*. A novel fibroblast growth factor-1 ligand with reduced heparin binding protects the heart against ischemia-reperfusion injury in the presence of heparin co-administration. Cardiovascular research. 2017 Nov 1;113(13):1585-602.

[9] Gasser E, Moutos CP, Downes M, Evans RM. FGF1—a new weapon to control type 2 diabetes mellitus. Nature Reviews Endocrinology. 2017 Oct;13(10):599-609.

[10] Ornitz DM, Itoh N. Fibroblast growth factors. Genome biology. 2001 Mar;2(3):reviews3005-1.

[11] Thallapuranam SK, Agarwal S, Gindampati RK, Jayanthi S, Wang T, Jones J, Kolenc O, Lam N, Niyonshuti I, Balachandran K, Quinn K, inventors. Engineered fgf1 and fgf2 compositions and methods of use thereof. United States patent application US 16/356,872. 2019 Sep 19.

[12] Culajay JF, Blaber SI, Khurana A, et al. Thermodynamic characterization of mutants of human fibroblast growth factor 1 with an increased physiological half-life. Biochemistry 2000;39:7153-7158.

[13] Copeland RA, Ji H, Halfpenny AJ, et al. The structure of human acidic fibroblast growth factor and its interaction with heparin. Arch Biochem Biophys 1991;289:53-61.

[14] Brych, S. R., Blaber, S. I., Logan, T. M., & Blaber, M. (2001). Structure and stability effects of mutations designed to increase the primary sequence symmetry within the core region of a β-trefoil. *Protein Science : A Publication of the Protein Society.* 10(12), 2587–2599.

[15] Zakrzewska, M., Krowarsch, D., Wiedlocha, A., and J. Otlewski. Design of fully active FGF-1 variants with increased stability. 2004. *Protein Engineering, Design & Selection,* 17(8), 603-611.

[16] Zakrzewska M, Krowarsch D, Wiedlocha A, et al. Highly stable mutants of human fibroblast growth factor-1 exhibit prolonged biological action. J Mol Biol 2005;352:860-875.

[17] Szlachcic, A., et al., Structure of a highly stable mutant of human fibroblast growth factor 1, Acta Cryst, 2009. D65: p. 67-73.

[18] Zakrzewska M, Wiedlocha A, Szlachcic A, Krowarsch D, Otlewski J, Olsnes S. Increased protein stability of FGF1 can compensate for its reduced affinity for heparin. Journal of Biological Chemistry. 2009 Sep 11;284(37):25388-403.

[19] Ortega, S., et al., Conversion of Cysteine to Serine Residues Alters the Activity, Stability, and Heparin Dependence of Acidic Fibroblast Growth Factor, J Biol Chem, 1991. 266(9): p. 5842-5846.

[20] Wong, P., Hampton, B., Szylobrgt, E., Gallagher, A.M., Jaye, M., Burgess, W.H., Analysis of Putative Heparin-binding Domains of Fibroblast Growth Factor-1. J Biol Chem, 1995. 270(43): p. 25805-25811.

[21] Kerr R, Agrawal S, Maity S, Koppolu B, *et al*. Design of a thrombin resistant human acidic fibroblast growth factor (hFGF1) variant that exhibits enhanced cell proliferation activity. Biochemical and biophysical research communications. 2019 Oct 15;518(2):191-6.

[22] M. A. Swartz, S. Hirosue and J. A. Hubbell, Sci. Transl. Med., 2012, 4, 148rv9.

[23] N. H. C. S. Silva, C. Vilela, I. M. Marrucho, C. S. R. Freire, C. Pascoal Neto and A. J. D. Silvestre, J. Mater. Chem. B, 2014, 2, 3715.

[24] O. Kirk, T. V. Borchert and C. C. Fuglsang, Curr. Opin. Biotechnol., 2002, 13, 345.

[25] J. E. Nielsen and T. V. Borchert, Biochim. Biophys. Acta, Protein Struct. Mol. Enzymol., 2000, 1543, 253.

[26] Wang, H. M., & Yu, C. (2011). Investigating the refolding pathway of human acidic fibroblast growth factor (hFGF-1) from the residual structure (s) obtained by denatured-state hydrogen/deuterium exchange. *Biophysical journal*, *100*(1), 154-164.

[27] Srimathi, T., Kumar, T. K. S., Kathir, K. M., Chi, Y. H., Srisailam, S., Lin, W. Y., ... & Yu, C. (2003). Structurally homologous all β-barrel proteins adopt different mechanisms of folding. *Biophysical journal*, *85*(1), 459-472.

[28] Tanford C. Protein denaturation. Adv Protein Chem. 1968;23:121–282.

[29] Thomas PD, Dill KA. Local and nonlocal interactions in globular proteins and mechanisms of alcohol denaturation. Protein Science. 1993;2:2050–2065.

[30] Buck M. Trifluoroethanol and colleagues: cosolvents come of age. Recent studies with peptides and proteins. Quarterly Rev Biophysics. 1998;31:297–355.

[31] Dill KA, Bromberg S, Yue K, Fiebig KM, Yee DP, Thomas PD, Chan HS. Principles of protein folding - A perspective from simple exact models. Protein Sci. 1995;4:561–602.

[32] Meyer BK, Ni A, Hu B, Shi L. Antimicrobial preservative use in parenteral products: Past and present. J Pharm Sci. 2007;96:3155–3167.

[33] Maa YF, Hsu CC. Aggregation of recombinant human growth hormone induced by phenolic compounds. Int J Pharm. 1996;140:155–168.

[34] Singh, S. M., Cabello-Villegas, J., Hutchings, R. L., & Mallela, K. M. (2010). Role of partial protein unfolding in alcohol-induced protein aggregation. *Proteins*, *78*(12), 2625–2637. https://doi.org/10.1002/prot.22778.

[35] Chen, G., Gulbranson, D. R., Yu, P., Hou, Z., & Thomson, J. A. (2012). Thermal stability of fibroblast growth factor protein is a determinant factor in regulating self-renewal, differentiation, and reprogramming in human pluripotent stem cells. *Stem cells (Dayton, Ohio)*, *30*(4), 623–630. https://doi.org/10.1002/stem.1021.

[36] Davis JE, Alghanmi A, Gundampati RK, Jayanthi S, Fields E, Armstrong M, Weidling V, Shah V, Agrawal S, prasanth Koppolu B, Zaharoff DA. Probing the role of proline− 135 on the structure, stability, and cell proliferation activity of human acidic fibroblast growth factor. Archives of biochemistry and biophysics. 2018 Sep 15;654:115-25.

[37] Grimsley GR, Scholtz JM, Pace CN (2009) A summary of the measured pK values of the ionizable groups in folded proteins. Protein Sci 18: 247–251.

[38] Kukić P, Farrell D, Søndergaard CR, Bjarnadottir U, Bradley J, et al. (2010) Improving the analysis of NMR spectra tracking pH-induced conformational changes: removing artefacts of the electric field on the NMR chemical shift. Proteins 78: 971–984.

[39] Gunner MR, Mao J, Song Y, Kim J (2006) Factors influencing the energetics of electron and proton transfers in proteins. What can be learned from calculations. Biochim Biophys Acta 1757: 942–968.

[40] Srivastava J, Barber DL, Jacobson MP (2007) Intracellular pH sensors: design principles and functional significance. Physiology 22: 30–39.

[41] Schneider LA, Korber A, Grabbe S, Dissemond J. Influence of pH on wound-healing: a new perspective for wound-therapy? *Arch Dermatol Res*. 2007;298(9):413-420.

[42] Hoffman R, Noble J, Eagle M. The use of proteases as prognostic markers for the healing of venous leg ulcers. *J Wound Care*. 1999; 8(6):273-276.

[43] Gethin G. The significance of surface pH in chronic wounds. *Wounds UK*. 2007;3(3):52-56.

[44] Xia, X., Babcock, J. P., Blaber, S. I., Harper, K. M., & Blaber, M. (2012). Pharmacokinetic Properties of 2 nd-Generation Fibroblast Growth Factor-1 Mutants for Therapeutic Application. *PloS one*, *7*(11), e48210.

[45] T. Konno, Y.O. Kamatari, N. Tanaka, H. Kamikubo, C.M. Dobson, K. Nagayama, Biochemistry 39 (2000) 4182–4190.

[46] F.D. Sönnichsen, J.E. Van Eyk, R.S. Hodges, B.D. Sykes, Biochemistry 31 (1992) 8790–8798.

[47] P.A. Raj, P. Balaram, Biopolymers 24 (1985) 1131–1146.

[48] R. Liu, P. Qin, L. Wang, X. Zhao, Y. Liu, X. Hao, Journal of Biochemical and Molecular Toxicology 24 (2010) 66–71.

[49] Chen, G., Gulbranson, D. R., Yu, P., Hou, Z., & Thomson, J. A. (2012). Thermal stability of fibroblast growth factor protein is a determinant factor in regulating self-renewal, differentiation, and reprogramming in human pluripotent stem cells. *Stem Cells*, *30*(4), 623-630.

[50] Gekko K, Ohmae E, Kameyama K, Takagi T. Acetonitrile-protein interactions: amino acid solubility and preferential solvation. BBA Protein Struct M. 1998;1387(1):195–205. doi: 10.1016/S0167-4838(98)00121-6.

CHAPTER VI

CONCLUSIONS AND FUTURE DIRECTIONS

Conclusions

Fibroblast growth factor (FGF) family is comprised of 23 highly regulated monomeric proteins which control a plethora of developmental and pathophysiological processes, including tissue repair, wound healing, angiogenesis, and embryonic development. Human acidic fibroblast growth factor (hFGF1) is a 16kDa protein characterized by its mitogenic properties and high affinity for heparin. It has been known that heparin protects the unstable form of the growth factor against heat and proteolytic degradation. Thus, the putative role of heparin is to prevent the degradation of the hFGF1 molecule. But, the kind of structure stabilization and new forces brought into place by heparin is still unclear.

The major focus of this dissertation was to construct a hFGF1 variant that exhibits increased thermal, chemical, and proteolytic stability, enhanced bioactivity, and reduced heparin binding affinity. These characteristics form the basis for a better wound healing agent. We also wanted to gain some insights into the role of heparin in hFGF1-FGFR complex formation and activation. In this context, wtFGF1 was subjected to mutation at positions 54 (Q54P), 61 (S61L), 107 (H107S), 126 (K126N), and 136 (R136E). Site directed mutagenesis technique was employed to construct the mutations mentioned above.

Interestingly, with contradicting studies showing that heparin either influences the receptor activation of hFGF1 or fosters hFGF1 stability with electrostatic interactions, the hFGF1-heparin complex becomes the most studied protein-glycosaminoglycan complex. Inferences from Chapter II indicate that although heparin affects the stability of the growth factor, it could have little implications on the proliferation efficiency of the protein. Isothermal

titration calorimetric studies reveal that the positions crucial on hFGF1 for heparin binding are K126 and R136. Additionally, other results pertaining to the mutation at positions Q54P, S61L, H107S, K126N, and R136E correspond to heparin-independent hFGF1 proficiency with increased thermal, chemical, and structural stability and improved cell proliferation activity.

The members of the FGF family has a characteristic β-trefoil conformation which helps in the functioning of the protein but there still remains an elusive understanding of its functional capability. In Chapter III, it was verified that with the decrease in the repulsion of positive charges in the heparin binding site, the structural stability of hFGF1 can be improved. Apart from this, limited enzymatic digestion, thermal and urea unfolding, and isothermal titration calorimetry were also performed. It was noticed that sFGF1 showed superior characteristics when compared to wild type in all aspects of the analyses mentioned. Furthermore, investigating the findings of molecular dynamic (MD) simulations, results showed that the flexibility of the heparin-binding site was hindered by the mutations, and increased stability was achieved due to the formation of salt bridges and hydrogen bonds. Also, with sFGF1 there was an elevated cell proliferation activity and a considerable rise in the activation of pathways such as Erk 1/2 and Akt. Thus, the above-mentioned results qualify sFGF1 as a promising wound healing drug.

In chapter IV, we indicate that modification of amino acids to reverse the charge in the heparin binding pocket of hFGF1 increases its stability without disrupting its structure. We have experimentally demonstrated that introduction of Q54P, K126N, and R136E mutations on wtFGF1 lead to reversible thermal and chemical denaturation of the growth factor. Thermal and urea induced unfolding and refolding results indicate that a triple variant of wtFGF1 (Q54P/K126N/R136E) render more stability and facilitates refolding of the growth factor. In fact, the triple variant has shown to exhibit hysteresis between unfolding and refolding processes

with difference in temperature and urea concentration gradient. MD simulations suggest that the triple variant render less flexibility to the heparin binding region and enhances the stability of hFGF1 by forming stable electrostatic interactions such as R133-E136 and N126-S130. ^{1}H-^{15}N HSQC experiment reveals that the triple variant does not significantly affect the gross three-dimensional structure of hFGF1. Interaction analyses from MD simulations and NMR thus indicate that the variant residues in the heparin binding region (R136E and K126N) along with Q54P mutation are critical to the stabilization of the protein observed in silico and the refolding process observed experimentally.

In chapter V, we noticed that although human acidic fibroblast growth factor renders many advantages in terms of wound healing and tissue repair, its potential is limited due to its short half-life and structural instability. Therefore, to increase the structural stability, several mutations were studied in hFGF1. The results showed that when compared to wtFGF1, sFGF1 was not only resistant to a wider pH range, but also stable in predominantly higher concentrations of aliphatic alcohols (ethanol, 2,2,2- trifluoroethanol (TFE), and acetonitrile). Additionally, sFGF1 is also stable in the cell culture media for up to 14 days, thereby implying that it could be potentially be used to design cost effective wound healing treatment options.

The implications of these findings imply that binding to heparin is not mandatory for the FGF-FGFR signal transduction, further challenging the central dogma of FGF receptor activation. In conclusion, binding of heparin to wtFGF1 and hFGF1 variants stabilizes and protects the proteins from thermal and proteolytic degradation prior to FGFR activation. However, with the engineered hFGF1, since heparin is not required for increased stimulation and complexation with the FGF receptor, it has the potential to play a pivotal role in shaping the development of wound healing treatment.

Significance of this dissertation

hFGF1 has an intrinsically low thermodynamic stability and almost half of the wild type hFGF1 population is denatured at physiological temperature. Several studies have been performed to increase the thermal and proteolytic stability of hFGF1. Prior work conducted in our lab resulted in the generation of variant hFGF1 referred to as single variant R136E, which is located in the heparin binding region. This study is focused on generating hFGF1 variants with four more mutations on R136E-hFGF1, to determine the significance of the heparin independent sFGF1 (Q54P, S61L, H107S, K126N, R136E).

Another important aspect of the heparin-binding region is that it contains the secondary thrombin cleavage site between Arginine-136 and Threonine-137. Thrombin is a serine protease that is generated after endothelial cell damage and during the coagulation cascade. It has also been demonstrated to cleave hFGF1 at Arg-136, thus, diminishing the mitogenic activity of hFGF1. Many studies have focused on designing hFGF1 variant with increased resistance to thrombin with the aim of enhancing its wound-healing potency. Studies have demonstrated that the binding of hFGF1 to heparin increases the possibility of degradation of the protein imposed by thrombin. Therefore; designing a hFGF1 variant with complete loss of heparin binding affinity will be advantageous in pharmaceutical wound healing applications. Topical applications of human fibroblast growth factor are believed to accelerate cell proliferation at wound sites while leaving other bodily processes intact. The significance of the hFGF1 variants studied in this dissertation widens the opportunity for the use of the growth factor in pharmaceutical industry.

Future directions

It is evident that there have been significant advances in improving the stability and decreasing the heparin binding affinity of hFGF1 through site directed mutagenesis technique. However, none of the hFGF1 variants reported so far in the literature exhibit complete loss of heparin binding ability. Here, we have generated a hFGF1 variant known as sFGF1 which has significantly higher thermal and proteolytic stability and confers zero heparin binding affinity.

While our variant has shown enhanced mitogenic activity, there has been a recent study of another hFGF1 variant (K132E) demonstrating increased metabolic activity and decreased potential to promote cell proliferation. Therefore, to take this research a step further we could consider combining both, the attributes of increased metabolic and mitogenic activities. This variant could especially be used in the field of diabetic research, wherein the role of hFGF1 variant will be to increase the glucose-lowering activity and enhance the cell proliferation ability. This variant great hope for the evolution of a new class of FGF-based protein therapeutics against Type-1 & Type-2 diabetes.

APPENDIX

Biosafety committee approval

Kumar lab biosafety protocol number – 13004

UNIVERSITY OF ARKANSAS

Office of Research Compliance

September 6, 2018

MEMORANDUM

TO:	Dr. Suresh Kumar Thallapuranam
FROM:	Ines Pinto, Biosafety Committee Chair
RE:	Protocol Renewal
PROTOCOL #:	13004
PROTOCOL TITLE:	Role of heparin in Acidic fibroblast growth factor signaling
APPROVED PROJECT PERIOD:	**Start Date** August 9, 2021 **Expiration Date** August 8, 2021

The Institutional Biosafety Committee (IBC) has approved your request, dated August 8, 2018, to renew IBC # 13004, "Role of heparin in Acidic fibroblast growth factor signaling".

The IBC appreciates your assistance and cooperation in complying with University and Federal guidelines for research involving hazardous biological materials.

1424 W. Martin Luther King, Jr. • Fayetteville, AR 72701
Voice (479) 575-4572 • Fax (479) 575-6527